THE *TOXOPLASMA GONDII* VACUOLAR H^+-ATPASE REGULATES INTRACELLULAR PH AND CALCIUM AND IMPACTS THE MATURATION OF ESSENTIAL SECRETORY PROTEINS

by

ANDREW JOSEPH STASIC

(Under the Direction of Silvia NJ Moreno)

ABSTRACT

Toxoplasma gondii is an Apicomplexan obligate intracellular parasite that infects as much as one-third of the world's population. The pathogenesis of Toxoplasma is linked to its lytic cycle which involves egress from a host cell, motility, attachment/invasion, and replication. While the parasite is preparing for egress, a large lysosomal vacuole forms, which is termed the plant-like vacuole (PLV) and that helps the parasite to resist the changing ionic conditions. In the PLV there is a vacuolar-H^+-ATPase (V-ATPase), an evolutionarily conserved multi-subunit complex that couples the hydrolysis of ATP to the pumping of protons across membranes. V-ATPases play diverse roles in eukaryotic cellular physiology including the acidification of intracellular compartments, vesicular trafficking, and creation of a proton gradient that can be used for the exchange of other ions. To study the *T. gondii* V-ATPase, I created a conditional mutant of the *a1* subunit (*iΔvha1-HA*). Depletion of the V-ATPase resulted significant defects to all major steps of the lytic cycle, indicating its importance to the parasite. In *T. gondii*, secretory organelles termed micronemes and rhoptries are required for invasion and modulation of the infected host

cell. The maturation of proteins destined to these organelles were decreased and often mislocalized in V-ATPase mutant parasites. Additionally, proteases responsible for the maturation of microneme and rhoptry proteins were defective in their own maturation. Further characterization of the *iΔvha1-HA* mutants revealed that the defects in the lytic cycle were in part due to defects in calcium signaling and homeostasis. It was further demonstrated that the proton gradient derived from the V-ATPase is responsible for calcium entry into the parasite and storage in the PLV and acidocalcisomes, organelles important for acidic calcium and polyphosphate storage. I demonstrate that loss of the V-ATPase results in defects in calcium uptake to the PLV and acidocalcisome. Loss of the proton gradient generated by the V-ATPase resulted in defects in synthesis and storage of polyphosphate in the acidocalcisome. This work underscores a novel role for V-ATPases in regulating the maturation of important proteins involved in virulence pathways, vesicular trafficking, and calcium and polyphosphate storage.

INDEX WORDS: *Toxoplasma gondii,* plant-like vacuole (PLV), acidocalcisomes, micronemes, rhoptries, endosomal-like compartments, vacuolar H^+ ATPase (V-ATPase), proton transport, lytic cycle, lysosome, pH homeostasis, polyphosphate, and calcium homeostasis.

THE *TOXOPLASMA GONDII* VACUOLAR H^+-ATPASE REGULATES INTRACELLULAR PH AND CALCIUM AND IMPACTS THE MATURATION OF ESSENTIAL SECRETORY PROTEINS

by

ANDREW JOSEPH STASIC

B.A., The University of Chicago, 2010

M.S., The University of Wisconsin—Madison, 2013

A Dissertation Submitted to the Graduate Faculty of The University of Georgia in Partial Fulfillment of the Requirements for the Degree

DOCTOR OF PHILOSOPHY

ATHENS, GEORGIA

2019

THE *TOXOPLASMA GONDII* VACUOLAR H^+-ATPASE REGULATES INTRACELLULAR PH AND CALCIUM AND IMPACTS THE MATURATION OF ESSENTIAL SECRETORY PROTEINS

by

ANDREW JOSEPH STASIC

Major Professor:	Silvia N. J. Moreno
Committee:	Vincent J. Starai
	Robert J. Maier
	Zhicheng Dou

Electronic Version Approved:

Suzanne Barbour
Dean of the Graduate School
The University of Georgia
May 2019

DEDICATION

This work is dedicated to my wife and infant son Andrew Charles (Charlie) Stasic. Conducting scientific research has tremendous highs and crushing lows. Regardless of how my daily science went, the love and support from my wife and son, gave me the strength to move past failed experiments and celebrate when manuscripts were accepted. I would like to thank my wife for following me all around the country for my various educational stops. Abbey sacrificed part of her professional career for me to follow mine. Words cannot express how thankful I am, and I will forever be grateful. I would also like to dedicate this work to my father, my mother, and my brother. My parents taught me to always do my best, to never give up easily, and to have an appreciation for science. Without their support and guidance throughout the years, I would not be the scientist or, most importantly, the man I am today. I am so blessed to have them in my life.

ACKNOWLEDGEMENTS

I would like to express my deepest gratitude to Dr. Silvia Moreno for allowing me to become part of her research lab. Silvia has been incredible supportive of my ideas on the direction of my project and instrumental in pushing me to investigate deeper. Silvia also provided invaluable assistance on data interpretation, guidance on presentations, manuscripts, and scholarships, and career advice. Years ago, I matriculated to UGA with the intention to continue studying my scientific passion—pathogenic microorganisms. During our first interview to discuss the possibility of rotating in Silvia's lab, I became fascinated by *Toxoplasma gondii*, the vacuolar H^+-ATPase, the importance of calcium, and the plant-like-vacuole—all of which became part central components of my research project. I was not sold on calcium part at first, but it later grew on me. I am grateful to have the opportunity to investigate this important pathogen and discover novel functions of the vacuolar H^+-ATPase and its implications for propagation of *Toxoplasma gondii*. With Silvia's guidance, I am honored to be able to present and share my numerous important observations with the scientific community. All of this work would simply not possible without out her guidance and support. I am grateful for our weekly research update meetings to discuss the previous week's progress and to be someone to talk to when experiments (or life) do not go according to the plan. Lastly, I am eternally grateful to Silvia for helping to shape the scientist I am today.

I would also like to acknowledge my former mentors Dr. Charles Kaspar and Dr. Amy Wong for giving me my first opportunity to conduct research and for putting up with

my scientific "growing pains." When I entered their labs, I had no formal research experience, but I was eager to learn and improve my skills as a scientist. They took a chance on me, and I hope that I have made them proud by nearing the completion of my doctoral degree. I would like to also thank them for training me in the areas of molecular biology, bacteriology, how to build figures, write manuscripts and protocols, and the basics of being a researcher. Most importantly, I would like to thank them for showing me how to organize primers, frozen strains, plasmids, and the curation of electronic data. These simple, yet critical, organizational techniques have been an integral part of my success during the preparation of this work by making me highly efficient and able to identify gaps in my research. Finally, I would also like to thank Chuck and Amy for helping shape the scientist I am today.

I would like to thank my committee members Drs. Vincent J. Starai, Robert J. Maier, Zhicheng Dou, and Boris Striepen (before he left UGA). I would like to thank Dr. Starai for training me on how to work with yeast and for the numerous plasmids or reagents I needed. I greatly appreciated your openness to talk about my project, for our numerous chats on science (or science fiction such as Dr. Who episodes), family life, and everything about yeast husbandry. I would also like to thank Dr. Starai for always volunteering to write a recommendation letter and always helping to advance my career in any way. I would like to thank Dr. Maier for allowing me to rotate in his lab, for providing valuable feedback on my project, and learning about his numerous fishing expeditions. I would like to thank Dr. Zhicheng Dou for driving from Clemson University to attend my committee meetings, for his suggestions and comments to strengthen my manuscripts, and for his willingness to write letters of support to further my career. I would also like to thank Dr.

Dou for his numerous collaborations on projects. I would like to thank Dr. Boris Striepen for his feedback during committee meetings and for providing numerous plasmids the tools for genetic modification of toxoplasma. I have greatly appreciated all of the suggestions and encouragement from my committee members over the years. They also helped advance my project and helped shape the scientist I am today.

Research does not occur in a vacuum, and I would like to thank all the current and former members of the Moreno and Docampo labs. I would like to thank all of them for their support, encouragement, advice, and friendship. You all have made my stay in the Moreno Lab most enjoyable. I would like to thank Dr. Nathan Chasen for first mentoring me on *T. gondii* maintenance, passaging, and basic genetic techniques, and for being someone to talk too about the plant-like vacuole—as we were *always* outnumbered by the calcium researchers. I would like to thank Dr. Andrea Myriam Hortua-Triana for always being extremely positive, providing copious amounts of encouragement, and being someone to speak with when an experiment did not go as planned. I will always cherish our hypothetical discussions on the solutions to fix all the ongoing problems in the world. I would like to thank Dr. Zhu-hong Li for being a wealth of knowledge on *T. gondii* and for his willingness to share it. I would like to thank Stephen Vella for his willingness to help acquire data with me, being someone to speak with in the calcium world, and for his seemingly endless connections to valuable plasmids or reagents from neighboring labs. I would like to thank Christina Moore for supplying the base structures I used on a few of my cartoons. I would like to thank Dr. Ciro Cordeiro for being a fantastic bench-mate, someone to give me new perspectives on my project, and for our scientific collaborations. Finally, I would like to thank Eric Dykes whom I mentored for over 2 years. I appreciated

his enthusiasm for science and his assistance in routine media making, mini-preps, and for being a reliable “parasite sitter” for my parasites when I was away from the lab. While mentoring Eric, I was able to vicariously relive the excitement when a PCR, western blot, or another major experiment was successful and provided meaningful data. While he has learned from me, I have learned much from mentoring him, and I will always cherish these memories. I have been blessed to have been trained by some of the best researchers throughout my training and it was an honor to pass on their legacy by training the next generation.

I would also like to thank Dr. Julie Nelson and Dr. Muthugapatti Kandasamy for their help with flow cytometry and microscopy, respectively. I would like to thank the Georgia Electron Microscopy lab for helping assist with my EM needs. I would like to thank Wandy Beatty for her help with immuno EM.

Lastly, I would like to thank all of my graduate friends who have made my experience in Athens worthwhile. I would like to thank Kawanda Foster and Emily Carpinonie for our game nights and dinner parties. I am very grateful for your friendship and memorable memories over the years.

TABLE OF CONTENTS

Page

LIST OF TABLES

Page

LIST OF FIGURES

Page

CHAPTER 1

INTRODUCTION

1.1 Introduction to the dissertation

The phylum Apicomplexa contains numerous human pathogens and members of this phylum are responsible of the death of millions of humans each year. One Apicomplexan parasite, *Toxoplasma gondii,* infects as much as one-third of the world's population, thus making it a highly successful parasite and a global burden. No effective human vaccines exist, and current treatments are only able to target certain life stages and have some side effects. The infected patients will remain infected for the remainder of their lives. Although most of the infected patients will suffer from little to no symptoms, death from this parasite is rare and occurs mostly in immunocompromised individuals. The US and various other countries have an increasing aging population, and this could lead to an increase in deaths from this parasite. Therefore, it is important to understand the biology and physiology of this parasite so that effective drug targets and effective treatments may one day be developed and used to treat or cure a toxoplasma infection.

In this work, I study an organelle which is termed the plant-like vacuole (PLV or the VAC). This organelle is unique because it contains proteins and functions similar to the vacuole found in plants. We believe that this organelle is important to the dissemination of the parasite and for its survival when it is briefly outside of the host cell. Before my work began, knockouts of a few proteins identified to associate with the PLV resulted in minor effects to the parasite lytic cycle. Until then, most of the PLV associated proteins

were considered dispensable or non-essential. Previous work suggested an important role of the proton gradient in the functions of this organelle and we decided to study the proton pump the vacuolar H^+ ATPase (V-ATPase). Proteomic analysis of a PLV fraction showed the presence of most of the subunits of the V-ATPase. The V-ATPase is an evolutionally conserved proton pump that performs dozens of functions in a typical eukaryote cell. My work focused on the V-ATPase and its importance to the PLV and the parasite. In this work I demonstrate that the V-ATPase is essential to the lytic cycle and important for ion and pH homeostasis. I believe understanding the role of the V-ATPase of *T. gondii* and its impact on the lytic cycle could one day lead to future drug targets and a better understanding of the physiology of this important pathogen. While humans have a V-ATPase as well, much evolution has occurred and the percent identity to the human subunits is low except in the conserved regions. It is possible that a drug could be used to target the parasite V-ATPase and leave the human V-ATPase unimpacted.

1.2 Structure of the dissertation

In this dissertation I focus on the characterization of the V-ATPase of *Toxoplasma gondii* and findings on its importance to the PLV. Chapter 2 presents a literature review of *Toxoplasma gondii* that include sections relevant to the work presented. This chapter covers much of the life cycle, lytic cycle, strains used, and major important organelles that are not present in the introductions found in the publications derived from this work. Chapter 3 is a literature review of the PLV. This chapter is the first consolidated literature review of the PLV and summarizes all the major findings of this organelle since its discovery in 2010. Chapter 4 is a literature review of the V-ATPase. Like chapter 2, this chapter includes more information that is not directly stated in the introductions found in

the publications derived from this work that would aid in the understanding of this dissertation. Chapter 5 begins to present the published work that was derived from this study. In this chapter I present the work on the characterization of the V-ATPase and the effects of a knockdown and demonstrate that the *a* subunit is a component of the V-ATPase complex. I demonstrate that the V-ATPase is present at the PLV, the plasma membrane, and immature rhoptries. I present evidence showing that the V-ATPase is important for all major steps of the lytic cycle, it creates the ionic environment that allows maturates to mature, which is important for the maturation of microneme and rhoptry proteins, and in addition it is important for pH homeostasis. For the first time, we demonstrate that the V-ATPase encircles immature rhoptries and postulate on the possible role in the acidification of immature rhoptries. Chapter 6 presents unpublished data on the impact of the V-ATPase interaction between pH and calcium homeostasis, and polyphosphate synthesis. In this chapter, I demonstrate that the V-ATPase is important for calcium entry, homeostasis, parasite egress, motility, and acidocalcisome normal functions. Chapter 7 presents a conclusion where my unanswered questions are posed for possible future study.

CHAPTER 2

LITERATURE REVIEW OF *TOXOPLASMA GONDII*

2.1 The discovery of *Toxoplasma gondii*

Dr. Charles Nicolle at the Pasteur Institute isolated a protozoan from the tissue of a rodent (*Ctenodactulus gundi*), which he originally thought to be *Leishmania* [1]. Later, the protozoan was identified as a new organism and termed based on its morphology; *Toxoplasma* ("toxo" meaning arc and "plasma" meaning life) and the host the parasite was discovered in, *gondii* [2]. In an odd twist of history, Dr. Nicolle incorrectly identified the Guinea pig host as "*Ctenodactylus gondi"* instead of *Ctenodactylus gundii,* and thus the parasite should have been named "*Toxoplasma gundii"* [2]. Consequently, *Toxoplasma gondii* was entered into the scientific lexicon. *Toxoplasma gondii* is a member of the Apicomplexan phylum of parasites that include notable species of *Plasmodium*, *Cryptosporidium*, *Babesia,* and *Cyclospora.* The vast majority of apicomplexans are unicellular and obligate intracellular parasites that share unique organelles which are used in invasion of a susceptible host.

2.2 Medical significance of *Toxoplasma gondii*

T. gondii infection in humans occurs through inadvertent consumption or contact with infected cat feces, undercooked meats, congenital transfer from mother to fetus, and in rare cases from organ transplantation (**Fig. 2.1**) [3-5]. In the United States, the seroprevalence of this infection is between 10% and 15% [6]. However, as many as 30-50% of the total human population are believed to be infected with *T. gondii,* making this

pathogen highly successful [7]. Another successful adaption of the parasite is its ability to invade nearly all nucleated cells [8].

A healthy immune system generally keeps the infection in check and infected individuals usually do not manifest symptoms. If symptoms do manifest, they are usually mild and include muscle aches and fever. In rare cases, immunocompetent individuals may suffer from ocular toxoplasmosis, a condition where the parasite replicates in the retina tissue and can lead to permanent blindness. In immunocompromised individuals and infants, symptoms are more severe and can include encephalitis, myocarditis, or pneumonitis [9-12]. Death from toxoplasmosis, the clinical term for a *T. gondii* infection, can occur in immunocompromised patients, especially those with AIDS [13]. During the 1980's AIDS epidemic, neurological toxoplasmosis cases and deaths from toxoplasma were significantly increased [14].

2.3 Treatment and prevention of *Toxoplasma gondii* infections

Treatment of toxoplasmosis usually includes pyrimethamine and sulfadiazine drugs, but these drugs only target the actively dividing parasites and often control rather than cure the infection [15]. Pyrimethamine inhibits the dihydrofolate reductase (DHFR) of *T. gondii* which prevents the regeneration of tetrahydrofolic acid, a metabolite essential for DNA and RNA synthesis in the parasite. Sulfadiazine drugs work by preventing folate synthesis. The parasite contains a unique organelle termed the apicoplast that contains a non-photosynthetic plastid remnant. Clindamycin, spiramycin, and azithromycin have been documented to treat toxoplasma infections successfully, but their target is not known but they are presumed target ribosome in the apicoplast [16-21]. Spiramycin can be

prescribed to control the infection of infected pregnant women due to its inability to cross the placenta [22].

Toxoplasmosis is considered a food borne disease and the best prevention strategy is to ensure all foods are fully cooked. Pregnant woman are advised to avoid cleaning up the cat litter box and wash their hands afterwards if they do clean up cat litter to prevent ingestion of oocysts [23]. The risk of ingestion of bradyzoites can be lessened by freezing meats, cooking meats to USDA guidelines, or gamma irradiating meats before consumption [24-26].

2.4 The life cycle of *Toxoplasma gondii*

The life cycle of *Toxoplasma gondii* is characterized by three main stages: oocytes, bradyzoites, and tachyzoites (**Fig. 2.1**). Felids are the definitive host for *Toxoplasma gondii* and become infected through carnivorism of infected prey. Once felids ingest the infected prey, *T. gondii* begins to differentiate into the merozoite stage where replication occurs in the felid gut enterocyte cells [27]. Merozoites differentiae into microgametocytes and macrogametocytes which are the sexual stages [27, 28]. After mating has occurred, the newly formed zygote matures and undergoes sporogony in cat feces [27, 28]. The oocysts can remain viable in the environment for years before they are ingested by an intermediate host [29-31]. The intermediate host, such as a mouse or a human, ingests oocysts through contaminated water or food. Once inside the new host, the oocysts differentiate into tachyzoites that disseminate the infection and are responsible for the acute form of the disease or differentiate into a cyst-forming bradyzoite that leads to the chronic infection.

The bradyzoite stage (**Fig. 2.1**), found during the chronic form of toxoplasmosis, is characterized as a slow replicating form of the parasite life cycle that is largely metabolically inactive [32]. Toxoplasma bradyzoites are typically found within tissue cysts in nervous, heart, and skeletal tissues [33-35]. Bradyzoites reside in a strong cyst wall that is able to survive the host stomach upon carnivorism of infected meats and allows the parasite to be transmitted clonally without undergoing the aforementioned sexual stage in felids [36, 37]. The conversion from tachyzoite to bradyzoite is not fully understood but stress appears to be a major contributor to the differentiation. Alkaline pH, heat shock, treatment with sodium arsenite, low CO_2 concentration, nitric oxide (NO) gas, atovaquone (a drug believed to target the parasite mitochondria), and nutrient starvation all have been reported to lead to bradyzoite formation [38-41]. There are no effective drugs against the bradyzoite stage, therefore the host is likely infected for life.

2.5 *Toxoplasma gondii* tachyzoites and the lytic cycle

Bradyzoites can differentiate into tachyzoites, which are responsible for the acute infection of the disease (**Fig. 2.1**). Tachyzoites are the fast replicating form of the parasite life cycle. The lytic cycle of *T. gondii* (**Fig. 2.2**) is linked to its pathogenesis as the parasites lyse the infected host cells to repeat the cycle. The lytic cycle begins with egress from the host cell, motility to another host cell, attachment/invasion of the host cell, and replication inside the host cell. *T. gondii* contain three major secretory organelles, micronemes, rhoptries, and dense granules. The parasite uses various SAGs to recognize and initiate host attachment [42]. Once invasion is initiated, the microneme organelle secretes microneme proteins (MICs) into the host cell. Shortly after the micronemes proteins are secreted, the parasite secretes rhoptry neck (RONs) proteins before secreting the remaining

rhoptry proteins (ROPs). RONs and apical membrane antigen (AMA1) work together to form a structure known as the moving junction [43]. The parasite uses its motor complex to move through the moving junction and pinches off from the plasma membrane to form the parasitophorous vacuole (PV) [44]. While the parasite is moving through the PV, host transmembrane proteins and proteins located in lipid rafts are stripped off, effectively removing much of the host membrane proteins [45]. Removal of host proteins from the PV membrane during invasion allows the PV to be nonfusogenic and avoid digestion by host lysosomal enzymes. Lastly, dense granule proteins are secreted to modify the PV to aid in the procurement of nutrients from the host [46].

Shortly after invasion, the parasite begins replicating (**Fig. 2.2**). *T. gondii* replicates by a process called endodyogeny, a form of asexual replication where the daughter cells grow inside the mother cell and consume the mother cell before separating [47]. The doubling time of *T. gondii* depends on the strain and host nutrient conditions but is generally accepted to be around 5-12 hours for a complete division cycle [48]. Tachyzoites replicate asexually and contain a haploid genome (1N). Replication of the parasites incudes S, G1, Mitosis, and cytokinesis, but the parasites appear to lack a G2 phase [48]. *T. gondii* parasites spend around 1.5 hours in S phase, where DNA is replicated [48]. Durnig S phase, there is a bimodal distribution of DNA where one population (cells in early to mid S phase) contain 1-1.7N and another population (late S Phase) 1.8N, suggesting that S phase slows or pauses at 1.8N [48]. During the late S phase (where the genome is 1.8N), budding of the Tachyzoite begins and the mitotic spindle starts to appear [49]. During this event the centrosomes are being doubled and the mitotic spindles are forming, while the parasite finishes DNA replication and the genome becomes 2N [49]. The parasite then

enters M phase which lasts 15-20 min [48]. At the beginning of the M phase, duplication of the centrosome and formation of the mitotic spindles are complete [50]. Chromosomes are attached to the mitotic spindles via microtubules and are eventually separated into the forming daughter cells [50]. The parasite then enters the Cytokinesis phase, which lasts less than 1 hr, and finishes budding off [48]. The first change in the tachyzoite G1 phase is a widening and doubling of the Golgi [51]. This event is followed by centriole duplication and leading into the S phase where the replication cycle continues [52].

About 36-48 hrs (or about 5-6 divisions) after infecting a host, the tachyzoites will egress from the host cell (**Fig. 2.2**). The exact mechanism of egress is not fully understood but the triggers appear to be decreasing pH in the PV, damage to the host cell leading to decreasing K^+ levels, increasing levels of abscisic acid, and calcium signaling [53-56]. Once the parasite is ready to egress, they secrete a Perforin-like protein (PLP1) that creates membrane pores that help rapidly permeabilize the PV and host membrane to help facilitate egress [57]. TgCDPK3 (a calcium dependent protein kinase) has also been shown to regulate microneme secretion and plays a role in calcium-dependent permeabilization of the parasitophorous vacuole membrane (PVM) [58, 59]. Activation of protein kinase G (PKG) has also been shown to play a role in egress [60]. Taken together, *T. gondii* egress appears to be a combination of physical changes to the PVM as well as complex signaling pathways that are trigged by changes in ion concentrations.

Once a parasite has egressed from its former host cell, the parasite must move, reorient, and attach and invade another host cell to complete the lytic cycle (Fig. 1.2). *T. gondii* has evolved a unique method of propelling itself. The machinery is collectively termed the glideosome, which uses the secretion of proteins that are actively translocated

towards the rear of the parasite to move. Gliding motility, the term to describe parasites actively moving, is important for the dissemination of the infection and propagation of the lytic cycle. *T. gondii* uses a complex group of proteins and machinery to move and invade host cells. The glidoesome is anchored to the underlying cytoskeleton called the inner membrane complex (IMC) which it uses for supporting movement. The IMC consists of flattened alveolar sacs located beneath the plasma membrane which are attached to the microtubule cytoskeleton and to filament like proteins termed the subpellicular network. The glideosome is composed of myosin A, glideosome-associated proteins (GAPs), myosin light chain (MLC1), actin, and microneme proteins that attach to the host or the surrounding surface [61-64]. To produce forward motion to propel the parasite to the next host cell, the parasite uses the myosin A motor complex to pull on the actin filaments to pull the parasites forward, while translocating the micronemes towards the posterior. The glideosome is activated either by binding calcium ions or through a secondary phosphorylation events that are controlled by the release of calcium ions [65].

2.6 *Toxoplasma gondii* strains

In North America, there are predominately three strains of *T. gondii* which are designated type I, II, and III [66]. These three types are considered clonal populations because they have minor genetic polymorphisms that must have emerged after a single genetic cross [67]. Each strain type differs in growth rate, virulence in mice (and humans), or the frequency of interconversion to tissue cysts. Type I strains are virulent in mice, replicate quickly, and have a lower rate of interconversion to the bradyzoite stage than the other types [8]. A commonly used laboratory strain of a type I is RH, which are the initials of a young boy who died from the infection, and was isolated from the boy's tissues in

1939 [68]. This became the first documented human case of infection isolated and was present in tissues from the cerebral cortex and spinal cord [68]. The majority of type I strains are lethal to mice with a single viable parasite [69]. Type I strains are more commonly associated with congenital and ocular toxoplasmosis [70]. Type II strains have higher mouse LD_{50}'s than type I, replicate slower, and readily form tissue cysts [8]. Type II strains are more commonly found in human isolates [8, 71]. In humans, type II strains are not as virulent as type I strains. Type III strains are similar to type II strains in that they replicate slower, have higher LD50s, and readily form cysts in intermediate hosts [8].

2.7 The RHΔ*ku80* TATi-1 strain

This work was conducted entirely using a Type I strain, RHΔ*ku80* TATi-1. This strain was chosen because the lytic cycle is most active, and it has been modified to allow for the study of conditional knockdowns of essential genes. The parental of RHΔ*ku80* TATi-1, is known as the RH strain. The RH strains are known to have a high frequency of non-homologous end joining (NHEJ) when transfected with DNA, making targeted gene disruptions or tagging more difficult. In mammalian cells, NHEJ is a complex process that repairs double stranded breaks and involves numerous proteins. Two proteins, Ku70 and Ku80, are important in binding to double stranded DNA breaks and facilitating NHEJ repair [72]. To increase the frequency of homologous recombination, the Ku80 gene *T. gondii* was knocked out to create the RHΔ*ku80* strain [73]. The deletion the Ku80 gene in this RH strain revolutionized the *Toxoplasma* community because it favored homologous recombination and allowed for increased targeted insertions or the ability to tag genes efficiently [73]. However, this strain still had the limitation that only non-essential genes

could be knocked out and that repair of DNA damage was reduced due to a deletion of Ku80.

In 2011, the study of conditional knockdowns was further advanced by the ability to insert a trans-activator trap identified (TATi) gene to create the RHΔ*ku80* TATi-1 strain [74]. This system works by inserting a tetracycline-inducible promoter and a constitutively expressed promoter (SAG4) upstream of the translational start codon of the gene of interest (GOI) (**Fig. 2.3A**) [74]. In the absence of anhydrotetracycline (ATc), this new promoter is constitutively expressed, and when ATc is added, the transcription of the GOI is significantly reduced (**Fig. 2.3B**). While the RHΔ*ku80* TATi-1 strain has been instrumental in allowing to understand the functions of essential genes, there are a few notable drawbacks to using this strain. First, the endogenous promoter is replaced with a constitutive promoter, which can cause expression of the gene at the wrong time in the cell cycle. Second, there is a chance of reversion where the addition of ATc has no effect on gene repression [75].

2.8 Important secretory organelles of *Toxoplasma gondii*

2.8.1 Micronemes

Micronemes are cigar shaped organelles that localize to the membrane periphery (**Fig. 2.4**) and secrete adhesive proteins termed MICs which play critical roles in invasion, egress, and parasite motility. In a typical toxoplasma cell, there can be 50-100 microneme organelles at the apical end. Currently there are at least 17 adhesion MICs and 6 proteins that associate or form complexes with the MICs [76]. MICs are transported through the endoplasmic reticulum (ER) to Golgi compartments and possibly through the trans-Golgi network (TGN) [77]. MICs are then transported from the Golgi/TGN to endosomal-like

compartments (ELCs) through which they are deposited to the microneme organelle by unknown mechanisms [77]. Some microneme proteins are constitutively secreted and other require some processing before secretion [78]. Constitutively expressed proteins typically lack sorting signals and are packaged into transport vesicles and secreted [78]. Those MICs that require additional processing are separated from the constitutively secreted MICs by forming aggregates at low pH and high calcium [79]. After aggregation, the sorting mechanism to the organelle remains unknown [77, 78].

Microneme secretion is a highly regulated process in *T. gondii*. A low potassium environment, such as when a host cell is ruptured, initiate parasite motility to begin the process of egress [56, 80, 81]. Parasite egress is characterized by increases in cytoplasmic calcium levels which have been demonstrated to lead to microneme secretion [56, 80, 81]. Micronemes secretion has been linked to increased levels of calcium as well as certain kinases [80, 81]. Chelation of intracellular calcium through BAPTA-AM has led to inhibited microneme secretion, supporting the role of calcium in microneme secretion [80]. The kinase inhibitors KT5926 and compound 1 have been reported to block microneme secretion [82-84]. Calcium dependent protein kinases (CDPKs) are kinases that become active in response to changes in calcium. When CDPK1 was ablated, calcium dependent microneme secretion was inhibited [85]. Cyclic GMP-dependent protein kinase (PKG), which phosphorylates a number of biologically important proteins, was found to be important for microneme secretion, gliding motility, and invasion [84]. Although a complex process, microneme secretion requires changes in calcium and certain kinase activity to secrete their contents.

MICs are secreted from the organelle to the parasite surface and are believed to attach to host cell receptors that include heparin sulfate proteoglycans, laminin, and ICAM-1 [78]. The parasite use MICs bound to the host cell receptors to create the moving junction which will ultimately lead to the parasite invading the cell. The parasite uses its actin-myosin motor to pull the parasite into the host cell and uses a rhomboid protease to cleave the MICs at the posterior end [86, 87].

One of the most abundant MICs in *T. gondii* is MIC2, which is constitutively expressed and forms a complex with M2AP [88]. M2AP requires a propeptide to be removed in order to secrete MIC2, although the propeptide is not required for M2AP folding or multimerization with MIC2 [78, 89, 90]. proM2AP is trafficked through the ELCs where it encounters compartments that aid in its maturation [90]. The MIC2-M2AP complex is important for gliding motility and invasion [89].

2.8.2 Rhoptries

Mature rhoptries are club shaped organelles that secrete ROPs that are secreted during invasion (**Fig. 2.4**). Mature rhoptries have a bulbous base and a neck that extends to the apical end of the parasite. Immature rhoptries are circular vesicles that allow for the maturation of rhoptry proteins. A typical *T. gondii* parasite can contain 6-12 mature rhoptries with each containing a distinct neck and bulb region [76]. Rhoptry proteins that localize to the neck are designated RON's and proteins that localize to the rhoptry bulb are designated ROP's. Although RONs and ROPs segregate to different sections of the rhoptry, there is no formal membrane that compartmentalizes these proteins [91]. Rhoptry proteins are believed to be trafficked through the ER, TGN, and through the ELCs to eventually end up in the mature organelle [77].

The biogenesis of rhoptries is poorly understood. What is known is that a vesicle that is destined to become the immature rhoptry buds from the trans-Golgi in a daughter tachyzoite. While this mechanism is unknown, dynamin related protein B (DrpB) and the sortilin-like receptor (TgSORTLR) have been postulated to play a role [92, 93]. How rhoptry proteins enter this immature rhoptry is not known, but the AP-1 clathrin adaptor component Tgμ1, TgSORTLR, vacuolar protein sorting (VPS) protein 9 (Vps9), and the retromer complex (Vps35, Vps26, and Vps29) are implicated in the biogenesis [93-96]. TgSORTLR appears to be able to guide rhoptry proteins through the immature rhoptries to then release its cargo, but how it recognizes different cargo is unknown [93]. Some rhoptry neck proteins, RON9 and RON10, have been shown to form a complex which is required for proper sorting of both proteins to the immature rhoptries [97]. Because rhoptry proteins initially occupy the same compartments as microneme proteins, it has been postulated that rhoptry proteins have distinct sorting receptors that direct them to their correct localization [77]. After pro-rhoptry proteins have successfully trafficked to the immature rhoptry, the pH of the immature rhoptry drops to pH 3.5-5.5 [98]. Until recently the acidification mechanism was a complete mystery. The vacuolar H^+ ATPase (V-ATPase) was recently demonstrated to surround the immature rhoptry membrane and likely be responsible for the acidification [99]. V-ATPase depletion resulted in numerous defects in the maturation of ROPs as well as rhoptry proteases that are known to mature ROPs [99]. Many of the rhoptry proteins are synthesized with a propeptide that is cleaved before secretion. In the acidic immature rhoptry, various proteases reside which are maturated and/or active and facilitate the maturation of rhoptry proteins [99-101]. Maturation of rhoptries is accompanied by increase in luminal pH and change in the morphology of the rhoptry,

which becomes bulbous and its neck elongated. A $Na+/H^+$ exchanger was associated with rhoptries and in combination with the V-ATPase, could be responsible for the changes in pH [99, 102]. The mechanism for organelle maturation is unknown but in V-ATPase knockdowns, the rhoptries fail to mature [99]. Thus, pH changes or the V-ATPase complex itself could be involved in rhoptry organelle maturation.

The processing of ROPs and RONs are generally proteolytically cleaved during transit [76]. Similar to micronemes, various proteases are likely responsible for rhoptry protein maturation. It was previously reported that a rhoptry localized subtilisin-like serine protease, TgSUB2, was involved in the maturation of ROP proteins [103]. Co-immunoprecipitates of TgSUB2 routinely pull down ROP1, ROP2, and ROP4, suggesting that these may be the target of this protease [103]. However, ablation of TgSUB2 resulted in no significant ROP maturation defects [100]. Recently, aspartic protease 3 (TgASP3) was determined to play a major role in the maturation of ROPs [100]. ASP3 was localized to the immature rhoptries and pH is likely required for ASP3 maturation and activity [99]. Most ROPs contain a signal peptide, a single transmembrane domain (TM) or a GPI anchor [76]. ROPs that do not contain a TM or GPI generally use myristylation and/or palmitoylation to achieve anchoring to the membrane [104]. To date, there are 26 ROPs, 9 RONs, and 7 rhoptry bulb associate proteins [76]. Some ROPs make their way to the host nucleolus and are able to regulate various host genes. ROP16 was identified as being able to down regulate host proinflammatory cytokine signaling and upregulate arginase-1 synthesis [105-107].

A few rhoptry neck proteins have been reported to play a role in the moving junction during parasite invasion. RON2, RON4, RON5, and RON8 form a complex that

is directly associated with the moving junction [108]. It is not known how RON2, RON4, RON5, and RON8 are matured.

The mechanism of how rhoptry proteins secrete their contents is not known. The potent actin inhibitor of actin polymerization cytochalasin D has been reported to allow parasites to discharge their contents, but prevents parasite invasion [109]. Because rhoptry proteins are discharged shortly after microneme proteins are secreted, proper attachment to the host may be required for proper rhoptry discharge. This was demonstrated by ablation of microneme proteins AMA1 and MIC8 that resulted in reduced rhoptry discharge [110, 111]. Although rhoptry proteins are secreted during the PV formation and associated with the PVM, there is no direct evidence that rhoptry proteins play a role in the formation of the PV [76].

2.8.3 Dense granules

The final secretory pathway that parasite uses are secretion of dense granules. Much less is known about dense granules than compared to micronemes and rhoptries. In electron microscopy, dense granules are electron dense vesicles (about 200 nm in diameter) that are secreted long after micronemes and rhoptries have discharged and play a major role in shaping the PV for the parasite (**Fig. 2.4**). The number of these organelles varies in each parasite, but up to 15 have been observed in the parasite [76]. Dense granule proteins are designated as GRAs and generally all have an N-Terminal hydrophobic sequence. It is not known if dense granules undergo a maturation process as seen with rhoptries. Dense granules have been postulated to be the default secretory pathway as many genetically modified proteins can end up being secreted through the dense granules [112].

The secretion of dense granules is not fully understood. Some GRA proteins like GRA1 are constitutively expressed and others appear to be secreted shortly after microneme and rhoptry discharge [99]. Unlike micronemes, increases in intracellular calcium do not trigger release of dense granules [113]. There is evidence that suggests that release of dense granules is highly regulated, but the mechanism for this regulated secretion remains unknown [114].

2.9 References

1. Nicolle, C. and L.H. Manceaux, *On a leishman body infection (or related organisms) of the gondi.* Comptes Rendus Hebdomadaires Des Seances De L Academie Des Sciences, 1908. **147**(1): p. 763-766.
2. Nicolle C and M. L, *The new protozoan of Gondi.* . Comptes Rendus Hebdomadaires Des Seances De L Academie Des Sciences 1909. **148**: p. 369-372.
3. Dunn, D., et al., *Mother-to-child transmission of toxoplasmosis: risk estimates for clinical counselling.* The Lancet, 1999. **353**(9167): p. 1829-1833.
4. Hill, D. and J.P. Dubey, *Toxoplasma gondii: transmission, diagnosis and prevention.* Clinical Microbiology and Infection, 2002. **8**(10): p. 634-640.
5. Miltgen, G., et al., *Fatal acute respiratory distress by Toxoplasma gondii in a toxoplasma seronegative liver transplant recipient.* Microbiologica -Bologna-, 2016. **39**(2): p. 160-2.
6. Jones, J.L., et al., *Toxoplasma gondii Seroprevalence in the United States 2009–2010 and Comparison with the Past Two Decades.* The American Journal of Tropical Medicine and Hygiene, 2014. **90**(6): p. 1135-1139.
7. Flegr, J., et al., *Toxoplasmosis – A Global Threat. Correlation of Latent Toxoplasmosis with Specific Disease Burden in a Set of 88 Countries.* PLoS ONE, 2014. **9**(3): p. e90203.
8. Dubey, J.P., *Chapter 1 - The History and Life Cycle of Toxoplasma gondii*, in *Toxoplasma Gondii (Second Edition)*. 2014, Academic Press: Boston. p. 1-17.
9. Michel, G., et al., *Lung toxoplasmosis after HLA mismatched bone marrow transplantation.* Bone marrow transplantation, 1994. **14**(3): p. 455-457.

10. Sahasrabudhe, N.S., et al., *Pathology of Toxoplasma myocarditis in acquired immunodeficiency syndrome.* Indian journal of pathology & microbiology, 2003. **46**(4): p. 649-651.

11. Shanks, G.D., R.R. Redfield, and G.W. Fischer, *Toxoplasma Encephalitis In An Infant With Acquired Immunodeficiency Syndrome.* The Pediatric Infectious Disease Journal, 1987. **6**(1): p. 70.

12. Luft, B.J. and J.S. Remington, *Toxoplasmic Encephalitis in AIDS.* Clinical Infectious Diseases, 1992. **15**(2): p. 211-222.

13. Coelho, L., et al., *Trends in overall opportunistic illnesses, Pneumocystis carinii pneumonia, cerebral toxoplasmosis and Mycobacterium avium complex incidence rates over the 30 years of the HIV epidemic: a systematic review.* Braz J Infect Dis, 2014. **18**(2): p. 196-210.

14. Luft, B., et al., *Outbreak Of Central-Nervous-System Toxoplasmosis In Western Europe And North America.* The Lancet, 1983. **321**(8328): p. 781-784.

15. Leport, C., et al., *Treatment of central nervous system toxoplasmosis with pyrimethamine/sulfadiazine combination in 35 patients with the acquired immunodeficiency syndrome.* The American Journal of Medicine, 1988. **84**(1): p. 94-100.

16. Araujo, F.G., R.M. Shepard, and J.S. Remington, *In vivo activity of the macrolide antibiotics azithromycin, roxithromycin and spiramycin against Toxoplasma gondii.* European Journal of Clinical Microbiology and Infectious Diseases, 1991. **10**(6): p. 519-524.

17. Dannemann, B., et al., *Treatment of toxoplasmic encephalitis in patients with aids: A randomized trial comparing pyrimethamine plus clindamycin to pyrimethamine plus sulfadiazine.* Annals of Internal Medicine, 1992. **116**(1): p. 33-43.

18. Fichera, M.E., M.K. Bhopale, and D.S. Roos, *In vitro assays elucidate peculiar kinetics of clindamycin action against Toxoplasma gondii.* Antimicrobial Agents and Chemotherapy, 1995. **39**(7): p. 1530-7.

19. Beckers, C.J., et al., *Inhibition of cytoplasmic and organellar protein synthesis in Toxoplasma gondii. Implications for the target of macrolide antibiotics.* The Journal of Clinical Investigation, 1995. **95**(1): p. 367-376.

20. Pfefferkorn, E.R., R.F. Nothnagel, and S.E. Borotz, *Parasiticidal effect of clindamycin on Toxoplasma gondii grown in cultured cells and selection of a drug-resistant mutant.* Antimicrobial Agents and Chemotherapy, 1992. **36**(5): p. 1091-1096.

21. Fichera, M.E. and D.S. Roos, *A plastid organelle as a drug target in apicomplexan parasites.* Nature, 1997. **390**: p. 407.

22. Desmonts, G. and J. Couvreur, *Toxoplasmosis in pregnancy and its transmission to the fetus.* Bulletin of the New York Academy of Medicine, 1974. **50**(2): p. 146-159.

23. Frenkel, J.K. and J.P. Dubey, *Toxoplasmosis and Its Prevention in Cats and Man.* The Journal of Infectious Diseases, 1972. **126**(6): p. 664-673.

24. Kotula, A.W., et al., *Effect of Freezing on Infectivity of Toxoplasma Gondii Tissue Cysts in Pork.* Journal of Food Protection, 1991. **54**(9): p. 687-690.

25. Dubey, J.P., et al., *Effect of High Temperature on Infectivity of Toxoplasma gondii Tissue Cysts in Pork.* The Journal of Parasitology, 1990. **76**(2): p. 201-204.

26. Dubey, J.P., et al., *Effect of gamma irradiation on unsporulated and sporulated Toxoplasma gondii oocysts.* International Journal for Parasitology, 1998. **28**(3): p. 369-375.

27. Ferguson, D.J.P., *Use of molecular and ultrastructural markers to evaluate stage conversion of Toxoplasma gondii in both the intermediate and definitive host.* International Journal for Parasitology, 2004. **34**(3): p. 347-360.

28. Hutchison, W.M., et al., *The life cycle of the coccidian parasite, Toxoplasma gondii, in the domestic cat.* Transactions of the Royal Society of Tropical Medicine and Hygiene, 1971. **65**(3): p. 380-398.

29. Dubey, J.P., *Toxoplasma gondii oocyst survival under defined temperatures.* The Journal of parasitology, 1998. **84**(4): p. 862-865.

30. Frenkel, J.K., A. Ruiz, and M. Chinchilla, *Soil Survival of Toxoplasma Oocysts in Kansas and Costa Rica*.* The American Journal of Tropical Medicine and Hygiene, 1975. **24**(3): p. 439-443.

31. Yilmaz, S.M. and S.H. Hopkins, *Effects of different conditions on duration of infectivity of Toxoplasma gondii oocysts.* J Parasitol, 1972. **58**(5): p. 938-9.

32. Denton, H., et al., *Enzymes of energy metabolism in the bradyzoites and tachyzoites of Toxoplasma gondii.* FEMS microbiology letters, 1996. **137**(1): p. 103-108.

33. Dubey, J.P., P. Thulliez, and E.C. Powell, *Toxoplasma gondii in Iowa sows: comparison of antibody titers to isolation of T. gondii by bioassays in mice and cats.* J Parasitol, 1995. **81**(1): p. 48-53.

34. Guimaraes, E.V., L. de Carvalho, and H.S. Barbosa, *Primary culture of skeletal muscle cells as a model for studies of Toxoplasma gondii cystogenesis.* J Parasitol, 2008. **94**(1): p. 72-83.

35. Hermes, G., et al., *Neurological and behavioral abnormalities, ventricular dilatation, altered cellular functions, inflammation, and neuronal injury in brains of mice due to common, persistent, parasitic infection.* J Neuroinflammation, 2008. **5**: p. 48.

36. Jacobs, L., J.S. Remington, and M.L. Melton, *The Resistance of the Encysted Form of Toxoplasma gondii.* The Journal of Parasitology, 1960. **46**(1): p. 11-21.

37. Zhang, Y.W., et al., *Initial characterization of CST1, a Toxoplasma gondii cyst wall glycoprotein.* Infection and immunity, 2001. **69**(1): p. 501-507.

38. Bohne, W., J. Heesemann, and U. Gross, *Reduced replication of Toxoplasma gondii is necessary for induction of bradyzoite-specific antigens: a possible role for nitric oxide in triggering stage conversion.* Infection and Immunity, 1994. **62**(5): p. 1761-1767.

39. Ihara, F. and Y. Nishikawa, *Starvation of low-density lipoprotein-derived cholesterol induces bradyzoite conversion in Toxoplasma gondii.* Parasites & Vectors, 2014. **7**(1): p. 248.

40. Soete, M., D. Camus, and J.F. Dubrametz, *Experimental Induction of Bradyzoite-Specific Antigen Expression and Cyst Formation by the RH Strain of Toxoplasma gondii in Vitro.* Experimental Parasitology, 1994. **78**(4): p. 361-370.

41. Tomavo, S. and J.C. Boothroyd, *Interconnection between organellar functions, development and drug resistance in the protozoan parasite, Toxoplasma gondii.* International Journal for Parasitology, 1995. **25**(11): p. 1293-1299.

42. Dzierszinski, F., et al., *Targeted disruption of the glycosylphosphatidylinositol-anchored surface antigen SAG3 gene in Toxoplasma gondii decreases host cell adhesion and drastically reduces virulence in mice.* Molecular Microbiology, 2000. **37**(3): p. 574-582.

43. Lamarque, M., et al., *The RON2-AMA1 Interaction is a Critical Step in Moving Junction-Dependent Invasion by Apicomplexan Parasites.* PLOS Pathogens, 2011. **7**(2): p. e1001276.

44. Egarter, S., et al., *The Toxoplasma Acto-MyoA Motor Complex Is Important but Not Essential for Gliding Motility and Host Cell Invasion.* PLOS ONE, 2014. **9**(3): p. e91819.

45. Mordue, D.G., et al., *Invasion by Toxoplasma gondii Establishes a Moving Junction That Selectively Excludes Host Cell Plasma Membrane Proteins on the Basis of Their Membrane Anchoring.* The Journal of Experimental Medicine, 1999. **190**(12): p. 1783.

46. Gold, Daniel A., et al., *The Toxoplasma Dense Granule Proteins GRA17 and GRA23 Mediate the Movement of Small Molecules between the Host and the Parasitophorous Vacuole.* Cell Host & Microbe, 2015. **17**(5): p. 642-652.

47. Francia, M.E. and B. Striepen, *Cell division in apicomplexan parasites.* Nature Reviews Microbiology, 2014. **12**: p. 125.

48. Radke, J.R., et al., *Defining the cell cycle for the tachyzoite stage of Toxoplasma gondii.* Molecular and Biochemical Parasitology, 2001. **115**(2): p. 165-175.

49. Gubbels, M.-J., M. White, and T. Szatanek, *The cell cycle and Toxoplasma gondii cell division: Tightly knit or loosely stitched?* International Journal for Parasitology, 2008. **38**(12): p. 1343-1358.

50. Gubbels, M.-J., et al., *A MORN-repeat protein is a dynamic component of the Toxoplasma gondii cell division apparatus.* Journal of Cell Science, 2006. **119**(11): p. 2236.

51. Pelletier, L., et al., *Golgi biogenesis in Toxoplasma gondii.* Nature, 2002. **418**: p. 548.

52. White, M.W., et al., *Genetic rescue of a Toxoplasma gondii conditional cell cycle mutant.* Molecular Microbiology, 2005. **55**(4): p. 1060-1071.

53. Borges-Pereira, L., et al., *Calcium Signaling throughout the Toxoplasma gondii Lytic Cycle: A STUDY USING GENETICALLY ENCODED CALCIUM INDICATORS.* Journal of Biological Chemistry, 2015. **290**(45): p. 26914-26926.

54. Nagamune, K., et al., *Abscisic acid controls calcium-dependent egress and development in Toxoplasma gondii.* Nature, 2008. **451**: p. 207.

55. Roiko, M.S., N. Svezhova, and V.B. Carruthers, *Acidification Activates Toxoplasma gondii Motility and Egress by Enhancing Protein Secretion and Cytolytic Activity.* PLOS Pathogens, 2014. **10**(11): p. e1004488.

56. Moudy, R., T.J. Manning, and C.J. Beckers, *The Loss of Cytoplasmic Potassium upon Host Cell Breakdown Triggers Egress of Toxoplasma gondii.* Journal of Biological Chemistry, 2001. **276**(44): p. 41492-41501.

57. Kafsack, B.F.C., et al., *Rapid Membrane Disruption by a Perforin-Like Protein Facilitates Parasite Exit from Host Cells.* Science, 2009. **323**(5913): p. 530-533.

58. McCoy, J.M., et al., *TgCDPK3 Regulates Calcium-Dependent Egress of Toxoplasma gondii from Host Cells.* PLOS Pathogens, 2012. **8**(12): p. e1003066.

59. Garrison, E., et al., *A Forward Genetic Screen Reveals that Calcium-dependent Protein Kinase 3 Regulates Egress in Toxoplasma.* PLOS Pathogens, 2012. **8**(11): p. e1003049.

60. Lourido, S., K. Tang, and L.D. Sibley, *Distinct signalling pathways control Toxoplasma egress and host-cell invasion.* The EMBO Journal, 2012. **31**(24): p. 4524.

61. Herm-Gotz, A., et al., *Toxoplasma gondii myosin A and its light chain: a fast, single-headed, plus-end-directed motor.* The EMBO Journal, 2002. **21**(9): p. 2149.

62. Gaskins, E., et al., *Identification of the membrane receptor of a class XIV myosin in Toxoplasma gondii.* The Journal of Cell Biology, 2004. **165**(3): p. 383.

63. Meissner, M., D. Schlüter, and D. Soldati, *Role of Toxoplasma gondii Myosin A in Powering Parasite Gliding and Host Cell Invasion.* Science, 2002. **298**(5594): p. 837.

64. Huynh, M.-H. and V.B. Carruthers, *Toxoplasma MIC2 Is a Major Determinant of Invasion and Virulence.* PLOS Pathogens, 2006. **2**(8): p. e84.

65. Nebl, T., et al., *Quantitative in vivo Analyses Reveal Calcium-dependent Phosphorylation Sites and Identifies a Novel Component of the Toxoplasma Invasion Motor Complex.* PLOS Pathogens, 2011. **7**(9): p. e1002222.

66. Howe, D.K. and L.D. Sibley, *Toxoplasma gondii Comprises Three Clonal Lineages: Correlation of Parasite Genotype with Human Disease.* The Journal of Infectious Diseases, 1995. **172**(6): p. 1561-1566.

67. Su, C., et al., *Recent Expansion of Toxoplasma Through Enhanced Oral Transmission.* Science, 2003. **299**(5605): p. 414-416.

68. Sabin, A.B., *Toxoplasmic encephalitis in children.* Journal of the American Medical Association, 1941. **116**(9): p. 801-807.

69. Howe, D.K., B.C. Summers, and L.D. Sibley, *Acute virulence in mice is associated with markers on chromosome VIII in Toxoplasma gondii.* Infection and Immunity, 1996. **64**(12): p. 5193-8.

70. McLeod, R., et al., *Chapter 4 - Human Toxoplasma Infection*, in *Toxoplasma Gondii (Second Edition)*. 2014, Academic Press: Boston. p. 99-159.

71. Howe, D.K., et al., *Determination of genotypes of Toxoplasma gondii strains isolated from patients with toxoplasmosis.* Journal of Clinical Microbiology, 1997. **35**(6): p. 1411-4.

72. Yoo, S., A. Kimzey, and W.S. Dynan, *Photocross-linking of an Oriented DNA Repair Complex: Ku BOUND AT A SINGLE DNA END.* Journal of Biological Chemistry, 1999. **274**(28): p. 20034-20039.

73. Huynh, M.-H. and V.B. Carruthers, *Tagging of Endogenous Genes in a Toxoplasma gondii Strain Lacking Ku80.* Eukaryotic Cell, 2009. **8**(4): p. 530-539.

74. Sheiner, L., et al., *A Systematic Screen to Discover and Analyze Apicoplast Proteins Identifies a Conserved and Essential Protein Import Factor.* PLOS Pathogens, 2011. **7**(12): p. e1002392.

75. JimÉNez-Ruiz, E., et al., *Advantages and disadvantages of conditional systems for characterization of essential genes in Toxoplasma gondii.* Parasitology, 2014. **141**(11): p. 1390-1398.

76. Lebrun, M., V.B. Carruthers, and M.-F. Cesbron-Delauw, *Chapter 12 - Toxoplasma Secretory Proteins and Their Roles in Cell Invasion and Intracellular Survival*, in *Toxoplasma Gondii (Second Edition)*. 2014, Academic Press: Boston. p. 389-453.

77. McGovern, O.L., et al., *Intersection of Endocytic and Exocytic Systems in Toxoplasma gondii.* Traffic, 2018: p. 336–353.

78. Huynh, M.-H., J.M. Harper, and V.B. Carruthers, *Preparing for an invasion: charting the pathway of adhesion proteins to Toxoplasma micronemes.* Parasitology Research, 2006. **98**(5): p. 389-395.

79. Chanat, E. and W.B. Huttner, *Milieu-induced, selective aggregation of regulated secretory proteins in the trans-Golgi network.* The Journal of Cell Biology, 1991. **115**(6): p. 1505.

80. B., C.V. and S.L. David, *Mobilization of intracellular calcium stimulates microneme discharge in Toxoplasma gondii.* Molecular Microbiology, 1999. **31**(2): p. 421-428.

81. Carruthers, V.B., S.N.J. Moreno, and D.L. Sibley, *Ethanol and acetaldehyde elevate intracellular [Ca2+] and stimulate microneme discharge in Toxoplasma gondii.* Biochemical Journal, 1999. **342**(2): p. 379.

82. M., D.J., C.V. B., and S.L. David, *Participation of myosin in gliding motility and host cell invasion by Toxoplasma gondii.* Molecular Microbiology, 1997. **26**(1): p. 163-173.

83. Kieschnick, H., et al., *Toxoplasma gondii Attachment to Host Cells Is Regulated by a Calmodulin-like Domain Protein Kinase.* Journal of Biological Chemistry, 2001. **276**(15): p. 12369-12377.

84. Wiersma, H.I., et al., *A role for coccidian cGMP-dependent protein kinase in motility and invasion.* International Journal for Parasitology, 2004. **34**(3): p. 369-380.

85. Lourido, S., et al., *Calcium-dependent protein kinase 1 is an essential regulator of exocytosis in Toxoplasma.* Nature, 2010. **465**: p. 359.

86. Brossier, F., et al., *A spatially localized rhomboid protease cleaves cell surface adhesins essential for invasion by Toxoplasma.* Proceedings of the National Academy of Sciences of the United States of America, 2005. **102**(11): p. 4146.

87. Dowse, T.J., et al., *Apicomplexan rhomboids have a potential role in microneme protein cleavage during host cell invasion.* International Journal for Parasitology, 2005. **35**(7): p. 747-756.

88. Jewett, T.J. and L.D. Sibley, *The Toxoplasma Proteins MIC2 and M2AP Form a Hexameric Complex Necessary for Intracellular Survival.* Journal of Biological Chemistry, 2004. **279**(10): p. 9362-9369.

89. Huynh, M.H., et al., *Rapid invasion of host cells by Toxoplasma requires secretion of the MIC2–M2AP adhesive protein complex.* The EMBO Journal, 2003. **22**(9): p. 2082.

90. Harper, J.M., et al., *A Cleavable Propeptide Influences Toxoplasma Infection by Facilitating the Trafficking and Secretion of the TgMIC2–M2AP Invasion Complex.* Molecular Biology of the Cell, 2006. **17**(10): p. 4551-4563.

91. Roger, N., et al., *Characterization of a 225 kilodalton rhoptry protein of Plasmodium falciparum.* Molecular and Biochemical Parasitology, 1988. **27**(2): p. 135-141.

92. Breinich, M.S., et al., *A Dynamin Is Required for the Biogenesis of Secretory Organelles in Toxoplasma gondii.* Current Biology, 2009. **19**(4): p. 277-286.

93. Sloves, P.-J., et al., *Toxoplasma Sortilin-like Receptor Regulates Protein Transport and Is Essential for Apical Secretory Organelle Biogenesis and Host Infection.* Cell Host & Microbe, 2012. **11**(5): p. 515-527.

94. Ngô, H.M., et al., *AP-1 in Toxoplasma gondii Mediates Biogenesis of the Rhoptry Secretory Organelle from a Post-Golgi Compartment.* Journal of Biological Chemistry, 2003. **278**(7): p. 5343-5352.

95. Sangaré, L.O., et al., *Unconventional endosome-like compartment and retromer complex in Toxoplasma gondii govern parasite integrity and host infection.* Nature Communications, 2016. **7**: p. 11191.

96. Sakura, T., et al., *A Critical Role for Toxoplasma gondii Vacuolar Protein Sorting VPS9 in Secretory Organelle Biogenesis and Host Infection.* Scientific Reports, 2016. **6**: p. 38842.

97. Lamarque, M.H., et al., *Identification of a New Rhoptry Neck Complex RON9/RON10 in the Apicomplexa Parasite Toxoplasma gondii.* PLOS ONE, 2012. **7**(3): p. e32457.

98. Shaw, M.K., D.S. Roos, and L.G. Tilney, *Acidic compartments and rhoptry formation in Toxoplasma gondii.* Parasitology, 1998. **117**(5): p. 435-443.

99. Stasic, A.J., et al., *The Toxoplasma Vacuolar H^+-ATPase regulates intracellular pH, and impacts the maturation of essential secretory proteins.* Cell Reports, 2019.

100. Dogga, S.K., et al., *A druggable secretory protein maturase of Toxoplasma essential for invasion and egress.* eLife, 2017. **6**: p. e27480.

101. E., H.B., et al., *Molecular Dissection of Novel Trafficking and Processing of the Toxoplasma gondii Rhoptry Metalloprotease Toxolysin-1.* Traffic, 2012. **13**(2): p. 292-304.

102. Karasov, A.O., J.C. Boothroyd, and G. Arrizabalaga, *Identification and disruption of a rhoptry-localized homologue of sodium hydrogen exchangers in Toxoplasma gondii.* International Journal for Parasitology, 2005. **35**(3): p. 285-291.

103. Miller, S.A., et al., *TgSUB2 is a Toxoplasma gondii rhoptry organelle processing proteinase.* Molecular Microbiology, 2003. **49**(4): p. 883-894.

104. Cabrera, A., et al., *Dissection of Minimal Sequence Requirements for Rhoptry Membrane Targeting in the Malaria Parasite.* Traffic, 2012. **13**(10): p. 1335-1350.

105. Yamamoto, M., et al., *A single polymorphic amino acid on Toxoplasma gondii kinase ROP16 determines the direct and strain-specific activation of Stat3.* The Journal of Experimental Medicine, 2009. **206**(12): p. 2747-2760.

106. Ong, Y.-C., M.L. Reese, and J.C. Boothroyd, *Toxoplasma Rhoptry Protein 16 (ROP16) Subverts Host Function by Direct Tyrosine Phosphorylation of STAT6.* Journal of Biological Chemistry, 2010. **285**(37): p. 28731-28740.

107. Butcher, B.A., et al., *Toxoplasma gondii Rhoptry Kinase ROP16 Activates STAT3 and STAT6 Resulting in Cytokine Inhibition and Arginase-1-Dependent Growth Control.* PLOS Pathogens, 2011. **7**(9): p. e1002236.

108. Besteiro, S., et al., *Export of a Toxoplasma gondii Rhoptry Neck Protein Complex at the Host Cell Membrane to Form the Moving Junction during Invasion.* PLOS Pathogens, 2009. **5**(2): p. e1000309.

109. Chasen, N.M., et al., *A Glycosylphosphatidylinositol-Anchored Carbonic Anhydrase-Related Protein of Toxoplasma gondii Is Important for Rhoptry Biogenesis and Virulence.* mSphere, 2017. **2**(3).

110. Mital, J., et al., *Conditional Expression of Toxoplasma gondii Apical Membrane Antigen-1 (TgAMA1) Demonstrates That TgAMA1 Plays a Critical Role in Host Cell Invasion.* Molecular Biology of the Cell, 2005. **16**(9): p. 4341-4349.

111. Kessler, H., et al., *Microneme protein 8 – a new essential invasion factor in Toxoplasma gondii.* Journal of Cell Science, 2008. **121**(7): p. 947.

112. Striepen, B., et al., *Targeting of soluble proteins to the rhoptries and micronemes in Toxoplasma gondii.* Molecular and Biochemical Parasitology, 2001. **113**(1): p. 45-53.

113. Chaturvedi, S., et al., *Constitutive Calcium-independent Release of Toxoplasma gondii Dense Granules Occurs through the NSF/SNAP/SNARE/Rab Machinery.* Journal of Biological Chemistry, 1999. **274**(4): p. 2424-2431.

114. Dubremetz, J.F., et al., *Kinetics and pattern of organelle exocytosis duringToxoplasma gondii/host-cell interaction.* Parasitology Research, 1993. **79**(5): p. 402-408.

FIGURES

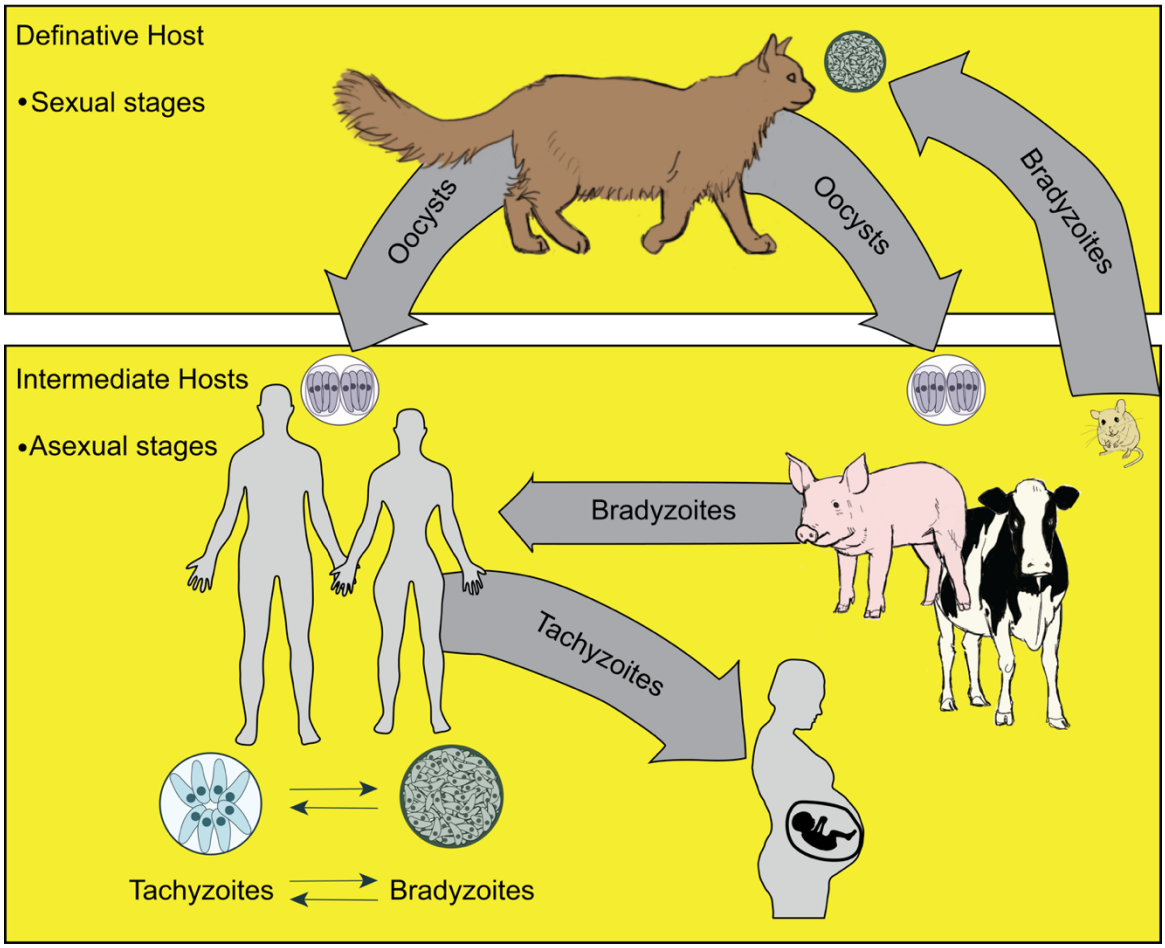

Figure 2.1. The life cycle of *Toxoplasma gondii.* The definitive host is the cat which becomes infected through carnivorism of infected prey. The cat sheds oocysts which infect the intermediate hosts. In rare cases, the *T. gondii* infection can be congenital and spread to the growing fetus.

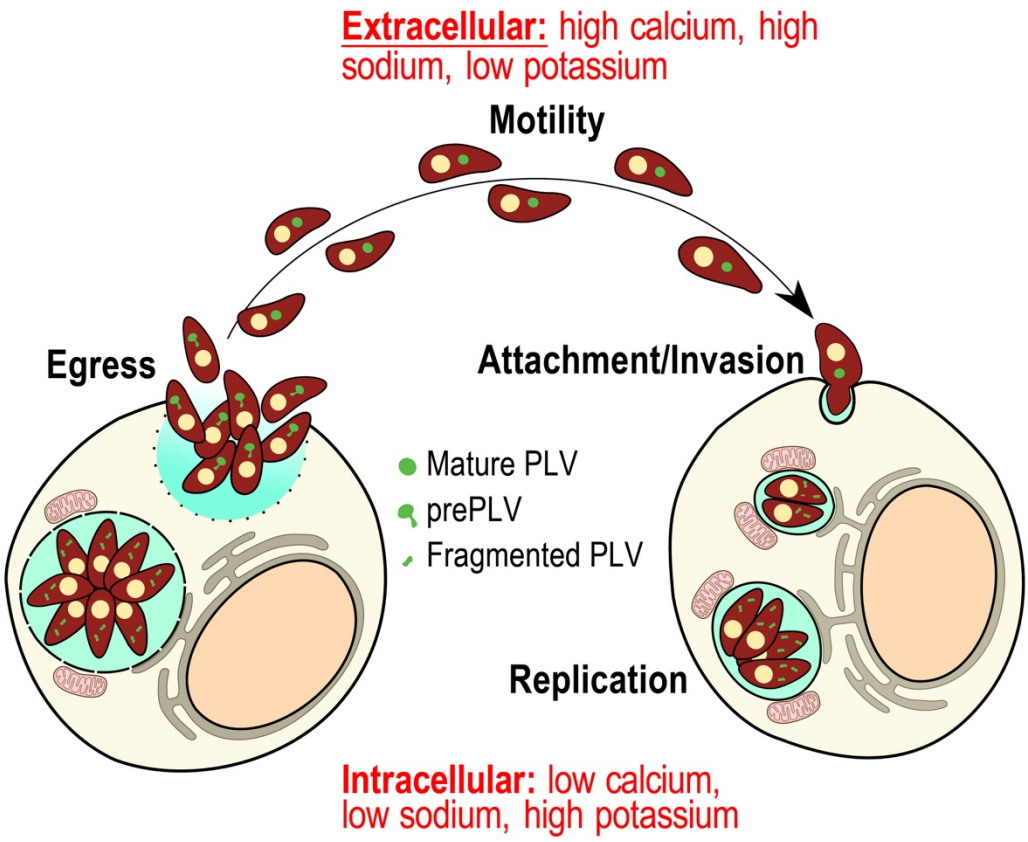

Figure 2.2. The lytic cycle of *Toxoplasma gondii*. The lytic cycle is characterized by egress from the host, motility, attachment/invasion, and replication by endodyogeny. The plant-like vacuole (PLV) forms just before egress, is prominent while extracellular, and fragments shortly upon entry. While parasites shift from intracellular to extracellular, ionic concentrations change dramatically.

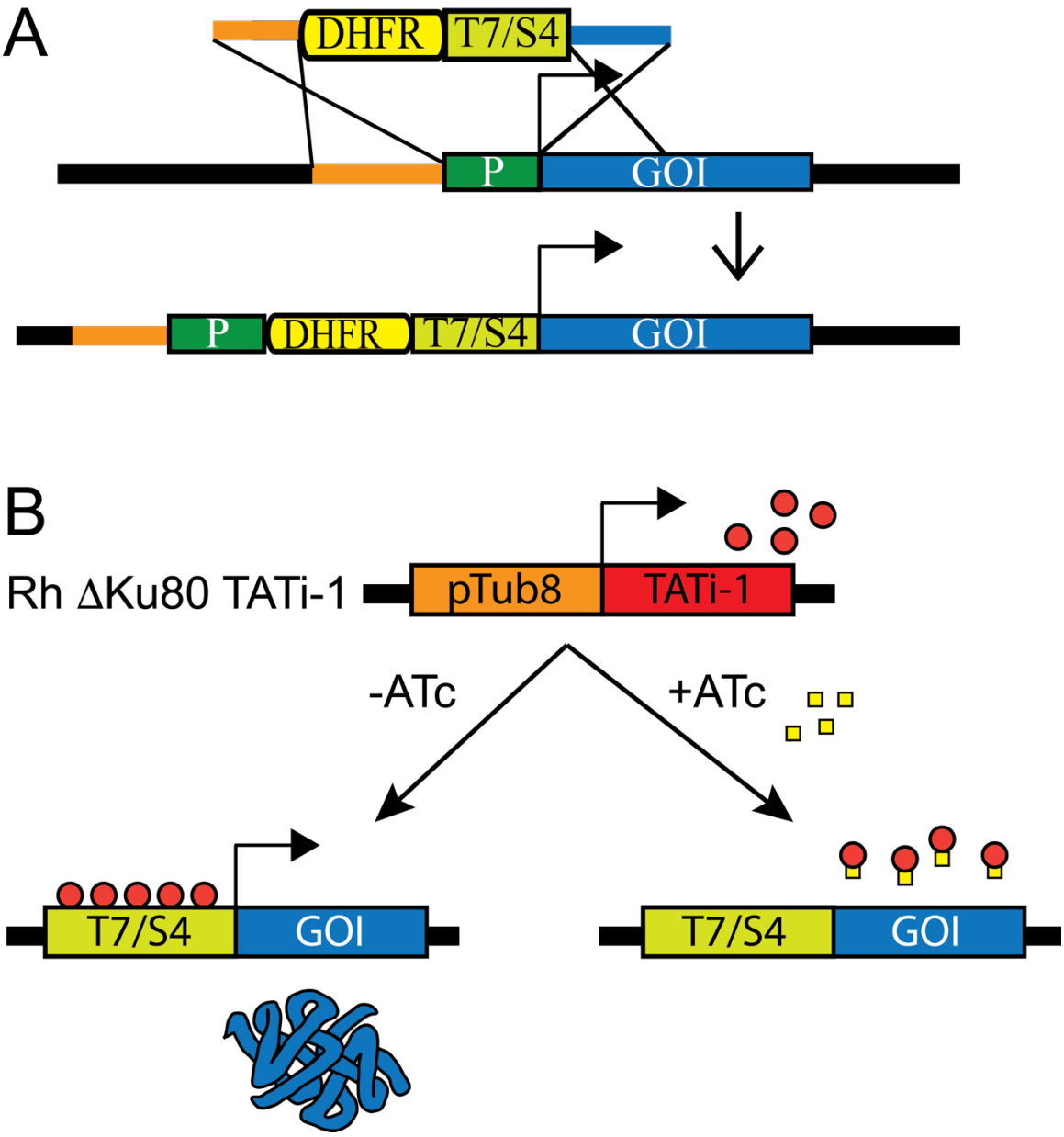

Figure 2.3: Promoter regulation of *T. gondii* essential genes. A) schematic for how homologous recombination is used to replace the endogenous protomer with a tetracycline repressible promoter. B) Cartoon showing how constitutive expression of the TATi-1 protein is able to repress genes in the presence of tetracycline.

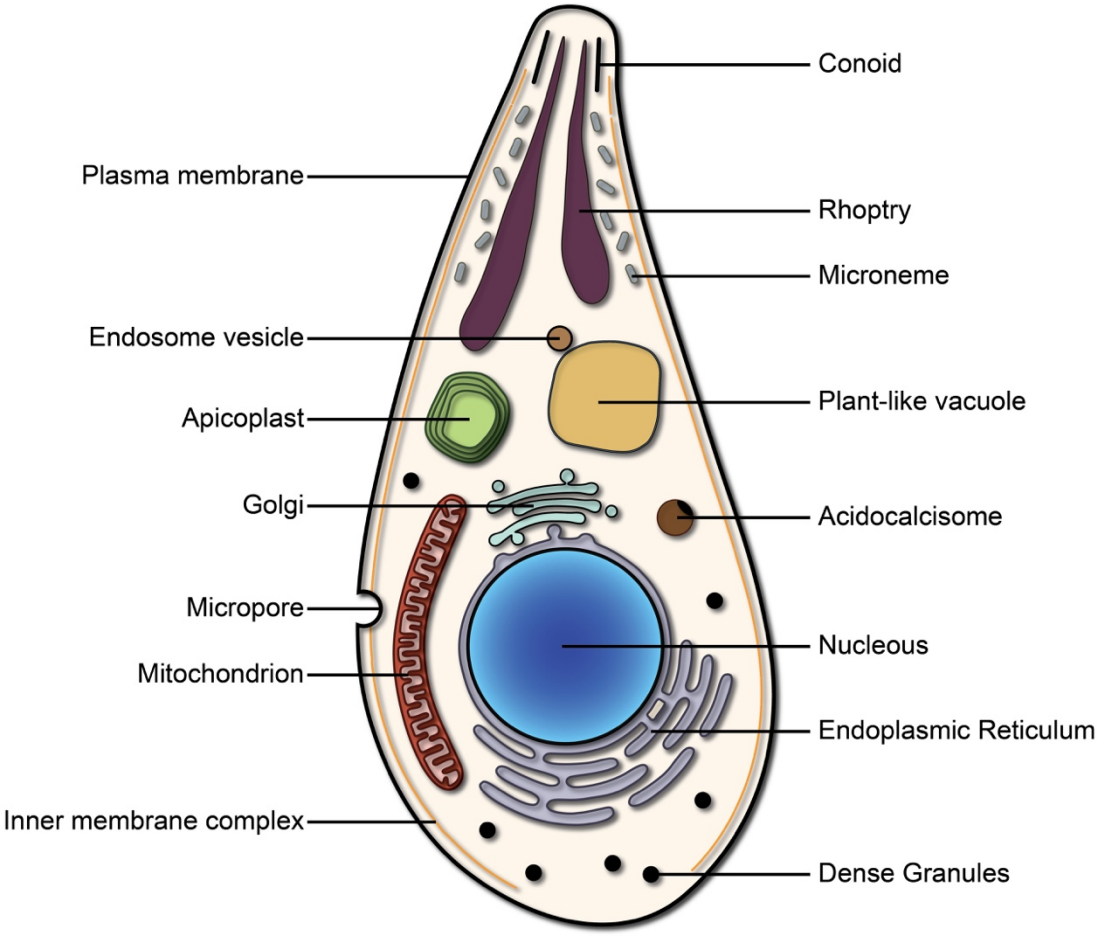

Figure 2.4: Major organelles of *Toxoplasma gondii*. A cartoon depicting the major organelles and features of *Toxoplasma gondii.*

CHAPTER 3

LITERATURE REVIEW OF *TOXOPLASMA GONDII* PLANT-LIKE VACOULE[1]

[1] Andrew J. Stasic and Silvia N.J. Moreno. Review to be submitted to *PLOS Pathogens*.

3.1 Plant like features in Apicomplexan parasites

The phylum Apicomplexa are a group of obligate intracellular parasites that contain numerous human pathogens. Members of the Apicomplexa phylum are responsible of the death of millions of humans each year. Most members of the Apicomplexa phylum possess a non-photosynthetic plastid termed the apicoplast. In *T. gondii,* the apicoplast is the most well-known and well characterized plant derived organelle. The apicoplast contains plant like features such as a 35 kilobase pairs (kbp) of circular DNA in a nonfunctional plastid that is comprised of genes that control transcription and translation but lacks any genes that are involved with photosynthesis [1]. The first endosymbiotic event being the acquisition of a plastid from a cyanobacterium into a heterotrophic eukaryote thought today to include photosynthetic alga and the second endosymbiotic event being the endosymbiosis of a photosynthetic alga [2]. Because of this endosymbiotic event, the apicoplast retains a number of genes that have plant-like characteristics [2, 3].

Apicomplexan parasites have other organelles, proteins, or other features which can be trace their origin to early plants [4]. Both *Toxoplasma gondii* and many *Plasmodium* species possess numerous organelles, proteins, or protein complexes that share a similarity to homologs commonly found in early to modern-day plants. Calcium dependent protein kinases appear to operate and be regulated by a mechanism similar to those found in plants [5, 6]. A recently identified essential tyrosine kinase (TgTKL1) was shown to contain an enhanced disease resistance 1 (EDR1) domain derived from plants that results in localization to the host nucleus [7]. A plant-like plasmodium kinase, PfCDPK5, was demonstrated to be required for parasite egress from the erythrocyte [8]. A phosphoenolpyruvate carboxykinase ($TgPEPCK_{mt}$) localizing to the *T. gondii*

mitochondrion was determined to be an ortholog of fungi and plants [9]. Two enzymes involved in the synthesis of trehalose have been identified as being of plant-like origin [10]. *Toxoplasma gondii* also contains an aquaporin that has high similarity to tonoplast intrinsic proteins in plants [11, 12]. *T. gondii* contains two glycolytic enzymes and two enolases that share significant homologies in plants [13, 14]. The important fatty acid synthesis enzyme, PfFab1, was determined to be plant-like [15].

In addition to numerous Apicomplexan proteins that can trace their origin back to plants, various plant pathways and/or hormones have been identified in Apicomplexa parasites. It has been recently reported that *T. gondii* produce cytokinins (which are involved in the regulation of cell proliferation, cell cycle progression, and plastid development) via a biosynthetic pathway similar to those found in higher plants [16]. The plant hormone abscisic acid (ABA) was found to be not only produced by *T. gondii* but also used for communication involving calcium signaling [17]. In *plasmodium*, the male specific sexual reproduction machinery is controlled by a mechanism similar to those found in flowering plants [18]. Metabolites and parasite orthologs of the α-linolenic acid (ALA) pathway typical found in plants were identified in *P. falciparum* [19].

In addition to the apicoplast organelle, an organelle in *T. gondii* similar to the lysosome was termed Plant-like vacuole or vacuolar compartment (PLV or VAC) because of its similarity in function and composition to the vacuole found in plants [12, 20]. The characterization of the PLV was first presented in 2010 as a joint endeavor of the Carruthers and Moreno lab. Characterization of this organelle identified cathepsin L protease (CPL), a vacuolar-H^+-pyrophosphatase (VP1), an enzyme only found in plants, and an aquaporin [12, 20, 21].

Since the identification of the PLV in 2010, numerous observations have been described in the literature, yet not comprehensive review on this important organelle exists. This review will be the first comprehensive review of this organelle and will highlight recent findings with an aim to demonstrate the importance of this organelle in the lytic cycle of *T. gondii*.

3.2 Major functions and composition of the plant vacuole

Plant cells possess a large central vacuole that occupies up to 90% of their volume in some cells [22]. The roles of the *plant vacuole* are vast but can be broadly categorized as storage of organic compounds, ion regulation, osmoregulation, and lysosome-like functions. Plants use the plant vacuole to store sugars, organic acids, proteins, and toxic elements and compounds [23-25]. Plant cells use the vacuole for ion regulation and for calcium homeostasis [26]. Osmoregulation is another important function of the plant vacuole and the tonoplast helps to create turgor pressure [27]. Finally, the plant vacuole contains various cathepsin proteases and possess similar functions to lysosomes present in animal cells [28]. The plant vacuole contains two major electrogenic proton pumps, a vacuolar H^+-ATPase (V-ATPase) and a vacuolar H^+-pyrophosphatase (V-PPase). These pumps work in conjunction to create a low pH (around pH 5.5) inside the plant vacuole. The proton motive force generated by both the V-ATPase and the V-PPase allow for the function of several antiporters and exchangers. The plant vacuole contains a Na^+/H^+ antiporter that has been shown to be important in salt tolerance [29]. The plant vacuole also contains a Ca^{2+}/H^+ antiporter that uses the proton gradient in the plant vacuole to exchange for calcium ions [30]. The plant vacuole also contains anion channels that transport Cl^-, NO_3^-, and malate [31]. The plant vacuole also contains aquaporins that allow

for water to enter into the plant vacuole and maintain turgor pressure [32]. Finally, the plant vacuole contains hydrolytic enzymes and functions similar to an animal cell lysosome [33, 34].

3.3 Overview of the plant-like-vacuole (and the associated vesicles of the endosomal like compartments) of *Toxoplasma gondii*

Toxoplasma gondii has a well-defined lytic cycle (**see Fig. 2.2**) that involves egress from the host cell, attachment/invasion, and replication inside the parasitophorous vacuole (PV). In extracellular tachyzoites, a large pronounced vacuole is formed that was termed the vacuolar compartment or the plant-like-vacuole (VAC or PLV; PLV hereafter) because of its similarity to the plant vacuole in its composition and functions. The PLV is a multi-vesicular organelle that becomes more evident in extracellular parasites and localizes towards the apical end of the parasite (**Fig. 1.4**). The formation of the PLV has been shown to be tied to the lytic cycle. When the parasites are extracellular, the PLV is fully formed [12]. However, upon entering host cells the PLV fragments shortly after invasion [12, 20]. The PLV in *T. gondii* expresses several orthologs of proteins commonly found in the *plant* vacuole (**Fig. 3.1**). These plant orthologs include a vacuolar H^+-pyrophosphatase (TgVP1), a cathepsin L protease (TgCPL), aquaporin 1 (TgAQP1) and a Na^+/H^+ exchanger [12, 20, 21, 35]. An overview of all the identified proteins present in the PLV is presented in **Fig. 3.1 (solid colors).**

Several studies investigating the roles of the PLV have shown that the PLV is important for salt homeostasis, calcium homeostasis, digestion of host derived proteins, maturation of secretory proteins, and forms part of the endosomal pathway [12, 20, 21, 36-39]. While these observations could very well be a direct function of the PLV, it should

be noted that the PLV emerges from endosomal like compartments (ELC) before coalescing into one large vacuole.

3.4 The biogenesis and fragmentation of the plant-like-vacuole.

The PLV is a multi-vesicular organelle and it appears to form during egress (data not shown) while it fragments right after invasion (PLV is fragmented after the first division) [12, 20]. Aside from egress and invasion, the exact signaling molecules or signaling pathways required for the PLV to form or fragment are not known. In addition, the exact mechanism(s) involved in the formation of the PLV is also not known. What is known is that downregulation of various proteins leads to biogenesis defects in the formation of the PLV. Knockdowns of vacuolar sorting protein 8 (Vsp8), Vsp11, Vps39, and a BEACH domain-containing protein (BDCP) lead to abnormal localization of the PLV marker CPL [40]. Although Vsp8 is part of the CORVET/HOPS system of vesicular traffic, the exact role that BDCP plays in the CORVET/HOPS or PLV formation remains unknown. A knockdown of the vacuolar-H^+-ATPase led to a fragmented PLV in extracellular tachyzoites using PLV markers CPL and VP1, which suggests that this pump plays some role in the PLV biogenesis but the exact role remains unknown [41]. Vacuolar-H^+-ATPases have been previously shown to play a role in vesicular trafficking and fusion in most eukaryotes and are essential, therefore it is possible that a lack of this pump could lead to a malformed PLV in *T. gondii* [42]. Rab7 is an important protein that plays a role in the regulation of endosomes and lysosomes [43, 44]. In *T. gondii*, Rab7 associates with the PLV which suggests that it may play a role in its formation [12].

Fragmentation of the PLV is poorly understood and so far has only been correlated with the cell cycle [20]. Within 1 hour after invasion, the PLV begins to fragment [20].

Three hours post-invasion, the PLV has mostly been fragmented and is fully fragmented 7 hours post-invasion (when parasites begin mitosis) [20].

3.5 The plant-like-vacuole and its role in salt homeostasis

While completing the lytic cycle, *T. gondii* is exposed to low levels of calcium and sodium and higher levels of potassium while intracellular and when the parasites egress they are exposed to higher levels of calcium and sodium and lower levels of potassium [12]. Coping with these changing ionic conditions is a of paramount concern for the dissemination of the parasite. One of the major functions of the vacuole in plants is to maintain salt homeostasis. The role of the PLV for ion homeostasis was first postulated when it was noticed that this organelle forms shortly after the parasites egresses and fragments shortly upon invasion of the new host [12]. Over expression of vacuolar H^+ pyrophosphatase (TgVP1) lead to increased survival in high concentrations of sodium, suggesting that sodium uptake into the PLV could be paired to proton translocation by TgVP1 [12]. Ablation of the Na^+/H^+ exchanger in *T. gondii*, which localizes to the PLV (**Fig. 3.1**), resulted in decreased survival in media containing 0.6 M KCl compared to parental clones [35]. This data suggested that the PLV plays a role in potassium homeostasis. PLV fractions exposed to pyrophosphate and NaCl, reached a steady state level and suggested that the PLV transports sodium upon energization with PP_i [12]. Overexpression of TgVP1 resulted in increased tolerance to 150 mM NaCl present in the media and formed significantly more plaques than parental cells under identical conditions [12]. TgVP1 knock out mutants exposed to hyposmotic conditions began to swell, suggesting that TgVP1 creates the proton gradient used to maintain sodium and chloride homeostasis in the PLV [21]. In hyperosmotic media, Na^+/H^+ exchanger KO clones had

significant lower survival in media with >0.75 M sorbitol, >0.5 M NaCl, >0.75 M sodium gluconate, and >0.6 M KCl [35]. Taken together, there is strong evidence to suggest that the PLV plays a role in salt tolerance in *T. gondii*.

3.6 The plant-like-vacuole and its role in calcium homeostasis

Miranda and colleagues found that enriched PLV fractions pre-energized with pyrophosphate released more protons than controls when calcium was added to the media, indicating evidence of a calcium/proton exchanger present at the PLV membrane [12]. Additional evidence of the PLV as a calcium store come from experiments looking at cytoplasmic Ca2+ and its increase in response to glycyl-L-phenylalanine-naphthylamide (GPN) [12]. GPN is hydrolyzed by cathepsin C in the lysosome of eukaryotes (or PLV in *T. gondii*), which results in an increased lysosome swelling, which ultimately results in releasing stored calcium out to the cytoplam [45]. The addition of GPN to extracellular parasites loaded with Fura2-AM, an intracellular chemical calcium indicator, resulted in increased levels of calcium in the cytoplasm [12]. The release of calcium from the PLV suggests that the PLV is a calcium store and could play a role in calcium homeostasis. The V-ATPase localizes in part to the PLV and creates a proton gradient that can be used to exchange for calcium ions (**Fig. 3.1**). Conditional knockouts of the V-ATPase resulted in a poorly formed PLV and intracellular levels of calcium were lower in the knockdowns (**see chapter 6**). Additionally, levels of Ca^{2+} release when GPN was added were lower in the V-ATPase knockdowns than in wild type cells (**see chapter 6**). These data suggest that a decrease in the pH of the PLV results in defects in calcium storage and thus defects in calcium homeostasis.

3.7 The plant-like-vacuole and its role in the storage of toxic components and elements

The vacuole found in *plants* is a major player in the storage of toxic elements and compounds and similarly, the PLV in *T. gondii* has been shown to be involved the storage of toxic elements. Overexpression of an aquaporin that is found in the PLV (**Fig. 3.1**) resulted in less circular parasites than wild type RH and accumulation of exogenous mercury in the PLV [12]. Recently, it was demonstrated that the PLV contains a zinc transporter (TgZnT) that localizes in the membrane of the PLV (**Fig. 3.1**) [46]. Ablation of TgZnT resulted in a defect in growth and, interestingly, overexpression of TgZnT resulted in a stronger growth defect [46]. A conditional TgZnT strain was shown to grow worse than the wild type in the presence of exogenous zinc [46]. It was also demonstrated that TgZnT was able to rescue growth in yeast in a heterologous yeast system devoid of zinc transporters [46]. Although TgZnT localizes to the PLV, it is unknown if zinc is actively transported into the PLV in *T. gondii.* However, these results suggest that *T. gondii* TgZnT is important for the propagation of the parasite and, due to its localization at the PLV, could likely be transporting zinc into to the PLV. Collectively, these observations demonstrate that the PLV plays a role in the protection from environmental stress.

3.8 Lysosome-like functions of the plant-like-vacuole

Typical eukaryote lysosomes function by creating an acidic environment where proteins, nucleic acids, lipids, and other molecules are degraded and recycled. These acidic vacuoles use degradative enzymes that aid in the recycling of material and proton pumps that maintain an acidic pH. *Toxoplasma gondii* does not have a formal lysosome organelle, but the PLV possess many characteristics found in a typical lysosome. Proteases,

specifically cathepsins, are commonly found in the lysosome and serve to degrade cellular proteins or proteins originating from endocytic events. *T. gondii* expresses 5 cathepsins; TgCPL, TgCPB, and TgCPC1-3 [36] and Two papain-family proteases together with TgCPL and TgCPB, have been localized to the PLV (**Fig. 3.1**) [12, 47]. Evidence of GPN released calcium support the idea that at least one cathepsin C (TgCPC) is present in the PLV or endosomal like compartments (ELCs) even though TgCPC1 and TgCPC2 are reported to be secreted in the parasitophorous vacuoles (PV) and TgCPC3 is reportedly only expressed in the sporozoite stage [48]. In Eukaryotes, cathepsins proteases are translated as a preprocathepsins where the propeptide is removed in the endoplasmic reticulum and the procathepsin is trafficked to the early endosome or lysosome. In the acidic environment of the lysosome, the procathepsin undergoes proteolytic processing, occasionally catalyzed by itself, to become active. In *T. gondii*, TgCPL and TgCPB are synthesized as an inactive procathepsin, trafficked to the PLV, and matured in at low pH [20, 47]. In *T. gondii*, TgCPL is expressed most prominently in the PLV, and its proteolytic activity was characterized [20]. A recent investigation reported that ΔTgCPL knockout strain accumulated host expressed GFP in the PLV, whereas a parasite with a properly functioning CPL did not display host derived GFP accumulation [38]. Recently, it was determined that host derived proteins are endocytosed in as little as 7 min. post invasion, trafficked to the PLV, and digested in under 30 min [37]. Ablation of TgCPL in the Prugniaud strain, a strain that favors the formation of bradyzoites, showed that the PLV was a major player in proteolytic activity in the chronic stage [49]. Additionally, the PLV was shown to play a role in autophagy as undigested organelles appeared in the PLV in ΔTgCPL knockouts [49]. Collectively, these results confirm that the PLV serves as a

digestive organelle and that TgCPL, and possibly TgCPB, are active proteases for at least some host derived proteins, including GFP.

The *Plasmodium* digestive vacuole is a lysosomal like organelle that is known to be the source of hemoglobin degradation. The *Plasmodium falciparum* digestive vacuole and the *T. gondii* PLV are believed to be homologous organelles possibly derived from a common ancestor that contained a lysosome-like organelle [50]. In *Plasmodium*, a pump termed the chloroquine resistance transporter (PfCRT) was shown to localize to the digestive vacuole and certain mutations in PfCRT ($PfCRT^{CQR}$) resulted in accumulation of peptides in the digestive vacuole [51]. In *T. gondii*, the orthologous chloroquine resistance transporter, TgCRT, was found to localize to the PLV (**Fig. 3.1**) [39]. These similarities in the localization suggested that the PLV and the *Plasmodium* digestive vacuole share similar lysosome-like functions. Ablation of TgCRT results in an enlarged PLV that can be up to 2.6 fold larger than wild type [52]. Recently the function of the TgCRT was identified to be maintenance of the integrity and proteolytic activity present in the PLV and facilitation of chloroquine transport [39, 52]. It is possible that that the enlarged PLV in ΔTgCRT knockouts could be caused by buildup of un-cleaved peptides due to repression of key proteases [52].

Another feature of lysosomes is their luminal low pH compared to other compartments and this acidic environment is maintained by various proton pumps. The PLV has two proton pumps, the vacuolar-H^+-pyrophosphatase (TgVP1) and the vacuolar-H^+-ATPase (V-ATPase) [12, 41]. Both the TgVP1 and the V-ATPase were found to be actively pumping protons in intact enriched PLV fractions (**Fig. 3.1**), suggesting that both the vacuolar-H^+-pyrophosphatase and the vacuolar H^+-ATPase are active at the PLV

membrane [12]. Lysotracker was able to accumulate in a compartment that the V-ATPase also localized, which demonstrated the acidic nature of the PLV [41]. Collectively, these observations support the acidic and lysosomal like-nature of the PLV.

3.9 The plant-like-vacuole and endosomal-like compartments for the maturation and localization of proteins important for invasion

Toxoplasma gondii contains three major secretary organelles that include rhoptries, micronemes, and dense granules. It has been proposed that proteins destined for all three organelles originate from a common organelle such as the trans-Golgi-network (TGN) before being trafficked to their respective destination [53]. From the TGN, rhoptry, microneme, and dense granule trafficking pathways diverge using mechanisms not fully understood [37, 54]. Mounting evidence suggests that the PLV and endosomal-like compartments (ELC) are part of the route used for the maturation of microneme proteins [37, 41]. Disruption of the PLV and ELC proton pump TgVP1 resulted in defects in microneme secretion, microneme organelle localization and host cell invasion/attachment [21]. Ablation of TgCPL, which resides primarily in the PLV, results in maturation defects of two important microneme proteins, TgM2AP and TgMIC3 [20]. Disruption of the V-ATPase, which localizes in part to the PLV and ELCs, resulted in defects in TgMIC3, TgMIC2, and TgM2AP localization, maturation, and secretion [41]. Rhoptry protein and organelle maturation was also impacted by disruption of the V-ATPase [41]. However, rhoptry or prorhoptries proteins did not colocalized in the PLV, indicating a different pathway is involved in rhoptry maturation than microneme maturation [41]. These results suggest that a complex pathway is involved in the maturation of microneme proteins that includes the PLV and its various vesicular compartments.

TgCPL in the PLV was also identified as the maturase for TgCPB [47] and because both localize to the PLV, it is likely that both work together in the degradation of polypeptides in the PLV. As TgCPL was shown to act as a maturase for certain microneme proteins, TgCPB has been reported to be involved in the maturation of ROP2, 3, and 4 [55]. Although TgCPL and TgCPB are lytic enzymes it appears that *T. gondii* is using them for the maturation of important invasion proteins.

3.10 The role of the plant-like-vacuole and endosomal-like compartments in the endo/exocytic pathways of *T. gondii*

Endocytosis is the cellular process of taking up material from outside of the plasma membrane and trafficking it to a digestive organelle. The endocytic pathway in mammalian cells and plants is an ordered and highly conserved process. In mammalian cells, an endocytic event begins as an early endosome (which labels with Rab5), traffics to the late endosome (which labels with Rab7), and finally fusion with the mature lysosome (this compartment also labels with Rab7) [56]. In plants, however, endocytosed cargo is usually sent to the trans-Golgi network before being routed through the early endosomes and finally ending up in the lysosome [57]. While endocytosis is involved in material uptake, exocytosis is the process of trafficking vesicles to the plasma membrane for secretion.

The mechanisms of endo/exocytic systems of *T. gondii* are poorly understood. Although there are many gaps in the understanding of the two pathways, the endocytic system is particularly poorly understood. The difficulty in understanding the endocytic pathway relies on the inability for chemical dyes to be endocytosed and a lack of known receptors or trackable ligands usually involved in the endocytic process. Without better

indicators of the *T. gondii* endocytic pathway, this process will take longer to be characterized. There have been some reported instances of endocytosed cargo making its way inside into vesicles presumably via the micropore, but the mechanism(s) remains unknown [58, 59]. *T. gondii* is also able to ingest host derived proteins through the intravacuolar network but the mechanism(s) also remains unclear [38]. These reports collectively show that *T. gondii* is capable of endocytic events, but much still needs to be studied about this process.

The endocytosed cargo makes its way to the PLV suggesting that the PLV could be the terminal end of the endocytic pathway. The PLV is a multi-vesicular post-Golgi compartment that is a highly dynamic and its formation and fragmentation suggests constant fusion and budding of internal vesicles. Proteomic studies of PLV-enriched fractions resulted in the identification of several Rab proteins, which are involved in intracellular trafficking [12]. On such Rab protein, Rab7, usually associated with early to late endosomes was shown to colocalize with the PLV marker TgVP1, suggesting that the PLV could play a role in the endocytic pathway [12, 60]. Although there is a lot to discover about how toxoplasma uses the endocytic system, recent reports suggest that the endosome like compartments (ELCs) and the PLV are major compartments of the endocytic system [36, 37]. Recent evidence suggests that ingested host proteins make their way through the ELCs and are finally trafficked to and digested by the PLV [37].

The exocytic system of *T. gondii* is better understood than the endocytic pathways. The secretory pathway in *T. gondii* is highly polarized with secretion occurring at the apical end and occurring from three distinct organelles, rhoptries, micronemes, and dense granules. Dense granule proteins pass through the Golgi, where the organelle forms as a

post Golgi vesicle that is then trafficked using MyoF actin motors to the parasites periphery [61]. Once at the periphery, the dense granule organelle finds a small gap in the IMC and accesses a docking site where the organelle can secrete when needed [61]. Dense granule trafficking appears to be the default pathway for proteins lacking targeting signals at their N-terminus and it does not appear to overlap with the endosomal-like compartments or the PLV [41]. Micronemes and rhoptries are trafficked through ELCs before being deposited at their respective organelle [37]. Previous reports have demonstrated that ablation of DrpB, a dynamin-related proteins (Drp) involved in vesicle traffic, SORTLR, a sortilin-like receptor important for protein trafficking, and TgCHC1, a clathrin heavy chain, resulted in loss of micronemes and rhoptries organelles [62-64]. However, it was recently shown that endocytic trafficking to the PLV does not require DrpB [37]. Therefore, DrpB likely plays a role in the downstream biogenesis of microneme and rhoptry organelles after cargo is endocytosed. TgCHC1 was localized to the Golgi and absent from the plasma membrane [64]. Ablation of TgCHC1 resulted in Golgi aberration, but like DrpB, TgCHC1 likely plays no role in the endocytic event and likely plays a role in stabilizing the Golgi [64]. Similar to DrpB and TgCHC1, TgSORTLR appears to be involved after the initial endocytic event and is important for secretory organelle biogenesis and trafficking of proteins [63].

HOPS (homotypic fusion and vacuole protein sorting) and CORVET (class C core vacuole/endosome tethering) are tethering complexes which are essential for the early to late endosome transition, lysosome biogenesis, and endolysosomal trafficking [65]. Vps11, a subunit of HOPS and CORVET tethering complexes, appears to be essential for

the biogenesis of all secretory organelles [66]. Therefore, Vps11 appears to be upstream to DrpB, TgSORTLR, and TgCHC1 but downstream to the initial endocytic event.

3.11 Importance of the plant-like-vacuole to *T. gondii*

Disruption of proton pumps, ion/H^+ exchangers, other PLV/ELC associated proteins, and certain proteases localized to the PLV/ELCs have routinely resulted in decreased invasion, replication, and/or egress phenotypes [12, 20, 21, 35, 41]. These observations suggest that a functional PLV is important for the parasite to continue with the steps of its lytic cycle. It is evident that the PLV or its endosomal compartments require proton pumping by either TgVP1 or the V-ATPase to create an acidic environment where proteases can mature. CPL and ASP3 both appear to require an acidic environment created by the V-ATPase in order to mature and function in the maturation of microneme or rhoptry proteins [41]. When the PLV is not acidic enough, the maturation of TgCPL or TgASP3 slows, which in return, results in decreased maturation of MIC3 and M2AP [41]. The mechanism of why microneme organelle location is impacted when proton pumps are knocked out or knocked down remains unknown at this time.

The PLV functions as the main digestive vacuole in *T. gondii* and disruption of proteases impacts cellular functions important for parasite propagation. While the PLV appears necessary for normal tachyzoite propagation, the PLV appears to be essential in the maintenance of the bradyzoite stage [49]. CPL knockouts in the chronic stage resulted in decreased viability in parasites due to lack of autophagosome turnover, suggesting the importance of the PLV for this stage of the life cycle [49]. TgCRT is a recently identified chloroquine resistance transporter, the orthologue to the PfCRT, that localizes to some compartments of the PLV and play a role in organelle integrity [52]. TgCRT knockouts

have swollen PLVs and have a growth defect due to decreased proteolytic activity [39, 52]. In the chronic stage, loss of TgCPL also results in a swollen PLV [49]. Collectively, these reports indicate that a swollen, defective PLV, leads to defects in growth in both the acute and chronic stages, further implicating the PLV as an important organelle for the propagation of the parasite.

3.12 Future outlook

While huge advances to our understanding of the PLV has occurred in the last 10 years, there still remains a number of deficiencies in our knowledge. The triggers that begin the formation and fragmentation of the PLV are not known. The data shows that it is correlated with invasion egress, and cell cycle but the triggering mechanism(s) remains unknown. Understanding the biogenesis of the PLV could be critical in finding drugs that prevent its formation and thus its function in the parasite. As of this writing, no Ca^{2+}/H^{+} exchanger or a Ca^{2+} ATPase have been identified at the PLV membrane, yet biochemical evidence exists to support their presence in the PLV. Identification and characterization of these proteins would provide valuable information in the understanding of the calcium storage function. Aside from the Na^{+}/H^{+} exchanger, no other ion channel or pump is known to be at the PLV and its storage of other ions (such as K^{+}, Mg^{2+}, and Cl^{-}) remains unknown. Understanding of the interplay between these ion exchangers and pumps could provide a deeper understanding of the ionic homeostatic function of the PLV.

3.13 References

1. Wilson, R.J.M., et al., *Complete Gene Map of the Plastid-like DNA of the Malaria Parasite Plasmodium falciparum.* Journal of Molecular Biology, 1996. **261**(2): p. 155-172.
2. van Dooren, G.G., et al., *Toxoplasma gondii Tic20 is essential for apicoplast protein import.* Proceedings of the National Academy of Sciences, 2008. **105**(36): p. 13574.
3. Amiar, S., et al., *Apicoplast-Localized Lysophosphatidic Acid Precursor Assembly Is Required for Bulk Phospholipid Synthesis in Toxoplasma gondii and Relies on an Algal/Plant-Like Glycerol 3-Phosphate Acyltransferase.* PLoS Pathog, 2016. **12**(8): p. e1005765.
4. Huang, J., et al., *A first glimpse into the pattern and scale of gene transfer in the Apicomplexa.* International Journal for Parasitology, 2004. **34**(3): p. 265-274.
5. Billker, O., S. Lourido, and L.D. Sibley, *Calcium-Dependent Signaling and Kinases in Apicomplexan Parasites.* Cell Host & Microbe, 2009. **5**(6): p. 612-622.
6. Kieschnick, H., et al., *Toxoplasma gondii Attachment to Host Cells Is Regulated by a Calmodulin-like Domain Protein Kinase.* Journal of Biological Chemistry, 2001. **276**(15): p. 12369-12377.
7. Varberg, J.M., et al., *TgTKL1 Is a Unique Plant-Like Nuclear Kinase That Plays an Essential Role in Acute Toxoplasmosis.* mBio, 2018. **9**(2): p. e00301-18.
8. Dvorin, J.D., et al., *A Plant-Like Kinase in Plasmodium falciparum Regulates Parasite Egress from Erythrocytes.* Science, 2010. **328**(5980): p. 910.

9. Nitzsche, R., et al., *A plant/fungal-type phosphoenolpyruvate carboxykinase located in the parasite mitochondrion ensures glucose-independent survival of Toxoplasma gondii.* Journal of Biological Chemistry, 2017. **292**(37): p. 15225-15239.

10. Yu, Y., H. Zhang, and G. Zhu, *Plant-Type Trehalose Synthetic Pathway in Cryptosporidium and Some Other Apicomplexans.* PLOS ONE, 2010. **5**(9): p. e12593.

11. Slavica, P.-D., S.J. E., and B. Eric, *A single aquaporin gene encodes a water/glycerol/urea facilitator in Toxoplasma gondii with similarity to plant tonoplast intrinsic proteins.* FEBS Letters, 2003. **555**(3): p. 500-504.

12. Miranda, K., et al., *Characterization of a novel organelle in Toxoplasma gondii with similar composition and function to the plant vacuole.* Molecular Microbiology, 2010. **76**(6): p. 1358-1375.

13. Dzierszinski, F., et al., *Differential expression of two plant-like enolases with distinct enzymatic and antigenic properties during stage conversion of the protozoan parasite Toxoplasma gondii.* Journal of Molecular Biology, 2001. **309**(5): p. 1017-1027.

14. Dzierszinski, F., et al., *The Protozoan Parasite Toxoplasma gondii Expresses Two Functional Plant-like Glycolytic Enzymes: Implications For Evolutionary Origin of Apicomplexans.* Journal of Biological Chemistry, 1999. **274**(35): p. 24888-24895.

15. McLeod, R., et al., *Triclosan inhibits the growth of Plasmodium falciparum and Toxoplasma gondii by inhibition of Apicomplexan Fab I.* International Journal for Parasitology, 2001. **31**(2): p. 109-113.

16. Andrabi, S.B.A., et al., *Plant hormone cytokinins control cell cycle progression and plastid replication in apicomplexan parasites.* Parasitology International, 2018. **67**(1): p. 47-58.

17. Nagamune, K., et al., *Abscisic acid controls calcium-dependent egress and development in Toxoplasma gondii.* Nature, 2008. **451**(7175): p. 207-210.

18. Hirai, M., et al., *Male Fertility of Malaria Parasites Is Determined by GCS1, a Plant-Type Reproduction Factor.* Current Biology, 2008. **18**(8): p. 607-613.

19. Lakshmanan, V., et al., *Metabolomic Analysis of Patient Plasma Yields Evidence of Plant-Like α-Linolenic Acid Metabolism in Plasmodium falciparum.* The Journal of Infectious Diseases, 2012. **206**(2): p. 238-248.

20. Parussini, F., et al., *Cathepsin L occupies a vacuolar compartment and is a protein maturase within the endo/exocytic system of Toxoplasma gondii.* Molecular Microbiology, 2010. **76**(6): p. 1340-1357.

21. Liu, J., et al., *A vacuolar-H^+-pyrophosphatase (TgVP1) is required for microneme secretion, host cell invasion, and extracellular survival of Toxoplasma gondii.* Molecular Microbiology, 2014. **93**(4): p. 698-712.

22. Taiz, L., *The Plant Vacoule.* The Journal of Experimental Biology, 1992. **172**(1): p. 113.

23. Korenkov, V., et al., *Enhancing tonoplast Cd/H antiport activity increases Cd, Zn, and Mn tolerance, and impacts root/shoot Cd partitioning in Nicotiana tabacum L.* Planta, 2007. **226**(6): p. 1379-1387.

24. Bouyssou, H., H. Canut, and G. Marigo, *A reversible carrier mediates the transport of malate at the tonoplast of Catharanthus roseus cells.* FEBS Letters, 1990. **275**(1): p. 73-76.

25. X., S.W., et al., *Cold acclimation induces changes in Arabidopsis tonoplast protein abundance and activity and alters phosphorylation of tonoplast monosaccharide transporters.* The Plant Journal, 2012. **69**(3): p. 529-541.

26. Tang, R.-J., et al., *Tonoplast calcium sensors CBL2 and CBL3 control plant growth and ion homeostasis through regulating V-ATPase activity in Arabidopsis.* Cell Research, 2012. **22**: p. 1650.

27. Nava, M., *Osmoregulation of leaf motor cells.* FEBS Letters, 2007. **581**(12): p. 2337-2347.

28. Yao-Min, C., et al., *Two proteases with caspase-3-like activity, cathepsin B and proteasome, antagonistically control ER-stress-induced programmed cell death in Arabidopsis.* New Phytologist, 2018: p. 1143-1155.

29. Apse, M.P., et al., *Salt tolerance conferred by overexpression of a vacuolar Na+/H+ antiport in Arabidopsis.* Science, 1999. **285**(5431): p. 1256.

30. Blackford, S., P.A. Rea, and D. Sanders, *Voltage sensitivity of H+/Ca2+ antiport in higher plant tonoplast suggests a role in vacuolar calcium accumulation.* Journal of Biological Chemistry, 1990. **265**(17): p. 9617-9620.

31. Tyerman, S., *Anion channels in plants.* Annual review of plant biology, 1992. **43**(1): p. 351-373.

32. Johansson, I., et al., *The role of aquaporins in cellular and whole plant water balance.* Biochimica et Biophysica Acta (BBA) - Biomembranes, 2000. **1465**(1): p. 324-342.

33. Boller, T. and H. Kende, *Hydrolytic Enzymes in the Central Vacuole of Plant Cells.* Plant Physiology, 1979. **63**(6): p. 1123.

34. Villiers, T.A., *Lysosomal Activities of the Vacuole in Damaged and Recovering Plant Cells.* Nature New Biology, 1971. **233**: p. 57.

35. Francia, M.E., et al., *A Toxoplasma gondii protein with homology to intracellular type Na+/H+ exchangers is important for osmoregulation and invasion.* Experimental Cell Research, 2011. **317**(10): p. 1382-1396.

36. Dou, Z. and V.B. Carruthers, *Cathepsin Proteases in Toxoplasma gondii*, in *Cysteine Proteases of Pathogenic Organisms*, M.W. Robinson and J.P. Dalton, Editors. 2011, Springer US: Boston, MA. p. 49-61.

37. McGovern, O.L., et al., *Intersection of Endocytic and Exocytic Systems in Toxoplasma gondii.* Traffic, 2018: p. 336–353.

38. Dou, Z., et al., *Toxoplasma gondii Ingests and Digests Host Cytosolic Proteins.* mBio, 2014. **5**(4).

39. Warring, S.D., et al., *Characterization of the Chloroquine Resistance Transporter Homologue in Toxoplasma gondii.* Eukaryotic Cell, 2014. **13**(11): p. 1360-1370.

40. Morlon-Guyot, J., et al., *A proteomic analysis unravels novel CORVET and HOPS proteins involved in Toxoplasma gondii secretory organelles biogenesis.* Cellular Microbiology, 2018. **0**(0): p. e12870.

41. Stasic, A.J., et al., *The Toxoplasma Vacuolar H^+-ATPase regulates intracellular pH, and impacts the maturation of essential secretory proteins.* Cell Reports, 2019.

42. Beyenbach, K.W. and H. Wieczorek, *The V-type H^+ ATPase: molecular structure and function, physiological roles and regulation.* Journal of Experimental Biology, 2006. **209**(4): p. 577-589.

43. Vanlandingham, P.A. and B.P. Ceresa, *Rab7 Regulates Late Endocytic Trafficking Downstream of Multivesicular Body Biogenesis and Cargo Sequestration.* Journal of Biological Chemistry, 2009. **284**(18): p. 12110-12124.

44. Meresse, S., J.P. Gorvel, and P. Chavrier, *The rab7 GTPase resides on a vesicular compartment connected to lysosomes.* Journal of Cell Science, 1995. **108**(11): p. 3349.

45. Haller, T., et al., *The lysosomal compartment as intracellular calcium store in MDCK cells: a possible involvement in InsP3-mediated Ca2+ release.* Cell Calcium, 1996. **19**(2): p. 157-165.

46. Chasen, N.M., et al., *The Vacuolar Zinc Transporter TgZnT Protects Toxoplasma gondii from Zinc Toxicity.* mSphere, 2019.

47. Dou, Z., I. Coppens, and V.B. Carruthers, *Non-canonical Maturation of Two Papain-family Proteases in Toxoplasma gondii.* Journal of Biological Chemistry, 2013. **288**(5): p. 3523-3534.

48. Que, X., et al., *Cathepsin Cs Are Key for the Intracellular Survival of the Protozoan Parasite, Toxoplasma gondii.* Journal of Biological Chemistry, 2007. **282**(7): p. 4994-5003.

49. Di Cristina, M., et al., *Toxoplasma depends on lysosomal consumption of autophagosomes for persistent infection.* Nature Microbiology, 2017. **2**: p. 17096.

50. Coppens, I., *Toxoplasma, or the discovery of a heterophage.* Trends in Parasitology, 2014. **30**(10): p. 467-469.

51. Martin, R.E., et al., *Chloroquine Transport via the Malaria Parasite's Chloroquine Resistance Transporter.* Science, 2009. **325**(5948): p. 1680.

52. Thornton, L.B., et al., *An ortholog of P. falciparum chloroquine resistance transporter (PfCRT) plays a key role in maintaining the integrity of the endolysosomal system in Toxoplasma gondii to facilitate host invasion.* PLOS Pathogens, 2019.

53. Ngô, H.M., H.C. Hoppe, and K.A. Joiner, *Differential sorting and post-secretory targeting of proteins in parasitic invasion.* Trends in Cell Biology, 2000. **10**(2): p. 67-72.

54. Coppens, I., et al., *Intracellular trafficking of dense granule proteins in Toxoplasma gondii and experimental evidences for a regulated exocytosis.* European Journal of Cell Biology, 1999. **78**(7): p. 463-472.

55. Que, X., et al., *The Cathepsin B of Toxoplasma gondii,Toxopain-1, Is Critical for Parasite Invasion and Rhoptry Protein Processing.* Journal of Biological Chemistry, 2002. **277**(28): p. 25791-25797.

56. Galvez, T., et al., *SnapShot: Mammalian Rab proteins in endocytic trafficking.* Cell, 2012. **151**(1): p. 234-234. e2.

57. Viotti, C., et al., *Endocytic and Secretory Traffic in Arabidopsis Merge in the Trans-Golgi Network/Early Endosome, an Independent and Highly Dynamic Organelle.* The Plant Cell, 2010. **22**(4): p. 1344-1357.

58. Nichols, B.A., M.L. Chiappino, and C.E.N. Pavesio, *Endocytosis at the micropore of Toxoplasma gondii.* Parasitology Research, 1994. **80**(2): p. 91-98.

59. Botero-Kleiven, S., et al., *Receptor-Mediated Endocytosis in an Apicomplexan Parasite (Toxoplasma gondii).* Experimental Parasitology, 2001. **98**(3): p. 134-144.

60. Bucci, C., et al., *Rab7: A Key to Lysosome Biogenesis.* Molecular Biology of the Cell, 2000. **11**(2): p. 467-480.

61. Heaslip, A.T., et al., *Dense granule trafficking in Toxoplasma gondii requires a unique class 27 myosin and actin filaments.* Molecular Biology of the Cell, 2016. **27**(13): p. 2080-2089.

62. Breinich, M.S., et al., *A Dynamin Is Required for the Biogenesis of Secretory Organelles in Toxoplasma gondii.* Current Biology, 2009. **19**(4): p. 277-286.

63. Sloves, P.-J., et al., *Toxoplasma Sortilin-like Receptor Regulates Protein Transport and Is Essential for Apical Secretory Organelle Biogenesis and Host Infection.* Cell Host & Microbe, 2012. **11**(5): p. 515-527.

64. Pieperhoff, M.S., et al., *The Role of Clathrin in Post-Golgi Trafficking in Toxoplasma gondii.* PLOS ONE, 2013. **8**(10): p. e77620.

65. Solinger, J.A. and A. Spang, *Tethering complexes in the endocytic pathway: CORVET and HOPS.* The FEBS Journal, 2013. **280**(12): p. 2743-2757.

66. Morlon-Guyot, J., et al., *Toxoplasma gondii Vps11, a subunit of HOPS and CORVET tethering complexes, is essential for the biogenesis of secretory organelles.* Cellular Microbiology, 2015. **17**(8): p. 1157-1178.

Figures

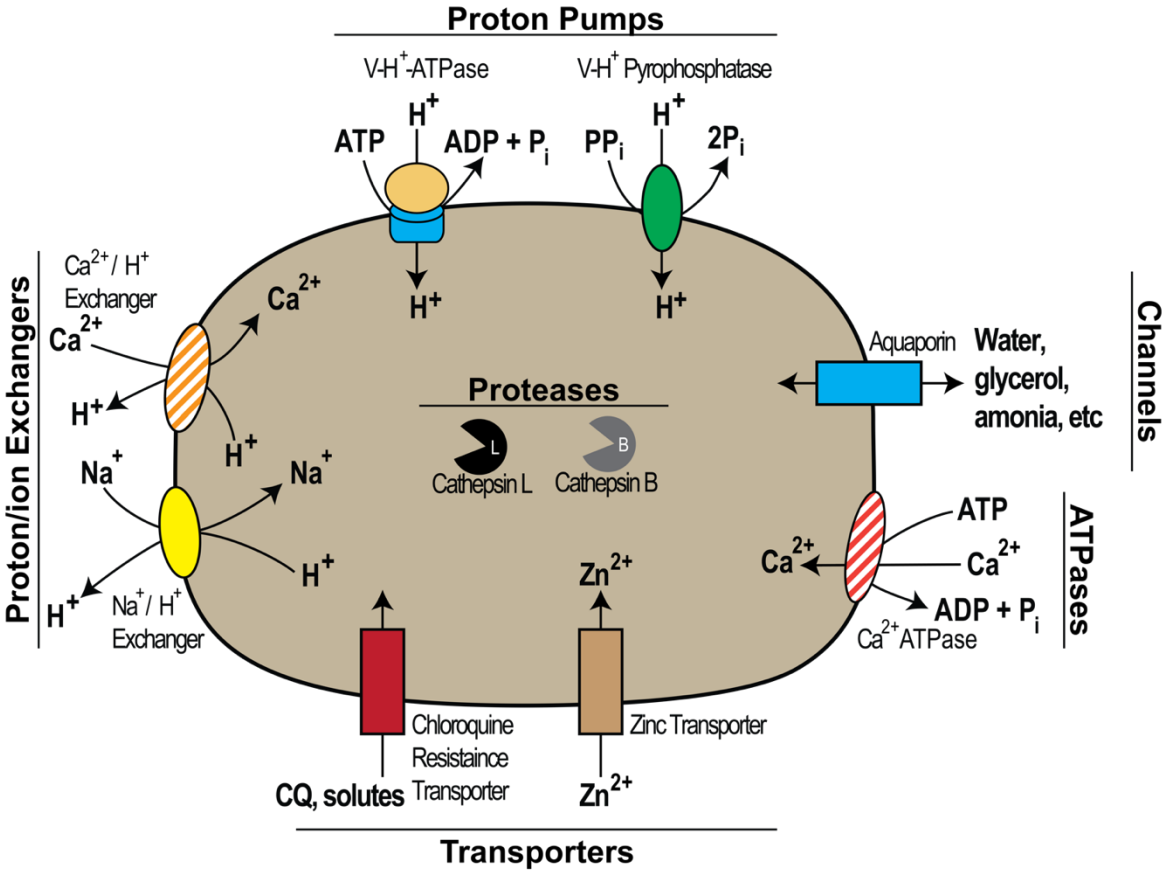

Figure 3.1: Major proteins found in the Plant-like vacuole. The PLV expresses ATPases, channels, transporters, proton/ion exchangers, proteases, and proton pumps. These numerous proteins are involved in maintaining proton gradients, ion homeostasis, and the maturation of proteins important for invasion. Solid colors indicate that the protein has been directly observed in the PLV, whereas striped colors indicate that protein has not been directly observed in the PLV but experimental evidence suggests their presence. CQ; Chloroquine.

CHAPTER 4

LITERATURE REVIEW OF VACUOLAR H^+-ATPASES

4.1 Introduction to this review

There have been numerous reviews on the function, structure, and regulation of the vacuolar H^+ ATPase (V-ATPase) since its formal identification in the 1970's (see refs [1-7]). However, this review will give a brief description of the structure, function, and regulation of the V-ATPase with current and updated information.

4.2 Introduction to the family of ATPases

There are 5 major families of ATPases that are present in a majority of living organisms and include vacuolar ATPases (or **V-Type ATPases**), phosphorylation ATPases (**P-Type ATPases** or **E1-E2 ATPases**), the phosphorylation factor ATPases (**F-Type ATPases**), archaebacterial ATPases (**A-ATPases**), and the extracellular ATPases (**E-Type ATPases**). V-ATPases are part of the family of V-Type ATPases and are functionally different from P-Type ATPase,s F-Type ATPases, A-ATPases, and E-Type ATPases. All ATPases couple the hydrolysis of ATP with a particular cellular function or role. These roles include the movement of protons, ions, or small solutes across a membrane or perform hydrolysis of nucleotide tri and/or diphosphates [1, 8-11]. V-, F-, and some P-Type ATPases pump protons across a membrane. Most P-Type ATPases pump cations or phospholipids and E-Type ATPases generally hydrolyze nucleotide tri and/or diphosphates. The V-Type ATPases are structurally and mechanistically similar to F-Type ATPases which are involved in ATP synthesis. However, there are notable major

differences between V- and F-Type ATPases in how they function, localize, and are activated. F-Type ATPases can undergo a reversible reaction, whereas the V-Type ATPases pump protons in a single direction and evolved to not be reversible. V-Type ATPases play no known role in the production of ATP like typical F-type ATPases. V-Type ATPases are commonly found in internal vesicles or lysosomes whereas the F-type ATPases are generally found in the mitochondria of eukaryotes.

A-ATPases are more evolutionarily similar to V-ATPases and function similar to F-Type ATPases [12]. This similarity has caused some to believe that modern V-Type ATPases must have evolved from early archaea [12]. P- and E-Type ATPases are structurally and functionally different from F- and V-Type ATPases in that they have significantly fewer subunits, are regulated by different mechanisms, and are not involved in the pumping of protons across a membrane.

Vacuolar H^+-ATPases (V-ATPase) are evolutionarily conserved protein complexes that couple the hydrolysis of ATP with the pumping of protons across a membrane (**Fig. 4.1**). Much of our understanding of the V-ATPase comes from studies on yeast (*Saccharomyces cerevisiae*), mainly in part because of the easiness of genetic manipulation and culturing, and because loss of V-ATPase subunits in yeast does not necessarily result in death [13]. All higher eukaryotes contain the V-ATPase and the complex is essential in all eukaryotes tested except *Saccharomyces cerevisiae* [13]. There are at least 16 prokaryote species that utilize the V-ATPase and archaea A-Type ATPases, which are evolutionarily closer to the V-Type ATPases [12, 14]. Thus, the V-ATPase is important across many domains of life. Traditionally, these protein complexes were localized in cytoplasmic vacuoles, but reports have demonstrated that the V-ATPase is present at the

plasma membrane in highly specialized cells [13, 15, 16]. Since its identification in the late 1970's, the V-ATPase has been extensively studied, making it one of the better understood protein complexes present in eukaryotes.

4.3 The structure of Vacuolar H^+ ATPases

V-ATPases are multi-subunit protein complexes composed of a cytoplasmic peripheral V_1 domain and a transmembrane integral V_O domain (**Fig. 4.1**). Together these two domains work together as a rotary machine that pumps protons against their concentration gradient. These two domains are able to dissociate/associate and therefore can play a role in regulation [17]. The V_1 domain is about 650 kDa and contains 8 protein subunits (designated A-H). In a typical yeast V-ATPase, there are 3 copies of the A and B subunits, 2 copies of the E and G subunits, 1 or 2 copies of the H subunit, and single copies of C, D, and F (**Fig. 4.1**) [7]. The A and B subunits alternate positions to form an hexamer and the A subunit is where the ATP is bound and hydrolyzed (**Table 4.1**) [18]. The D and F subunits play a role in the central stalk that serves as the rotor that couples the energy from ATP hydrolysis to the rotation of the proteolipid ring (c, c', and c'' subunits in the V_O domain) [17]. The C, E, G, H, and the N-terminus part of subunit a (V_O domain) form the peripheral stalk which acts as a stator and prevents the reversible action of the V-ATPase [17].

The V_O domain in yeast is about 260 kDa and contains up to 6 unique subunits (designated a, d, c, c', c'', and e). The V_O domain is the site where protons are translocated from the cytoplasm to the lumen of a vesicle or extracellular space. The *a* subunit is the largest subunit of the whole complex and spans both the V_1 and V_O domains. The hydrophilic N terminus faces the cytoplasmic side and contains a pore where protons can

enter and be translocated through the complex. The C-terminal domain of subunit *a* contains 8 or 9 transmembrane domains and, although deeply imbedded in the plasma membrane, likely faces the cytoplasmic side [19-21]. Vph1p, the *a* subunit in yeast, was shown to contain an important arginine residue (Arg 735) that is critical for proton transport and important for ATPase activity [22]. The proteolipid ring consist of 4-5 copies of the c subunit with single copies of the c' and c'' subunits [7]. In higher eukaryotes, the c' is usually absent and often contain an accessory subunit, known as Ac45, that may play a role in Ca^{2+} dependent peptide secretion [23, 24]. The proteolipid ring is highly hydrophobic, arranged in a ring, and each contains a Glu residue located in transmembrane 4 for the c and c' subunits and transmembrane 3 of the c'' subunit [7, 25]. The Glu residue, due to its negative charge, binds protons as it travels around the rotating proteolipid. On top of the c subunit proteolipid ring resides a cork shaped d subunit which connects the rotating peripheral stalk [26]. The e subunit, which is absent in most other eukaryotes, associates with the Vph1p in yeast and serves no known function.

4.4 The functions of Vacuolar H^+ ATPases

In animal cells, V-ATPases are responsible for the acidification of clathrin-coated vesicles, endosomes, lysosomes, Golgi-derived vesicles, multivesicular bodies, and chromaffin granules. The majority of these functions are driven by proton gradients delivered by the V-ATPases. The mechanism of how protons are pumped is best understood in yeast. Protons enter through a hemi-channel in the a subunit and bind to a buried Glu residue in the c subunit proteolipid ring [7]. The hydrophobic environment of the lipid bilayer causes the protons to stay bound to the Glu residue as the proteolipid rotates. The A and B subunits facilitate ATP hydrolysis which leads to rotation of the D

and F subunits. The d subunit in the V_O domain rotates because it is connected to the D and F subunits. When the bound proton completes one rotation in the proteolipid ring, the buried arginine residue in the a subunit facilitates the displacement of the proton across the membrane through a luminal hemi-channel [7, 22].

Because the V-ATPase pumps protons at the expense of ATP, knowing the number of subunits can predict pump energetics and an approximate ratio of protons pumped per ATP (H^+/ATP). Stoichiometry predicts that the H^+/ATP ratio would be about $2H^+$/ATP because a typical yeast V-ATPase contains 6 proton carrying c subunits [27]. Experimentally, however, it was demonstrated that hydrolysis of a single ATP was dependent on the pH gradient [28]. Kettner et al demonstrated that when the pH gradient of the cytoplasm and the vacuole differed by 2.5 or 1.5 pH units, a single ATP molecule could energize the flow of 2.9 protons or 4.1 protons, respectively [28].

The pumping of protons from this complex have been linked to numerous functions. V-ATPases have been implicated in receptor mediated endocytosis in rat hepatocytes by creating a pH gradient between the endocytic compartments [29]. In yeast, the functions of the V-ATPase include pH homeostasis and osmotic stress [30, 31]. Although somewhat controversial, it has been reported that acidification from the V-ATPase is required for homotypic vacuole fusion in yeast [32].

While the primary function of this complex is to act as proton pump to acidify vacuoles (referred to as the canonical functions), there are numerous functions in the cell that V-ATPases provide that do not directly involve proton pumping (referred to as the non-canonical functions). The *a* subunit has been routinely shown to be important for targeting of the V-ATPases complex in the cell [33-35]. Mammalian cells have 4 a subunit

isomers and each targets different compartments. Even after decades of research studying the protein complex, new features of the V-ATPases, both canonical and noncanonical, are routinely being discovered. Thus, the importance of V-ATPases for organisms has proven to be complex and multifunctional.

4.5 Assembly of Vacuolar H^+ ATPases

The assembly of the V-ATPase occurs in the endoplasmic reticulum (ER), but the two domains can disassociate/associate independently and their disassociations can be regulated. **Table 4.2** summarizes the functions of the accessory proteins necessary to build or transport the V-ATPase from the ER. In the ER Vma12p, Vma21p, Vma22p, Voalp, and Pkr1p are known protein chaperons that play a role in the V-ATPase assembly. Vma21p promotes the assembly of the proteolipid into a ring and aids in the binding of subunit d [7, 36]. Vma12p and Vma22p interact with the *a* subunit and facilitates its assembly with the proteolipid ring [37-39]. If either Vma12p or Vma22p are absent, subunit *a* is rapidly degraded and the V_O domain is unable to assemble [40]. Voa1p was also shown to play a role in the assembly of the V-ATPase by association with *vma21* and the core proteolipid [41]. Voa1p disassociates from the V_O domain once all the components have been assembled [41]. When the *a* subunit binds to the Vma21p/proteolipid complex, Vma12p and Vma22p dissociate from the forming complex [40]. *PKR1* also appears to work in conjunction with other V-ATPase assembly factors to aid in the stability of the complex [42]. Ablation of *PKR1* was also shown to be important for subunit a stability, assembly of the V_O domain, and export out of the ER [42].

When and how the V_1 and V_O domain proteins assemble is not completely understood. Independent or concerted assembly are two models that have been proposed

for how the V_1 domain is assembled [40]. In the concerted assembly model, a single A subunit of the V_1 domain forms a complex with the *a* subunit of the V_O domain [40]. Following binding of both domains, the remaining V_1 domain proteins auto-assemble to create the complete complex. In the independent assembly model, the V_1 domain proteins form spontaneously in the cytoplasm and then bind to a fully formed V_O domain [40].

Once the V-ATPase is assembled, it needs to move out of the ER in order to perform its functions. It was previously demonstrated that *hph1* and *hph2* are required for V-ATPase posttranslational translocation from the ER [43]. Both *hph1* and *hph2* are homologous integral ER membrane portions which likely work with the ER translocation pore complex known as Sec62/Sec63 [43]. Ablation of *hph1* and *hph2* also resulted in instability of the a subunit, suggesting that these proteins may also play some role in assembly [43]. Vma21p is known to interact with the c' subunit and aids in the export from the ER [44]. Ablation of *PKR1* resulted in a 90% decrease of V_O domain export out of the ER [42]

4.6 Regulation of Vacuolar H^+ ATPases

Regulation of the V-ATPase is most often associated with environmental stress. Unlike P-Type ATPases that change activity based on phosphorylation levels, the V-ATPase use different mechanisms to regulate assembly and activity. One unique feature about the V-Type ATPases is that once the V-ATPase is fully assembled, its activity can be regulated by adjusting the level of the V_1-V_O complex assembly. One way to achieve differing levels of complex assembly is through the reversible dissociation of the two domains. During complex disassembly, the V_1 domain is released in the cytosol while the V_O domain remains bound to the membrane. While the V_O domain remains fully intact in

the membrane, the c subunit of the V_1 domain detaches from the complex while the other subunits of the V_1 domain remain attached. The separation of both domains results in a complete loss of ATPase activity and proton translocation. Complex dissociation was first discovered during glucose deprivation in yeast [45]. Once favorable conditions improve, i.e. more glucose is present in the cytoplasm, the complex is able to form again and resume ATPase and proton translocation activity. No new proteins need to be synthesized for reassembly, making for a quick response when conditions improve.

The RAVE complex (regulator of the ATPase of vacuolar and endosomal membranes) is the first assembly complex to be implicated in both assembly and reassembly of the V_1 and V_O domains. The RAVE complex is composed of Rav1p, Rav2p and Skp1p and involved in glucose-triggered assembly of the V-ATPase. Rav1p is the central component of the RAVE complex that holds together Rav2p and Skp1p and interacts with the V_1 domain proteins E and G [46]. Rav2p interacts with Rav1p and is important for V_1-V_O assembly [46]. Skp1p is a member of SCF ubiquitin ligases which play roles in immunity, signaling, cell division, and transcription [47]. Skp1p interacts with Rav1p and is essential for V_1 assembly [47]. It is believed that RAVE complex may work by docking the peripheral stock to the membrane bound V_O domain by interacting with the V_1 C subunit [48]. Interestingly, it was demonstrated that the C subunit was not able to assemble with the V_1-V_O domains in the absence of the RAVE complex [48]. While the RAVE complex was initially discovered in yeast, homologues of this complex can be found in a variety of eukaryotes. The *d* subunit of the V_O domain has been suggested as playing a role in the reversible dissociation of the V_1 and V_O complex [26].

While the assembly and disassembly were initially discovered in yeast, other work has suggested that altering assembly state may be more universal. Human proximal tubular HK-2 cells and renal epithelial LLC-PK1 cells were the first identified mammalian cells to change assembly state in response to glucose levels [49, 50]. In both of these human cell lines, cytoplasmic glucose levels were shown to result in loss of organellular acidification and release of the V_1 domain into the cytoplasm. Assembly of the V-ATPase in LLC-PK1 cells was concentration dependent in a manner similar to yeast [49, 51].

Because glucose levels were linked to complex association and disassociation, several investigators looked for glucose dependent signal transduction pathways as a possible mechanism of V-ATPase regulation. Glycolytic enzymes such as aldolase and phosphofructokinase (PKF) have been implicated in V-ATPase assembly [21, 52-54]. Ablation of aldolase has been shown to prevent V-ATPase assembly [52]. A point mutation that disrupts aldolase from binding to the B and E subunits but remains catalytical active resulted in reduced assembly of V_1 and V_O [53]. These studies suggested that aldolase could be an important glucose sensor and may trigger complex assembly. PFK was shown to bind to V_O subunits and loss of PFK resulted in reduced assembly and proton pumping [21, 55]. Further evidence that glucose plays a role in complex assembly comes from studies with phosphatidylinositol 3-kinase (PI3K) [50]. Chemical inhabitation of PI3K resulted in significantly reduced glucose stimulated assembly and trafficking [50]. Collectively, these results strongly suggest that V-ATPase assembly is regulated by glucose concentration.

Recently other mechanisms of regulation and assembly have been demonstrated that are independent of glucose levels. Increased salt stress was previously demonstrated

to increase V-ATPase activity [56]. High extracellular pH was also shown to increase V-ATPase activity and assembly [57]. Additionally, cells exposed to high extracellular pH were unable to undergo reversible disassembly and continued proton translocation when glucose levels were depleted [57]. The level of V-ATPase assembly in mammalian immature dendritic cells was shown to change in response to changing lysosomal pH [58].

4.7 References

1. Forgac, M., *Structure and function of vacuolar class of ATP-driven proton pumps.* Physiological reviews, 1989. **69**(3): p. 765-796.
2. Stevens, T.H. and M. Forgac, *Structure, function and regulation of the vacuolar (H^+)-ATPase.* Annu Rev Cell Dev Biol, 1997. **13**: p. 779-808.
3. Forgac, M., *Structure and properties of the vacuolar (H^+)-ATPases.* J Biol Chem, 1999. **274**(19): p. 12951-4.
4. Nishi, T. and M. Forgac, *The vacuolar (H^+)-ATPases--nature's most versatile proton pumps.* Nat Rev Mol Cell Biol, 2002. **3**(2): p. 94-103.
5. Cotter, K., et al., *Recent Insights into the Structure, Regulation, and Function of the V-ATPases.* Trends Biochem Sci, 2015. **40**(10): p. 611-622.
6. Beyenbach, K.W. and H. Wieczorek, *The V-type H^+ ATPase: molecular structure and function, physiological roles and regulation.* Journal of Experimental Biology, 2006. **209**(4): p. 577-589.
7. Forgac, M., *Vacuolar ATPases: rotary proton pumps in physiology and pathophysiology.* Nature Reviews Molecular Cell Biology, 2007. **8**: p. 917.
8. Plesner, L., *Ecto-ATPases: Identities and Functions*, in *International Review of Cytology*, K.W. Jeon and J. Jarvik, Editors. 1995, Academic Press. p. 141-214.
9. Palmgren, M.G. and P. Nissen, *P-type ATPases.* Annu Rev Biophys, 2011. **40**: p. 243-66.
10. Pedersen, P.L. and L.M. Amzel, *F-type ATPases. Introduction.* J Bioenerg Biomembr, 1992. **24**(5): p. 427-8.

11. Mukohata, Y. and M. Yoshida, *The H^+-translocating ATP synthase in Halobacterium halobium differs from F_0F_1-ATPase/synthase.* J Biochem, 1987. **102**(4): p. 797-802.

12. Gogarten, J.P., et al., *Evolution and isoforms of V-ATPase subunits.* The Journal of Experimental Biology, 1992. **172**(1): p. 137.

13. Manolson, M.F., et al., *STV1 gene encodes functional homologue of 95-kDa yeast vacuolar H^+-ATPase subunit Vph1p.* Journal of Biological Chemistry, 1994. **269**(19): p. 14064-14074.

14. Lolkema, J.S., Y. Chaban, and E.J. Boekema, *Subunit Composition, Structure, and Distribution of Bacterial V-Type ATPases.* Journal of Bioenergetics and Biomembranes, 2003. **35**(4): p. 323-335.

15. Wieczorek, H., et al., *Structure and regulation of insect plasma membrane H^+V-ATPase.* Journal of Experimental Biology, 2000. **203**(1): p. 127.

16. Hayashi, M., et al., *Vacuolar H^+-ATPase Localized in Plasma Membranes of Malaria Parasite Cells, Plasmodium falciparum, Is Involved in Regional Acidification of Parasitized Erythrocytes.* Journal of Biological Chemistry, 2000. **275**(44): p. 34353-34358.

17. Arata, Y., J.D. Baleja, and M. Forgac, *Localization of Subunits D, E, and G in the Yeast V-ATPase Complex Using Cysteine-Mediated Cross-Linking to Subunit B.* Biochemistry, 2002. **41**(37): p. 11301-11307.

18. Shao, E., et al., *Mutational Analysis of the Non-homologous Region of Subunit A of the Yeast V-ATPase.* Journal of Biological Chemistry, 2003. **278**(15): p. 12985-12991.

19. Leng, X.-H., T. Nishi, and M. Forgac, *Transmembrane Topography of the 100-kDa a Subunit (Vph1p) of the Yeast Vacuolar Proton-translocating ATPase.* Journal of Biological Chemistry, 1999. **274**(21): p. 14655-14661.

20. Wang, Y., M. Toei, and M. Forgac, *Analysis of the Membrane Topology of Transmembrane Segments in the C-terminal Hydrophobic Domain of the Yeast Vacuolar ATPase Subunit a (Vph1p) by Chemical Modification.* Journal of Biological Chemistry, 2008. **283**(30): p. 20696-20702.

21. Su, Y., et al., *The a-Subunit of the V-type H^+-ATPase Interacts with Phosphofructokinase-1 in Humans.* Journal of Biological Chemistry, 2003. **278**(22): p. 20013-20018.

22. Kawasaki-Nishi, S., T. Nishi, and M. Forgac, *Arg-735 of the 100-kDa subunit a of the yeast V-ATPase is essential for proton translocation.* Proceedings of the National Academy of Sciences, 2001. **98**(22): p. 12397.

23. Jansen, E.J.R., et al., *Accessory subunit Ac45 controls the V-ATPase in the regulated secretory pathway.* Biochimica et Biophysica Acta (BBA) - Molecular Cell Research, 2008. **1783**(12): p. 2301-2310.

24. Supek, F., et al., *A novel accessory subunit for vacuolar H^+-ATPase from chromaffin granules.* Journal of Biological Chemistry, 1994. **269**(39): p. 24102-24106.

25. Wilkens, S. and M. Forgac, *Three-dimensional Structure of the Vacuolar ATPase Proton Channel by Electron Microscopy.* Journal of Biological Chemistry, 2001. **276**(47): p. 44064-44068.

26. Iwata, M., et al., *Crystal structure of a central stalk subunit C and reversible association/dissociation of vacuole-type ATPase.* Proceedings of the National Academy of Sciences, 2004. **101**(1): p. 59.

27. Cross Richard, L. and V. Müller, *The evolution of A-, F-, and V-type ATP synthases and ATPases: reversals in function and changes in the H^+/ATP coupling ratio.* FEBS Letters, 2004. **576**(1-2): p. 1-4.

28. Kettner, C., et al., *Electrophysiological Analysis of the Yeast V-Type Proton Pump: Variable Coupling Ratio and Proton Shunt.* Biophysical Journal, 2003. **85**(6): p. 3730-3738.

29. Harada, M., et al., *Bafilomycin A1, a specific inhibitor of vacuolar-type H^+-ATPases, inhibits the receptor-mediated endocytosis of asialoglycoproteins in isolated rat hepatocytes.* Journal of Hepatology, 1996. **24**(5): p. 594-603.

30. Tarsio, M., et al., *Consequences of Loss of Vph1 Protein-containing Vacuolar ATPases (V-ATPases) for Overall Cellular pH Homeostasis.* Journal of Biological Chemistry, 2011. **286**(32): p. 28089-28096.

31. Li, S.C., et al., *Vacuolar H^+-ATPase Works in Parallel with the HOG Pathway To Adapt Saccharomyces cerevisiae Cells to Osmotic Stress.* Eukaryotic Cell, 2012. **11**(3): p. 282.

32. Strasser, B., et al., *The V-ATPase proteolipid cylinder promotes the lipid-mixing stage of SNARE-dependent fusion of yeast vacuoles.* The EMBO Journal, 2011. **30**(20): p. 4126.

33. Dettmer, J., et al., *Vacuolar H^+-ATPase Activity Is Required for Endocytic and Secretory Trafficking in Arabidopsis.* The Plant Cell, 2006. **18**(3): p. 715.

34. Bagh, M.B., et al., *Misrouting of v-ATPase subunit V0a1 dysregulates lysosomal acidification in a neurodegenerative lysosomal storage disease model.* Nature Communications, 2017. **8**: p. 14612.

35. Marshansky, V. and M. Futai, *The V-type H^+-ATPase in vesicular trafficking: targeting, regulation and function.* Current Opinion in Cell Biology, 2008. **20**(4): p. 415-426.

36. Graham, L.A., A.R. Flannery, and T.H. Stevens, *Structure and Assembly of the Yeast V-ATPase.* Journal of Bioenergetics and Biomembranes, 2003. **35**(4): p. 301-312.

37. Hirata, R., et al., *VMA12 is essential for assembly of the vacuolar H^+-ATPase subunits onto the vacuolar membrane in Saccharomyces cerevisiae.* Journal of Biological Chemistry, 1993. **268**(2): p. 961-967.

38. Jackson, D.D. and T.H. Stevens, *VMA12 Encodes a Yeast Endoplasmic Reticulum Protein Required for Vacuolar H^+-ATPase Assembly.* Journal of Biological Chemistry, 1997. **272**(41): p. 25928-25934.

39. Hill, K.J. and T.H. Stevens, *Vma22p Is a Novel Endoplasmic Reticulum-associated Protein Required for Assembly of the Yeast Vacuolar H^+-ATPase Complex.* Journal of Biological Chemistry, 1995. **270**(38): p. 22329-22336.

40. Smardon, A.M. and P.M. Kane, *Chapter 1 - Vacuolar H^+ ATPase Assembly*, in *Handbook of H^+-ATPases*, S. Nakamura, Editor. 2014, Pan Standford Publishing Pte. Ltd: Singapore. p. 1-30.

41. Ryan, M., et al., *Voa1p Functions in V-ATPase Assembly in the Yeast Endoplasmic Reticulum.* Molecular Biology of the Cell, 2008. **19**(12): p. 5131-5142.

42. Davis-Kaplan, S.R., et al., *PKR1 Encodes an Assembly Factor for the Yeast V-Type ATPase.* Journal of Biological Chemistry, 2006. **281**(42): p. 32025-32035.

43. Piña, F.J., et al., *Hph1 and Hph2 Are Novel Components of the Sec63/Sec62 Posttranslational Translocation Complex That Aid in Vacuolar Proton ATPase Biogenesis.* Eukaryotic Cell, 2011. **10**(1): p. 63-71.

44. Malkus, P., et al., *Role of Vma21p in Assembly and Transport of the Yeast Vacuolar ATPase.* Molecular Biology of the Cell, 2004. **15**(11): p. 5075-5091.

45. Kane, P.M., *Disassembly and Reassembly of the Yeast Vacuolar H^+-ATPase in Vivo.* Journal of Biological Chemistry, 1995. **270**(28): p. 17025-17032.

46. Smardon, A.M., M. Tarsio, and P.M. Kane, *The RAVE Complex Is Essential for Stable Assembly of the Yeast V-ATPase.* Journal of Biological Chemistry, 2002. **277**(16): p. 13831-13839.

47. Seol, J.H., et al., *Skp1 forms multiple protein complexes, including RAVE, a regulator of V-ATPase assembly.* Nature Cell Biology, 2001. **3**: p. 384.

48. Smardon, A.M. and P.M. Kane, *RAVE Is Essential for the Efficient Assembly of the C Subunit with the Vacuolar H^+-ATPase.* Journal of Biological Chemistry, 2007. **282**(36): p. 26185-26194.

49. Nakamura, S., *Glucose activates H^+-ATPase in kidney epithelial cells.* American Journal of Physiology-Cell Physiology, 2004. **287**(1): p. C97-C105.

50. Sautin, Y.Y., et al., *Phosphatidylinositol 3-Kinase-Mediated Effects of Glucose on Vacuolar H+-ATPase Assembly, Translocation, and Acidification of Intracellular Compartments in Renal Epithelial Cells.* Molecular and Cellular Biology, 2005. **25**(2): p. 575-589.

51. Parra, K.J. and P.M. Kane, *Reversible Association between the $V_1$and V_0 Domains of Yeast Vacuolar H^+-ATPase Is an Unconventional Glucose-Induced Effect.* Molecular and Cellular Biology, 1998. **18**(12): p. 7064-7074.

52. Lu, M., et al., *The Glycolytic Enzyme Aldolase Mediates Assembly, Expression, and Activity of Vacuolar H^+-ATPase.* Journal of Biological Chemistry, 2004. **279**(10): p. 8732-8739.

53. Lu, M., et al., *Physical Interaction between Aldolase and Vacuolar H^+-ATPase Is Essential for the Assembly and Activity of the Proton Pump.* Journal of Biological Chemistry, 2007. **282**(34): p. 24495-24503.

54. Lu, M., et al., *Interaction between Aldolase and Vacuolar H^+-ATPase: EVIDENCE FOR DIRECT COUPLING OF GLYCOLYSIS TO THE ATP-HYDROLYZING PROTON PUMP.* Journal of Biological Chemistry, 2001. **276**(32): p. 30407-30413.

55. Su, Y., et al., *Human H^+ATPase a4 subunit mutations causing renal tubular acidosis reveal a role for interaction with phosphofructokinase-1.* American Journal of Physiology-Renal Physiology, 2008. **295**(4): p. F950-F958.

56. Li, S.C., et al., *Vacuolar H^+-ATPase Works in Parallel with the HOG Pathway To Adapt Saccharomyces cerevisiae Cells to Osmotic Stress.* Eukaryotic Cell, 2012. **11**(3): p. 282-291.

57. Diakov, T.T. and P.M. Kane, *Regulation of Vacuolar Proton-translocating ATPase Activity and Assembly by Extracellular pH.* Journal of Biological Chemistry, 2010. **285**(31): p. 23771-23778.

58. Trombetta, E.S., et al., *Activation of Lysosomal Function During Dendritic Cell Maturation.* Science, 2003. **299**(5611): p. 1400.

59. Shao, E. and M. Forgac, *Involvement of the Nonhomologous Region of Subunit A of the Yeast V-ATPase in Coupling and in Vivo Dissociation.* Journal of Biological Chemistry, 2004. **279**(47): p. 48663-48670.

60. Gimble, F.S. and J. Thorner, *Homing of a DNA endonuclease gene by meiotic gene conversion in Saccharomyces cerevisiae.* Nature, 1992. **357**: p. 301.

61. Hirata, R. and Y. Anraku, *Mutations at the putative junction sites of the yeast VMA1 protein, the catalytic subunit of the vacuolar membrane H^+-ATPase, inhibit its processing by protein splicing.* Biochemical and Biophysical Research Communications, 1992. **188**(1): p. 40-47.

62. Liu, J. and P.M. Kane, *Mutational Analysis of the Catalytic Subunit of the Yeast Vacuolar Proton-Translocating ATPase.* Biochemistry, 1996. **35**(33): p. 10938-10948.

63. Păunescu, T.G., et al., *Expression of the 56-kDa B2 subunit isoform of the vacuolar H^+-ATPase in proton-secreting cells of the kidney and epididymis.* American Journal of Physiology-Cell Physiology, 2004. **287**(1): p. C149-C162.

64. Holliday, L.S., et al., *The Amino-terminal Domain of the B Subunit of Vacuolar H^+-ATPase Contains a Filamentous Actin Binding Site.* Journal of Biological Chemistry, 2000. **275**(41): p. 32331-32337.

65. Liu, Q., et al., *Site-directed Mutagenesis of the Yeast V-ATPase B Subunit (Vma2p).* Journal of Biological Chemistry, 1996. **271**(4): p. 2018-2022.

66. Drory, O., F. Frolow, and N. Nelson, *Crystal structure of yeast V-ATPase subunit C reveals its stator function.* EMBO reports, 2004. **5**(12): p. 1148.

67. Vitavska, O., H. Wieczorek, and H. Merzendorfer, *A Novel Role for Subunit C in Mediating Binding of the H^+-V-ATPase to the Actin Cytoskeleton.* Journal of Biological Chemistry, 2003. **278**(20): p. 18499-18505.

68. Vitavska, O., H. Merzendorfer, and H. Wieczorek, *The V-ATPase Subunit C Binds to Polymeric F-actin as Well as to Monomeric G-actin and Induces Cross-linking of Actin Filaments.* Journal of Biological Chemistry, 2005. **280**(2): p. 1070-1076.

69. Curtis, K.K., et al., *Mutational analysis of the subunit C (Vma5p) of the yeast vacuolar H^+-ATPase.* J Biol Chem, 2002. **277**(11): p. 8979-88.

70. Oot, R.A. and S. Wilkens, *Subunit Interactions at the V_1-V_o Interface in Yeast Vacuolar ATPase.* Journal of Biological Chemistry, 2012. **287**(16): p. 13396-13406.

71. Graham, L.A., K.J. Hill, and T.H. Stevens, *VMA8 encodes a 32-kDa V_1 subunit of the Saccharomyces cerevisiae vacuolar H^+-ATPase required for function and assembly of the enzyme complex.* J Biol Chem, 1995. **270**(25): p. 15037-44.

72. Xu, T. and M. Forgac, *Subunit D (Vma8p) of the yeast vacuolar H^+-ATPase plays a role in coupling of proton transport and ATP hydrolysis.* J Biol Chem, 2000. **275**(29): p. 22075-81.

73. Ho, M.N., et al., *Isolation of vacuolar membrane H(+)-ATPase-deficient yeast mutants; the VMA5 and VMA4 genes are essential for assembly and activity of the vacuolar H(+)-ATPase.* J Biol Chem, 1993. **268**(1): p. 221-7.

74. Owegi, M.A., et al., *Mutational analysis of the stator subunit E of the yeast V-ATPase.* J Biol Chem, 2005. **280**(18): p. 18393-402.

75. Makyio, H., et al., *Structure of a central stalk subunit F of prokaryotic V-type ATPase/synthase from Thermus thermophilus.* The EMBO Journal, 2005. **24**(22): p. 3974.

76. Aviezer-Hagai, K., V. Padler-Karavani, and N. Nelson, *Biochemical support for the V-ATPase rotary mechanism: antibody against HA-tagged Vma7p or Vma16p but not Vma10p inhibits activity.* J Exp Biol, 2003. **206**(Pt 18): p. 3227-37.

77. Charsky, C.M.H., N.J. Schumann, and P.M. Kane, *Mutational Analysis of Subunit G (Vma10p) of the Yeast Vacuolar H^+-ATPase.* Journal of Biological Chemistry, 2000. **275**(47): p. 37232-37239.

78. Geyer, M., et al., *Subunit H of the V-ATPase Binds to the Medium Chain of Adaptor Protein Complex 2 and Connects Nef to the Endocytic Machinery.* Journal of Biological Chemistry, 2002. **277**(32): p. 28521-28529.

79. Wilkens, S., T. Inoue, and M. Forgac, *Three-Dimensional Structure of the Vacuolar ATPase: LOCALIZATION OF SUBUNIT H BY DIFFERENCE IMAGING AND CHEMICAL CROSS-LINKING.* Journal of Biological Chemistry, 2004. **279**(40): p. 41942-41949.

80. Parra, K.J., K.L. Keenan, and P.M. Kane, *The H Subunit (Vma13p) of the Yeast V-ATPase Inhibits the ATPase Activity of Cytosolic V_1 Complexes.* Journal of Biological Chemistry, 2000. **275**(28): p. 21761-21767.

81. Jefferies, K.C. and M. Forgac, *Subunit H of the Vacuolar (H^+) ATPase Inhibits ATP Hydrolysis by the Free V_1 Domain by Interaction with the Rotary Subunit F.* Journal of Biological Chemistry, 2008. **283**(8): p. 4512-4519.

82. Geyer, M., O.T. Fackler, and B.M. Peterlin, *Subunit H of the V-ATPase involved in endocytosis shows homology to beta-adaptins.* Mol Biol Cell, 2002. **13**(6): p. 2045-56.

83. Kawasaki-Nishi, S., T. Nishi, and M. Forgac, *Yeast V-ATPase Complexes Containing Different Isoforms of the 100-kDa a-subunit Differ in Coupling Efficiency and in Vivo Dissociation.* Journal of Biological Chemistry, 2001. **276**(21): p. 17941-17948.

84. Toyomura, T., et al., *From Lysosomes to the Plasma Membrane: LOCALIZATION OF VACUOLAR TYPE H^+-ATPase WITH THE a3 ISOFORM DURING OSTEOCLAST DIFFERENTIATION.* Journal of Biological Chemistry, 2003. **278**(24): p. 22023-22030.

85. Hurtado-Lorenzo, A., et al., *V-ATPase interacts with ARNO and Arf6 in early endosomes and regulates the protein degradative pathway.* Nature Cell Biology, 2006. **8**: p. 124.

86. Hiesinger, P.R., et al., *The v-ATPase V_0 Subunit a1 Is Required for a Late Step in Synaptic Vesicle Exocytosis in Drosophila.* Cell, 2005. **121**(4): p. 607-620.

87. Peri, F. and C. Nüsslein-Volhard, *Live Imaging of Neuronal Degradation by Microglia Reveals a Role for V_0-ATPase a1 in Phagosomal Fusion In Vivo.* Cell, 2008. **133**(5): p. 916-927.

88. Sun-Wada, G.-H., et al., *The a3 isoform of V-ATPase regulates insulin secretion from pancreatic β-cells.* Journal of Cell Science, 2006. **119**(21): p. 4531.

89. Marshansky, V., *The V-ATPase a2-subunit as a putative endosomal pH-sensor.* Biochemical Society Transactions, 2007. **35**(5): p. 1092.

90. Zhang, W., et al., *V-ATPase V_0 Sector Subunit a1 in Neurons Is a Target of Calmodulin.* Journal of Biological Chemistry, 2008. **283**(1): p. 294-300.

91. Wang, D., et al., *C^{2+}–Calmodulin regulates SNARE assembly and spontaneous neurotransmitter release via v-ATPase subunit V_0a1.* The Journal of Cell Biology, 2014. **205**(1): p. 21.

92. Bayer, M.J., et al., *Vacuole membrane fusion.* The Journal of Cell Biology, 2003. **162**(2): p. 211.

93. Morel, N., J.-C. Dedieu, and J.-M. Philippe, *Specific sorting of the a1 isoform of the V-H^+ ATPase a subunit to nerve terminals where it associates with both synaptic vesicles and the presynaptic plasma membrane.* Journal of Cell Science, 2003. **116**(23): p. 4751.

94. Stasic, A.J., et al., *The Toxoplasma Vacuolar H^+-ATPase regulates intracellular pH, and impacts the maturation of essential secretory proteins.* Cell Reports, 2019.

95. Hirata, T., et al., *Subunit Rotation of Vacuolar-type Proton Pumping ATPase: RELATIVE ROTATION OF THE G AND c SUBUNITS.* Journal of Biological Chemistry, 2003. **278**(26): p. 23714-23719.

96. Huss, M., et al., *Concanamycin A, the Specific Inhibitor of V-ATPases, Binds to the V_o Subunit c.* Journal of Biological Chemistry, 2002. **277**(43): p. 40544-40548.

97. Sennoune, S.R., D. Luo, and R. Martinez-Zaguilán, *Plasmalemmal vacuolar-type H^+-ATPase in cancer biology.* Cell Biochemistry and Biophysics, 2004. **40**(2): p. 185-206.

98. Bowman, B.J. and E.J. Bowman, *Mutations in Subunit c of the Vacuolar ATPase Confer Resistance to Bafilomycin and Identify a Conserved Antibiotic Binding Site.* Journal of Biological Chemistry, 2002. **277**(6): p. 3965-3972.

99. Powell, B., L.A. Graham, and T.H. Stevens, *Molecular Characterization of the Yeast Vacuolar H^+-ATPase Proton Pore.* Journal of Biological Chemistry, 2000. **275**(31): p. 23654-23660.

100. Sun, S.Z., X.S. Xie, and D.K. Stone, *Isolation and reconstitution of the dicyclohexylcarbodiimide-sensitive proton pore of the clathrin-coated vesicle proton translocating complex.* Journal of Biological Chemistry, 1987. **262**(30): p. 14790-14794.

101. Hirata, R., et al., *VMA11 and VMA16 Encode Second and Third Proteolipid Subunits of the Saccharomyces cerevisiae Vacuolar Membrane H^+-ATPase.* Journal of Biological Chemistry, 1997. **272**(8): p. 4795-4803.

102. Umemoto, N., Y. Ohya, and Y. Anraku, *VMA11, a novel gene that encodes a putative proteolipid, is indispensable for expression of yeast vacuolar membrane H^+-ATPase activity.* Journal of Biological Chemistry, 1991. **266**(36): p. 24526-32.

103. Whyteside, G., et al., *Assembly of the yeast vacuolar H^+-ATPase and ATP hydrolysis occurs in the absence of subunit c".* FEBS Letters, 2005. **579**(14): p. 2981-2985.

104. Nishi, T., S. Kawasaki-Nishi, and M. Forgac, *Expression and function of the mouse V-ATPase d subunit isoforms.* J Biol Chem, 2003. **278**(47): p. 46396-402.

105. Owegi, M.A., et al., *Identification of a Domain in the Vo Subunit d That Is Critical for Coupling of the Yeast Vacuolar Proton-translocating ATPase.* Journal of Biological Chemistry, 2006. **281**(40): p. 30001-30014.

106. Sambade, M. and P.M. Kane, *The Yeast Vacuolar Proton-translocating ATPase Contains a Subunit Homologous to the Manduca sexta and Bovine e Subunits That Is Essential for Function.* Journal of Biological Chemistry, 2004. **279**(17): p. 17361-17365.

107. De-Qin, Y., et al., *V-ATPase subunit ATP6AP1 (Ac45) regulates osteoclast differentiation, extracellular acidification, lysosomal trafficking, and protease exocytosis in osteoclast-mediated bone resorption.* Journal of Bone and Mineral Research, 2012. **27**(8): p. 1695-1707.

TABLES

Table 4.1: Known functions and/or cellular interactions of the V-ATPase subunits and assembly/accessory proteins

Domain	Subunit	Total/ Cell	Yeast Gene	Stator/ Rotary	Subunit Function and Cellular Interactions	Reference
V_1	A	3	*vma1*	Stator	ATP hydrolysis, regulation, endonuclease[1]	[18, 59-62]
	B	3	*vma2*	Stator	Non-catalytic ATP site, binds actin and aldolase	[52, 63-65]
	C	1	*vma5*	Stator	Regulation, stalk stability, binds actin, stabilizes binding of E and G subunits, complex assembly	[66-70]
	D	1	*vma8*	Rotary	Rotating stalk, complex assembly, and coupling of proton transport	[71, 72]
	E	2	*vma4*	Stator	Complex assembly, binds RAVE complex and aldolase	[46, 52, 73, 74]
	F	1	*vma7*	Rotary	Rotating mechanism, complex assembly	[75, 76]
	G	2	*vma10*	Stator	Binds RAVE complex, stabilizes E subunit	[46, 77]
	H	1	*vma13*	Stator	Regulation, binds NEF, endocytosis	[78-82]
V_O	a	1	*vph1, stv1*	Stator	H^+ translocation, targeting/trafficking, vesicle exocytosis, interacts with t-SNAREs, vesicular/phagosomal fusion, insulin regulation, binds Phosphofructokinase-1, binds aldolase, binds calmodulin, endosomal pH-sensor, virulence	[21, 22, 53, 83-94]
	$c^{2,3}$	4	*vma3*	Rotary	Principal player H^+ translocation, assembly, rotation, DCCD binding site	[95-100]
	c'^{4}	1	*vma11*	Rotary	H^+ translocation, rotation, assembly, binds assembly factor *vma21*	[44, 99, 101, 102]
	c''^{4}	1	*vma16*	Rotary	H^+ translocation, rotation	[99, 101, 103]
	d	1	*vma6*	Rotary	Coupling of proton transport/ATP hydrolysis and association/dissociation of vacuole-type ATPase	[26, 104, 105]
	e^{5}	1	*vma9*	Stator	Unknown	[7, 106]
	-	1	*ac45*	Rotary	Ca^{2+}-dependent peptide secretion, lysosomal trafficking, extracellular acidification and protease exocytosis	[23, 24, 107]

[1]VMA1 is synthesized as a 119 kDa fragment that, through an unusual protein splicing reaction, creates a 50 kDa protein (PI-Scel) that has endonuclease activity. The A subunit itself does not have any known endonuclease activity.
[2]Subunit c is the site where concanamycin A and bafilomycin A_1 binds and inhibits the V-ATPase.
[3]Subunit c is present in the proteolipid ring and is believed to have many copies present
[4]Part of the proteolipid ring and likely expressed as a single copy per complex.
[5]The e subunit is generally not found in other organisms except yeast cells.

Table 4.2: Known assembly or accessory proteins associated with the V-ATPase

	Gene	Organism[1]	Function	Reference
Assembly/ ER Transport	*voa1*	yeast	Binds *vma21*, aids in assembly of proteolipid ring	[41]
	vma12	yeast	Mediates assembly of subunit a with proteolipid, anchors *vma22* to ER membrane	[37, 38]
	vma21	yeast	Assembly and stability of the V_O domain proteolipid, ER transport	[44]
	vma22	yeast	Mediates assembly of subunit a with proteolipid, binds to *vma12*	[39]
	aldolase	yeast	V-ATPase assembly and regulation	[52-54]
	pkr1	yeast	General V-ATPase assembly and ER export	[42]
	hph1	yeast	Posttranslational translocation of V-ATPase, stability of *vph1,* interacts with the Sec62/Sec63 complex in V-ATPase biogenesis	[43]
	hph2	yeast	Posttranslational translocation of V-ATPase, stability of *vph1,* interacts with the Sec62/Sec63 complex in V-ATPase biogenesis	[43]
V_1-V_O complex association/ dissociation	*rav1*	yeast	Component of RAVE, glucose trigged V-ATPase assembly,	[46]
	rav2	yeast	Component of RAVE, glucose trigged V-ATPase assembly,	[46]
	skp1	yeast	Component of RAVE, glucose trigged V-ATPase assembly,	[46, 47]

[1]Organism where the first description of the function was identified.

FIGURES

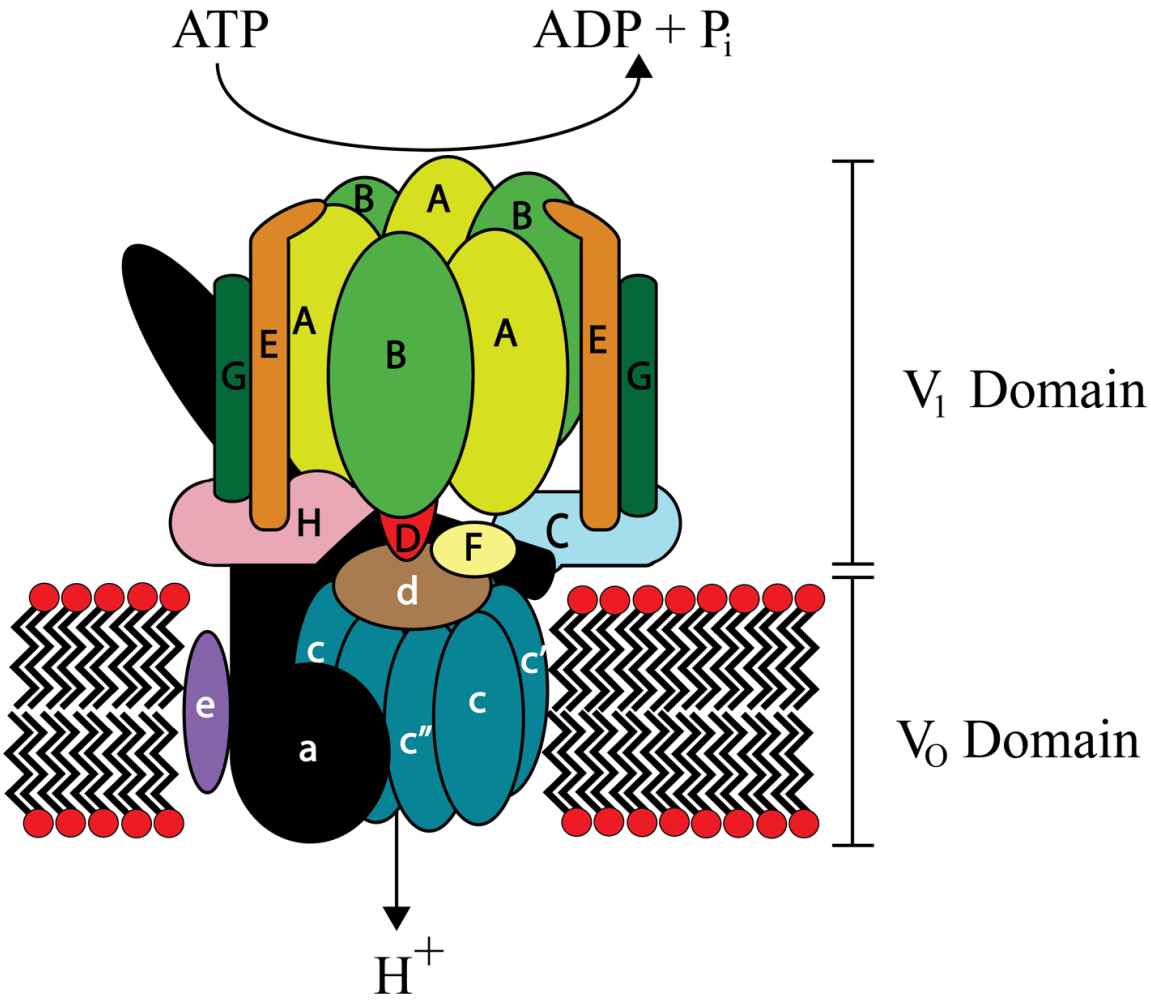

Figure 4.1. A typical yeast Vacuolar H^+ ATPase. The vacuolar H^+ ATPase consists of two domains donated by uppercase (V_1 domain) and lowercase (V_O domain). Structure loosely based off of [7].

CHAPTER 5

THE TOXOPLASMA VACUOLAR H^+-ATPASE REGULATES INTRACELLULAR PH, AND IMPACTS THE MATURATION OF ESSENTIAL SECRETORY PROTEINS[2]

[2] Andrew J. Stasic, Nathan M. Chasen, Eric J. Dykes, Stephen Vella, Beejan Asady, Vincent J. Starai, and Silvia N.J. Moreno. Accepted by *Cell Reports*. Reprinted here with permission of the publisher.

5.1 Abstract

Vacuolar-proton ATPases (V-ATPases) are conserved complexes that couple the hydrolysis of ATP to the pumping of protons across membranes. V-ATPases are known to play diverse roles in cellular physiology. We studied the *Toxoplasma gondii* V-ATPase complex and discovered a dual role of the pump in protecting parasites against ionic stress and in the maturation of secretory proteins in endosomal-like compartments. *Toxoplasma* V-ATPase subunits localize to the plasma membrane and to acidic vesicles and characterization of conditional mutants of the *a*1 subunit highlighted the functionality of the complex at both locations. Microneme and rhoptry proteins are required for invasion and modulation of host cells and they traffic via endosome-like compartments in which proteolytic maturation occurs. We show that the V-ATPase supports the maturation of rhoptry and microneme proteins, and their maturases, during their traffic to their corresponding organelles. This work underscores a role for V-ATPases in regulating virulence pathways.

5.2 Graphical abstract

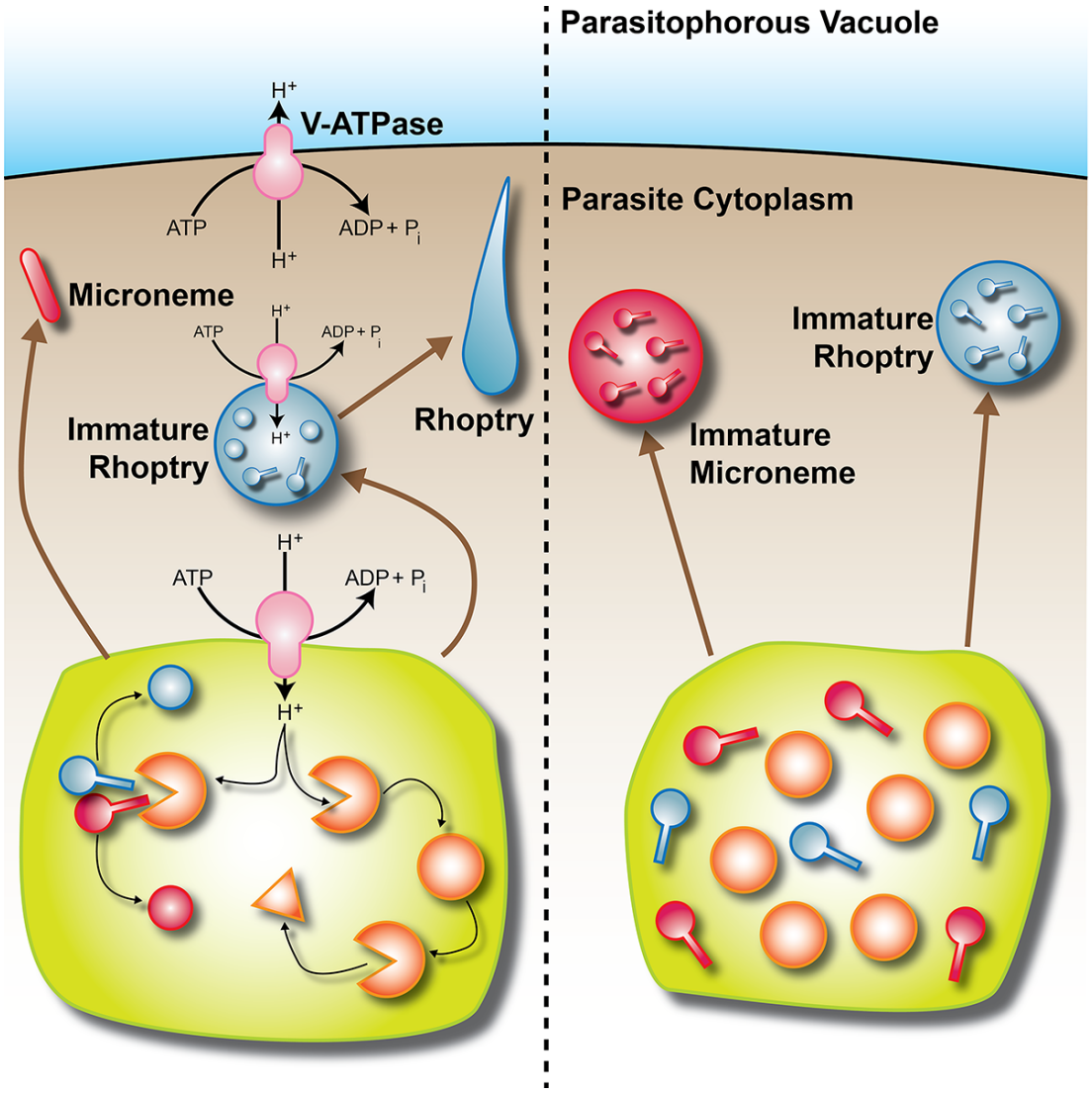

5.3 Introduction

Toxoplasma gondii is an Apicomplexan parasite that infects a wide range of hosts, including humans. *T. gondii* infections are usually asymptomatic in healthy adults, but in immunosuppressed individuals, infections can cause serious complications and be fatal. The pathogenicity of this obligate intracellular parasite is linked to its lytic cycle, which consists of invasion of mammalian cells, replication inside a parasitophorous vacuole (PV), and egress [1]. As *T. gondii* progresses through its lytic cycle, it encounters dramatic changes in the ionic (Ca^{2+}, Na^{+}, K^{+}, Cl^{-}) and nutrient composition of its surrounding milieu. Sophisticated regulatory mechanisms are in place for the parasite to deal with these changes and also to use these ionic gradients for its own benefit such as filling its intracellular Ca^{2+} stores [2]. *T. gondii* tachyzoites, the fast-growing form, replicate inside host cells, which lyses upon exit of the parasite, a phase responsible for the pathology of *Toxoplasma*. Our laboratory has previously characterized an organelle termed the Plant-Like Vacuole or PLV (also termed VAC) that becomes prominent in extracellular tachyzoites and fragments shortly after invasion in intracellular parasites. The PLV is thought to protect parasites against ionic and osmotic stress [3, 4]. The PLV houses lytic enzymes like cathepsins, plant-like pumps like the vacuolar proton pyrophosphatase, and channels like aquaporins, and acts to regulate ions and/or as a post Golgi sorting compartment for secretory proteins destined to the micronemes, rhoptries, and acidocalcisomes. The PLV plays a central role during the extracellular phase of the parasite not only in resisting environmental stress but also in preparing parasites for subsequent host cell invasion. Most of the functions of this organelle depend on its ability to maintain an acidic gradient at its membrane, which, in

plants is driven by 2 distinct electrogenic proton pumps: the H^+-translocating inorganic pyrophosphatase (VP1) and the vacuolar-H^+-ATPase (V-ATPase).

The V-ATPase is an evolutionarily conserved proton (H^+) pump that couples the hydrolysis of ATP with the translocation of H^+ across membranes, often into the lumen of a vesicle. Typically, these protein complexes consist of at least 14 different subunits that compose a membrane anchoring **V_0 domain** (*a, c, c′, c″, d,* and *e* subunits) and a peripheral **V_1 domain** (subunits A to H) [5]. In this work, we characterized the *a*1 subunit of the *T. gondii* V-ATPase complex. Subunit *a* is a 100 kDa transmembrane protein containing an amino-terminal cytoplasmic domain and a carboxy-terminal hydrophobic domain with 8–9 transmembrane helices [6]. We investigated the link between the *T. gondii* V-ATPase and PLV function to gain knowledge of the mechanism by which this organelle protects parasites against ionic stress and its role in sorting and maturation of essential secretory proteins like microneme and rhoptry proteins. Our data showed that the V-ATPase is also functional at the plasma membrane of *T. gondii* tachyzoites where it pumps H^+ out of the parasite. We propose a model for the dual role of this multipurpose pump and its adaptation to the unique needs of intracellular and extracellular tachyzoites and their parasitism.

5.4 Results

Genomic organization and expression of the *T. gondii vha1* gene.

V-ATPases are complexes composed of two domains, V_1 and V_0 (**Fig. S5.1A**), which couple the hydrolysis of ATP with transport of H^+. Subunit *a* of the V_0 domain is a 100-kDa integral membrane protein that spans both domains of the complex and is involved in its assembly [5] (**Fig. S5.1A**). The N-terminal domain connects V_1 and V_0, and stabilizes the complex during rotary catalysis. The C-terminal domain is membrane-

embedded, contains eight transmembrane helices, and is involved in proton transport [7]. *T. gondii* appears to express two *a* isoforms, *a*1 and *a*2 (TGGT1_232830 and TGGT1_290720, respectively). We chose to characterize *a*1 because of its central role in translocating H^+ and its potential interaction with both domains V_0 and V_1. Subunit *a*1 (TGGT1_232830) had a higher BLAST expectant score compared with the yeast Vph1p (**Table 5.1**), stronger evidence for expression, and a stronger phenotype score than *a*2 according to ToxoDB [8]. We termed this gene *Tgvha1* (*vha1* henceforth), which encodes for a predicted protein of 909 amino acids (Vha1) with an N-terminal signal peptide covering the first 26 amino acids. The topology of Vha1 predicts the presence of 7 transmembrane domains (**Fig. S5.1B**).

The V-ATPase localizes to the plasma membrane and the PLV.

To study the localization of the V-ATPase in *T. gondii*, the *vha1* gene was endogenously tagged with a 3xHA at the C-terminus (**Fig. 5.1A**) using the pLIC plasmid approach [9, 10]. The *vha1-HA* parasites were isolated and insertion of the tag was confirmed by PCR (**Figs. S5.1C, D**) and further evaluated by western blots with αHA antibodies (**Fig. 5.1B**). Immunofluorescence assays (IFAs) with αHA antibodies showed plasma membrane localization in intracellular (**Fig. 5.1Ci**) and extracellular parasites and co-localization with the plasma membrane protein, surface antigen 1 or SAG1 (**Fig. 5.1Cii and S5.2A**). Specific localization of Vha1 to the plasma membrane was shown by *Clostridium septicum* alpha-toxin treatment, which induces separation of the plasma membrane away from the Inner Membrane Complex (IMC) [11]. IFAs showed that Vha1 did not co-localize with the IMC marker (**Fig. S5.2B**). In intracellular parasites we observed labeling of vesicles (**Fig. 5.1C and S5.2A**) but the plasma membrane labeling

was the most predominant (**Fig. 5.1C**). In extracellular parasites, in addition to the plasma membrane, Vha1 labeled a large vacuole (**Figs. 5.1Cii-iv and S5.2C**) that co-localized with cathepsin L (TgCPL or CPL) and the vacuolar proton pyrophosphatase (VP1), which label the PLV and other Endosome Like Compartments (ELC) [4] [3] (**Figs. 5.1Ciii and iv and S5.2C**). Immuno-EM confirmed the presence of Vha1 at the plasma membrane and the PLV (**Fig. 5.1D**). The localization of Vha1 to the PLV became more noticeable with longer exposure of parasites to the extracellular milieu (**Fig. S5.2G**). We also showed PLV localization by super resolution microscopy (**Fig. 5.1Ciii, and S5.2C**) and confirmed this localization by IFAs with specific antibodies generated in mice against the *a*1 subunit (**Fig. S5.2H-I**). Western blots of *Toxoplasma* lysates developed with the affinity purified mouse serum showed a band corresponding to the correct size of Vha1 (**Figs. S5.2H**). The traffic of the V-ATPase to the PLV and its underlying mechanism remains to be characterized. We do not believe that it is being turned over or degraded because no degradation products showed in immunoblots (**Fig. S5.2H**) and our data indicates that the complex is functional at the PLV.

We previously showed ATP-stimulated proton transport in a PLV enriched fraction (Miranda et al, 2010, Fig. 6B) supporting activity of the V-ATPase in the PLV. We tagged the *a*1 subunit with the Green fluorescent protein mNeonGreen [8] and parasites expressing Vha1-mNeonGreen were loaded with LysoTracker, a lysosomal marker that labels acidic compartments. LysoTracker co-localized with the Vha1-mNeon at the PLV in extracellular tachyzoites, confirming the acidic nature of the PLV and its co-localization with the V-ATPase (**Fig. 5.1E**).

We also studied the localization of subunits E (TGGT1_305290; henceforth *vhE*) and G (TGGT1_246560; henceforth *vhG*) following a similar genetic strategy as described. Subunits E (VhE) and G (VhG) form part of the peripheral V_1 domain and are involved in establishing the stator of the V-ATPase complex and interact with the regulator of ATPase of vacuoles and endosomes (RAVE) complex [12]. Both VhG and VhE localized to the plasma membrane and co-localized with VP1 in intracellular and extracellular tachyzoites (**Figs. 5.1F, G, and S5.2E-F**). We also tagged *vhG* with a Ty tag in parasites expressing *vha1-HA* (**Fig. S5.2D**) to study co-localization. IFAs with αTy and αHA, showed co-localization of both subunits supporting their role within the complex (**Fig. S5.2D**). Our results established that the *T. gondii* V-ATPase localizes to the plasma membrane and the PLV, which becomes more prominent in extracellular parasites.

***vha1* can partially rescue growth in *a* subunit-deficient yeast**.

The specific function of the *vha1* gene product as part of the V-ATPase complex was investigated by expressing the *T. gondii vha1* gene in *Saccharomyces cerevisiae Δvph1Δstv1* mutants [13]. These mutants do not express either of their *a* subunits (Vph1p and Stv1p, which localize to the yeast vacuole or Golgi, respectively) and are unable to grow at pH ≥ 7 due to deficient acidification of the yeast vacuole [14]. The *T. gondii vha1-HA* gene was cloned in the galactose inducible expression plasmid, pYES2/NT C, and transformed in the Δ*vph1*Δ*stv1* yeast strain (**Fig. 5.2A**). The *vha-HA* gene was expressed in the Δ*vph1*Δ*stv1* strain in CSM-ura media with 2% galactose while no expression was seen in 2% glucose (**Fig. 5.2B).** The Δ*vph1*Δ*stv1* strain does not grow at pH 7, but expression of the *vha-HA* gene partially restored growth in this medium (**Figs. 5.2C and S5.3A)**. Quantification of the slopes during exponential growth (4-16 hours for WT and 8-

32 hours for *vph1*Δ*stv1*Δ yeast) showed that *vph1*Δ*stv1*Δ expressing *vha1-HA* grew significantly better than *vph1*Δ*stv1*Δ yeast transformed with the empty vector (EV) (**Fig. 5.2C**). Using a similar strategy, the gene of the subunit *a*2 (*vha2*) was expressed in the *vph1*Δ*stv1*Δ strain (**Figs. S5.3A)** and it also partially complemented their growth. Expression of GFP-Vha1 showed localization of Vha1 to the yeast vacuole (and other internal compartments) (**Fig. S5.3B**). GFP-Vph1 was also expressed as control, which localized mostly to the yeast vacuole (**Fig. S5.3B**). These results showed that the *T. gondii a*1 subunit can function as part of the V-ATPase complex, providing genetic evidence of its conserved biochemical function.

Vha1 and the lytic cycle of *T. gondii*.

We generated conditional *i*Δ*vha1-HA* mutants by using a tetracycline-regulated transactivator system and the parental line TATiΔku80, which combines regulated gene expression [10] with high efficiency of homologous recombination [15] (**Figs. 5.3A and S5.4A**). Proper insertion and orientation of the promoter was shown by PCR (**Fig. S5.4B)** and western blots confirmed regulation of Vha1 expression. Vha1 was not evident by western after 24 h of growth with anhydrotetracyclin (ATc) (**Fig. 5.3A**) and IFAs did not detect the Vha1 signal after 3 days with ATc (**Fig. S5.4C**, +*ATc*). We also created a complemented strain, *i*Δ*vha1-HA-CM* that constitutively expressed *vha1* from a tubulin promoter at the *uprt* gene locus [16] (**Figs. 5.3B and S5.4D**) for control experiments. Note that the western in Fig. 3B was done using αHA (left panel) and the polyclonal antibody αVha1 generated in this work (right panel), which shows that the complemented *vha1* is expressed even in the presence of ATc (**Fig. S5.2H**).

The pathogenicity of *T. gondii* stems from its lytic cycle, which is initiated by active invasion of host cells, replication and egress (**Fig. 5.3C**). To establish whether Vha1 is important for parasite growth, we performed plaque assays of *vha1-HA*, *iΔvha1-HA*, *iΔvha1-HA-CM,* and the parental strain TATiΔku80 under identical conditions with (+) and without (-) ATc (**Fig. 5.3D**). *iΔvha1-HA+ATc* could not form plaques demonstrating that the expression of *vha1* was critical for at least one major step of the lytic cycle. We introduced a cytosolic tdTomato into the *iΔvha1-HA* and *iΔvha1-HA-CM* cells to analyze growth kinetics. To determine the impact of ATc on growth, tdTomato expressing parasites were preincubated with ATc and the drug removed at the indicated times (**Fig. S5.5A**). We observed that 4 days with ATc blocked growth completely while some growth was seen after 1-2 days +ATc (**Fig. S5.5A**). Based on these results, we studied a variety of phenotypic features with 1, 2, or 3 days of ATc treatment. We reasoned that longer exposure to ATc would likely result in stronger phenotypic characteristics but could be the result of non-specific effects. *iΔvha1-HA* parasites grown +ATc for three days were tested for viability using the trypan blue exclusion assay to rule out that they were dead or dying (**Fig. S5.5B**). We evaluated the daily growth rate and found that *iΔvha1-HA*+ATc parasites grew significantly slower than the controls (*iΔvha1-HA*-ATc) and complemented (*iΔvha1-HA-CM*+ATc) lines (**Figs. 5.3E and S5.5C**). To assay for replication, parasites were pre-incubated (+ATc) or not (-ATc) with ATc for 24 h and passaged to new fibroblast cells + or - ATc, respectively. After 24 h of exposure to ATc, followed by another 24 h in a new passage (48 h +ATc), there was a significant reduction in the ability of *iΔvha1-HA*+ATc to replicate as shown by the low number of parasites per PV counted (**Fig. 5.3F,** *red columns*).

We next analyzed each step of the lytic cycle and found that 2 days +ATc reduced invasion of host cells 7-fold and attachment 5-fold (**Fig. 5.3G**); these defects were ameliorated in the *iΔvha1-HA-CM* line. We studied egress by stimulating intracellular tachyzoites with nigericin or saponin + calcium [17] and the *iΔvha1-HA+ATc* mutants showed a significant delay in their response to these inducers of egress (**Figs. 5.3H** and **S5.5D**). There was a significant difference in the % of lysed PVs after 30 min of exposing intracellular parasites to 10 μM nigericin (66.9% and 68.9% for the *iΔvha1-HA-ATc* and *iΔvha1-HA-CM+ATc*, respectively, and 30.5% for *iΔvha1-HA+ATc*) (**Fig. 5.3H**). We also measured time to egress after induction with 2 mM Ca^{2+} in the presence of 0.01% saponin to permeabilize host cells. *iΔvha1-HA-ATc* and *iΔvha1-HA-CM+ATc* parasites took 303 ± 35 and 342 ± 80 sec, respectively, to exit host cells, while *iΔvha1-HA+ATc* took 527 ± 45 seconds (**Fig. S5.5D)**. We also evaluated motility, an essential part of the lytic cycle of *T. gondii* and found that the mutants +ATc traveled 57 μm less than the controls -ATc and 69 μm less than the complemented strains +ATc (**Fig. 5.3I**). In summary, these results show that the activity of the V-ATPase impacts every step of the lytic cycle of *T. gondii*.

The role of Vha1 in intracellular pH.

Intracellular pH (pH_i) must be strictly controlled because of the narrow optimum pH of most enzymatic processes [18]. Because of this, cells regulate their pH_i by active transport of H^+ across membranes. We showed that the maintenance of the cytoplasmic pH of *T. gondii* tachyzoites was sensitive to bafilomycin A_1, a specific inhibitor of V-ATPases [19] and a role for the V-ATPase in pH_i regulation was deduced. We therefore tested pH_i in the *iΔvha1-HA+ATc* mutants (extracellulars) by loading them with the pH indicator BCECF-AM (**Figs. 5.4A, B**). pH_i of *iΔvha1-HA*+ATc tachyzoites appeared to vary in a

similar way to the pH_i of *iΔvha1-HA*-ATc parasites when exposed to extracellular pHs between 5.5 and 8.5 (**Fig. 5.4B**). Apparently under these conditions, *iΔvha1-HA*+ATc mutants are still able to regulate pH_i, which is reasonable considering the importance of maintaining physiological pH_i levels within a normal range. To study the function of the V-ATPase at the plasma membrane we measured H^+ extrusion using the free acid form of BCECF in a weakly buffered solution (**Fig. 45.C**) [20]. This protocol measures changes in extracellular pH (pH_e), that results from H^+ extruded from the cell into the extracellular milieu. Addition of glucose, which stimulates glycolytic activity, resulted in medium acidification (**Fig. 5.4C** *see green and blue slopes*). Changes in pH_e of -0.40 to -0.46 pH units were observed with the control (*iΔvha1-HA*-ATc) or the complemented (*iΔvha1-HA-CM*+ATc) parasites. However, mutant *iΔvha1-HA+ATc* tachyzoites produced a change in pH_e of only -0.19 pH units (**Fig. 5.4C** and inset). The H^+ extrusion activity was blocked by bafilomycin A_1 for all three cell lines, *iΔvha1-HA*–ATc, *iΔvha1-HA*+ATc, and *iΔvha1-HA-CM*+ATc (**Fig. 5.4D**). These data highlighted the role for the *T. gondii* V-ATPase in extrusion of H^+ upon stimulation of metabolic activity with glucose.

Exposing *iΔvha1-HA*-ATc (controls) tachyzoites to 10 mM propionic acid caused transient acidification of the cytosolic pH, which is quickly recovered to normal values within 50 s of the acid pulse (**Fig. 5.4E,** *blue tracing*). Recovery of *iΔvha1-HA*+ATc parasites after acid treatment was very slow and at 100 seconds post-treatment their pH_i was still low, while the pH of control parasites was completely recovered **(Fig. 5.4E,** *yellow and red tracings***)**. The complemented line, *iΔvha1-HA-CM+ATc* was able to restore its pH_i, almost as fast and efficiently as parental parasites (**Fig. 5.4E,** *green tracing***).** Bafilomycin A_1 blocked recovery of pH_i in all lines (+ or -ATc and complemented strain) (**Fig. 5.4F)**,

showing that the V-ATPase functions to protect *T. gondii* from acid stress by pumping protons out of the parasite cytosol.

Deficient H^+ pumping at the plasma membrane may also impact membrane potential. We used the membrane potential-sensitive fluorescent probe bisoxonol [19] and found that the *iΔvha1*-HA+ATc parasites were modestly depolarized (higher fluorescence ratio) compared to their controls (**Fig. 5.4G)**. These data indicated that the proton pumping activity of the V-ATPase generated a H^+ gradient at the plasma membrane that contributes partially to the build-up of the membrane potential. Likely, other mechanisms are at play and prevent cells from becoming completely depolarized.

Co-localization of Lysotracker with Vha1 in the PLV (**Fig. 5.1E**) of *iΔvha1-HA*-ATc cells supports the acidic nature of the PLV. When we loaded *iΔvha1-HA*+ATc parasites with Lysotracker instead of a single vacuole labeled, we observed several puncta showing fragmentation of the PLV (**Fig. 5.4H, I**), which could result from defective biogenesis. We next performed IFAs of *iΔvha1-HA*+ATc parasites with the PLV markers VP1 and CPL and we also observed labeling of both markers in vesicles distributed through the cell (**Fig. 5.4J** *arrowheads*) including some labeling of the endoplasmic reticulum (ER) (**Fig. 5.4J** *arrows*). It is possible that the PLV is not forming properly in extracellular *iΔvha1-HA*+ATc tachyzoites, probably due to defective vesicle fusion (**Fig. 5.1 iii and iv**). The labeling with αVP1 was similar to the one observed with LysoTracker, indicating that the defective formation of the PLV was likely leading to an accumulation of VP1 vesicles, which were acidic but failed to fuse. We were unable to evaluate the difference in acidification because of the non-quantitative nature of Lysotracker. We expressed a genetically encoded pH indicator (mCherry-SEpHluorin) in the PLV (see supplemental

movie 1) of control *iΔvha1-HA* cells but because of the fragmented nature of the PLV, it was not possible to estimate pH in the vesicles formed in *iΔvha1-HA*+ATc mutants (data not shown). Our data supports a role for the V-ATPase in trafficking of vesicles to or from the PLV.

Vha1 is important for the localization, maturation, and secretion of micronemes.

Micronemes are secretory organelles involved in the invasion of host cells by tachyzoites [21]. Several microneme proteins undergo proteolytic maturation while traveling to the micronemes and a role for endosomal compartments in this maturation has been shown [22]. In extracellular tachyzoites the V-ATPase translocates from the plasma membrane to the PLV, which harbors microneme maturase activity [4]. Parasite attachment and invasion is associated with the secretion of micronemes [21], and since *iΔvha1-HA+ATc* parasites display defects in attachment and invasion, we studied microneme secretion. We tested the release of MIC2, into the excreted/secreted antigen fraction collected from supernatants of extracellular tachyzoites without stimulation (**Fig. 55.A,** *constitutive*) or after induction by ethanol (**Fig. 5.5A,** *1% ethanol*). Mutants *iΔvha1-HA+ATc* parasites were not able to secrete micronemes constitutively and they responded poorly to stimulation by ethanol (**Fig. 5.5A**). The amount of total MIC2 protein in the *iΔvha1-HA* lysate was similar to that of parental and complemented strains. **Fig. 5.5B** shows the quantification of three independent experiments using GRA1 secretion as control. We found that after 3 days with ATc, *iΔvha1-HA*+ATc tachyzoites are deficient at secreting MIC2 while secretion of GRA1 was normal (indicating viable parasites) (**Fig. 5.5B**). The complemented line, *iΔvha1-HA–CM* showed normal secretion of MIC2 even after 3 days +ATc. We also tested the secretion of the apical membrane antigen 1

(TgAMA1), a transmembrane protein that localizes to the micronemes [23]. Secretion of TgAMA1 was also significantly reduced in the *iΔvha1-HA+ATc* line (**Fig. S5.6A, B**).

MIC2 forms an heterohexameric complex with M2AP (MIC2-associated protein) and the complex MIC2-M2AP plays fundamental roles in gliding motility and invasion. M2AP is initially translated with a propeptide that is removed in an endosomal compartment and blocking the removal of the propeptide affects trafficking of the M2AP-MIC2 complex to the periphery. [22]. We studied processing and trafficking of M2AP in the *iΔvha1-HA*+ATc cells (3 days) and observed a significant accumulation of the immature form (**Fig. 5.5C-D**). MIC3 is an homodimeric adhesin that is synthesized as a precursor that is proteolytically processed during its traffic through the secretory pathway on its way to the micronemes. This processing is important for the binding function of the protein [24]. Mature MIC3 abundance was significantly reduced in *iΔvha1-HA+ATc* mutants when compared to controls (**Figs. 5.5E, F**). Parental lines (*TATiΔku80+ATc*) were tested for M2AP and MIC3 maturation in the presence of ATc and is shown in **Fig. S5.6C-E.** ATc did not affect maturation of these proteins in parental lines.

We next looked at the distribution of microneme proteins by IFAs of *iΔvha1-HA+ATc* mutants (**Figs. 5.5G-I**). There was a notable difference in the distribution of MIC3 in the *iΔvha1-HA+ATc* mutants. MIC3 labeling was increased in perinuclear areas and accumulated in internal vesicles likely destined to the secretory pathway (**Fig. 5.5G, +ATc,** *arrows*). This was distinct from the neatly distributed labeling of MIC3 at the periphery of parasites that express normal levels of Vha1 *(iΔvha1-HA*-ATc) (**Fig. 5.5G, -ATc**). It was previously reported that unprocessed MIC3 builds up in perinuclear compartments such as the ER and/or Golgi compartments and accumulates in the secretory

pathway during parasite division [25]. Our data points towards retention of MIC3 in the ER and secretory pathway because of its defective processing, a consequence of inactive V-ATPase (**Fig. 5.5G,** *arrowheads*). MIC3 and M2AP are synthesized almost simultaneously but pro-M2AP was mainly observed in endosome-like compartments while pro-MIC3 was observed in both the ER-Golgi and endosome-like compartments [25]. We studied the localization of M2AP in the *iΔvha1-HA*+ATc mutants (**Fig. 5.5H)** and saw a remarkable difference in their distribution. M2AP labeling in the controls *iΔvha1-HA*-ATc showed the typical peripheral distribution while labeling in the *iΔvha1-HA*+ATc mutants was clustered within the central region of the extreme apical end (**Fig. 5.5H,** *compare – and +ATc*). proM2AP labeling was increased in the *iΔvha1-HA+ATc* mutants **(Fig. 5.5I).** Disruption of M2AP [22] results in secretory retention of MIC2, leading to reduced MIC2 secretion from the micronemes and impaired invasion. MIC2 localization was also altered and it accumulated in vesicles with intense labeling toward the apical end of the cell close to the plasma membrane (**Fig. S5.6F**).

Transmission EM of *iΔvha1-HA*+ATc showed that their micronemes are not able to dock or fuse at the periphery, instead presenting a more central location in the apical region of the tachyzoite (**Fig. 5.5J**). These micronemes also exhibited a rounded morphology rather than the typical cigar shape [26] (**Fig. 5.5J**). We found significantly fewer micronemes at the periphery in the *iΔvha1-HA*+ATc mutants (**Fig. 5.5K).** These results showed that the V-ATPase plays a significant role in microneme maturation, function, and organelle distribution.

Vha1 and maturation of rhoptries.

The majority of rhoptry bulb proteins are initially translated with an ER signal peptide and a pro-peptide that acts as a trafficking signal for the rhoptries [27]. Because pro-peptides are proteolytically cleaved within endosomal compartments [28], we questioned if the activity of the V-ATPase would impact maturation of rhoptries. Immunoblots of lysates from *iΔvha1-HA*-ATc and *iΔvha1-HA*+ATc tachyzoites revealed that the maturation of the rhoptry proteins ROP4, ROP7, and TgCA_RP [29] were altered, as demonstrated by a significant increase in the percentage of immature protein (**Figs. 5.6A, B**). The effect of ATc on the maturation of Rhoptries and maturases of parental cell lines is shown in Fig. S7. Rhoptry maturation was tested in S7A-B.

We next compared IFAs of *iΔvha1-HA*-ATc and *iΔvha1-HA*+ATc tachyzoites with antibodies against the pro-peptide of ROP4 (αproROP4), which labels immature rhoptries [30]. We found a significant increase in the number of *iΔvha1-HA+ATc* tachyzoites that contained immature rhoptries. Immature rhoptries were only seen in dividing tachyzoites and we observed labeling in tachyzoites that were not in the division stage of their cell cycle, as determined by IMC labeling (**Fig. 5.6C,** *not dividing*). When tachyzoites were dividing (following the IMC labeling), αproROP4 and αCA_RP labeling appeared indistinguishable between *iΔvha1-HA*-ATc and *iΔvha1-HA*+ATc tachyzoites, with the only observation of an increased number of nascent rhoptries in the residual body of *iΔvha1-HA*+ATc vacuoles (**Fig. 5.6C,** *dividing*). Trafficking from the ER appeared to be normal as indicated by the localization of rhoptry bulb proteins. When the parasites had completed division, we still saw labeling of αproROP4 in the *iΔvha1-HA*+ATc mutants. We quantified the number of PVs containing tachyzoites with immature rhoptries and we

saw a significant increase (>80%) of αproROP4 labeling in the *iΔvha1-HA*+ATc (3 days) mutants (**Fig. 5.6D**). The number of tachyzoites containing daughter cells (labeled with αIMC1) was not significantly different in *iΔvha1-HA*+ATc mutants; suggesting that this step of endodyogeny is not affected. Routine electron microscopy of *iΔvha1-HA*+ATc parasites showed a striking phenotype where there is no evidence of mature rhoptries (**Figs. 5.6E, F**). Our data supports a role for the V-ATPase in the maturation of rhoptry proteins and the morphological changes associated with the formation of the characteristic elongated mature rhoptries.

We performed IFAs with αCA_RP (rhoptries) αproROP4 (immature rhoptries), and αHA in *iΔvha1-HA* parasites (no ATc) using super resolution microscopy. We saw labeling of Vha1 in vesicles that surround immature rhoptries (**Figs. 5.6G,** *arrows* **and S5.8A**) but none in mature rhoptries (**Fig. S5.8B**). With the aim to confirm that this localization is consistent for the entire V-ATPase complex, we performed IFAs on *vhE-HA* and *vhG-HA* and saw that both E and G encircled immature rhoptries, supporting the presence of the whole complex at this location (**Figs. S5.8C, D**). Immature rhoptries were previously shown to be acidic (pH 3.5-5.5) [31] and our data shows the potential mechanism of acidification. It remains to be determined how the V-ATPase-labeled vesicles split allowing the mature rhoptry proteins to traffic to the rhoptries while the V-ATPase follows a different path to other endosomal compartments.

The V-ATPase and proteolytic activities.

We investigated the role of the V-ATPase on the maturation of known endosomal proteases. CPL, an enzyme present in the PLV and shown to play a role in the maturation of M2AP and MIC3 [4], is proteolytically processed and acidic pH is required for both its

maturation and its function. CPL maturation was affected in *iΔvha1-HA+ATc* mutants as accumulation of immature CPL was seen 48 h after treatment with ATc (**Figs. 5.7A, B**), while ATc had no effect on the maturation of CPL in parental lines (*TATiΔku80)* (**Fig. S5.7C-D**).

A rhoptry localized subtilisin-like serine protease, TgSUB2 was proposed to be involved in maturation of ROP proteins [32], although TgSUB2 knock-outs did not show ROP maturation defects [33]. It has been reported that some subtilisin proteases require pH below 7 for their own maturation [34, 35], but this information is not known for TgSUB2. The activity of subtilisin proteases on their substrate, however, may need neutral or slightly alkaline pH [36]. We tested the maturation of TgSUB2 in the *iΔvha1-HA*+ATc mutants and found a significant difference in the ratio between mature and immature forms of TgSUB2 as compared with the same ratio present in the controls, *iΔvha1-HA*-ATc (**Figs. 5.7C, D)**. These results demonstrate that matured SUB2 is reduced in the *iΔvha1-HA*+ATc mutants, however, the effect on the proteolytic function of TgSUB2 remains to be seen.

Aspartic proteases require low pH for maturation and activity [37] and it was reported that aspartic protease 3 (ASP3) was the maturase for microneme and rhoptry proteins in *T. gondii* [33]. To investigate if maturation of ASP3 was affected in *iΔvha1-HA* cells, we tagged ASP3 using the 5'UPRT-pTub8-Asp3-3Ty-3'UPRT plasmid in the *iΔvha1-HA* line. We exposed these parasites (*iΔvha1-HA-ASP3-Ty)* to ATc to reduce the expression of *vha1* and performed westerns and observed an increase in immature ASP3 (and decrease of mature form) compared to the level present in *iΔvha1-HA-ATc* cells (**Fig 5.7E, F**). Both lines showed a noticeable level of immature and mature forms (**Figs. 5.7E**). ASP3 was localized to the ELC [33], so we performed co-localization IFAs with αHA in

the *vha1-HA* line. In dividing intracellular tachyzoites, we observed that ASP3 colocalized with proROP4 and Vha1 labeling encircled the signal of proROP4 (**Fig. 5.7G,** *dividing PV*). Our results indicate that the H^+ gradient generated by the V-ATPase in immature rhoptries is likely responsible for the generation of the ideal environment required for ASP3 maturation to its proteolytically active product (**Fig. 5.7G,** *dividing PV*). Our results support a role for the V-ATPase in regulating pH of endosomal compartments where important maturation of critical secretory proteins occurs.

5.5 Discussion

The function of the V-ATPase complex is to pump H^+ against a concentration gradient and this activity impacts the physiology of every eukaryotic cell [38]. The gradient generated by the activity of the V-ATPases in organelles and in membranes of eukaryotic cells is used as a driving force for a number of secondary transport processes [39]. V-ATPases are ATP-dependent H^+ pumps that localize to a variety of cellular membranes in eukaryotic cells [40] including endosomes, lysosomes, Golgi-derived vesicles, secretory vesicles and, in some cells, also the plasma membrane [5]. The activity of V-ATPases in the endocytic pathway results in a pH gradient that decreases from pH ~6.0 in early endosomes to pH 5.0–5.5 in lysosomes [41]. Intra-endosomal acidification is required for the enzymatic activity of hydrolytic enzymes [42] among other functions.

The *Toxoplasma* genome shows evidence for the presence of most subunits of the V-ATPase with two *a* subunit isoforms, *a*1 and *a*2 (TgGT1_232830 and TgGT1_290720). In this work we characterized the *a*1 subunit. Expression of the *Toxoplasma vha1* gene partially complemented the growth of the mutant strain *S. cerevisiae vph1/Δstv1* at pH 7 [14]. This result showed that Vha1 functions as part of the V-ATPase complex and the

function of the V-ATPase complex could be studied by manipulating the expression of the *vha1* gene. The expression of the *a*2 gene in the same strain of *S. cerevisiae* also partially complemented their growth indicating that *a*2 may also function as part of the complex. We focused on the characterization of *a*1 because it had higher homology to other *a* subunits of V-ATPases of yeast, plants, and mammalian cells and also because the sequence of *a*2 contained an extra domain of 12-15 kDa at the C-terminus, the domain important for H^+ translocation, which is not found in yeast, plants, or mammalian cells.

The V-ATPase of *T. gondii* showed H^+-pumping activity at the plasma membrane, which acted in the recovery of normal cytosolic pH from acid loads. The active H^+ extrusion into the surrounding media shows that the V-ATPase is fully functional at the plasma membrane and H^+s generated from normal metabolic functions, or artificially induced with acid load, are pumped outside the cell. It is likely that other mechanisms are functional, like a P-type ATPase or a sodium/proton exchanger [43] thus explaining why parasites are still alive at 48 h even though the absence of Vha1 expression.

The H^+ gradient generated by the activity of the V-ATPase at the plasma membrane contributed to the generation of a membrane potential and mutant parasites were slightly depolarized [19]. This depolarization is modest because, most likely, parasites would not survive if their membranes were considerably depolarized. Changes in membrane potential are often linked with ion influx or efflux [44].

The expression of the *vha1* gene could be regulated with ATc in the *iΔvha1-HA* mutants. These parasites showed a strong growth defect and strong phenotypic differences, already observed 48 h after ATc treatment and even stronger differences were observed when cells were grown longer with ATc. All of the major steps of the lytic cycle were

defective, including maturation and secretion of micronemes, invasion, motility, and egress, supporting an essential role for the V-ATPase. The invasion defect was evident two days after ATc treatment, earlier than the microneme secretion defect, which is only evident three days after ATc treatment. The H^+ pumping activity is already non-functional at day 2 of ATc so it is likely that the invasion decrease at this stage is due to a defect in signaling, which is linked to H^+ gradients generated by the V-ATPase [45].

Intracellular replication was affected in the *iΔvha1-HA+ATc* mutants and our interpretation is that metabolically active intracellular parasites produce large quantities of acid, which needs to be extruded by the pumps at the plasma membrane. We measured intracellular pH in extracellular parasites and that did not appear to be affected when cells were exposed to regular changes in extracellular pH. However, when the parasite cytosol was challenged with propionic acid the recovery response observed was defective in the mutants. This supports an important function for the pump in protecting cytoplasmic pH and when the pump is defective, would cause alterations of intracellular pH, disrupting cell fitness and replication.

Secretory organelles, like rhoptries and micronemes, are made de novo in daughter parasites during the process of endodyogeny, the mechanism by which *Toxoplasma* replicates [1]. A large body of evidence indicates that the biogenesis of rhoptries and micronemes occurs at the Golgi [26]. Trafficking of cargo to the micronemes involves the participation of endosome-like compartments and their proteolytic maturation involves the participation of specific maturases [4, 33]. pro-MICs have been observed in structures bearing late endosomal markers [22] and nascent micronemes have been observed in close proximity to the PLV. Specific inhibitors of the V-ATPase, like bafilomycin A_1, reduced

the maturation of CPL, an enzyme that localizes to the PLV, shown to be self-processed [46] and to be involved in the maturation of microneme proteins [4].

Disruption of the activity of the V-ATPase negatively impacted the maturation of MIC3 and M2AP, two microneme proteins that are processed before storage in the microneme compartment [47]. Defective maturation of M2AP leads to miss-targeting of MIC2 as it was shown that proteolytic stabilization of the MIC2–M2AP complex within the micronemes is important for the correct packaging within micronemes favoring its rapid secretion onto the parasite surface [22]. The localization of M2AP, MIC3, proM2AP and MIC2 were altered in *iΔvha1-HA* mutant parasites and microneme organelles were not correctly oriented. We proposed a model for the role of the V-H^+-ATPase in the maturation of micronemes (**Fig. 5.7H**). Two potential endosome acidic compartments, one expressing higher levels of the VP1 (VP1 compartment as in [22, 48]) and a second one where the V-ATPase predominates (PLV/VAC). Acidification of these organelles could be important for either the maturation process of relevant maturases and/or for their specific proteolytic activity on their substrates, as for example essential adhesins secreted for invasion. The presence of more than one of these compartments could represent the means by which lytic activity is regulated by limiting and/or allowing contact with substrates. Vha1 depletion disrupted the biogenesis of the PLV and this resulted in mistargeting of important secretory proteins.

Rhoptries are club shaped secretory organelles with a discrete neck and bulb region uniquely present in Apicomplexan parasites. Mature rhoptries become club-shaped when mature and they secrete proteins during the process of host cell invasion, an essential function for parasite virulence [49]. A number of rhoptry proteins are secreted during host

cell invasion and participate in the building of the PV. In addition, some rhoptry proteins are targeted to the host cell nucleus to control host functions [49]. In intracellular parasites, the V-ATPase labeled immature rhoptries, which have been previously shown to be acidic (pH 3.5-5) in comparison to the more neutral mature rhoptries (pH 5-7) [31]. Pro-rhoptries form transiently between the Golgi and the apical area just prior to cytokinesis [49] but the mechanism by which these vesicles form is not known [50]. How proteins are delivered to the rhoptries is also not clear, however adaptins have been implicated in this trafficking [50, 51].

Many of the proteins destined to the bulb of the rhoptries (ROPs) contain an N-terminal ER signal peptide and an N-terminal pro-peptide that is cleaved during rhoptry maturation. It was proposed that the N−terminal ROP pro-peptides could be cleaved by subtilisin-like proteases, like TgSUB2, at the SΦX(E/D) motif first identified in ROP1 [32, 52]. Subtilisin-like proteases typically undergo autocatalytic cleavage of a pro-peptide that initially helps with folding, but must be cleaved before proteolytic activity can occur on substrate proteins [53]. The autocatalytic cleavage and substrate protease activity of subtilisin-like proteases typically have different pH optimums. In the case of subtilisin E from *Bacillus subtilis,* the optimal pH for autocatalytic cleavage of the pro-peptide is pH 7.0, whereas the optimal proteolytic activity on substrate proteins is pH 8.5 [36]. TgSUB2 has an atypical cleavage site, which occurs after an acidic residue instead of a basic residue, raising the possibility that the optimal conditions for its cleavage activity are also atypical. There is no experimental evidence to support TgSUB2 maturation in the neutral environment of the ER [32].

Aspartic protease 3 (ASP3), an aspartyl protease of the ELC, was critical for invasion and egress of *Toxoplasma* albeit did not appear to be implicated in parasite replication, gliding motility and attachment [33]. It was also proposed that the activity of ASP3 superseded the previously proposed roles for SUB2 [32] and CPL [4] for the maturation of rhoptries and microneme proteins respectively. The acidification role of the V-ATPase is relevant for the efficient maturation of SUB2 and also ASP3. In this model SUB2 autocatalytic cleavage occurs in the immature rhoptries at low pH and acidification of immature rhoptries would affect maturation of SUB2, but the role of this enzyme in ROP proteins secretion and maturation is less clear. Maturation and/or activity of ASP3 in pro-rhoptries would be impacted by the acidification role of the V-ATPase explaining the delay in ASP3 maturation and the defective rhoptries in the *iΔvha1-HA+ATc* mutants. It is evident that the phenotype of *iΔvha1-HA+ATc* parasites partly mimics the phenotypes of *iΔASP3(+ATc)* on maturation of rhoptries and micronemes. However, *iΔvha1-HA+ATc* parasites also present other phenotypic features probably linked to the role of the pump at the plasma membrane. See our model for the role of the V-H^+-ATPase in maturation of rhoptries (**Fig. 5.7I**).

This work is the first characterization of the V-ATPase protein complex at the molecular level in *Toxoplasma gondii*. The work revealed interesting and significant features of this complex such as its distinct localization in intracellular and extracellular parasites and its functionality at the plasma membrane and the endosomal system. The V-ATPase proton pump activity supports the processing/synthesis of microneme and rhoptry proteins, which are critical for the lytic cycle of *Toxoplasma*, a central feature of the pathogenesis of the parasite. Especially intriguing is its localization with immature

rhoptries and downstream dissociation from rhoptries likely to allow the maturation of the organelle. The traffic of Vha1 to the PLV, soon after egress of tachyzoites and its functional role at the lysosomal-like organelle where it acts in the acidification and maturation of secreted proteins, is also an intriguing feature to adjust to the needs of extracellular tachyzoites.

In summary, our findings highlight the function of this pump in higher order physiological processes essential for *Toxoplasma* parasitism. In doing so, the activity of the pump impacts the processing/synthesis of virulence factors. Disruption of these delicate mechanisms will alter the most essential aspect of the parasitological cycle of *Toxoplasma*. Our work directly connects the proton pumping activity of the V-ATPase complex to processes necessary for *Toxoplasma* virulence.

5.6 Acknowledgments

We thank Vern Carruthers for anti- MIC2, proM2AP and CPL antibodies, Maryse Lebrun for anti-MIC3, and Kami Kim for anti-TgSUB2. We thank Dominique Soldati-Favre for the plasmids for C-terminal tagging of ASP3. Melissa Storey generated the Vha1 antibody. We thank the Georgia Electron Microcopy Center for assisting with the EM images and the Biomedical Microscopy Core, Coverdell, for the use of their microscopes. Wandy Betty from Washington University, St Louis performed the immunoEM of Figure 1. We thank Zhicheng Dou, Drew Etheridge and Vern Carruthers for suggestions and reading the manuscript. Funding for this work was provided by the National Institutes of Health (AI-096836 to SNJM and AI-100913 to VJS). NC was supported by a pre-doctoral fellowship from the American Heart Association (14PRE19100003). AJS was partly funded through a UGA OVPR fellowship as part of the T32 training grant T32AI060546.

5.7 Author contributions

Conceptualization, S.N.J.M. and A.J.S..; Methodology, A.J.S., N.M.C., E.D., S.V. and B.A.; Investigation, A.J.S., N.M.C., B.A. and V.J.S.; Writing, A.J.S. and S.N.J.M.; Editing, V.J.S and S.A.V. Supervision, S.N.J.M.

5.8 Declaration of interests

The authors declare no competing interests.

5.9 References

1. Black, M.W. and J.C. Boothroyd, *Lytic Cycle of Toxoplasma gondii.* Microbiology and Molecular Biology Reviews, 2000. **64**(3): p. 607-623.
2. Pace, D.A., et al., *Calcium Entry in Toxoplasma gondii and Its Enhancing Effect of Invasion-linked Traits.* Journal of Biological Chemistry, 2014. **289**(28): p. 19637-19647.
3. Miranda, K., et al., *Characterization of a novel organelle in Toxoplasma gondii with similar composition and function to the plant vacuole.* Molecular Microbiology, 2010. **76**(6): p. 1358-1375.
4. Parussini, F., et al., *Cathepsin L occupies a vacuolar compartment and is a protein maturase within the endo/exocytic system of Toxoplasma gondii.* Molecular Microbiology, 2010. **76**(6): p. 1340-1357.
5. Forgac, M., *Vacuolar ATPases: rotary proton pumps in physiology and pathophysiology.* Nat Rev Mol Cell Biol, 2007. **8**(11): p. 917-929.
6. Leng, X.H., T. Nishi, and M. Forgac, *Transmembrane topography of the 100-kDa a subunit (Vph1p) of the yeast vacuolar proton-translocating ATPase.* J Biol Chem, 1999. **274**(21): p. 14655-61.
7. Wang, Y., M. Toei, and M. Forgac, *Analysis of the Membrane Topology of Transmembrane Segments in the C-terminal Hydrophobic Domain of the Yeast Vacuolar ATPase Subunit a (Vph1p) by Chemical Modification.* Journal of Biological Chemistry, 2008. **283**(30): p. 20696-20702.
8. Sidik, S.M., et al., *A Genome-wide CRISPR Screen in Toxoplasma Identifies Essential Apicomplexan Genes.* Cell, 2016. **166**(6): p. 1423-1435.e12.

9. Huynh, M.H. and V.B. Carruthers, *Tagging of endogenous genes in a Toxoplasma gondii strain lacking Ku80.* Eukaryot Cell, 2009. **8**(4): p. 530-9.

10. Sheiner, L., et al., *A Systematic Screen to Discover and Analyze Apicoplast Proteins Identifies a Conserved and Essential Protein Import Factor.* PLOS Pathogens, 2011. **7**(12): p. e1002392.

11. Wichroski, M.J., et al., *Clostridium septicum Alpha-Toxin Is Active against the Parasitic Protozoan Toxoplasma gondii and Targets Members of the SAG Family of Glycosylphosphatidylinositol-Anchored Surface Proteins.* Infection and Immunity, 2002. **70**(8): p. 4353-4361.

12. Smardon, A.M., M. Tarsio, and P.M. Kane, *The RAVE Complex Is Essential for Stable Assembly of the Yeast V-ATPase.* Journal of Biological Chemistry, 2002. **277**(16): p. 13831-13839.

13. Perzov, N., et al., *Characterization of yeast V-ATPase mutants lacking Vph1p or Stv1p and the effect on endocytosis.* Journal of Experimental Biology, 2002. **205**(9): p. 1209-1219.

14. Manolson, M.F., et al., *STV1 gene encodes functional homologue of 95-kDa yeast vacuolar H^+-ATPase subunit Vph1p.* Journal of Biological Chemistry, 1994. **269**(19): p. 14064-14074.

15. Fox, B.A., et al., *Efficient gene replacements in Toxoplasma gondii strains deficient for nonhomologous end joining.* Eukaryot Cell, 2009. **8**(4): p. 520-9.

16. Donald, R.G. and D.S. Roos, *Insertional mutagenesis and marker rescue in a protozoan parasite: cloning of the uracil phosphoribosyltransferase locus from*

Toxoplasma gondii. Proceedings of the National Academy of Sciences, 1995. **92**(12): p. 5749-5753.

17. Borges-Pereira, L., et al., *Calcium Signaling throughout the Toxoplasma gondii Lytic Cycle a study using genetically encoded calcium indicators.* Journal of Biological Chemistry, 2015. **290**(45): p. 26914-26926.
18. Demaurex, N., *pH Homeostasis of Cellular Organelles.* Physiology, 2002. **17**(1): p. 1-5.
19. Moreno, N.J.S., et al., *Vacuolar-type H^+-ATPase regulates cytoplasmic pH in Toxoplasma gondii tachyzoites.* Biochemical Journal, 1998. **330**(2): p. 853.
20. Pace, D.A., et al., *Overexpression of a Cytosolic Pyrophosphatase (TgPPase) Reveals a Regulatory Role of Pyrophosphate in Glycolysis for Toxoplasma gondii.* The Biochemical journal, 2011. **440**(2): p. 229-240.
21. Carruthers, V.B., O.K. Giddings, and L.D. Sibley, *Secretion of micronemal proteins is associated with toxoplasma invasion of host cells.* Cell Microbiol, 1999. **1**(3): p. 225-35.
22. Harper, J.M., et al., *A cleavable propeptide influences Toxoplasma infection by facilitating the trafficking and secretion of the TgMIC2-M2AP invasion complex.* Mol Biol Cell, 2006. **17**(10): p. 4551-63.
23. Hehl, A.B., et al., *Toxoplasma gondii Homologue of Plasmodium Apical Membrane Antigen 1 Is Involved in Invasion of Host Cells.* Infection and Immunity, 2000. **68**(12): p. 7078.

24. Cérède, O., et al., *The Toxoplasma gondii protein MIC3 requires propeptide cleavage and dimerization to function as adhesin.* The EMBO Journal, 2002. **21**(11): p. 2526-2536.

25. El Hajj, H., et al., *Molecular signals in the trafficking of Toxoplasma gondii protein MIC3 to the micronemes.* Eukaryot Cell, 2008. **7**(6): p. 1019-28.

26. Tomavo, S., et al., *Protein Trafficking through the Endosomal System Prepares Intracellular Parasites for a Home Invasion.* PLOS Pathogens, 2013. **9**(10): p. e1003629.

27. Hoppe, H.C., et al., *Targeting to rhoptry organelles of Toxoplasma gondii involves evolutionarily conserved mechanisms.* Nat Cell Biol, 2000. **2**(7): p. 449-56.

28. Ngo, H.M., M. Yang, and K.A. Joiner, *Are rhoptries in Apicomplexan parasites secretory granules or secretory lysosomal granules?* Mol Microbiol, 2004. **52**(6): p. 1531-41.

29. Chasen, N.M., et al., *A Glycosylphosphatidylinositol-Anchored Carbonic Anhydrase-Related Protein of Toxoplasma gondii Is Important for Rhoptry Biogenesis and Virulence.* mSphere, 2017. **2**(3): p. e00027-17.

30. Carey, K.L., et al., *The Toxoplasma gondii Rhoptry Protein ROP4 Is Secreted into the Parasitophorous Vacuole and Becomes Phosphorylated in Infected Cells.* Eukaryotic Cell, 2004. **3**(5): p. 1320.

31. Shaw, M.K., D.S. Roos, and L.G. Tilney, *Acidic compartments and rhoptry formation in Toxoplasma gondii.* Parasitology, 1998. **117**(5): p. 435-443.

32. Miller, S.A., et al., *TgSUB2 is a Toxoplasma gondii rhoptry organelle processing proteinase.* Molecular microbiology, 2003. **49**(4): p. 883-894.

33. Dogga, S.K., et al., *A druggable secretory protein maturase of Toxoplasma essential for invasion and egress.* eLife, 2017. **6**: p. e27480.

34. Anderson, E.D., et al., *Activation of the furin endoprotease is a multiple-step process: requirements for acidification and internal propeptide cleavage.* The EMBO journal, 1997. **16**(7): p. 1508-1518.

35. Gawlik, K., et al., *Autocatalytic activation of the furin zymogen requires removal of the emerging enzyme's N-terminus from the active site.* PLoS One, 2009. **4**(4): p. e5031.

36. Shinde, U., X. Fu, and M. Inouye, *A pathway for conformational diversity in proteins mediated by intramolecular chaperones.* Journal of Biological Chemistry, 1999. **274**(22): p. 15615-15621.

37. Szecsi, P.B., *The aspartic proteases.* Scand J Clin Lab Invest Suppl, 1992. **210**: p. 5-22.

38. Saroussi, S. and N. Nelson, *Vacuolar H^+-ATPase-an enzyme for all seasons.* Pflugers Arch, 2009. **457**(3): p. 581-7.

39. Beyenbach, K.W. and H. Wieczorek, *The V-type H^+ ATPase: molecular structure and function, physiological roles and regulation.* Journal of Experimental Biology, 2006. **209**(4): p. 577.

40. Toei, M., R. Saum, and M. Forgac, *Regulation and isoform function of the V-ATPases.* Biochemistry, 2010. **49**(23): p. 4715-23.

41. Hurtado-Lorenzo, A., et al., *V-ATPase interacts with ARNO and Arf6 in early endosomes and regulates the protein degradative pathway.* Nat Cell Biol, 2006. **8**(2): p. 124-136.

42. Nishi, T. and M. Forgac, *The vacuolar (H^+)-ATPases--nature's most versatile proton pumps.* Nat Rev Mol Cell Biol, 2002. **3**(2): p. 94-103.

43. Arrizabalaga, G., et al., *Ionophore-resistant mutant of Toxoplasma gondii reveals involvement of a sodium/hydrogen exchanger in calcium regulation.* The Journal of Cell Biology, 2004. **165**(5): p. 653.

44. Åkerman, K.E.O., *Changes in membrane potential during calcium ion influx and efflux across the mitochondrial membrane.* Biochimica et Biophysica Acta (BBA) - Bioenergetics, 1978. **502**(2): p. 359-366.

45. Roiko, M.S., N. Svezhova, and V.B. Carruthers, *Acidification Activates Toxoplasma gondii Motility and Egress by Enhancing Protein Secretion and Cytolytic Activity.* PLOS Pathogens, 2014. **10**(11): p. e1004488.

46. Dou, Z., I. Coppens, and V.B. Carruthers, *Non-canonical maturation of two papain-family proteases in Toxoplasma gondii.* J Biol Chem, 2013. **288**(5): p. 3523-34.

47. Soldati, D., J.F. Dubremetz, and M. Lebrun, *Microneme proteins: structural and functional requirements to promote adhesion and invasion by the apicomplexan parasite Toxoplasma gondii.* International Journal for Parasitology, 2001. **31**(12): p. 1293-1302.

48. Liu, J., et al., *A vacuolar-H^+-pyrophosphatase (TgVP1) is required for microneme secretion, host cell invasion, and extracellular survival of Toxoplasma gondii.* Molecular Microbiology, 2014. **93**(4): p. 698-712.

49. Dubremetz, J.F., *Rhoptries are major players in Toxoplasma gondii invasion and host cell interaction.* Cell Microbiol, 2007. **9**(4): p. 841-8.

50. Ngô, H.M., et al., *AP-1 in Toxoplasma gondii Mediates Biogenesis of the Rhoptry Secretory Organelle from a Post-Golgi Compartment.* Journal of Biological Chemistry, 2003. **278**(7): p. 5343-5352.

51. Venugopal, K., et al., *Dual role of the Toxoplasma gondii clathrin adaptor AP1 in the sorting of rhoptry and microneme proteins and in parasite division.* PLOS Pathogens, 2017. **13**(4): p. e1006331.

52. Turetzky, J.M., et al., *Processing and secretion of ROP13: A unique Toxoplasma effector protein.* International Journal for Parasitology, 2010. **40**(9): p. 1037-1044.

53. Ikemura, H. and M. Inouye, *In vitro processing of pro-subtilisin produced in Escherichia coli.* Journal of Biological Chemistry, 1988. **263**(26): p. 12959-12963.

54. Chtanova, T., et al., *Dynamics of Neutrophil Migration in Lymph Nodes during Infection.* Immunity, 2008. **29**(3): p. 487-496.

55. Kafsack, B.F., C. Beckers, and V.B. Carruthers, *Synchronous invasion of host cells by Toxoplasma gondii.* Mol Biochem Parasitol, 2004. **136**(2): p. 309-11.

56. O'Brien, K.M., E.L. Lindsay, and V.J. Starai, *The Legionella pneumophila Effector Protein, LegC7, Alters Yeast Endosomal Trafficking.* PLOS ONE, 2015. **10**(2): p. e0116824.

57. Huynh, M.-H. and V.B. Carruthers, *Toxoplasma MIC2 Is a Major Determinant of Invasion and Virulence.* PLOS Pathogens, 2006. **2**(8): p. e84.

58. Koivusalo, M., et al., *Amiloride inhibits macropinocytosis by lowering submembranous pH and preventing Rac1 and Cdc42 signaling.* J Cell Biol, 2010. **188**(4): p. 547-63.

5.10 STAR methods

Contact for Reagent and Resource Sharing

Further information and requests for resources and reagents should be directed to and will be fulfilled by the Lead Contact, Silvia Moreno (smoreno@uga.edu).

Experimental Model and Subject Details

Parasites and Host Cell Culture

T. gondii tachyzoites were maintained at 37°C in either immortal or mortal human foreskin fibroblasts (hTERT, ATCC® CRL-4001; HFF, ATCC® SCRC-1041) monolayers cultured in Dulbecco's modified Eagle's medium with high glucose supplemented with 1% HyClone fetal bovine serum (GE Healthcare Life Sciences). Parasites were regularly passed to new flasks containing new host cells when approximately 50-80% of the parasites have lysed out of the old culture. Flasks were maintained at 37°C with 5% CO_2. All strains and host cell lines were determined to be mycoplasma negative with the MycoScope kit (Genlantis). All parasite lines and host cells used in this study are listed in the key resource table (**Table 5.4**).

Parasite mutants were passed under similar conditions but the media was supplemented with the appropriate antibiotic used for selection.

Yeast growth

Yeast were grown on yeast peptone dextrose (YPD) agar plates or in liquid YPD at 30°C. Yeast were also grown on CSM-ura media on agar plates or broth as described below. For transformations, 1 ml of cultures was used to inoculate 10-15 ml of fresh YPD media at 30°C. Yeast were grown until the OD_{600} reached 1.5-2.0.

Method Details:

Epitope-tagging

Carboxy-terminus tagging was done in the parental line RHTatiΔku80 (*TatiΔku80*) [10] a parasite line that contains the tetracycline-regulated transactivator system that allows conditional expression of genes and also in which the *ku80* gene was deleted increasing efficiency of homologous recombination. Primers 1-6 (**Table 5.2**) were used to create C terminal insert fragments of genes *vha1* (TgGT1_232830), *vhE* (TgGT1_305290), and *vhG* (TgGT1_ 246560) (**Table 5.1**) that were suitable for cloning into a pLIC-3XHA, pLIC-mNeonGreen, or pLIC-GFP plasmids. Linearized plasmids were transfected into *TATiΔku80* cells followed by drug selection. Upstream gene locus primers 7-9 (**Table 5.2**) and a pLIC reverse primer (primer 10) were used to verify proper insertion in the correct gene locus. Western blot analyses with rat αHA (1:200) confirmed the presence of the 3xHA tagging. The cell lines isolated were termed according to the tagged gene and the tag used as *vha1-HA, vhE-HA, vhG-HA*, *vha1-mNeonGreen*, *vha1-GFP*. For tdTomato expressing cell lines, parasites were transfected with a tdTomato plasmid [54] (a gift from Boris Striepen, University of Georgia), enriched using a Bio-Rad S3 cell sorter, and subcloned. C-terminal Ty1 or myc tagging of aspartic protease 3 (ASP3; TgGT1_246550) was performed in the *iΔvha1-HA* strain by co-transfecting a plasmid that contained *CAS9* and a protospacer against the *UPRT gene* locus along with a plasmid that contained the *ASP3-3Ty1 cDNA* or a pLIC plasmid with a C-terminal myc tag, both plasmids generous gifts from Dominique Soldati-Favre [33]. Correct ASP3 C-terminal tags were confirmed by PCR (Primers 26, 27, and/or 10) and western blots with anti-Ty1 or anti-myc.

Inducible Knockdown

For *vha1* knockdowns, a tetracycline-regulatable element [10] was inserted upstream of the translational start codon via double homologous recombination. Primers 11-14 (**Table 5.2**) were used to generate the upstream UTR and gene fragments respectively for promoter insertion. Primes 15-18 were used to confirm insertion in the correct genetic locus. Repression of *vha1* was accomplished with 0.5 mg/ml anhydrotetracycline. The clonal line isolated after transfection, selection, and subcloning was named *iΔvha1-HA.*

Complementation of *iΔvha1-HA* Parasites

Complementation was achieved by cloning the cDNA of the *vha1* gene, using primers 19 and 20 (**Table 5.2**), into a UPRT cDNA shuttle vector, which contains the 5' and 3' UTR's of the *UPRT* and a tubulin promoter. The plasmid was transfected into *iΔvha1-HA* cells expressing tdTomato and selected using 5 μM 5-fluorodeoxyuridine (FUDR). Primers 18 and 21 (**Table 5.2**) were used to verify if *vha1* cDNA was inserted into the UPRT gene. The line isolated was named *iΔvha1-HA-CM.*

Immunofluorescence Assays

For IFAs of intracellular tachyzoites, hTERT or HFF monolayers were grown on 18 mm glass coverslips for 24 h and at this time infected with 5 X 10^5 parasites and allowed to grow for another 24 h. After 18-24 hours, parasites were fixed in 3% paraformaldehyde for 15 min.

For extracellular parasites, freshly lysed tachyzoites were collected, centrifuged and washed with Buffer A with glucose (BAG) (116 mM NaCl, 5.4 mM KCl, 0.8 mM $MgSO_4$, 50 mM HEPES, and 5.5 mM dextrose). Extracellular parasites were affixed to pre-

coated coverslips with polylysine and fixed in 3% paraformaldehyde for 15 min. After fixation, both intracellular and extracellular were treated identically. Parasites were permeabilized with 0.25% Triton X-100 at room temperature for 10 minutes. Blocking followed with 3% bovine serum albumin (BSA) in PBS at pH 8.0 for 30 min at room temperature. Primary and secondary antibodies were prepared in PBS at pH 8.0. Coverslips with parasites were washed 5 times after each antibody incubation and mounted on glass slides. IFA images were taken with an Olympus IX-71 inverted fluorescence microscope with a Photometrix CoolSnapHQ CCD camera driven by DeltaVision software or with a Zeiss ELYRA S1 (SR-SIM) super-resolution microscope. Images were deconvolved using Applied Precision's Softworx imaging suite using 10 cycles of enhanced ratio deconvolution or with ZEN 2011 software with SIM analysis module for SR-SIM images. For all IFAs, a control of TATi*ΔKu80* incubated with secondary antibody alone were used to subtract non-specific background.

The antibodies used for IFAs were: rat αHA (1:25); mouse αTy: (1:1,000), mouse αCPL (1:100), mouse αMIC2 (1:500), mouse αMIC3 (1:400), rabbit αM2AP (1:500), rabbit αproM2AP (1:250), mouse αSAG1 (1:100), mouse αMyc (1:100), mouse αVha1 (1:100), and rabbit αVP1 (1:4,000). The secondaries were all used at a concentration of 1:1,000.

For the experiment looking at pro-rhoptry labeling the specific antibody against immature rhoptry α-proROP4 (UVT-70, 1:500) (a gift from Gary Ward), the rhoptry bulb antibody α-TgCA_RP (Guinea Pig 1:1000) and an inner membrane complex marker that labels the IMC (α-IMC1 Mouse, 1:500), and allows to identification of dividing tachyzoites were used. For the quantification of this result, 100 vacuoles (containing 2-8 tachyzoites)

were examined for the presence or absence of tachyzoites containing nascent rhoptries (α-proROP4 labeling) and/or undergoing cytokinesis (α-IMC1 labeling of daughter cells).

Electron Microscopy:

Routine electron microscopy was performed at the Georgia Electron Microcopy Center. Parasites were fixed in 2.5% glutaraldehyde and 2% paraformaldehyde and post-fixed in 2% osmium tetroxide in 0.1 M cacodylate buffer (pH 7.2). Samples were then "En bloc" stained in 0.5% uranyl acetate and dehydrated in an ascending ethanol series and embedded in Spurr's plastic (Spurr, 1969). Cells were polymerized in an Eppendorf tube at 70 degrees Celsius for 12 hours. Embedded cells were sectioned on grids post-stained with uranyl acetate and lead nitrate. Grids were viewed in a JEOL JEM-1011 transmission electron microscope operated at 80 kV. The most apical point of the plasma membrane was defined, and then a line was drawn from this most apical end extending into the cytosol of the parasite 400 nM. Anything within this zone, was defined as apical micronemes and not peripheral. Anything within 100 nM of the plasma membrane and out of the apical zone was defined as periphery. Micronemes were identified by their higher electron density relative to other structures and organelles of the parasite. Structures with greater or equivalent electron density like dense granules, rhoptry necks, and acidocalcisomes are significantly larger and different in shape to be easily distinguishable from micronemes. Rhoptries were considered mature if any visible portion of the rhoptry was longer than 200 nM (in any direction). Rhoptries were identified by either their bulbs or necks, with necks having characteristically tubular morphology with high relative electron density and rhoptry bulbs with much less electron density than the necks and the cytosol. Parasites with a minimum of 1 microneme or rhoptry structure were enumerated.

Immuno-electron Microscopy.

Immuno-electron microscopy was done using Vha1-HA or Vha1-GFP tagged parasites. Parasites were manually lysed through a 25 gauge needle and incubated in DMEM media with serum for 0 or 1.5 hours at 37°C shaking incubator. Cells were pelleted, washed with PBS, then fixed with 4% paraformaldehyde and 0.05% glutaraldehyde for 1 hour on ice and washed once with phosphate buffered saline once. Sample preparation and images were performed by Dr. Wandy Beatty at the Department of Molecular Microbiology, Washington University School of Medicine, St. Louis, MO 63110.

Generation of mouse anti-Vha1 serum

Primers 22 and 23 (**Table 5.2**) were used to clone the first 327 amino acids of the *vha1 gene* into the bacterial inducible expression plasmid pQE-80L. Expression was induced with 1 mM Isopropyl β-D-1-thiogalactopyranoside (IPTG) for 2 hours at 37°C. Before and after the addition of IPTG, a sample corresponding to 1 OD_{600} was taken. The cells were sonicated, and the supernatant and pellet fractions were run on a 10% SDS-PAGE gel. Induction of expression with IPTG resulted in a significant band corresponding to the correct size of 36 kDa. Recombinant protein was purified from the bacteria lysate with a Thermo scientific HisPur Ni-NTA chromatography cartridge. Mice were inoculated intraperitoneally with 100 μg of purified and sterilized peptide solution mixed with Freund's complete adjuvant and boosted twice every 2 weeks with 50 μg of peptide and Freund's incomplete adjuvant. Antigen-adjuvant mixture was injected intraperitoneally (0.1 ml/injection) and blood was collected every two weeks to determine antibody titers. At the end of the immunization period mice were anesthetized, and blood was collected by

cardiac puncture. This serum was tested against parasite lysates and compared with the αHA labeling of *vha1-HA* lysates to confirm correct size and antibody purity (~37 kDa). Parasite lysates were run on a 10% SDS-PAGE gel and transferred to a nitrocellulose membrane for developing with αHA and the αVha1 serum. The observed bands were around 100 kDa. The serum was affinity purified and the αVha1 antibody was used for IFAs and westerns. Work with mice was carried out in strict accordance with the Public Health Service Policy on Humane Care and Use of Laboratory Animals and Association for the Assessment and Accreditation of Laboratory Animal Care guidelines. The animal protocol was approved by the University of Georgia's Committee on the Use and Care of Animals (protocol A2015 02-025-R2). All efforts were made to humanely euthanize the mice after collecting blood.

Plaque Assays

Plaque assays were performed with confluent hTERT host cells grown in six-well plates. Parasites obtained from T-25 flasks were pelleted, washed with PBS, counted using a hemocytometer and diluted in DMEM-HG for infection of each well with 200 parasites. Plates were incubated with or without ATc at 37°C. After 8 days of undisturbed growth, wells were washed twice with PBS, fixed with 100% ethanol for 5 minutes, and washed twice with PBS. Washed wells were stained with 5X crystal violet, washed twice with PBS, and allowed to dry for 4 hours before being photographed.

Red/Green Invasion Assay

The Red/Green invasion assay was performed as described [55] with some modifications. HFF fibroblasts were grown in a 12 well plate containing 18 mm coverslips for 24 h. The ideal monolayer should be at 70-80% confluency for this experiment. The

plate was placed on ice prior to the experiment. Freshly harvested and purified parasites were resuspended in ice-cold invasion media (3% serum and 10 mM HEPES in DMEM) at a concentration of 2.0 x parasites per ml. The media from the pre-chilled 12 well plate was aspirated and replaced with 1 ml of media plus 1 ml of the parasite suspension (2 x 10^7 parasites in 2 ml) and the plate incubated on ice for 20 min. At this point, the12 well plate is transferred to a 37°C water bath and parasites allowed to invade host cells for 5 min. Invasion is stopped by washing each well with PBS twice, immediately fixing with 3% paraformaldehyde, and blocked with 10% fetal bovine serum (FBS) for 20 min. Extracellular parasites are labeled with Rabbit αSAG1 polyclonal antibody (1:1000) (a generous gift from John Boothroyd) 60 min at room temperature. Wells were washed with PBS 5 times to remove antibody, permeabilizated with 1% Triton X-100 in PBS for 10 minutes, and washed 3 times. Parasites were then probed with anti-SAG1 monoclonal antibody (1:500) (Thermo Fisher) for 60 min at room temperature. Cells were washed with PBS 5 times to remove antibody. Secondaries against rabbit (red; 1,1000) and mouse (green; 1:500) were used to distinguish invasion from attachment. Secondaries were incubated for 60 minutes at room temperature and washed with PBS 5 times. Counting of red and green labeled parasites was compiled from three independent experiments by counting ten fields of view selected at random.

Replication and Growth Assays

Parasite strains were transfected with a plasmid that overexpresses the *tdTomato gene*. FACS sorting was performed to select a stable tdTomato expressing line. tdTomato-expressing parasites were incubated with or without ATc for 24 hours. These parasites (1 x 10^5) were used to infect (37°C for 30 min) sub-confluent HFF cells previously grown on

coverslips. Following this incubation, parasites were washed twice to remove any extracellular parasites and incubated with or without ATc for an additional 24 hours. After 48 hours of total ATc incubation, *Toxoplasma*-infected cells were washed twice with PBS and fixed with 3% paraformaldehyde for 10 min. Between 115-150 parasitophorous vacuoles (PV) per condition were counted and the number of parasites inside each PV enumerated. These experiments were repeated a minimum of three times.

Growth was assayed by infecting confluent hTERT cells in 96 well plates with 4,000 tdTomato-expressing parasites with or without ATc in the media. Parasites were allowed to grow in DMEM media without phenol red for 6 days. Each day a fluorescensce reading was recorded on a BioTek Synergy H1 hybrid plate reader. A standard curve was used to correlate parasite numbers, (1×10^6 to 1×10^1) with fluorescence values.

Egress and Motility Assays

For egress experiments, tdTomato-expressing parasites were grown with ATc for 2 days on hTERT host cells grown on 18 mm coverslips. Two coverslips per cell line of interest (one to serve as the experimental and the other as a control) were infected with 2×10^5 parasites in DMEM media and incubated for 24 hours at 37°C. Coverslips were then washed with PBS three times with pre-warmed PBS (pH 7.4) to 37°C. Egress was triggered with 10 μM nigericin from a stock solution made in DMSO and compared with a coverslip treated with DMSO alone as control. Coverslips were incubated at 37°C for 30 minutes. After the incubation, coverslips were fixed with 3.5% paraformaldehyde for 20 min at room temperature. Coverslips were then washed once with PBS and then mounted on a slide. For each sample, the number of intact parasitophorous vacuoles in 10 randomly selected fields was recorded. To determine % of egress the following equation was used:

$$100\% - \left(\frac{\text{number of vacuoles, nigericin sample}}{\text{number of vacuoles, DMSO control}} \text{ X } 100\right)$$

Only PV's with 2 or more parasites were counted.

An additional egress assay was performed using 0.01% saponin. HFF cells were seeded onto 35 mm MatTek culture dishes 24 hours prior to use. tdTomato-expressing parasites were pre-grown for 24 hours with ATc in hTERTs host cells, harvested, and used to infect the HFFs previously grown in MatTek culture dishes. After an additional 24 hours (48 hours total with ATc), parasites were assayed using time-lapse microscopy. This was done by removing the DMEM-HA media and replacing it with 2 ml of Ringer buffer with 2 mM calcium. Parasites were equilibrated for 2 minutes before adding 20 µl of a 0.01% saponin solution to the dish. A minimum of 6 PV's per field of view were assayed and the time for each PV to egress was enumerated. If no PV's egressed after 20 minutes from the time of saponin addition, those PVs were assigned an egress time of 1,200 sec.

Motility was assayed by resuspending parasites in Ringer buffer without calcium (155 mM NaCl, 3 mM KCl, 1 mM $MgCl_2$, 3 mM NaH_2PO_4, and 10 mM Hepes, and 10 mM dextrose) with 100 µM EGTA. tdTomato-expressing parasites incubated with or without ATc were tested. 24 hours prior to the experiment, 35 mm MatTek dishes were treated with 10% FBS to provide sufficient protein to form a surface conducive to motility. MatTek dishes were washed once with PBS and loaded with 2 ml of Ringer without Ca^{2+}. MatTek dishes were chilled on ice and 5 x 10^5 parasites were added and allowed to adhere to the surface for 1.5 min. Dishes were then placed in a Zeiss LSM 710 Confocal Microscope environmental chamber set to 37°C. 1.8 mM Ca^{2+} was added at the indicated time and the motility assay was recorded via time lapse microscopy. Length of trials was

manually traced in ImageJ using the MTrackJ plugin. For each trial, the motility of 5 parasites from 4 independent trials per strain (*iΔvha1-HA*-ATc, *iΔvha1-HA* +ATc, and *iΔvha1-HA-CM*+ATc) was quantified and averaged. The length of parasite movement is reported in μm.

Yeast Transformation

A colony of yeast grown on yeast peptone dextrose (YPD) agar plates was inoculated in 10 ml of YPD liquid media overnight at 30°C. 1 ml of the overnight culture was used to inoculate 10-15 ml of fresh YPD media at 30°C. Yeast were grown until the OD_{600} reached 1.5-2.0. Yeast was centrifuged and the pellet resuspended in 200 μl of 0.1 M lithium in water for 15 sec and centrifuged. Yeast were resuspended in 80 μl of 0.1 M lithium acetate and the volume adjusted to 100 μl, which was split into two 50 μl tubes. Each 50 μl tube was centrifuged, and the pellets resuspended in as described in **Table 5.3**.

Tubes were vortexed for 1 min and incubated first at 30°C for 30 min and then at 42°C for 30 min. Yeast were plated on Complete Supplement Mixture medium lacking uracil (CSM-ura) plates at 30°C for 3 days.

Yeast complementation.

The yeast mutant *vph1Δstv,* that does not express either of the V-ATPase *a* subunits was used for functional complementation studies because these mutants are unable to grow a neutral pH. Primers 24-25 and 28-29 (**Table 5.2**) were used to clone *vha1-HA* or *vha2* cDNA, respectively, into the pYES2NT/c yeast galactose inducible plasmid by restriction digest. Plasmids were transformed into WT and *Δvph1Δstv1* yeast and plated on CSM-ura pH 6.5 agar plates. Colonies were analyzed via PCR for the presence of correct inserts. For

inducible expression analysis, yeasts were grown in CSM-ura media at pH 5.5 with 2 % galactose or glucose.

Yeast were grown in YPD broth or CSM-ura media and normalized to OD_{600}. Yeast grown in media were pelleted to remove old media and then resuspended in 200 µL lysis buffer (0.1 M NaOH, 0.05 M EDTA, 2% SDS, with 2% 2-Mercaptoethanol) and boiled for 10 min. After boiling, 5 µL of 4 M acetic acid was added and the suspension was vortexed for 30 seconds. Lysed yeast were boiled again for 10 minutes and 50 µl of loading buffer was added (0.25 M Tris-HCl, 50% glycerol, 0.05% Bromophenolblue). 20 µg (quantified via nanodrop) of lysate was run on a 10% SDS-PAGE gel for western analysis with rat αHA (1:200) antibodies. To test for complementation of growth, strains were grown on CSM-ura media at pH 7.0 with 2 % galactose for 48 (liquid) or 96 h (plates) at 30°C. For growth in liquid CSM-ura, yeast strains were normalized to an OD_{600} of 1 and diluted 1:10 in liquid media in triplicate. Plates were read in a BioTek Synergy H1 hybrid tester every hour for 48 h under high orbital shaking incubated at 37°C. For growth on agar plates, yeast strains first grown in suspension were normalized to an OD_{600} of 1 and serially diluted 1:10 on the plates and the experiment repeated three times. Plates were photographed 96 h after inoculation. For the localization of *vha1* in yeast, primers 28-31 were used to amplify *vha1* or *vph1* cDNA to clone via yeast gap repair into the pGO36 plasmid [56] which will fuse GFP to the gene. Yeast were grown on CSM-ura plates for 4 days and colonies were isolated.

pH_i Measurements.

Intracellular pH (pH_i) of *iΔvha1-HA* and *iΔvha1-HA–CM* grown plus and minus ATc was determined fluorometrically by loading parasites with 2′,7′-Bis(2-carboxyethyl)-

5(6)-carboxyfluorescein acetoxymethyl ester (BCECF-AM) (Thermo Fisher Scientific). Purified extracellular tachyzoites were resuspended at a final density of 1 x 10^9/ ml and loaded with 9 μM BCECF-AM in BAG containing 1.5% sucrose at 37°C for 20 min. At the end of the loading time parasites were washed twice with BAG and resuspended to a final concentration of 1 X 10^9 cells/ml in the same buffer and kept on ice protected from light. For fluorescence measurements, a 50 μl aliquot of the cell suspension was diluted into 2.45 ml of standard buffer (135 mM NaCl, 5 mM KCl, 1 mM $MgSO_4$, 1 mM $CaCl_2$, 5 mM glucose and 10 mM Hepes/Tris, pH 7.4) to a final density of 2 x 10^7 cells/ml. The cell suspension was allowed to equilibrate for 2.5 min. in a cuvette before being placed in an Hitachi F-7000 fluorescence spectrophotometer (Hitachi High Technologies). Fluorescence ratios were calculated with excitations at 505 and 440 nm and emission at 530 nm. A standard curve was created using parasites in high potassium standard buffer (140 mM KCl, 1 mM $MgSO_4$, 1 mM $CaCl_2$, 5 mM glucose and 10 mM Hepes/Tris, pH 7.4) at pH's ranging from 5.5 to 8 (in 0.5 pH increments) and by adding 5.2 μM of nigericin to the cell suspension. The pH of the buffer and the fluorescence value reached after the stabilization of the trace was used for building the standard curve. The standard curve was then used to determine pH_is. To determine the effect of changing extracellular pH (pH_e) on pH_i, *iΔvha1-HA* + and - ATc loaded with BCECF-AM were incubated in standard buffer at the indicated varying pH_e. For the recovery experiments, loaded parasites in suspension were exposed to 10 mM propionic acid, which was added to the cuvette at the indicated time.

Proton Extrusion Measurements

Proton extrusion was determined fluorometrically by suspending parasites in a weakly buffered solution containing the free form of BCECF (Thermo Fisher Scientific). A 100 µl aliquot of a cell suspension (at 1 x 10^9 cell/ml) was diluted into 2.45 ml of a weak buffer (135 mM NaCl, 5 mM KCl, 1 mM $MgSO_4$, 1 mM $CaCl_2$, 0.1 mM HEPES, and 0.1 mM Tris-Base) with 0.38 µM BCECF free acid. The cell suspension was added to a cuvette and placed in a Hitachi F-7000 fluorescence spectrophotometer. 25 mM glucose was added to stimulate metabolic activity and proton extrusion. A standard curve of known pH's was used to determine the change of extracellular pH.

Membrane Potential Measurements

Membrane potential was measured fluorometrically with bisoxonol. Bisoxonol (0.2 µM) was added to 5 x 10^7 cells suspended in 2.5 ml of standard buffer at pH 7.5 or 7.0 at 37°C and the fluorescence excitation was set at 540 nm and emission at 580 nm. The cell suspension was added to a cuvette and placed in a Hitachi F-7000 fluorescence spectrophotometer. The last 100 seconds of the tracing were averaged at each pH and the ratio of pH 7.5/7.0 determined.

Lysotracker Measurements

Purified parasites (at a concentration of 1 x 10^8) were loaded with 10 µM Lysotracker red by incubating them for 30 min at 37°C in BAG, washed twice with BAG, and placed in 35 mm MatTek dishes in Ringer buffer. For quantification of Lysotracker stained compartments, the number of vacuoles from 10 fields of view with at least 5 parasites was tallied. To minimize bias, counting was performed double blinded.

Microneme Secretion

Parasites were collected from a <10% lysed culture, passed through a 23 gauge needle, filtered through 3 μm nucleopore membrane, pelleted, and resuspended in ice cold invasion media (20 mM HEPES in DMEM-HG without serum). For constitutive expression, 4 x 10^8 parasites were incubated at 37°C in a shaking water bath for 30 min. Parasites were pelleted and the supernatant was collected and used for western analysis. For induced expression, 4 x 10^8 parasites were incubated in microneme secretion buffer (9.8 mL of invasion media with 200 μL of 10% ethanol), incubated in a shaking 37°C water bath for 2 minutes, and the supernatant was collected. The supernatants and lysate were run on a 12.5% SDS-PAGE gel for 45 minutes at 100 volts. Immunoblots were probed with αMIC2 (1:4,000), αAMA1 (1:500), and αGRA1 (1:1,000).

Microneme Maturation

M2AP and MIC3 maturation were measured by using an antibody created against the propeptide part of M2AP [22] (1:1,000) or against MIC3 [24] (1:40). *iΔvha1-HA* parasites were incubated with ATc for 0 to 3 days, parasite lysate was generated, and run on a 10% SDS-PAGE gel and probed with αM2AP, αMIC3 or αTubulin (1:30,000). The intensity of the bands obtained in the immunoblots were analyzed using pixel density by ImageJ or Image Studio (where indicated). Quantification was determined either by a ratio of immature/mature or mature/tubulin respectively.

Maturation of proteases

Maturation of CPL was performed using an antibody against CPL, which recognizes both the mature and immature forms. *iΔvha1-HA* parasites were grown with ATc for 0 to 3 days, lysed, run on an 10% SDS-PAGE gel, which was transferred to a

nitrocellulose membrane for western analysis. αCPL at 1:500 was used to identify proCPL from mature CPL. Determination of the mature from immature was done based on the sizes described in [4]. For TgSUB2 maturation, αTgSUB2 (1:500) [32] was used for westerns as described above. Determination of the mature from immature was done based on sizes described in [32]. For aspartic protease 3 (ASP3) maturation, the plasmid 5'UPRT-pTub8-Asp3-3Ty-3'UPRT from Dominique Soldati-Favre's lab [33] was transfected into *iΔvha1-HA* parasites. αTy1 (1:1,000) was used for westerns of membranes containing lysates generated as above. Determination of the mature from immature was based on sizes described in [33]. For all quantifications, pixel densities generated using ImageJ of the propeptide and mature peptide was measured to determine maturation.

Maturation of Rhoptry Proteins

Maturation of rhoptry proteins was analyzed using α-ROP4 (UVT-68, Rabbit 1:500), α-ROP7 (1:1,000), and α-TgCA_RP (Guinea Pig 1:1,000) via western blots which were done similarly to the ones described above for microneme and protease maturations. Quantification of band intensity was performed using signal intensity determined by LI-COR Image Studio Software. Percentage of immature protein was determined by dividing the band intensity of the immature band by the total combined intensity of mature and immature bands.

Quantification and Statistical Analysis

All statistical analyses were performed using GraphPad Prism 6. Unless otherwise noted, all error bars are presented as the standard error of the mean (SEM) and from a minimum of three independent trials. Significant differences were only considered if P values were < 0.05, where $*P < 0.05$; $**P < 0.01$; $***P < 0.001$; and $****P < 0.0001$. NS

designates when the comparison is not statistically significant. Experiment-specific statistical information is provided in the figure legends or associated method details including trials (n), standard error of the mean SEM, and statistical test performed.

Tables

Table 5.1: Identification of *T. gondii* V-ATPase subunits.

	Subunit[a]	Yeast Gene[b]	Toxo ID	Proposed Name	E value[c]	% Similar[d]	CRISPR Score[e]
V_1	A	*vma1*	TGGT1_256970	VhA	2.00E-126	58%	-3.61
	B	*vma2*	TGGT1_219800	VhB	0	73%	-5.49
	E	*vma4*	TGGT1_305290	VhE	5.00E-28	32%	-1.40
	C	*vma5*	TGGT1_315620	VhC	4.00E-38	30%	-3.59
	F	*vma7*	TGGT1_310960	VhF	3.00E-31	52%	-2.18
	D	*vma8*	TGGT1_281920	VhD	7.00E-60	50%	-4.69
	G	*vma10*	TGGT1_246560	VhG	8.00E-06	35%	-5.05
	H	*vma13*	TGGT1_208590	VhH	3.00E-13	24%	-4.78
V_O	a1	*vph1*	TGGT1_232830	Vha1	1.00E-98	29%	-3.73
	a2	*vph1*	TGGT1_290720	Vha2	3.00E-78	29%	-3.30
	c	*vma3*	TGGT1_212310	Vhc	4.00E-40	54%	-4.29
	c'	*vma11*	nf[f]	-	-	-	-
	c''	*vma16*	TGGT1_291310	Vhc''	7.00E-45	55%	-5.45
	d	*vma6*	TGGT1_259010	Vhd	7.00E-68	35%	-4.84
	e	*vma9*	nf	-	-	-	-

[a] Subunits of a typical Vacuolar-H^+-ATPase.

[b] Gene corresponding to the listed subunit from *Saccharomyces cerevisiae*.

[c] Expectation value generated from BLASTp analysis.

[d] Percent similarity of protein compared to *Saccharomyces cerevisiae*.

[e] CRISPR Phenotype score.

[f] None found.

Table 5.2: Primers used in this study

Primer	Sequence	Use
1	TACTTCCAATCCAATTTAATGCTGAAGCCGGAAGTAGCAG	3XHA tagging *vha1*
2	TCCTCCACTTCCAATTTTAGCCGCATCATCCTCGCCTTGGAG	
3	TACTTCCAATCCAATTTAATGCGAAGGCGAAGAAACTCGAAACCCAG	3XHA tagging *vhE*
4	TCCTCCACTTCCAATTTTAGCTTGATGGCTCGGGAATAAGGTATG	
5	TACTTCCAATCCAATTTAATGCCTTCTCCCAGAAGTCCAACGAAC	3XHA tagging *vhG*
6	TCCTCCACTTCCAATTTTAGCCGGTGCGACGCCTCGTTTG	
7	CCATGGTGCAGTCAAGTAC	*vha1* upstream verification
8	GTCTCTCGAGGACTTCAACATTG	*vhE* upstream verification
9	CACCATCGTCAACAAAGCGAAGG	*vhG* upstream verification
10	CGATACCGTCGACCTCGAGTAG	pLIC reverse primer
11	GCTTGAGCAAGGGTGGGTATGC	Used to make the upstream fragment of promoter insertion
12	GCCTGTCTCAGTGTCCCAACAGAC	
13	ATGACCACTCTACGCAGCGAGC	Used to make the gene fragment of promoter insertion
14	CGTCCAGCAAACTCTGCAACC	
15	TGAGTATTGCCACTTTTCCTGTG	Used to confirm correct insertion upstream of *vha1*
16	ATCTGCACACCTGGTCTCGATG	
17	CGTGAGGCTGGTACCTGGTCG	*sag4* forward
18	GCAGCCATGTGCCAGCGG	*vha1* 5' end reverse
19	GGCGCGCCATGACCACTCTA	Used to clone vha1 cDNA into UPRT cDNA shuttle vector
20	GGTACCCGCATCATCCTCGCCTTGGAG	
21	GCCTGCGATTCCCGTATTGGTCAC	*uprt* upstream Forward
22	GGATGCATGGATCCATGACCACTCTACGCAGCGAG	Used to clone the first 327 amino acids of Vha1 into pQE-80L vector
23	ACTTTATACTGCAGCTAACTGAGAAAATATTTCTCATAGGCAGCG	
24	GCGGCCGCACATGACCACTCTACG	

25	GCGGCCGCACTTAGGCATAATCTG	Inserting Vha1 cDNA into pYESNT/c
26	GCGCGACCAAAGATATACCCCG	*uprt* Downstream Reverse
27	GCACAACGACGACAACAGTGC	*asp3* cDNA Forward
28	ATGGATGAACTATACAAGTCCGGACTCAGATCTATGACCACTCT ACGCAGCGAG	Used to put *vha1* cDNA into pGO36 plasmid
29	GTCGACTGCAGAATTCGAAGCTTGAGCTCGAGATCTCTACGCAT CATCCTCGCCTTG	
30	ATGGATGAACTATACAAGTCCGGACTCAGATCTATGGCAGAGA AGGAGGAAGCG	Used to put *vph1* cDNA into pGO36 plasmid
31	GTCGACTGCAGAATTCGAAGCTTGAGCTCGAGATCTTTAGCTTG AAGCGGAAGAGCTTG	

Table 5.3: Yeast transformation reaction.

Experimental Tube	**Control Tube**
240 μL 50% sterile PEG3350	240 μL 50% sterile PEG3350
36 μL 1 M Lithium Acetate	36 μL 1 M Lithium Acetate
50 μL Salmon sperm DNA (2 mg/mL)	50 μL Salmon sperm DNA (2 mg/mL)
DNA (100-500 ng) plus water to 34 μL	34μL water (no DNA)

Table 5.4: Key Resource Table

REAGENT or RESOURCE	SOURCE	IDENTIFIER
Antibodies		
αMIC2	Vern Carruthers	[22]
αMIC3	Maryse Lebrun	[24]
αM2AP	Vern Carruthers	[22]
αproM2AP	Vern Carruthers	[22]
αGRA1	Vern Carruthers	[57]
αCPL	Vern Carruthers	[4]
αVha1	This Paper	TgVha1
αTgSUB2	Kami Kim	[32]
αHA High Affinity, from rat IgG1	Sigma-Aldrich	Cat#11867423001
αTy1	Drew Etheridge	Lab Stock
αTubulin	Sigma-Aldrich	Cat#T5168
αVP1	Silvia Moreno	[3]
αSAG1	John Boothroyd and Fisher	N/A
αROP4 (UVT-68)	Gary Ward	[30]
αROP7	Peter Bradley	[29]
αCA_RP	Silvia Moreno	[29]
αMyc	Sigma-Aldrich	Cat#M5546
Alexa Fluor 350 Antibody	Thermo Fisher Scientific	Cat#A20180

Alexa Fluor 488 Antibody	Thermo Fisher Scientific	Cat#A20181
Alexa Fluor 546 Antibody	Thermo Fisher Scientific	Cat#A20183
αAMA1	Dominique Soldati-Favre	[23]
α-IMC1	Drew Etheridge	N/A
Bacterial and Virus Strains		
Mix and Go	Zymo Research	Cat#T3007
BL21-CodonPlus (DE3)-RILP	VWR	Cat#76193-370
Biological Samples		
TATiΔKu80 Toxoplasma gondii	Boris Striepen	[10]
vha1-HA, TATiΔKu80 Toxoplasma gondii	This work	N/A
vhE-HA, TATiΔKu80 Toxoplasma gondii	This work	N/A
vhG-HA, TATiΔKu80 Toxoplasma gondii	This work	N/A
vha1-HA, vhG-Ty1; TATiΔKu80 Toxoplasma gondii	This work	N/A
iΔvha1-HA; TATiΔKu80 Toxoplasma gondii	This paper	N/A
iΔvha1-HA-CM; TATiΔKu80 Toxoplasma gondii	This work	N/A

iΔvha1-mNeonGreen; TATiΔKu80 Toxoplasma gondii	This work	N/A
iΔvha1-GFP; TATiΔKu80 Toxoplasma gondii	This work	N/A
Δvph1Δstv1	This work	N/A
WT Yeast	Vincent Starai	BY47472
Chemicals, Peptides, and Recombinant Proteins		
2h, 7h-bis-(2-carboxyethyl)-5(6)-carboxyfluorescein (BCECF)	Thermo Fisher Scientific	Cat#B1151
2h, 7h-bis-(2-carboxyethyl)-5(6)-carboxyfluorescein-acetoxymethyl (BCECF-AM)	Thermo Fisher Scientific	Cat#B1170
Anhydrotetracycline (ATc)	Sigma-Aldrich	Cat#1035708
5-fluorodeoxyuridine (FUDR)	Sigma-Aldrich	Cat#F0503
isopropyl β-D-1-thiogalactopyranoside (IPTG)	Sigma-Aldrich	Cat#I5502
Bafilomycin A1	Sigma-Aldrich	Cat#B1793
Saponin	Sigma-Aldrich	Cat#47036
Nigericin	Sigma-Aldrich	Cat#N7143
Dulbecco's modified Eagle medium--High Glucose	Sigma-Aldrich	Cat#D5796

Freund's Complete Adjuvant	Thermo Fisher Scientific	Cat#77140
Freund's incomplete adjuvant	Thermo Fisher Scientific	Cat#77145
HisPur Ni-NTA chromatography cartridge	Thermo Fisher Scientific	Cat#90098
16% Paraformaldehyde	Electron Microscopy Sciences	Cat#15700
Bovine Serum (Calf Serum)	Thermo Fisher Scientific	Cat#16030074
Complete Supplement Mixture medium lacking uracil (CSM-ura)	Sunrise Science	Cat#1004-100
Galactose	Sigma-Aldrich	Cat#1287700
LysoTracker™ Red DND-99	Thermo Fisher Scientific	Cat#L7528
DiSBAC2(3) (Bis-(1,3-Diethylthiobarbituric Acid)Trimethine Oxonol)(bisoxonol)	Thermo Fisher Scientific	Cat#B413
Experimental Models: Cell Lines		
Human Foreskin Fibroblast immortalized with hTERT	ATCC	BJ-5ta ATCC® CRL-4001
Human Foreskin Fibroblast (HFF)	ATCC	HFF-1 ATCC® SCRC-1041

Oligonucleotides		
	See Table 5.2	
Recombinant DNA		
pLIC-3XHA	Boris Striepen	[10]
pLIC-mNeon-Green	This work	N/A
pLIC-GFP	This work	N/A
ptdTomato overexpression plasmid	Boris Striepen	[54]
UPRT Vha1 cDNA shuttle vector	This work	This paper
5'UPRT-pTub8-Asp3-3Ty-3'UPRT	Dominique Soldati-Favre	[33]
pSAG1-CAS9-U6-sgUPRT	David Sibley	Addgene plasmid #54467
promoter insertion plasmid	Boris Striepen	[10]
pGO-GFP	Vincent Starai	[56]
Software and Algorithms		
FIJI (imageJ)	https://fiji.sc	Version 2.0.0-rc-69/1.52i
Graphpad	https://www.graphpad.com	Version 6
Microsoft excel	Microsoft.com	Version 16.22
Microsoft word	Microsoft.com	Version 16.22
Adobe Illustrator	Adobe.com	Version CS6
Adobe Photoshop	Adobe.com	Version CS6

Image Studio	Licor.com	Version 5

Figures

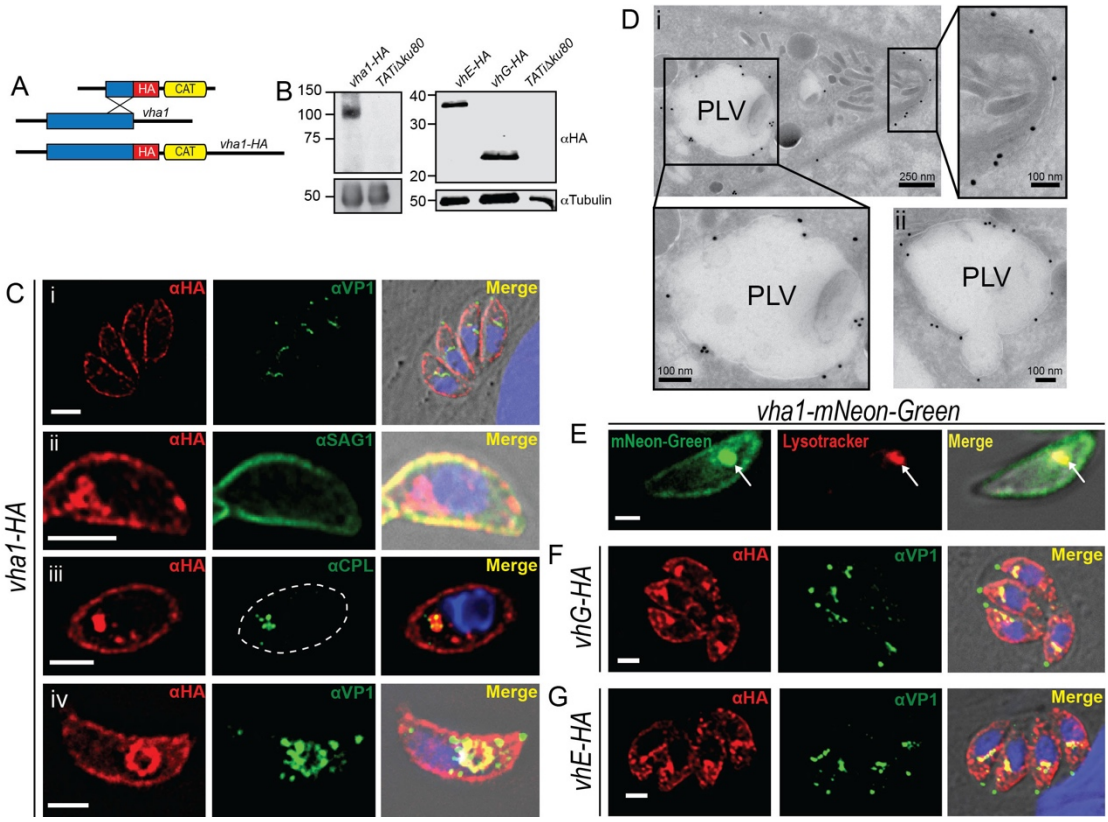

FIGURE 5.1: **Vha1 localization.** A) 3xHA tagging: HA, hemagglutinin; CAT, chloramphenicol acetyltransferase. B) Western blots of lysates from *vha1-HA* (left panel), *vhE-HA* and *vhG-HA* (right panel) parasites with αHA antibody. C) IFAs of *vha1-HA* cells with αHA showing i) localization of Vha1 in intracellular tachyzoites; ii) co-localization with αSAG1; iii) super resolution IFA's showing co-localization with CPL (PLV marker). Dashed lines mark parasites; iv) extracellular tachyzoites showing co-localization with VP1. D) Immuno-EM with αHA showing i) labeling at the plasma membrane and PLV; ii) PLV fusing with vesicles. E) *vha1-mNeonGreen* clones showing co-localization of mNeonGreen with lysotracker. F) IFAs of intracellular *vhG-HA* tachyzoites with αHA and αVP1. G) IFAs of intracellular tachyzoites expressing *vhE-HA* with αVP1 and

αHA. The Mander's colocalization coefficient of VP1/Vha1 and CPL/Vha1 from 3 independent trials was 0.33 and 0.62, respectively. Scale bars: 2 μm.

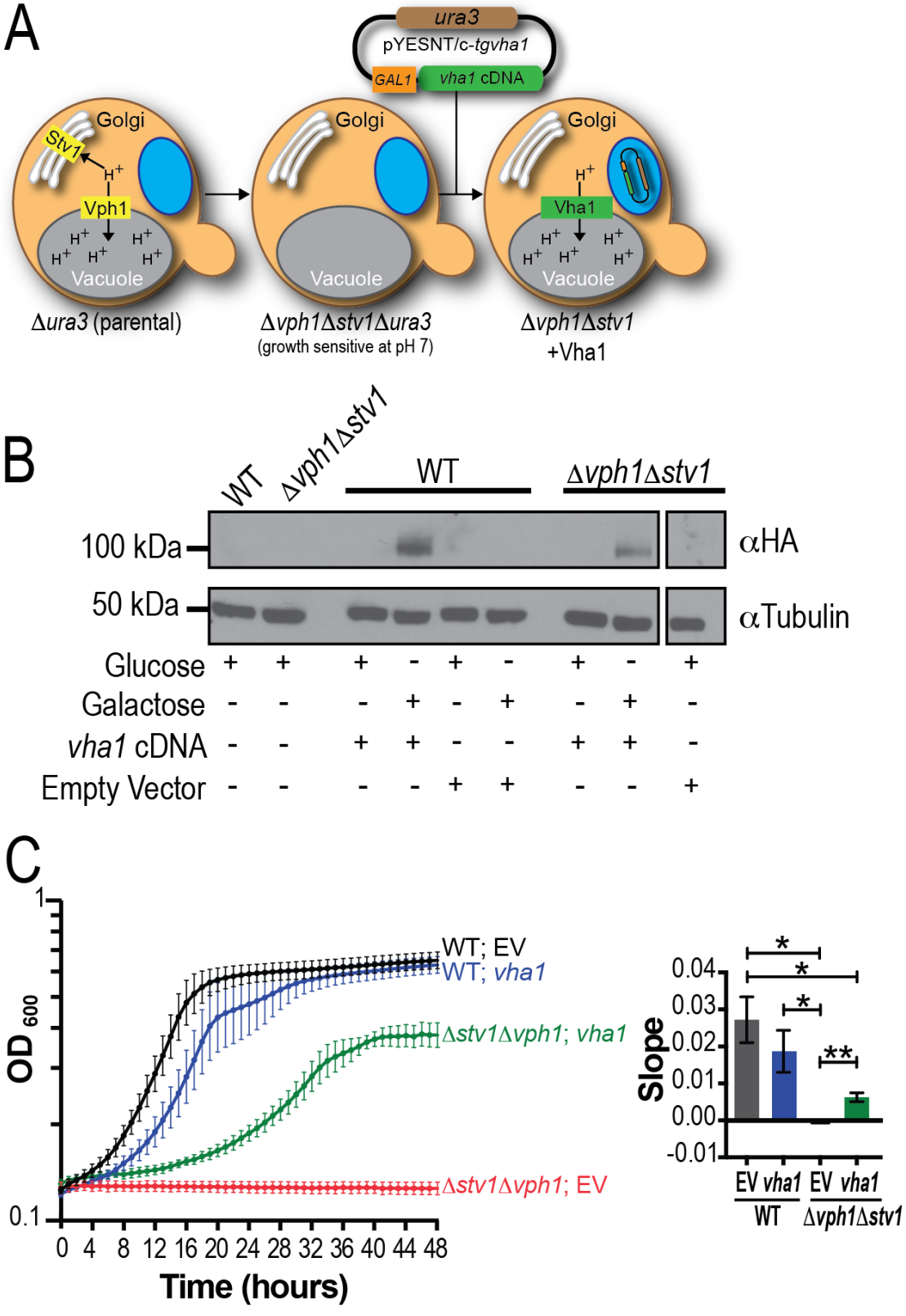
A
ura3
pYESNT/c-tgvha1
GAL1
vha1 cDNA
Golgi
Stv1
Vph1
Vha1
Vacuole
Δura3 (parental)
Δvph1Δstv1Δura3
(growth sensitive at pH 7)
Δvph1Δstv1
+Vha1
B
WT
Δvph1Δstv1
WT
Δvph1Δstv1
100 kDa
50 kDa
αHA
αTubulin
Glucose
Galactose
vha1 cDNA
Empty Vector
C
OD 600
Time (hours)
WT; EV
WT; vha1
Δstv1Δvph1; vha1
Δstv1Δvph1; EV
Slope
EV vha1 EV vha1
WT
Δvph1Δstv1

FIGURE 5.2: **Functional analysis of Vha1 in *Saccharomyces cerevisiae*.** A) Strategy used for complementation of *vph1Δstv1Δ S. cerevisiae* with the *vha1* gene. GAL1, galactose inducible promoter; *ura3*, metabolic marker that contains the *ura3* gene. B) Western blot of *vph1Δstv1Δ* lysates grown on glucose or galactose (pH 5.5) transfected with pYES2 containing the *vha1-HA* cDNA. Control strains were transformed with an empty pYES2/NT C vector or no vector. C) Growth of WT and *Δvph1Δstv1* yeast harboring *vha1* cDNA (*vha1*) or empty vector (EV) grown in CSM-ura pH 7.0 with 2% galactose for 48 h. Data are from 3 independent trials done in triplicate. Quantification of the slopes during exponential growth (4-16 hours in WT yeast and 8-32 hours in Δ*vph1*Δ*stv1* yeast) using one-way ANOVA test where $*P < 0.05$ and $**P < 0.01$.

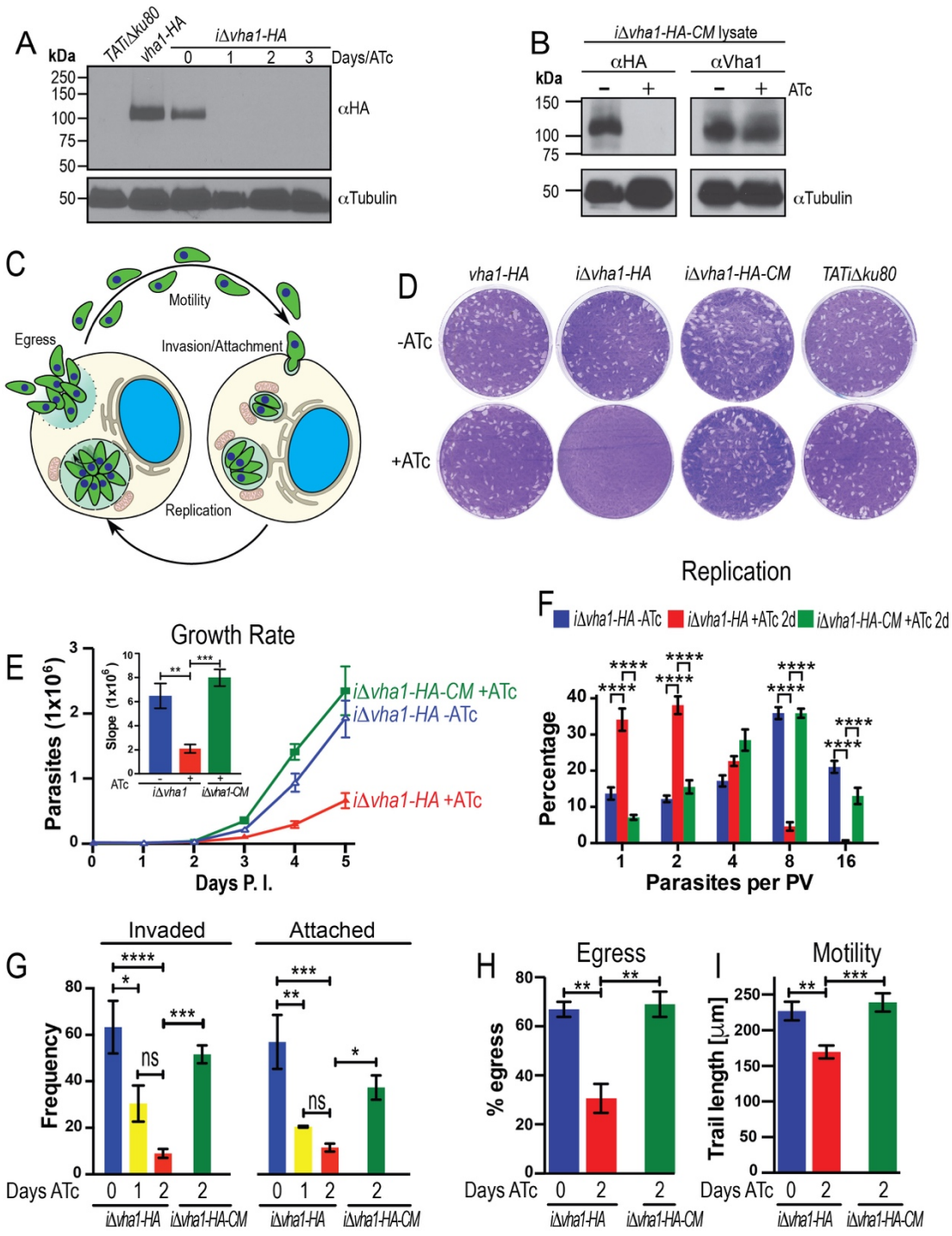

FIGURE 5.3: **The V-ATPase and the *T. gondii* lytic cycle.** A) Western blots of lysates from parental (*TATiΔku80*), *vha1-HA*, and *iΔvha1-HA* grown + or - ATc parasites. Immunoblots were developed with rat αHA (1:200). Anti-tubulin was the loading control.

B) Western blots of lysates of *iΔvha1-HA-CM* parasites showing no expression of the endogenous copy of *vha1* in the presence of ATc while the extra copy of Vha1 was constitutively expressed as evident with the mouse αVha1 antibody (1:500) (see Fig. S2H for more details on the antibody). C) Overview of the lytic cycle. D) Plaque assays of *vha1-HA*, *iΔvha1-HA*, *iΔvha1-HA*-CM and TATiΔ*ku80* clones grown + or - ATc (0.5 μg/ml). Each well was infected with 200 parasites and grown for 8 days, fixed and stained with crystal violet. E) 4,000 tdTomato-expressing parasites were grown in hTERT cells for 5 days. Data are presented as the average of 3 independent trials done in triplicate. Inset: slopes from days 2-5. F) Growth kinetics of *iΔvha1-HA* and *iΔvha1-HA-CM* + or -ATc. Parasites from 115-150 PVs were counted per clone in three independent trials. G) Red-green assay for quantification of attachment and invasion of *T. gondii*. Data was from 3-4 independent experiments counting ten random fields per clone. H) Egress triggered with 10 μM nigericin for 30 min at 37°C. Data was from 3 independent experiments counting ten random fields per clone and comparing them to a DMSO control. Only PVs with 2 or more parasites were enumerated. I) tdTomato-expressing parasites were resuspended in ringer buffer without Ca^{2+} and motility was stimulated with 1.8 mM Ca^{2+}. The average length (microns) parasites traveled is reported from 5-6 individual parasites from 3 independent trails. Values are means ± SEM. Panels E) and F) were compared with two-way ANOVA test and panels G), H), and I) were compared with one-way ANOVA test, where $*P < 0.05$; $**P < 0.01$; $***P < 0.001$, $****P < 0.0001$.

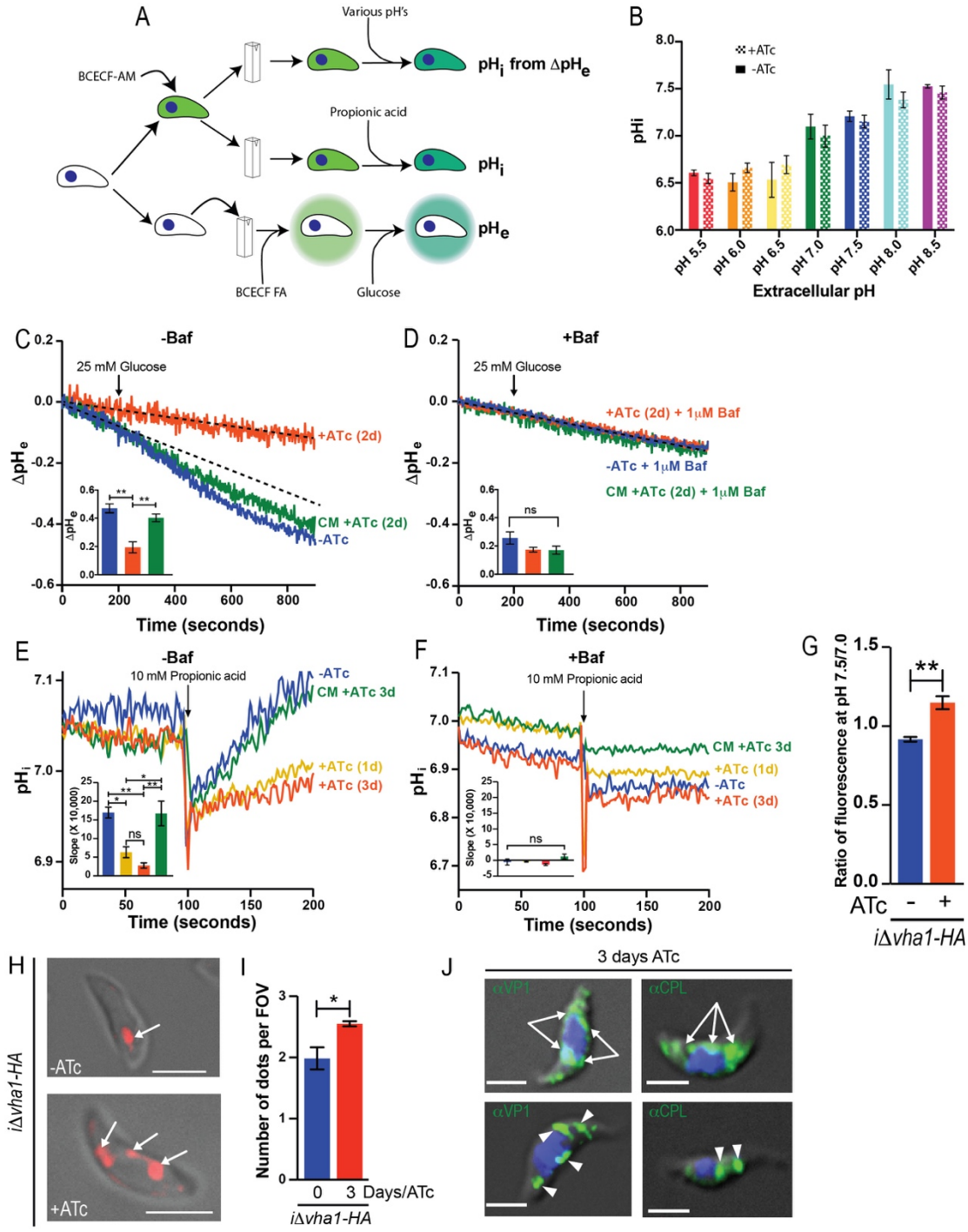

FIGURE 5.4: **Function of Vha1 in *T. gondii*.** A) Protocol used to measure intracellular pH (pH_i), extracellular pH (ΔpH_e), and proton extrusion (pH_e). B) pH_i measurements of *iΔvha1-HA* cells at various extracellular pH's. Parasites were loaded with the pH indicator

BCECF-AM and fluorescence measurements were done as described in Methods. Data was from 3 independent trials. C) Representative tracings of proton extrusion of *iΔvha1-HA* + or - ATc after adding 5 mM glucose. BCECF free acid in a weakly buffered solution was used. Changes in pH were followed as described in Methods. Inset shows analysis from 3-6 independent trials. Dashed line represents the –Atc slope before adding glucose. D) Same as C but cells were pretreated with 1 μM bafilomycin for 3 min. Insets show quantifications of slopes. E) Acid load and pH recovery of parasites loaded with BCECF-AM. 10 mM propionic acid (PA) was added where indicated to suspensions of *iΔvha1-HA* and *iΔvha1-HA-CM* (3 days ATc) grown +ATc for 0, 1, 3 days. Quantifications are from 3-4 independent trials. F) Same as E but cells were pretreated with 1 μM bafilomycin for 3 min. Insets show the quantification of slopes from 105 to 200 sec from 3 independent trials. G) Membrane potential measurements of *iΔvha1-HA* cells grown + or - ATc for 2 days and incubated with bisoxanol. Fluorescence measurements at pH 7.5 to 7.0 were compared and are from 3 independent trials. H) *iΔvha1-HA* parasites + or -ATc (0 or 3 days, respectively) and loaded with 10 μM LysoTracker red for 30 min at 37°C in BAG. I) Quantification of compartments stained by LysoTracker. 5-15 cells per field of view were counted and a minimum of 8 fields. Graph shows quantifications of puncta in *iΔvha1-HA* parasites + and - ATc. J) IFA of *iΔvha1-HA*+ATc (3 days) parasites and probed with αVP1 or αCPL. Arrows point to ER localization and arrowheads point to discrete puncta of VP1 or CPL staining. Statistical analysis was performed using a student's T-Test (G, I) or one-way ANOVA (B, C-F) where $*P < 0.05$; $**P < 0.01$; $***P < 0.001$, $****P < 0.0001$, ns, not significant.

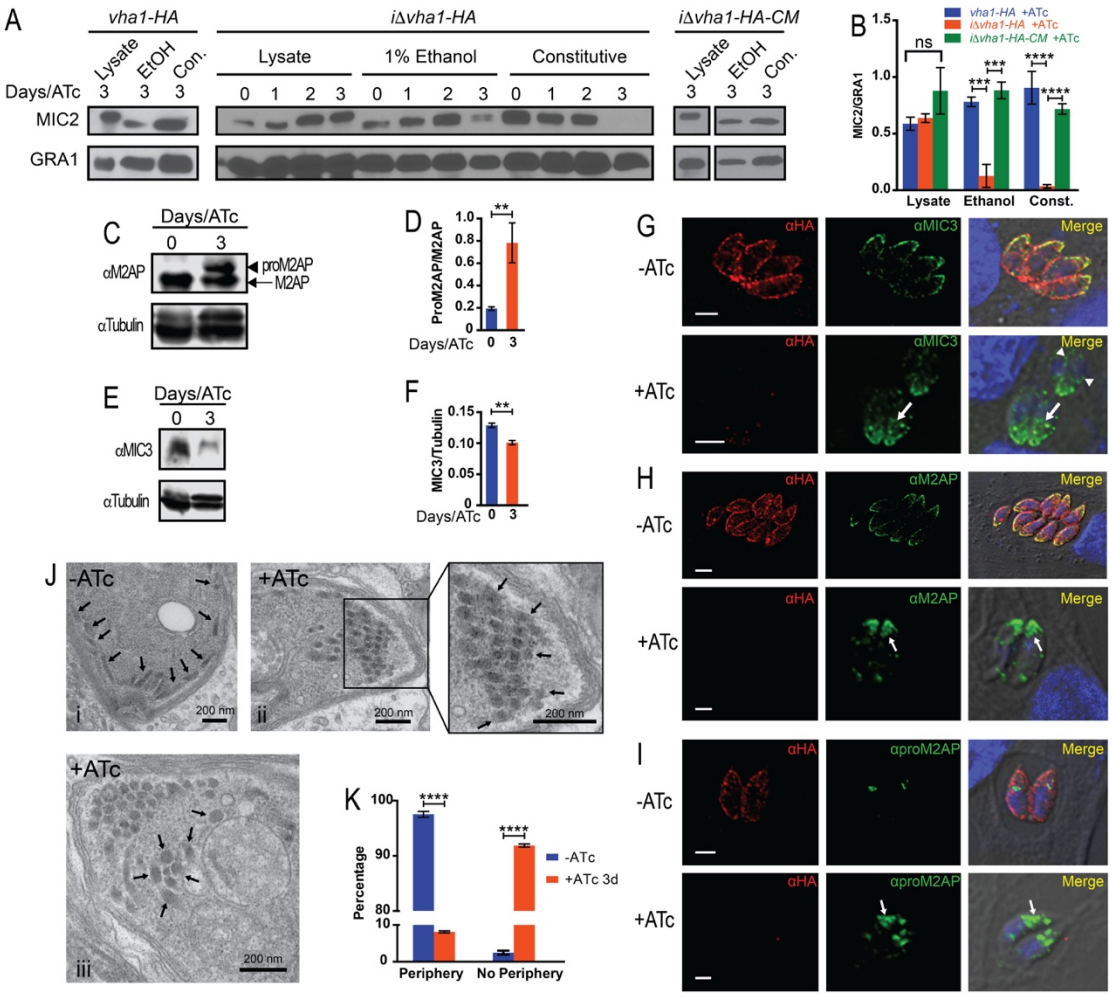

FIGURE 5.5: **V-ATPase and microneme secretion.** A) Microneme secretion of *vha1-HA*, *iΔvha1-HA,* and *iΔvha1-HA-CM* parasites. Parasites were incubated in invasion media alone for constitutive expression (con.) or in the presence of 1% ethanol (EtOH). Lysate samples were also included. Supernatants were analyzed by Western blots with anti-MIC2 or anti-GRA1. B) Quantification of MIC2 secretion by pixel density from ImageJ (ratio of MIC2/GRA1) from 4-5 independent trials. Values are means ± SEM. C) Western blots of total lysates of *iΔvha1-HA* + and - ATc showing the increase in the signal for proM2AP (arrowhead) compared to mature M2AP (arrow). D) Ratio of the signal intensity of proM2AP and M2AP. Bar graphs shows quantification of at least three independent trials.

E) Western blots of total lysates of *iΔvha1-HA* parasites +ATc for 3 days or -ATc (0) probed with αMIC3. F) Quantification of the ratio of intensity of the bands for MIC3/tubulin from three independent trials. G) IFAs with αMIC3 and αHA showing localization of MIC3 in *iΔvha1-HA* parasites grown + and - ATc. Arrowheads point to perinuclear labeling and arrows point staining not at the periphery. H) IFAs with αM2AP and αHA showing the localization of M2AP in *iΔvha1-HA* parasites grown + and - ATc. I) IFAs with αproM2AP and αHA in *iΔvha1-HA* parasites grown + and - ATc. J) Transmission EM of *iΔvha1-HA* parasites grown -ATc (i) or +ATc for 3 days (ii-iii). i) Arrows point toward peripheral micronemes and apical end; ii) Micronemes are indicated by the arrows at the apical end in parasites +ATc for 3 days. iii) micronemes are more centrally located in parasites incubated +ATc for 3 days. K) Quantification of EM images from 3 independent preparations comparing the localization of micronemes of *iΔvha1-HA* grown + and - ATc for 3 days. Methods explain how was done the quantification. Approximately 59-72 parasites were enumerated from 3 independent trials. D, F were quantified by pixel density using Image Studio from 3 independent trials. Graph error bars are SEM. Statistical analysis was performed using a one-way ANOVA where $^{**}P < 0.01$; $^{***}P < 0.001$, $^{****}P < 0.0001$, ns, not significant.

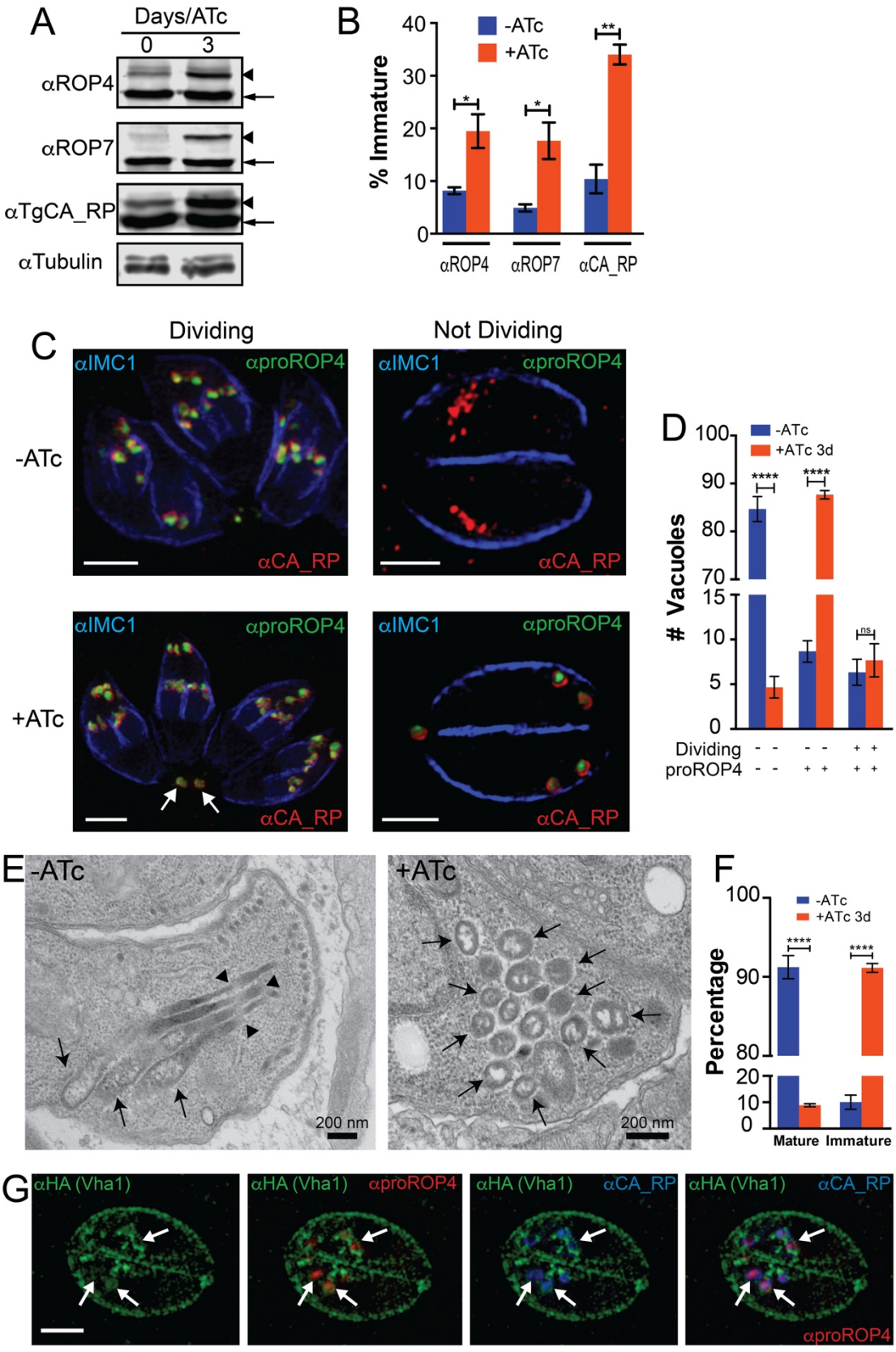
A
Days/ATc
0
3
αROP4
αROP7
αTgCA_RP
αTubulin
B
% Immature
-ATc
+ATc
αROP4
αROP7
αCA_RP
C
Dividing
Not Dividing
-ATc
+ATc
αIMC1
αproROP4
αCA_RP
D
Vacuoles
-ATc
+ATc 3d
Dividing
proROP4
E
-ATc
+ATc
200 nm
F
Percentage
Mature
Immature
G
αHA (Vha1)
αproROP4
αCA_RP

FIGURE 5.6: The V-ATPase and rhoptry maturation. A) Western blots of total lysates of *iΔvha1-HA* tachyzoites grown + and -ATc (3 days) and probed for rhoptry bulb proteins ROP4, ROP7, or TgCA_RP. Immature forms are indicated with arrowheads and mature forms with arrows. B) Comparison between the percentage of immature ROP4, ROP7, or TgCA_RP between lysates of *iΔvha1-HA* parasites grown + or – ATc. C) IFAs of *iΔvha1-HA* tachyzoites grown + or –ATc and probed with αIMC (highlights nascent daughter cells in dividing parasites), αproROP4 (labels immature rhoptries) and αCA_RP (rhoptries). These are super-resolution images showing the labeling with αproROP4 of dividing parasites (αIMC1 labels nascent daughters, *left panels*) and non-dividing parasites (*right panels*). Scale bars: 2 μm. D) Quantification of PVs with parasites expressing immature and mature rhoptries in *iΔvha1-HA* tachyzoite vacuoles grown + and - ATc. There was a significant increase of αproROP4 labeling in non-dividing parasites with ATc (*red columns*). E) Routine EM of *iΔvha1-HA* tachyzoites grown -ATc (left, *-ATc*) showing normal rhoptries and their characteristic rhoptry neck (*arrowheads)* and bulb regions (*arrows)*. In *iΔvha1-HA* +ATc (3 days), mature rhoptries are absent, and accumulation of vesicular immature rhoptry structures was seen (*arrows).* F) Quantification of the EM images showing significant reduction in the number of tachyzoites containing mature rhoptries after treatment with ATc. Approximately 52-73 parasites were enumerated from 3 trials. G) Super resolution IFA showing co-localization of Vha1 with proROP4 (1:500) and TgCA_RP (1:1,000) in intracellular parasites. Statistical analysis was done using a Student's T-test where $*P < 0.05$; $**P < 0.01$; $****P < 0.0001$, n. s., not significant.

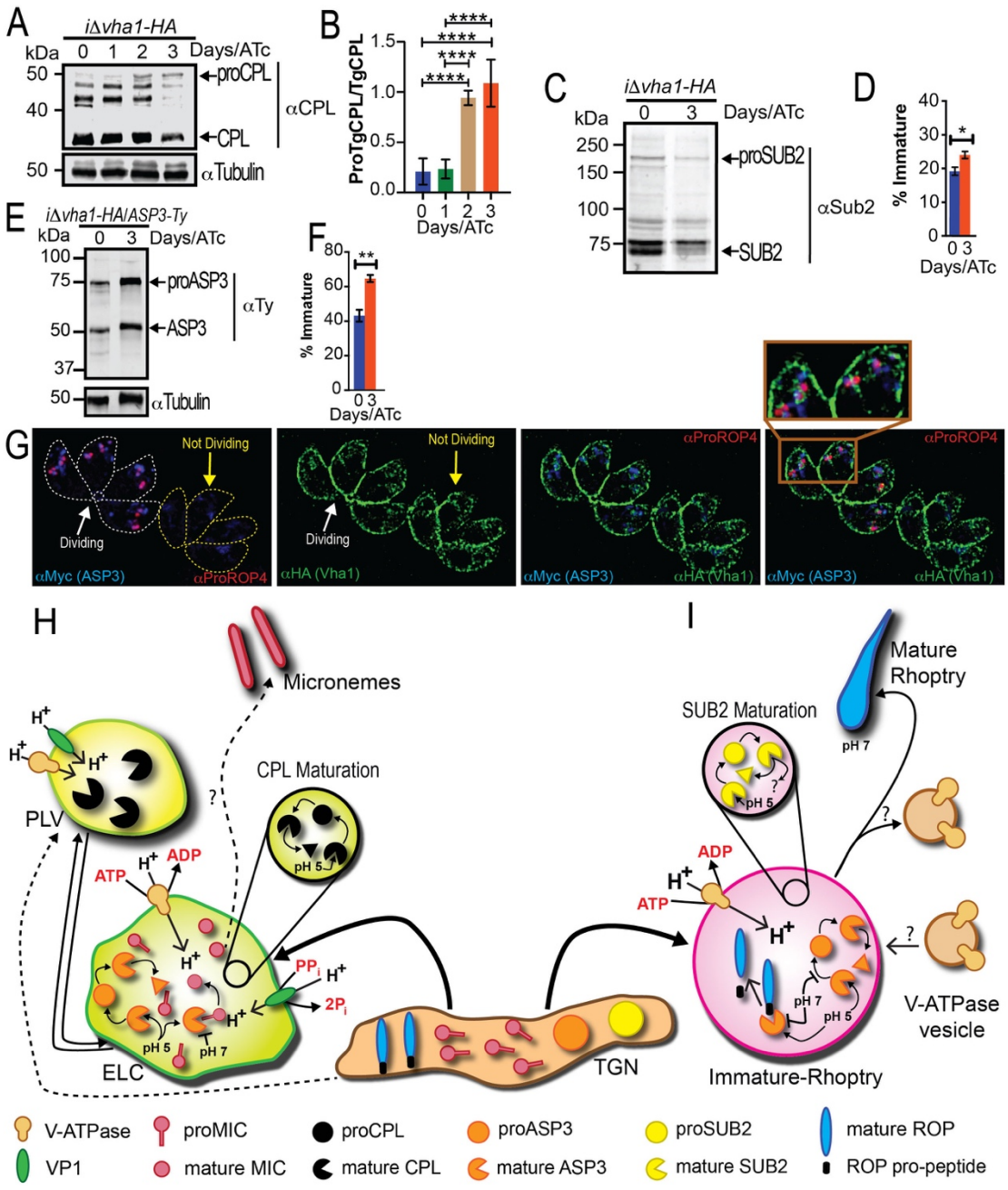

FIGURE 5.7: The V-ATPase and protease maturation. A) Western blots with αCPL (1:500) of lysates from *iΔvha1-HA* +ATc parasites showing accumulation of proCPL. B) Quantification of bands shown in A from 4-5 trials. Experiments were standardized to tubulin and the ratio of proCPL/CPL was determined by ImageJ. C) Western blots of lysates from *iΔvha1-HA* tachyzoites grown + and -ATc (3 days) and probed with αTgSUB2

(1:500). D) Quantification of immature SUB2 as percentage of total SUB2. Quantification was from lysates of *iΔvha1-HA* grown + and –ATc. E) Western blots with αTy of *iΔvha1-HA-ASP3-Ty* parasites. Parasites were grown +ATc for 0 or 3 days. F) Quantification of the maturation of ASP3 as percentage of immature form from total ASP3. G) Super-resolution images showing ASP3 co-localization with proROP4 and V-ATPase, which surrounds ASP3 and proROP4 in dividing cells (lines outline parasites). Statistical analysis was done using a one-way ANOVA or student's T-Test where $*P < 0.05$; $**P < 0.01$; $****P < 0.0001$, ns, not significant. H) **Proposed maturation of micronemes:** Newly synthesized MICs are transported from the Golgi to the Trans Golgi Network and then to the ELC. The ELC is acidified by both, VP1 and V-ATPase. The PLV is mainly acidified by the V-ATPase and we propose that this compartment would be more acidic and most likely would not contain MICs. Maturation of CPL occurs by self-cleavage. Maturation of ASP3 occurs in the ELCs. In the V-ATPase acidified endosome, proMICs encounter mature ASP3 and/or other lytic enzymes. Cleavage of pro-peptides may occur at this point and once the late endosome is matured, processed MICs would be transported to the micronemes. I) **Rhoptry biogenesis:** immature ROP proteins, immature SUB2, and ASP3 traffic through the TGN. The V-ATPase associates with the forming rhoptry creating the acidic environment that is important for SUB2 and ASP3 maturation. In pro-rhoptries, APS3 would be active and able to process immature ROPs. According to this model the activity of SUB2 would likely be decreased at low pH. The V-ATPase separates by an unknown mechanism allowing the pH of the mature rhoptry to become more neutral and rhoptry organelles to mature.

Supplemental figures

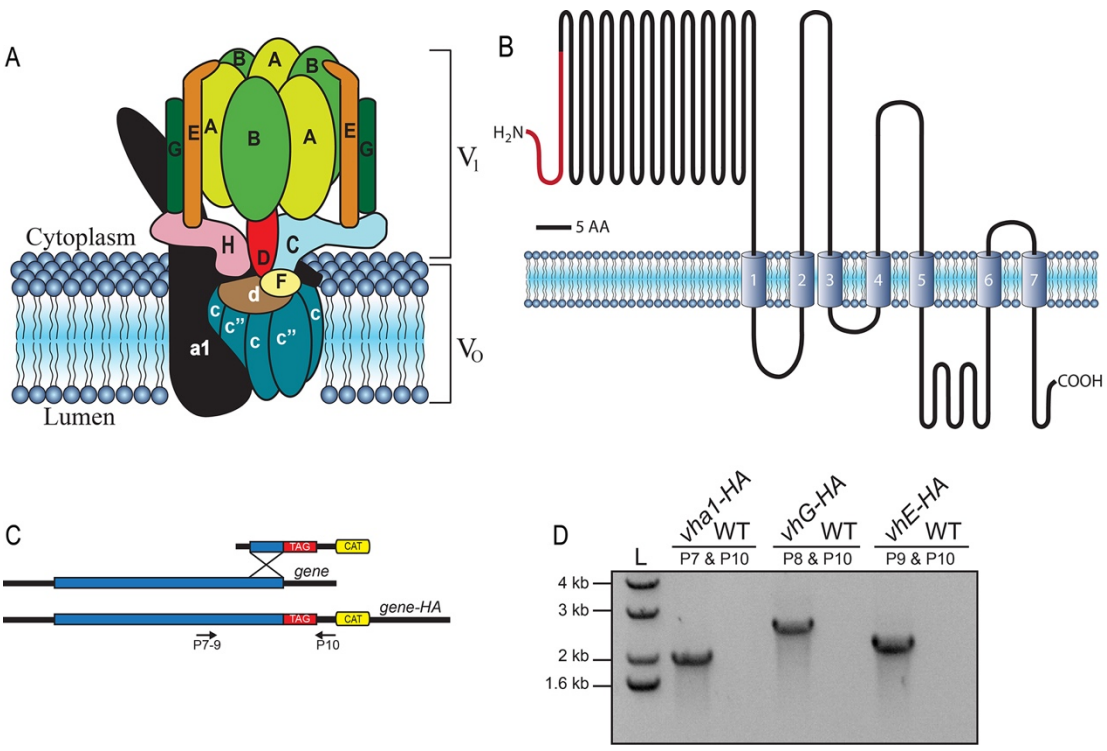

FIGURE S5.1: **The Vacuolar H$^+$-ATPase of *Toxoplasma gondii.*** A) Scheme of the various subunits and domains of the V-ATPase in *T. gondii*. Structural design adapted from [5]. B) Vha1 sequence modeling using Protter version 1.0, which predicts 7 transmembrane domains. The 27 amino acids that form the predicted signal peptide are marked in red. Scale bar is 5 amino acids. C) Scheme of the primers used to determine correct tag insertion. D) PCR using an upstream gene specific forward primer (Primers 7-9) and reverse pLIC primer (Primer 10). Primer sets specific for *vha1*, *vhG*, *vhE* being HA tagged were also compared against a TATi*Δku80* strain (WT).

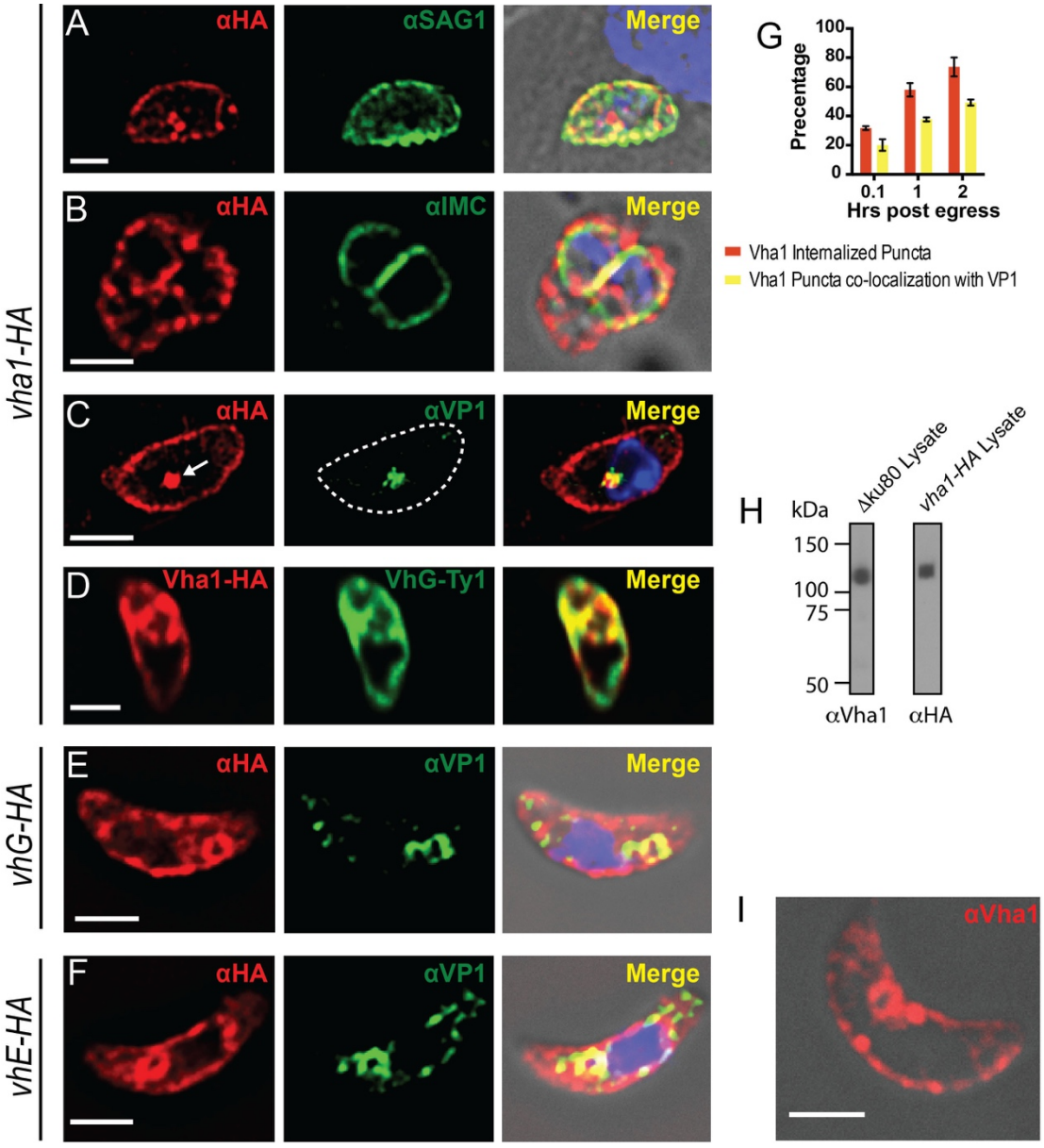

FIGURE S5.2: The *T. gondii* V-H$^+$-ATPase localizes to the plasma membrane and the plant-like vacoule. A) IFAs of *iΔvha1-HA* intracellular parasites with anti-HA and anti-SAG1 in hTERT host cells. B) Immunofluorescence assays of extracellular tachyzoites treated for 4 hours with alpha toxin as detected using αHA αIMC1 (Inner Membrane Complex). C) Super resolution IFA's using αHA and PLV marker αVP1. Arrow points to an internal puncta that co-localizes with VP1. Dashed line shows the outline of the

parasite. D) Vha1-HA parasites expressing *vhG-Ty* (subunit G was C-terminally tagged with a Ty tag). E) IFAs of extracellular parasites expressing VhG-HA with αHA (1:25) and rabbit αVP1 (1:4,000). F) IFAs of extracellular parasites expressing VhE-HA with αHA and αVP1. G) Quantification of IFA images showing the formation of a large central Vha1 puncta and its co-localization with VP1 in function of time. H) Western blots of *TATiΔku80* or Vha1-HA lysates probed with αVha1 (1:500) or αHA (1:200), respectively. I) IFA of extracellular parasites with αVHa1 (1:500). IFA scale bars are 2 μm.

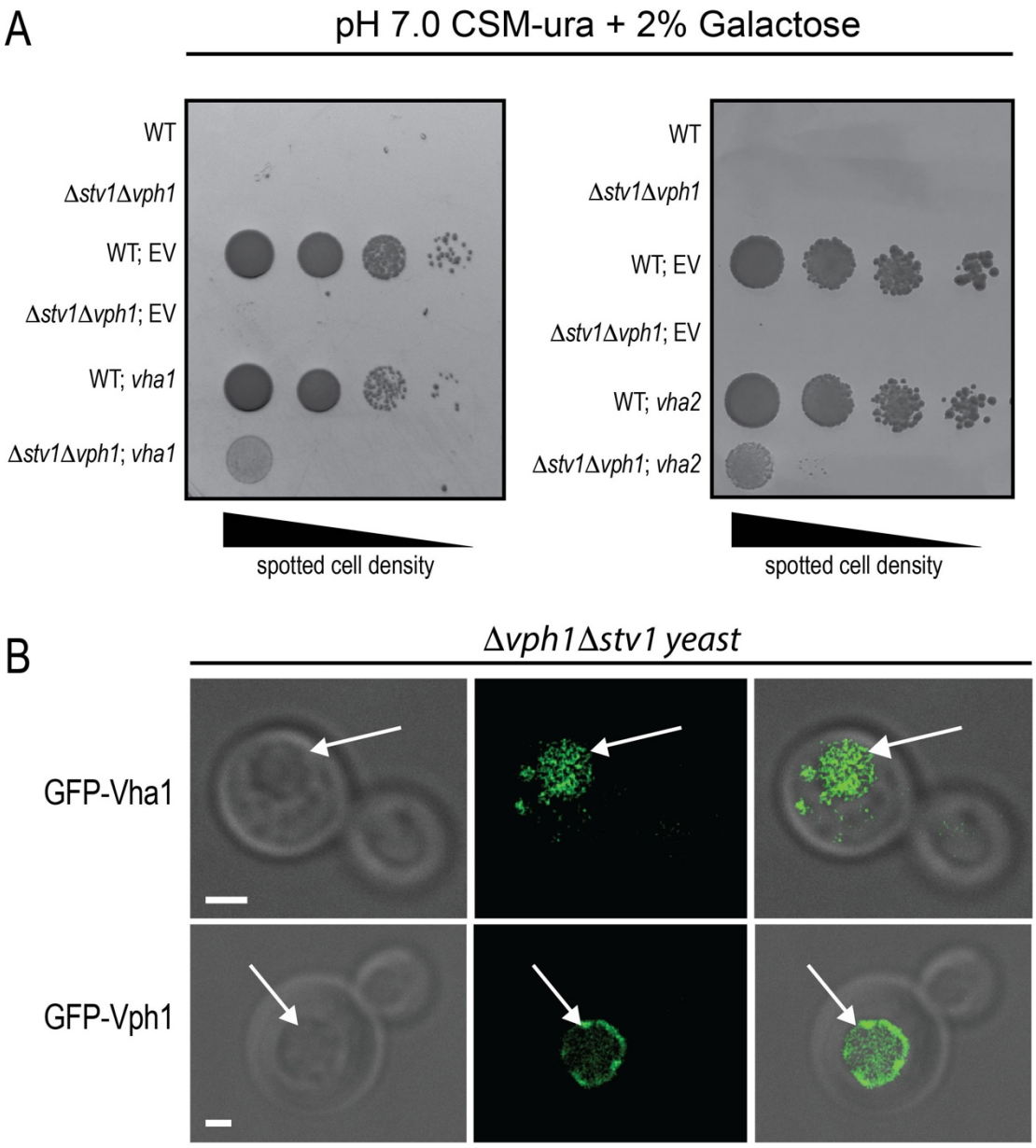

FIGURE S5.3. Yeast complementation and localization of VHa1 in *Δvph1Δstv1* yeast. A) Spotted serial dilutions of yeast suspensions normalized to an OD of 1 of yeast expressing Vha1 (*left panel)* or Vha2 (*right panel*). WT, wild type yeast; EV, empty pYES2 vector; *vha1/vha2*, pYES2 vector with *vha1* or *vha2* cDNA. Suspensions were grown on CSM-ura plates with 2% galactose at pH 7.0 for 96 hours. Blots are representative of 3

independent trials done in duplicate. B) cDNA from *vha1* or *vph1* were fused to GFP and transformed into *Δvph1Δstv1* yeast. Arrows point to the the yeast vacuole.

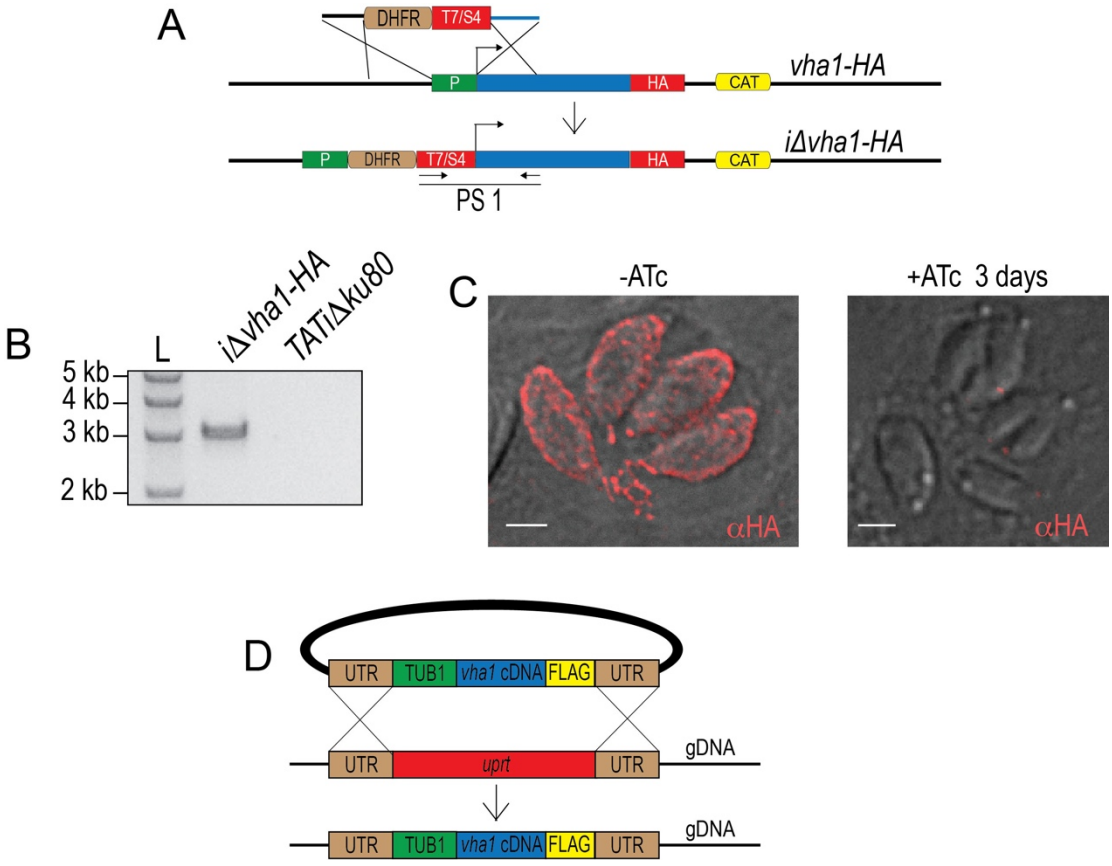

FIGURE S5.4: **Conditional knock down of the *vha1 gene.*** A) Cartoon showing the promoter insertion strategy and localization of primers used for genetic validation. CAT, chloramphenicol acetyltransferase; HA, 3 hemagglutinin epitope tags; T7/S4, tetracycline inducible promoter; DHFR, pyrimethamine resistance cassette; P, endogenous promoter; PS1, primer set 1. B) PCR with PS1 to confirm integration of cassette upstream of the translational start codon. C) IFA's with αHA (1:25) showing the regulation of expression of *vha1* by ATc. D) Cartoon showing the strategy used for complementation of the *iΔvha1-HA* parasites with *vha1* cDNA into the *uprt* gene locus. Scale bars are 2 μm.

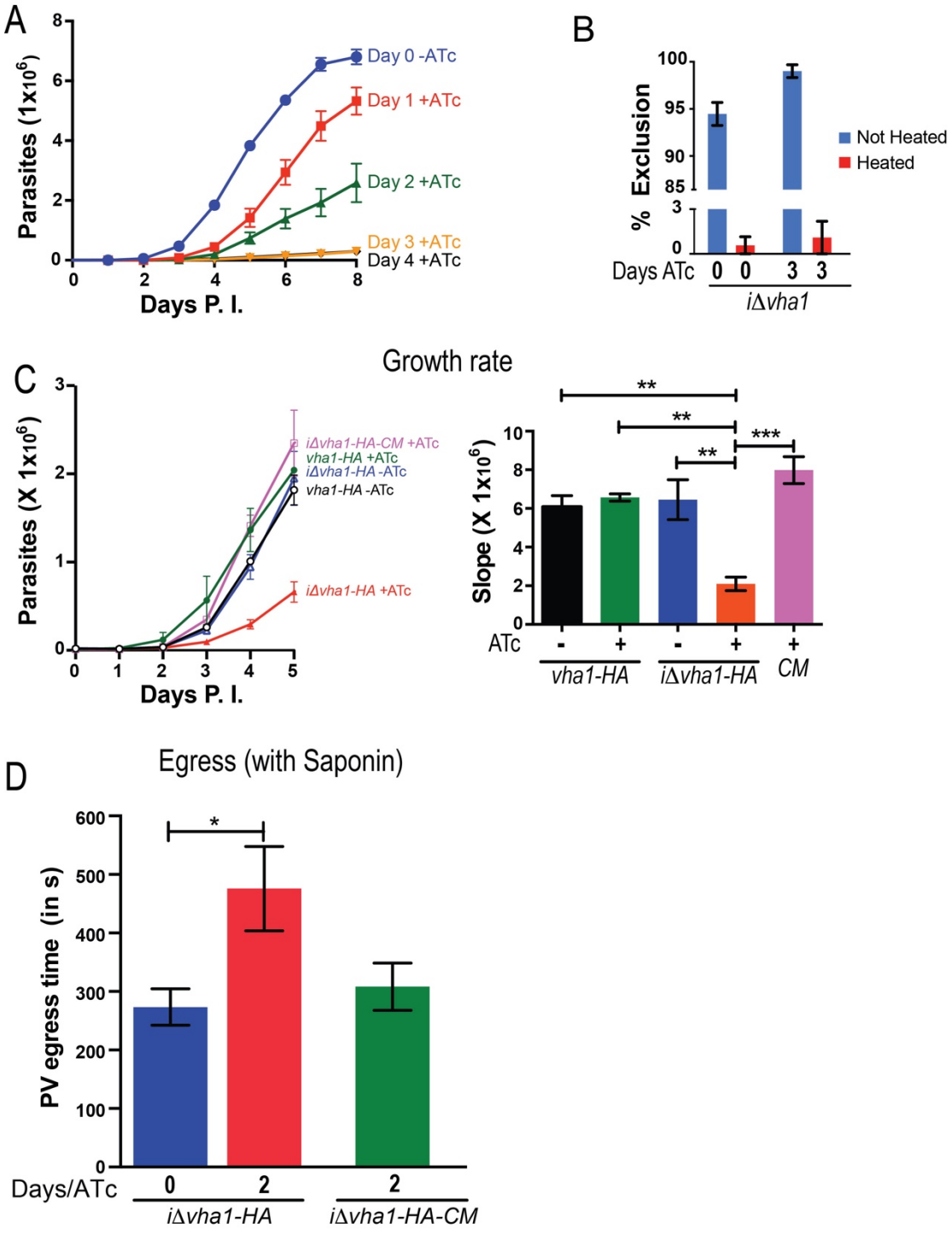

FIGURE S5.5. Vha1 plays roles in the lytic cycle of the parasite. A) Growth of *iΔvha1-HA* parasites pre-incubated for the indicated days with ATc, washed twice, and added to fresh host cells without ATc and their growth monitored. Around 100 tDtomato expressing

parasites were seeded in confluent hTERT cells in a 96 well plate and allowed to grow for 8 days. Data represented is the average of three independent trials done in triplicate. B) Trypan exclusion of *iΔvha1-HA* parasites incubated with or without ATc for 0 or 3 days. Parasites were either heat treated at 70°C for 5 min or not heat treated and exposed to 1.5% trypan, washed twice, and the number excluding trypan blue enumerated. Data are from three independent trials. C) Growth rate of *vha1-HA, iΔvha1-HA,* and *iΔvha1-HA*-CM tDtomato expressing parasites. Slopes were calculated from days 2-5. Data are from three independent trials. D) *iΔvha1-HA* and *iΔvha1-HA-CM* parasites incubated for 0 (-) or 2 (+) days with ATc were exposed to 0.01% saponin after 120 seconds. 3 independent trails were performed in duplicate where the time to egress after saponin addition was recorded. $*P < 0.05$; $**P < 0.01$; $***P < 0.001$.

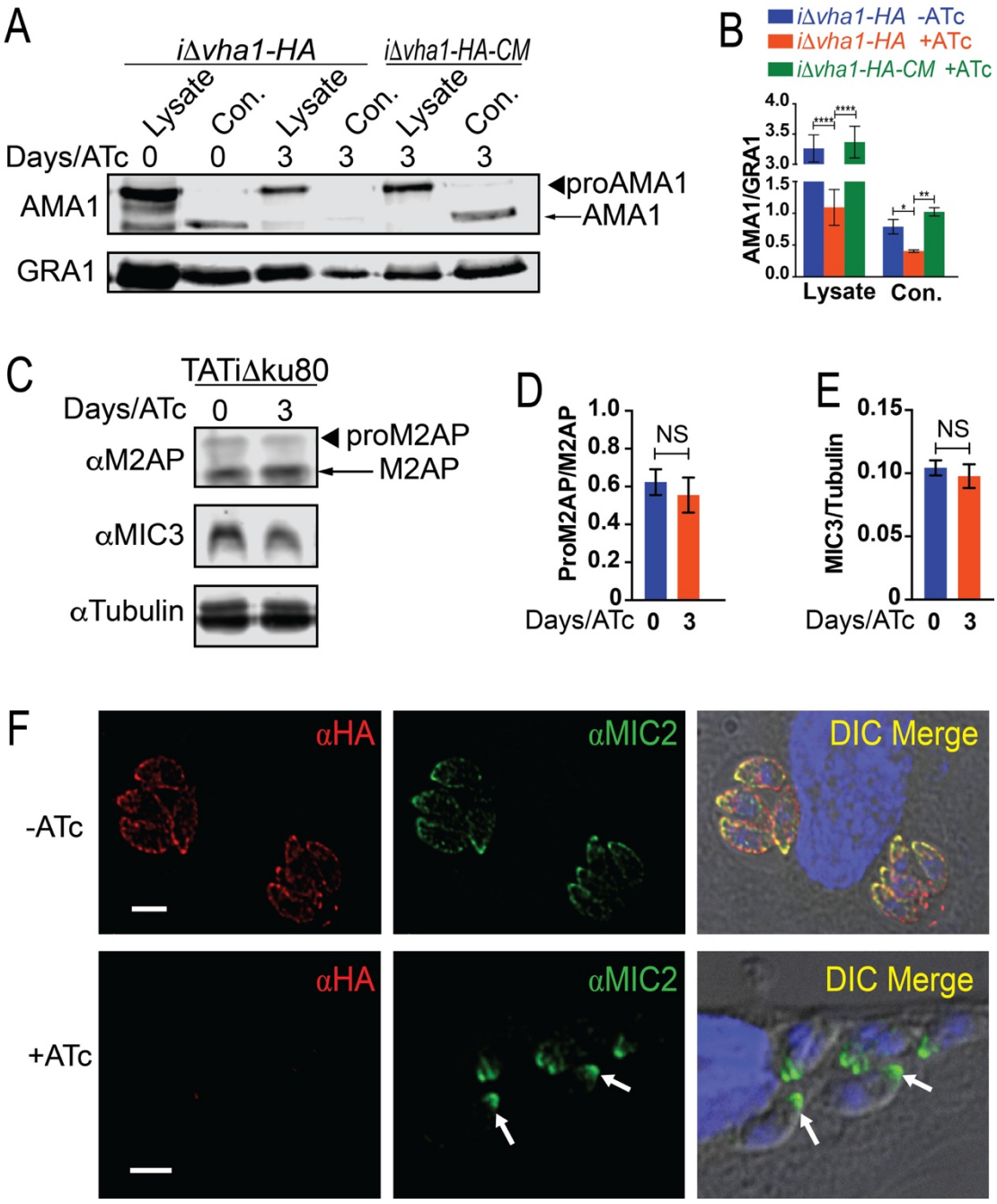

FIGURE S5.6. Microneme proteins secretion and localization. A) Western blots of total lysates and constitutive secretion (con.) of *iΔvha1-HA* or *iΔvha1-HA-CM* parasites grown with and without ATc. Parasites were incubated for 30 min in invasion media (DMEM-HG with 20 mM HEPES) and supernatant (Con.) and pellet (Lysate) were

separated by centrifugation. Immunoblots developed with αAMA1 (1:500) showed labeling of immature AMA1 (arrow head) and mature AMA1 (arrow) of *iΔvha1-HA* or *iΔvha1-HA-CM* parasites grown with and without ATc. GRA1 control is shown in the bottom panel with αGRA1 (1:1,000). B) Ratio of AMA1/GRA1 as determined by pixel density using Image Studio from 3 independent trials. C) Western blots of total lysates of *vha1-HA* parasites grown with and without ATc showing the staining of proM2AP (arrow head) compared to mature M2AP (arrow) (top panel), MIC3 (mid panel) and Tubulin control (bottom). Blots were probed with αM2AP (1:1,000) and αMIC3 (1:40). D) Ratio of proM2AP/M2AP pixel density. E) Ratio of density of the bands of mature MIC3/Tubulin. F) IFAs of *iΔvha1-HA* parasites grown with or without ATc (3 days) using rat αHA (1:25) and αMIC2 (1:400). Arrows point to non-peripheral atypical labeling. Scale bars are 2 μm. Graph error bars are SEM. Statistical analysis were performed using a one way ANOVA where $*P < 0.05$; $**P < 0.01$; $****P < 0.0001$.

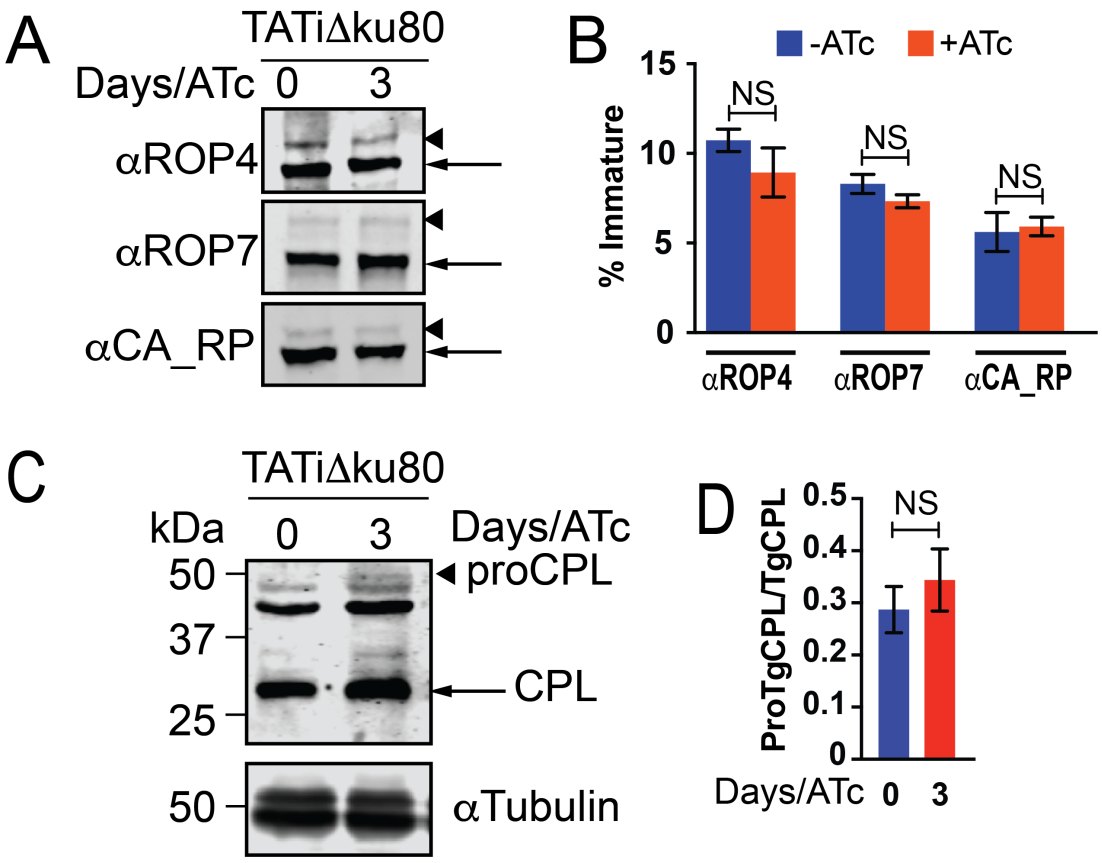

FIGURE S5.7. Parental controls for rhoptry maturation. A) Western blots of total lysates of *vha1-HA* parasites grown with and without ATc showing normal maturation of ROP4, ROP7, and TgCA_RP. The antibody uses were αROP4 (UVT-68, Rabbit 1:500), α-ROP7 (1:1,000), and α-TgCA_RP (Guinea Pig 1:1,000). Arrowhead indicates immature protein and arrow denotes mature protein. B) Quantification of bands shown in F by ratio of immature/mature. 3 independent biological replicates were performed. C) Western blots of total lysates of *vha1-HA* parasites grown with and without ATc showing the maturation of CPL. Blots were probes with αCPL (1:500). G) Quantification of immature/mature CPL. A and C were quantified by pixel density using Image Studio from 3 independent trials. Graph error bars are SEM. Statistical analysis were performed using a Student's *t* test where NS is not significant.

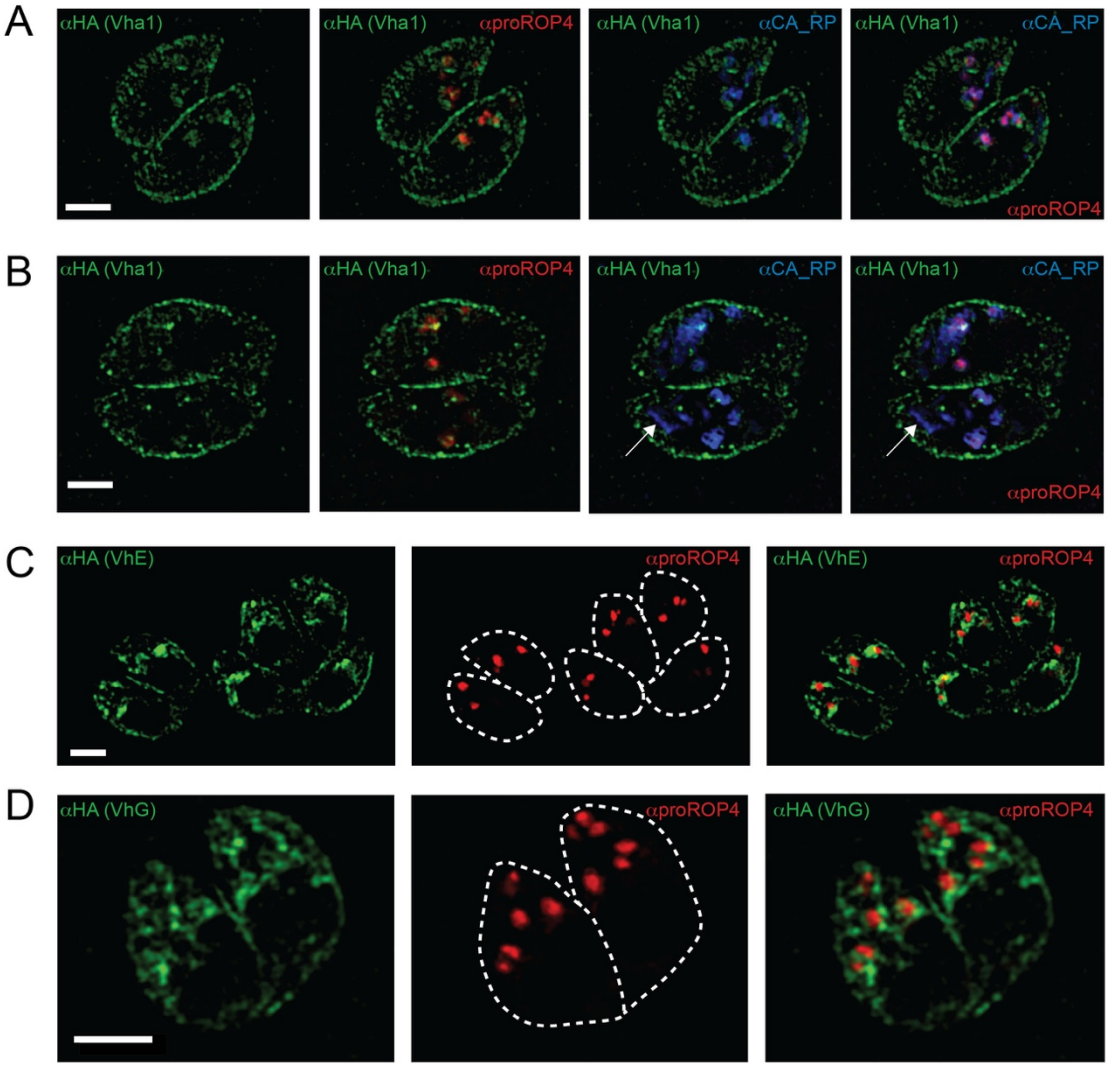

FIGURE S5.8. The V-H$^+$-ATPase associates with pro-rhoptries. A) Super resolution IFA of *iΔvha1-HA* without ATc fixed 24 hours after invasion with 4% paraformaldehyde. Antibodies against HA, labeling VHa1, (rat-anti-HA, 1:25, green), anti-proROP4 (Mab UVT-70, 1:500, red), and anti-TgCA_RP (Guinea Pig, 1:1000, blue) were used for intracellular localizations. B) Super resolution IFA of intracellular *iΔvha1-HA* clones without ATc using antibodies against HA (1:25), proROP4 (1:500), and TgCA_RP (1:1000). Cells were fixed 24 hours after invasion with 4% paraformaldehyde. C) Super resolution IFA of VhE-HA parasite clones using anti-HA (labeling subunit E) and anti-

proROP4 (1:500, red). Cells were fixed 24 hours after invasion with 4% paraformaldehyde. D) Same as C but with VhG-HA clones. Scale bars are 2 μm.

Supplemental Video 5.1: pH indicator mCherry-SEpHluorin expressed in the PLV. Related to Figures 1 and 4. *iΔvha1-HA* parasites were transfected with a plasmid that targeted mCherry-SEpHluorin [58] to the PLV. Extracellular parasites were placed in MatTek dishes with Ringer buffer at pH 7.3. At 15 seconds, 20 mM NH_4Cl was added. Due to the acidic nature of the PLV, the green channel (which responds to changes in pH) was not seen until after alkalization, confirming that the PLV is normally acidic. The change in fluorescence indicates that the indicator is functional.

CHAPTER 6

CROSSTALK BETWEEN PH, CALCIUM HOMEOSTASIS, AND POLYPHOSPHATE FACILITATED BY THE VACUOLAR H^+-ATPASE OF *TOXOPLASMA GONDII*[3]

[3]Andrew J. Stasic, Eric J. Dykes, Stephen A. Vella, Ciro D. Cordeiro, Mojtaba S. Fazli, Shannon Quinn, Zhicheng Dou, Roberto Docampo, and Silvia N.J. Moreno. To be submitted to the *Journal of Biological Chemistry.*

6.1 Abstract

Toxoplasma gondii is an important human pathogen that must cope with changing ionic concentrations. Calcium influx and signaling pathways are important to the propagation of the parasite and calcium imbalances lead to decreased virulence. *T. gondii* utilizes a vacuolar-H^+-ATPase (V-ATPase), an evolutionarily conserved multi subunit complex that couples the hydrolysis of ATP to the pumping of protons across membranes and creates a proton gradient across membranes that can be used for the transport of other ions. *T. gondii* contains two major acidic stores, the plant-like vacuole and the acidocalcisome which are likely acidified by the V-ATPase. We found that disruption of the V-ATPase affects calcium influx and results in uncontrolled cytoplasmic increase in the presence of extracellular calcium. We also demonstrate that *T. gondii* utilizes the plant-like vacuole and the acidocalcisome for maintaining its cytoplasmic Calcium levels under control when the endoplasmic reticulum is chemically blocked. Lytic cycle steps that are stimulated by a Ca^{2+} threshold are negatively affected if the V-ATPase is non-functional. The synthesis of polyphosphates and electron density of acidocalcisomes are both dependent of the acidic environment created by the V-H-ATPase. The V-ATPase co-localized with the vacuolar transporter chaperone 4, a protein that synthesizes polyphosphate in the acidocalcisome. Depletion of proton transport to acidocalcisomes illustrates the interaction between protons gradients, calcium, and polyphosphate in *T. gondii*. Our work underscores the importance of ion gradients in maintaining a delicate equilibrium that when altered results in detrimental cell function.

6.2 Introduction

Toxoplasma gondii is an important Apicomplexan parasite the infects approximately one-third of the world's population. Although usually asymptomatic in healthy adults, death or serious complications from *T. gondii* infections occur in immunocompromised individuals. The pathogenicity of this obligate intracellular parasite is linked to its lytic cycle, which is comprised of invasion of host cells, replication inside a parasitophorous vacuole (PV), stimulation of motility, and egress from the host cell [1]. As *T. gondii* progresses through its lytic cycle, the ionic composition of the surrounding environment to which it is exposed changes dramatically. When the parasites are intracellular, they are exposed to a Ca^{2+} concentration around 100 nM and after egress they are exposed to a Ca^{2+} concentration around 1.8 mM [2]. Sophisticated regulatory mechanisms are in place for the parasite to deal with these changes and also to use these ionic gradients for its own benefit such as filling its intracellular calcium stores [3]. The lytic cycle is highly influenced by the level of cytosolic free calcium and has been implicated in all of the important steps [2].

T. gondii contains a organelle termed the plant-like vacuole or vacuolar compartment (PLV or VAC) that has been shown to play a role in calcium homeostasis, environmental toxicity, and salt homeostasis [4, 5]. The PLV contains two known proton pumps, the vacuolar proton pyrophosphatase (TgVP1) and the vacuolar proton ATPase (V-ATPase) [6, 7]. The vacuolar proton pyrophosphatase couples the hydrolysis of pyrophosphate with the pumping of protons across a membrane, whereas the V-ATPase couples the hydrolysis of ATP to the pumping of protons across a membrane. Ablation of TgVP1 resulted in a mild growth phenotype [6] but repression of the a1 subunit of the V-

ATPase (TgVha1) resulted in complete ablation of the major steps of the lytic cycle [7]. It was reported that the V-ATPase localizes to the plasma membrane, PLV, and immature rhoptries in *T. gondii* [7]. While unusual for a V-ATPase to localize to the plasma membrane, the majority of the protons extruded from *T. gondii* were due to the V-ATPase and contributes, in some capacity, to maintaining membrane potential [7, 8]. It has been documented that the transport of calcium ions across membranes has been linked to proton exchange [9, 10]. Additionally, changes in membrane potential are often linked with ion influx or efflux [11], thus the V-ATPase could be playing a role in ion transport by contributing to membrane potential.

Toxoplasma gondii also possesses three recognized major organelles in the storage of calcium, the endoplasmic reticulum (ER), the PLV, and acidocalcisome (AC) [4, 12]. Only the PLV and the AC are presently known to be acidic calcium stores in *T. gondii*. Acidocalcisomes are electron dense, highly acidic, and contain polyphosphates (polyP), calcium, magnesium, sodium, and zinc [13]. Acidocalcisomes use the vacuolar proton pyrophosphatase and/or the V-ATPase to generate the proton gradient in this organelle [13].

Polyphosphate synthesis is accomplished through vacuolar transporter chaperon (VTC) complex that hydrolyzes ATP to create polyphosphate chains inside the lumen of the organelle [13]. Due to the inherently negative charge of polyP, it is often complexed with various cations that include calcium [14]. Yeast have 4 known proteins involved in the yeast VTC complex (VTC1-4), but genetic evidence from *Toxoplasma* supports the presence of only two subunits, VTC2 (TgGT1_298630) and VTC4 (TGGT1_299080). VTC2 is an integral membrane protein that is part of the VTC complex but the function of

this subunit is not fully understood and postulated to play a role in vacuole fusion [15]. VTC4 is also believe to play a role in vacuole fusion and is the subunit responsible for the polymerization of polyP in the AC [15, 16]. It was shown that VTC2 did not colocalize with the *Toxoplasma* vacuolar proton pyrophosphatase (TgVP1) [17] and VTC4 has not been characterized.

In this study, we demonstrate that the V-ATPase plays a role in calcium influx, calcium homeostasis, and disfunction of the pump result in calcium deficiencies that lead to defects in the lytic cycle. We characterize the role of the V-ATPase in the role acidic stores in calcium homeostasis and signaling.

6.3 Results

Constitutive leakage of Ca^{2+} in cells with inactive V-ATPase.

V-ATPases are multi-subunit complexes composed of two domains, V_1 and V_0, which couple the hydrolysis of ATP with the transport of protons across a membrane [18]. Disruption of the V-H^+-ATPase in *Toxoplasma gondii* resulted in major defects in the lytic cycle, including invasion, replication, motility, and egress, as well as defects in proton homeostasis and the maturation of proteins important for invasion or egress [7]. The *T. gondii* V-ATPase localizes to the endosomal-like compartments (ELCs), the plant-like vacuole (PLV or VAC), the immature rhoptries (while replicating), and the plasma membrane [7] (**Fig. 6.1A**). The PLV and ELCs are known to be calcium stores [4, 6, 19]. The cytosolic basal concentration of Ca^{2+} is tightly regulated in all cells as it is the case with *T. gondii* [20]. Additionally, calcium plays a major role in the lytic cycle [3, 20, 21] and thus changes in calcium entry or homeostasis could result in major defects of the lytic cycle. Calcium homeostasis is important for fine-tuning of Ca^{2+}-dependent functions.

Plasma membrane Ca^{2+} channels are important players that open and close allowing Ca^{2+} influx contributing to transient increases in cytosolic Ca^{2+} concentration. These calcium influxes can result in the activation of downstream intracellular signaling pathways [22, 23]. It was previously demonstrated that exposing parasites to 1.8 mM extracellular Ca^{2+} resulted in an increase in cytosolic Ca^{2+} ($[Ca^{2+}]_c$) followed by recovery and leveling of the cytoplasmic levels [3]. This recovery is the result of the pumping activity of Ca^{2+}-ATPases at the plasma membrane or intracellular organelles, most likely the endoplasmic reticulum [24], the plant like vacuole [4], and/or the acidocalcisome [25, 26]. It was recently demonstrated that the V-ATPase localizes with the PLV [7] and has been postulated to be present in the acidocalcisome membrane [27]. Because depletion of V-ATPase resulted in loss of function of all the major steps of the *T. gondii* lytic cycle we hypothesize that defects in calcium signaling are responsible of these defects.

We first studied Ca^{2+} influx and for this we used Fura2-AM loaded *iΔvha1-HA* cells previously treated with ATc for 0, 2, or 3 days to study cytosolic Ca^{2+} changes in response to extracellular Ca^{2+} (**Fig. 6.1B**). We added 1.8 mM Ca^{2+} to the suspension of parasites previously incubated in a Ca^{2+}-depleted buffer [3] (**Fig. 6.1C, D**). Under these conditions, control parasites expressing a fully functional V-ATPase (*iΔvha1-HA* grown without ATc or complemented *iΔvha1-HA-CM*+ATc) allow some Ca^{2+} into the cytoplasm, which is rapidly controlled (**Fig. 6.1C, *blue and green tracings, respectively)***. However, mutant parasites previously exposed to ATc (*iΔvha1-HA+ATc)* were unable to control the cytoplasmic levels of Ca^{2+}, which leaked into the cytoplasm continuously. This was especially remarkable in cells exposed to ATc for 3 days. We quantified the $\Delta[Ca^{2+}]_c$ after the addition of 1.8 mM Ca^{2+} and found that parasites incubated without ATc had an average

$\Delta[Ca^{2+}]_c$ of 19.0 nM Ca^{2+}, and the complemented strain (*iΔvha1-HA-CM*) had an average $\Delta[Ca^{2+}]_c$ of 34.0 nM Ca^{2+} (**Fig. 6.1D**). Parasites incubated with ATc for 2 or 3 days had an average $\Delta[Ca^{2+}]_c$ of 186.9 and 1,090.9 nM Ca^{2+} after addition of extracellular Ca^{2+} (**Fig. 6.1D**). Although the major players regulating calcium entry are not known, these results indicate that a fully functioning V-ATPase is an important player in calcium influx, possibly by controlling the parasite membrane potential.

We next wanted to determine any effects on the other calcium stores, ER, PLV and acidocalcisomes. The addition of thapsigargin (TG) blocks the sarco/endoplasmic reticulum Ca^{2+}-ATPase (SERCA) and calcium is leaked into the cytoplasm by an unknown mechanism [12, 28]. By adding extracellular calcium and blocking the uptake of calcium to the ER, the function of the acidic storage can be studied. The addition of 2 μM TG, leads to increased $[Ca^{2+}]_c$ due to leakage from the ER followed by a recovery phase that can be executed by the uptake by acidic stores or by pumping it out of the parasite. In the V-ATPase depleted parasites, the recovery phase is highly impacted demonstrating that a functional V-ATPase is required in the membrane of the acidic stores to regulate $[Ca^{2+}]_c$ (**Fig. 6.1E, *blue and green tracing*s**). Adding Ca^{2+} after TG in the knockdowns, led to a cytosolic increase that continuously increased without evidence for recovery (**Fig. 6.1E, *maroon tracing***) as compared with the parental line (**Fig. 6.1E, *blue tracing***) and the complemented one (**Fig. 6.1E, *green tracing***). The *iΔvha1-HA+ATc* parasites showed a similar leaky phenotype as shown in **Fig. 6.1C** after exposure to 1.8 mM calcium.

Upon switching the order of additions, the leaky calcium phenotype was more pronounced in the *iΔvha1-HA +ATc* parasites (**Fig. 6.1F**). The *iΔvha1-HA +ATc* did not show any recovery after the addition of both TG and 1.8 mM calcium, whereas the -ATc

and complemented strain showed some recovery (**Fig. 6.1F**). These results indicate that the activity of the V-ATPase either at the plasma membrane or at the PLV is important for cytosolic Ca^{2+} recovery following an increase. It is likely that the proton gradient generated at the PLV, acidocalcisome or plasma membrane is important for the uptake of Ca^{2+} into these organelles [7].

The V-ATPase plays a role in acidic calcium storage.

It was previously demonstrated that the PLV accumulates the lysotracker dye indicating its acidic nature [7]. Additionally, it was previously demonstrated that the PLV stores Ca^{2+}, which can be released into the cytosol by the cathepsin C substrate glycyl-L-phenylalanine-naphthylamide (GPN), which when hydrolyzed causes swelling of lysosomal compartment and calcium leakage into the cytosol [4, 29, 30]. GPN, which causes leakage of Ca^{2+} from lysosomal compartments (PLV) showed a reduced effect when added to Fura2-AM loaded *iΔvha1-HA* parasites incubated for 3 days with ATc in comparison to *iΔvha1-HA*-ATc parasites (**Fig. 6.2A**). These results suggested that the PLV of mutant parasites contains less Ca^{2+}, supporting a role for the proton gradient in Ca^{2+} storage or that the PLV is less acidic and GPN is not hydrolyzed efficiently. Adding TG, led to an increase of cytosolic Ca^{2+}, which was significantly lower in *iΔvha1-HA*+ATc (**Fig. 6.2A**). Switching the order of additions resulted in a more pronounced calcium release to GPN in both ATc conditions, but the release of calcium in the +ATc conditions was significantly less than parasites grown without ATc (**Fig. 6.2B**). When TG was added first, the response was similarly less pronounced in parasites grown with ATc (**Fig. 6.2B**). The slopes after the addition of GPN and TG was also quantified and found to be significantly lower in the +ATc condition (data not shown). Surprisingly, the addition of

nigericin had no significant change in calcium release in either ATc condition (data not shown).

In addition to the PLV, *Toxoplasma gondii* also contains another known acidic calcium storage organelle, the acidocalcisome. This organelle is characterized by its high acidity, high concentration of calcium, and high polyphosphate content [13]. It was previously shown that neutralization with NH_4Cl caused a release of calcium from the acidocalcisome [12, 25]. We next wanted to neutralize all acidic calcium compartments to see the impact on cytosolic calcium. The addition of 10 mM NH_4Cl did not result in cytosolic increase of Ca^{2+} in clones previously grown +ATc clones on either the first or second addition, whereas the -ATc parasites released calcium into the cytoplasm upon both additions (**Fig. 6.2C, D**). In both cases, TG had significant differences in the amount of calcium release when TG was added (**Figs. 6.2C, D**).

Because *T. gondii* contains 2 *a* subunit isoforms [7], we assayed whether the addition of bafilomycin would have any impact on the function of both isoforms. The addition of bafilomycin first resulted in no significant calcium release (**Fig. 6.2E**). However, the addition of TG first followed by bafilomycin resulted in an increase of cytosolic Ca^{2+} which was significantly higher in the control cells (-ATc) than the +ATc clones (**Fig. 6.2F**). These data suggested upon addition of extracellular Ca2+, the ER is the faster and more efficient organelle for its uptage, but when retention is chemically blocked, the PLV can take-up free cytoplasmic calcium. In V-ATPase depleted parasites, calcium accumulates in the cytoplasm because both the ER (because of TG) and the PLV are not functioning.

Recently, it was reported a chloroquine resistant transporter (CRT) with homology to the *Plasmodium falciparum* PfCRT localized to the PLV [31]. Depletion of TgCRT results in an abnormal swelling of the PLV and the function of the TgCRT was reported to be involved in maintaining the integrity and lytic activity of the proteases present in the PLV [31, 32]. We reported previously that downregulation of the V-ATPase resulted in numerous defects in the maturation and activity of proteases due to lack of sufficient acidification of the compartments where the maturation occurs [33]. We postulated that the PLV would be more alkaline in Δ*crt* mutants because of the defects in PLV membrane integrity and therefore have difficulty maintaining and storing calcium. We found that the addition of bafilomycin (after blocking ER uptake with TG) resulted in virtually no increase in cytoplasmic calcium (**Fig. 6.2G *orange tracing***) in the Δ*crt* mutants while parental strain (Δ*ku80*) and Δcrt^{CRT} both had significantly higher calcium increase upon the addition of bafilomycin (**Fig. 6.2G *compare purple and green tracings with orange***). These data demonstrate that the V-ATPase is absolutely required for calcium uptake into the PLV.

Protons are important for the storage and maintenance of polyphosphate.

Acidocalcisomes are a major store polyphosphate (polyP), where are long chains of phosphate [12-14]. PolyP chains are inherently negatively charged and are often complexed with cations, including calcium, zinc, iron, potassium, sodium, and magnesium [34]. In these organelles the V-ATPase and VP1 pump protons into the lumen which can then be exchanged for calcium. The acidocalcisome also expressed members of the VTC complex, which synthesizes polyP chains and uses ATP as energy source [35]. It was previously demonstrated that inhibitors of the V-ATPase resulted calcium release from the

AC as use of calcium ionophores were associated with polyP hydrolysis [36]. These observations suggest an association with protons from the V-ATPase, calcium release from the AC, and the stability of polyP. Thus, we postulated that depletion of the V-ATPase would likely impact polyP storage and synthesis by disruption of calcium storage. To confirm this link, we first needed to localize the V-ATPase with a subunit of the VTC complex. We chose VTC4, which is the catalytic subunit of the VTC complex [35], and C-terminally Ty1 tagged VTC4 (TgGT1_299080) in the *iΔvha1-HA* strain to determine co-localization with the V-ATPase. IFAs showed that VTC4 appears as small puncta (**Fig. 6.3A**), which suggest acidocalcisome localization [17], and VTC4-Ty1 co-localized with Vha1-HA (**Fig. 6.3A *arrows***). We also observed colocalization and contact of the AC with the PLV (**Fig. 6.3B *and inset***), confirming a previous observation in which both organelles were in close contact [4]. Because depletion of the V-ATPase results in a fragmented PLV [7], we postulated that a similar effect could occur to the acidocalcisomes and impact its content. Acidocalcisomes are electron dense organelles and can be easily seen by transmission electron microscopy (EM) of whole tachyzoites. We showed that V-ATPase depleted parasites contained fewer acidocalcisomes than control parasites incubated without ATc (**Figs. 6.3C, D**). We next tested polyP levels and for this we extracted them parallel from *iΔvha1-HAΔvp1*+ATc, *iΔvha1-HAΔvp1*-ATc and *iΔvha1-HAΔvp1-CM*+ATc *T. gondii* tachyzoites and resolved them in a 35% PAGE system (**Fig. 6.3E**). The level of polyPs was significantly lower when the V-ATPase was down regulated with ATc (*iΔvha1-HAΔvp1*+ATc), which was ameliorated in the complemented strain (**Fig. 6.3E**). We next extracted and quantified short chain polyP from *iΔvha1-HA* (with or without ATc), *Δvp1*, *iΔvha1-HAΔvp1*+ATc, and *iΔvha1-HA-CM*+ATc to compare the effects of depletion of

both proton pumps on polyP levels. Depletion of either the V-ATPase or the vacuolar proton pyrophosphatase (VP1) resulted in significantly lower levels of endogenous polyP (**Fig. 6.3F**). Interestingly, the *iΔvha1-HAΔvp1* double mutant contained similar levels of polyP as the respective single mutants suggesting that disruption to either pump causes significant deficiencies to polyP synthesis and storage that are not additive by the double disruption (**Fig. 6.3F**). These data show that protons, Ca^{2+}, and polyPs are working in conjunction in this organelle to store calcium and polyPs.

Vha1 knockdowns contain lower cytosolic calcium.

We next wanted to study the impact of the disruption of the PLV and acidocalcisome on intracellular calcium. Deletion of TgA1 and TgVP1 resulted in higher cytosolic $[Ca^{2+}]_c$ [4, 25] but, we found that *iΔvha1-HA* +ATc cells had basal intracellular free calcium levels were normal or even lower than control cells grown without ATc (**Fig. 6.4A**). The V-ATPase knockdowns contain an altered membrane potential [7], and this defect could alter the plasma membrane mechanism that keeps intracellular Ca^{2+} levels at ~100 nM. We also created a genetic ratiometric calcium indicator (**Fig. 6.4B**) that contained the GCaMP6f [37] and mScarlet genes with a porcine teschovirus-1 (P2A) [38] interspaced between both genes in the *iΔvha1-HA* strain (**Fig. 6.4B**). The P2A region causes ribosome skipping and thus allows for the two peptides to be synthesized from a single mRNA allowing for a true ratiometric observation. We isolated clones of *iΔvha1-HA* termed *iΔvha1-HA-GmS*, and assayed them for growth and found that they did not show significant differences when compared with the parental cells with or without ATc (**Fig. 6.4C**). To ensure that the ratiometric system was being expressed during ATc addition and to confirm that it was not being degraded with the addition of ATc,

immunoblots were done and shown in **Fig. 6.4D**. The GCamp6f-3Ty1 peptide was predicted to be 54 kDa, the mScarlet peptide was predicted to be 34 kDa, and the full length without ribosome skipping would be 88 kDa. We found minimal expression of the full-length peptide, suggesting that the P2A ribosome skipping system was efficiently working (**Fig. 6.4D**). Next, we observed live *iΔvha1-HA-GmS* clones incubated with or without ATc to confirm that the ratiometric system was working in live cells (**Fig. 6.4E**). We attempted to use these clones to determine the basal $[Ca^{2+}]_c$. However, this proved difficult because although the level of green signal (measuring calcium) was lower than the -ATc signal, the red signal unexplainably decreased as well and impacted the ratio (**Fig. 6.4E**). The GCaMP6f still responded to calcium changes and we determined that calculating the change in the ratio (ΔGCaMP6/mScarlet) was more accurate than one static measurement to determine basal $[Ca^{2+}]_c$.

Vha1 knockdowns have a delayed egress phenotype.

We previously reported that the V-ATPase knock downs had an egress phenotype [7], however the mechanism of this phenotype was not explored. Because calcium signaling is important for all the major steps of the lytic cycle [20], we wanted to test if egress was affected in the *iΔvha1-HA-GmS* clones. To assay egress stimulated by calcium agonists, we incubated *iΔvha1-HA-GmS* clones grown with or without ATc in confluent hTERT host cells on a 35 mm MatTek dish (**Fig. 6.5A**). The MatTek dish was washed twice with ringer buffer without calcium (**Fig. 6.5A**). Calcium agonists such as ionomycin and zaprinast have been instrumental in understanding calcium fluxes in Toxoplasma cytosol and its link to lytic cycle steps [21, 39]. After 30 seconds of time lapse, 100 nM and 25 μM ionomycin or zaprinast were added to stimulate egress (**Fig. 6.5A**). We found

that treatment with ATc resulted in parasites with a delayed egress response to ionomycin (**Figs. 6.5B, C**) or to 25 μM zaprinast, as we observed a significant increase in the length of time that parasites took to egress (**Figs. 6.5D, E**). Collectively, these data demonstrated that the V-ATPase plays a role in calcium signaling, which is critical for stimulating egress.

A calcium threshold is required for egress.

We next wanted to investigate the presence of a threshold for cytosolic calcium, which would be required for egress and for this we first grew *iΔvha1-HA-GmS* clones with or without ATc in confluent hTERT host cells on a 35 mm MatTek dish to determine the ratio of green to red in each parasite inside PVs (**Fig. 6.6A**). The addition of 100 nM ionomycin resulted in an increase in calcium (green signal), which was compared to the red signal (**Fig. 6.6B**). Parasites grown without ATc showed an increase in the green fluorescence and eventually egressed (**Fig. 6.6B**). Parasites incubated with ATc also showed an increase in their ratio (**Fig. 6B)**, but we noticed that a large number of them failed to egress (**Fig. 6.6B *no egress***). After quantifying the individual tracings of all the parasites in the PV, we observed that a threshold of calcium is required in order to egress (**Figs. 6.6C, D *dashed line***). Addition of 25 μM zaprinast, resulted in similar results where the +ATc clones failed to egress and the ratio values were below the required threshold (**Figs. 6.6E-G**). These results suggest that a minimum level of cytosolic calcium is required to stimulate the parasite to egress from the host and that the V-ATPase plays a major role in this requirement.

V-ATPase and motility.

Calcium signaling is important for microneme secretion, egress, and motility [21, 39, 40]. It has been previously shown that microneme secretion, motility (raw distance

travelled), and egress are impacted in the Vha1 knockdown clones [7], but the impact of calcium fluxes as it relates to motility and velocity have not been carefully analyzed. To study motility, we transfected *iΔvha1-HA* parasites with a plasmid that will express tdTomato in the cytoplasm or used *iΔvha1-HA-GmS* and *iΔvha1-HA-GmS-CM* parasites (**Fig. 6.7A**). We studied motility by stimulating tdTomato-expressing parasites with 1.8 mM Ca^{2+} and time-lapse microscopy. Using a new tracking algorithm developed to calculate parasite velocities [41], we found that the Vha1 knockdowns had significantly slower average and maximum velocities compared to control parasites grown without ATc (**Figs. 6.7B and Supp. Movie 2)**. We found that the average velocity of *iΔvha1-HA* –ATc, *iΔvha1-HA*+ATc, *iΔvha1-HA-CM*+ATc tachyzoites were 5.3, 1.28, and 3.8 μm/sec, respectively and the average maximum velocity was 18.9, 6.6, and 21.8 μm/sec, respectively. Because Ca^{2+} induced motility was impacted in the Vha1 knockdowns, we assayed if a Ca^{2+} threshold would also play a role in the decrease velocity of the mutants. We stimulated *iΔvha1-HA-GmS* and *iΔvha1-HA-GmS-CM* parasites with 1.8 mM calcium and measured the ratio at the start (before addition of calcium) and the frame prior to movement, and determined that parasites incubated with ATc had a reduced amplitude change in ratio compared to the -ATc parasites (**Fig. 6.7D**). The -ATc and CM parasites had an average change in fluorescence ratio of 0.57 and 0.55, respectively. *iΔvha1-HA-GmS* parasites that did move more that 5 μm had an average change in fluorescence ratio of 0.33 and those that failed to move or moved <5 μm had an average change in fluorescence ratio of -0.04. These data showed that the V-ATPase is involved in the calcium signaling that precedes stimulation of motility.

6.4 Materials and methods

Chemicals, reagents, and cell cultures.

Fluo4-AM and Fura2-AM was obtained from Invitrogen (Life Technologies, Inc.). Anhydrotetracycline (ATc), Thapsigargin (TG), nigericin, bafilomycin, calcium chloride, ammonium chloride, and ionomycin (iono) were purchased from Sigma Aldrich. Glycyl-L-phenylalanine-naphthylamide (GPN) was from Santa Cruz biotech. hTERT or HFF human fibroblasts cells were maintained in Dulbecco's modified Eagle medium (DMEM) with 10% cosmic calf serum at 37°C with 5% CO_2. *Toxoplasma gondii* strains *iΔvha1-HA, iΔvha1-HA-CM,* and *TATiΔku80* parasites were used in this study [7, 42] and were cultured as described [12].

Genetic manipulations.

iΔvha1-HA parasites were transfected with a plasmid that contained GCaMP6-Ty1-P2A-mScarlet-3xHA (See **fig. 6.3B**) and FACS sorted by both green and red fluorescence. Stable clones (termed *iΔvha1-HA-GmS)* were selected with a good dynamic range of green fluorescence upon addition of extracellular calcium. Plaque assays and western controls were performed to ensure that the genetic calcium indicator did not impact parasite growth (See **Fig. 6.3C, D**). To create complemented cell line, vha1 cDNA was introduced into the *uprt* gene locus as previously described [7]. Verification of insertion was confirmed via immunoblot and PCR (data not shown). Stable clones of *iΔvha1-HA-GmS-vha1* (termed *GmS-CM*) were selected and were found to be able to grow in the presence of ATc. Vacuolar transporter chaperon 4 (VTC4; TGGT1_299080) was C-terminally Ty1 tagged in the iΔvha1-HA strain using the CRISPR protospacer GCCAACGTTTCGGCAGCCGA. Primers 5' ctgcaaattgacgcgggagttaaaaaactgaagtcggtaatgcgtgaattggatgcattg 3' and 5'

aaggaagcaagtcacggcaccatcgagcagggagaggaaccatcctgcaagtgcatagaa 3' were used to amplify 40 base pairs of homology upstream and downstream of the translational stop codon and 3Ty1-DHFR from a template tagging plasmid. This strain is termed *i*Δ*vha1-HA-VTC4-Ty1*.

Measuring intracellular Ca^{2+} with Fura2-AM.

Intracellular Ca^{2+} was determined fluorometrically by loading parasites with Fura2-AM as described previously [3]. Briefly, parasites were harvested, washed with buffer A with glucose (BAG; 116 mM NaCl, 5.4 mM KCl, 0.8 mM $MgSO_4$, 50 mM Hepes, pH 7.3, and 5.5 mM glucose), and filtered through a 5 μm filter. Parasites were resuspended to 1 x 10^9 parasites/ml in BAG + 1.5% sucrose with 5 μM Fura2-AM. Parasite suspensions were incubated for 26 min in a 26°C water bath with mild agitation. Cells were washed twice with BAG to remove extracellular dye and were resuspended at a final density of 1 x 10^9 cells/ml. A 50 μL aliquot of this suspension was added to 2.45 mL of Ringer buffer without calcium (155 mM NaCl, 3 mM KCl, 1 mM $MgCl_2$, 3 mM NaH_2PO_4, and 10 mM Hepes, and 10 mM dextrose) for fluorometric measurements. The excitation wavelength was set at 340 and 380 nm, and emission at 510 nm. *i*Δ*vha1-HA* and *i*Δ*vha1-HA-CM* parasites were incubated with ATc for 0, 2, or 3 days and loaded with Fura2-AM. 1.8 mM calcium was added at the indicated times in the tracings. Quantification of changes in $[Ca^{2+}]_c$ was performed by measuring the change between the initial and final Ca^{2+} concentration. Thapsigargin (TG), bafilomycin A and other agonists were added at the indicated times and concentrations. Quantifications of the slopes were determined by the increase in fluorescence during the first 10-20 sec after addition of calcium ionophores or calcium agonists. 3-6 independent trials were performed for quantifications. To determine the

initial calcium levels in Fura2-AM loaded parasites, the initial Ca^{2+} readings from suspensions were determined from 4-6 independent trials averaging the first 50 seconds of each tracing.

Measuring intercellular Ca^{2+} with GCaMP6f.

The *i*Δ*vha1-HA-GmS* strain was used for these measurements [38]. *i*Δ*vha1-HA-GmS* parasites were incubated with ATc for 0, 2, or 3 days and viewed under an Olympus IX-71 inverted fluorescence microscope with a Photometrix CoolSnapHQ CCD camera driven by DeltaVision software. The exposure duration, gain, laser intensity, and filter settings were identical for all images taken for quantification. DeltaVision Softworx software was used to measure pixel intensity of red and green signal of individual parasites (averaged per PV) in 4-6 independent experiments. The ratio of red to green fluorescence in parasites was used to quantify relative intracellular calcium levels.

Chemical induced parasite egress.

24 hours prior to microscopy observation, parasites were inoculated onto confluent hTERT host cells 30 mm MatTek dishes. 100 nM ionomycin or 25 μM Zaprinast were added at 30 sec of the time lapse and videos were allowed to record for up to 15 min. Images were acquired by time lapse microscopy with identical settings for each of the 6 independent trials. In each field of view, the time post addition of the stimulant until the first evidence of parasite egress from a PV was enumerated. The first 5 quickest egressing PV's were averaged for each independent trial. If ≤ 5 PV's showed no parasite egress, each PV (up to 5 total) were assigned the maximum time of the time lapse (15 min.). For each independent trial, the individual fluorescence values of red and green signal of all the members in per PV were recorded. The ratio of red to green signal was determined for the

individual parasites that either egressed or did not egress. To quantify the relative level of calcium required for egress, the ratios from all members of the same PV were averaged and the averaged values of 4-6 independent trials (per PV) are reported.

Motility analysis.

Changes in motility of the parasites was performed as previously described [21] with some modifications. tdTomato-expressing or GCaMP6f-2PA-mScarlet parasites grown with or without ATc were used to visualize motility or quantify Ca^{2+} levels. 24 hours prior to microscopy, 35 mm MatTek dishes were incubated with 10% FBS to provide sufficient protein to allow a surface conducive to motility. MatTek dishes were washed once with PBS and loaded with 2 ml of Ringer buffer without Ca^{2+}. MatTek dishes were chilled on ice, parasites were added to the dish and allowed to equilibrate for 15 min. Dishes were then placed in the Zeiss LSM 710 Confocal Microscope environmental chamber set at 37°C. 1.8 mM Ca^{2+} was added and motility was imaged and quantified as previously described [41]. Briefly, for each independent trial the average and maximum observed velocity were determined, each individual parasite velocity was sorted from highest to lowest, and the top 20 highest velocities per independent trial were used to determine quantification. There were 3 or 4 independent trials of *i*Δ*vha1-HA*–ATc, *i*Δ*vha1-HA* +ATc, and *i*Δ*vha1-HA-CM* +ATc assayed in this fashion. For measuring relative calcium levels, *i*Δ*vha1-HA* or *i*Δ*vha1-HA-CM* GCaMP6f-2PA-mScarlet expressing parasites were used. The ratio of green to red fluorescence before the addition of 1.8 mM Ca^{2+} addition and the frame before the parasite movement (where movement is defined as a distance traveled greater than 5 um) was determined and the change in the

ratio reported. Data from 3 independent trials and the change in fluorescence ratio of 10 parasites per trial are reported.

Polyphosphates and acidocalcisome analysis.

Short chain polyphosphate from 1 x 10^9 parasites was extracted as previously described [43] with some modifications. First, *iΔvha1-HA*, *Δvp1*, *iΔvha1-HAΔvp1,* and *iΔvha1-HA-CM* were incubated with or without ATc for 3 days and were washed with BAG. Extraction of short chain polyP was done according to a previous protocol for resolution in a 35 % polyacrylamide gel [43]. For polyP quantification, we used 10^8 parasites and quantification of polyP levels was determined using the Malachite Green assay as previously described [43, 44]. For Electron microscopy, parasites were washed and placed on copper grids, which were allowed to air dry. Once dry, parasites were imaged on a transmission electron microscope JEOL JEM1011. Images were randomized and assayed double blinded. Quantification of acidocalcisomes are from 2 independent trials where a total of 67 -ATc and 57 +ATc were enumerated. Immunofluorescence microscopy was performed as previously described [7] on *iΔvha1-HA-VTC4-Ty1*. Rat-anti-HA (1:25) and mouse-anti-Ty1 (1:1,000) were used to probe the localization of acidocalcisomes.

Statistical analysis.

All statistical analyses were performed using GraphPad Prism. Unless otherwise noted, all error bars are presented as the standard error of the mean (SEM) and from a minimum of three independent trials. Differences were considered significant if *P* values were < 0.05.

6.5 Discussion

It has been well documented that Ca^{2+} signaling regulates all the steps of the lytic cycle of *Toxoplasma gondii,* like invasion, egress, motility and microneme secretion [3, 20, 21, 25, 45, 46]. The mechanisms involved in calcium influx, signaling, and homeostasis are poorly understood. This is in part due to the evolutionary distance between Apicomplexan parasites and mammalian model systems [47]. Ca^{2+} influx plays important roles in refilling intracellular organelle stores and also in activating calcium signaling pathways [20, 48]. Failure to properly regulate calcium entry and signaling can lead to calcium cytotoxicity and can lead to cell death [49]. Thus, it is imperative that *T. gondii* maintain calcium homeostasis to ensure propagation.

Once calcium enters into the cytoplasm, it can be pumped into organelles for storage. The known organelles that store calcium in *T. gondii* are the endoplasmic reticulum (ER), and two acidic storage organelles, the plant-like vacuole and the acidocalcisome (AC). The ER is known to play important roles in calcium signaling and homeostasis in many organisms [50]. The model from Hortua Triana et al [20] postulates that the ER is the largest contributor to calcium uptake, homeostasis, and signaling. Thus, extra cytoplasmic calcium will be pumped into the ER primarily by a SERCA-type Ca^{2+} ATPase and stored. Chemical inhibition of a SERCA pump results in an increase of $[Ca^{2+}]_c$ levels (through leakage by an unknown mechanism) and then recovery to basal levels [3, 21, 51]. We aimed to understand the contribution of the PLV and acidocalcisomes to this Ca^{2+} recovery phase.

In the membrane of the PLV the V-ATPase is involved in pumping protons into its lumen [7]. This fits with the major function of the V-ATPase, which is to pump protons

against their concentration gradient. The localization of these pumps are typically in internal vesicles, and in the case of *T. gondii*, localized to the PLV, immature rhoptries, and plasma membrane [7, 52]. In addition, there is biochemical evidence that supports its localization to acidocalcisome [12, 53], but no co-localization investigations in *T. gondii* had been previously done. We demonstrate for the first time, that the *T. gondii* V-ATPase co-localized with VTC4, a subunit of the polyphosphate synthesis complex, which is usually found in acidocalcisomes [13]. We investigated calcium homeostasis in the *iΔvha1-HA* because the proton gradient generated at the PLV and AC by the V-ATPase could be used for Ca^{2+} transport or exchange, which would impact $[Ca^{2+}]_c$. It was previously shown that the PLV stores Ca^{2+}, which could be released into the cytoplasm with GPN, and by a Ca^{2+}/H^+ exchanger activity in PLV enriched fractions [4]. It was also shown that a Ca^{2+}-ATPase, TgA1, which localized to the AC was important for calcium homeostasis [25]. Both of these organelles play important roles in acidic calcium storage and we studied the impacts of depletion of the V-ATPase. During our investigation, we found that depletion of the V-ATPase resulted in defects in calcium storage in both the PLV and the AC. The amount of Ca^{2+} released into the cytoplasm in response to GPN was significantly reduced in *iΔvha1-HA* parasites that grew in the presence of ATc. This result supports the role of the V-ATPase in creating the proton gradient used for Ca^{2+} transport into the PLV. To determine the role of the V-ATPase and Ca^{2+} storage at the acidocalcisome, we added 10 mM NH_4Cl to *iΔvha1-HA*+ATc parasites and observed little to no Ca^{2+} release in the Vha1 knockdowns. These results demonstrate that all acidic calcium stores in these mutants are deficient in their Ca^{2+} storage levels, a consequence of a non-functional V-ATPase. Further evidence that the V-ATPase plays a role in calcium uptake at the PLV and/or AC was

demonstrated. First, the addition of bafilomycin after the addition of TG resulted in a significant increase in calcium in the -ATc and complemented clones, but virtually no release in parasites incubated with ATc. These data demonstrate that the proton gradient is essential for calcium storage both in the PLV and AC. Second, blocking the ER by TG, followed by addition of 1.8 mM calcium, resulted in calcium leakage into the parasites (**Fig. 6.1E**). When the reagents were switched, the Vha1 mutants continued to leak calcium into the cytosol, supporting the role of the PLV and AC in regulating cytosolic Ca^{2+}. Third, it was reported that membrane integrity of the PLV was impacted in a chloroquine resistant transporter (TgCRT) which localizes at the PLV [32]. The addition of bafilomycin after blocking ER uptake resulted in significant calcium release in the WT and complemented strain and little to no release in the ΔCRT mutant. Because TgCRT has been shown to only localize to the PLV [32], these results demonstrate that protons are absolutely essential to the storage of calcium in the PLV. These observations also suggest that after uptake by the ER, the PLV is the next major organelle for Ca^{2+} uptake. Direct uptake of calcium by the AC likely is tertiary and most likely due to organelle interactions with the PLV.

Ca^{2+} entry into *Toxoplasma gondii* is poorly understood but essential to the propagation of the parasite [3, 21]. The low resting level of $[Ca^{2+}]_c$ is essential for maintaining the large dynamic range that is required for Ca^{2+} signals. The role of Ca^{2+}-buffering organelles involves storage and extrusion to maintain this $[Ca^{2+}]_c$. This finely tuned control of $[Ca^{2+}]_c$ is critical for the downstream modulation of signaling pathways that result in specific cellular functions [22]. Cells use a variety of mechanisms for regulating the opening and closing of plasma membrane channels that allow Ca^{2+} influx [54]. In addition, a highly efficient Ca^{2+}-ATPase at the plasma membrane pumps Ca^{2+}

outside the cell [26]. In *Toxoplasma* the molecular identity of the channels that allow Ca^{2+} influx is still unknown and so is its regulation. We do know that extracellular Ca^{2+} enters the tachyzoite in a highly regulated process and this process is sensitive to specific inhibitors of voltage gated calcium channels [6]. We studied $[Ca^{2+}]_c$ changes under conditions of Ca^{2+} influx in the *iΔvha1-HA* and observed that these parasites are not able to regulate the cytoplasmic levels as efficiently as their parental clones. This Ca^{2+} leaky phenotype was similar to the one observed with the Na^+/H^+ exchanger knock-out mutants [55]. This result indicated an important role for the PLV or AC in buffering $[Ca^{2+}]_c$. A deficient proton gradient would disrupt the PLV or AC capacity to uptake Ca^{2+} from the cytosol and probably other ions. It is also possible that buildup of protons at the plasma membrane would neutralize a portion of the negative charges responsible for the membrane potential and this would alter the regulation of the permeability of plasma membrane calcium channels. Changes in the membrane potential have been linked to calcium influx in mammalian cells [56]. In Toxoplasma, Ca^{2+} is critical for the activation of effectors that stimulate/enhance important steps of the *Toxoplasma gondii* lytic cycle. Disruption of these delicate mechanisms will alter the most essential aspect of the parasitological cycle of *Toxoplasma*. We propose the model (presented in **Fig. 6.8**) where Ca^{2+} uptake mostly occurs by the ER. When calcium uptake by the ER is blocked, both the PLV or the AC are able to sequester increases in $[Ca^{2+}]_c$. The loss of the V-ATPase results in abnormal PLV, which is defective in calcium uptake, and creates an alkaline AC, which no longer contains a strong proton gradient (**Fig. 6.8**). In our model we propose that loss of V-ATPase results in depolarization of the plasma membrane leading to defects in the activation of calcium

channels. These channel defects lead to equilibration with the external calcium concentration (**Fig. 6.8**).

Because calcium is important for all the steps of the lytic cycle and depletion of the V-ATPase resulted in defects of the lytic cycle [3, 7, 20, 21, 45, 46], we postulated calcium signaling and/or homeostasis might be responsible for the observed defects. We used a genetically encoded calcium indicator (GCaMP6f) to investigate the role of calcium to the lytic cycle in V-ATPase depleted parasites. Much to our surprise, we observed lower levels of $[Ca^{2+}]_c$ in our mutants than the parental or complemented. We attributed these results to defects in the activation of voltage gated calcium channels resulting in equilibrating with the external calcium levels in the V-ATPase depleted parasites. Ca^{2+} release from intracellular stores has been reported to directly modulate an unknown Ca^{2+} channel and Ca^{2+} release from intracellular stores enhances motility, microneme secretion, and host invasion [3]. Using GCaMP6f in V-ATPase depleted parasites, we observed that time of egress increased with ionomycin or zaprinast as incubation with ATc increased. Our data are in line with previously reported egress times using the calcium ionophore ionomycin and also support the presence of an unidentified Ca^{2+} channel that is involved with increases in $[Ca^{2+}]_c$ that is required to trigger egress [21]. Upon further observation, we determined that intracellular calcium increases must pass a threshold in order to trigger signaling pathways that lead to egress. While the V-ATPase depleted parasites are intracellular, they are equilibrated with the host $[Ca^{2+}]_c$ levels (around 50-100 nM), and the intracellular stores such as the ER contain lower concentrations of Ca^{2+}. Thus, when ionomycin or zaprinast cause increases in $[Ca^{2+}]_c$, the V-ATPase depleted parasites take longer to reach the threshold (if at all) and are delayed or, in some cases, fail to initiate

egress. Similarly, when we studied motility, we found a correlation between velocity and increases in $[Ca^{2+}]_c$ that is consistent with previous reports [7, 21]. We found that the V-ATPase depleted mutants had lower velocities than the parental or complemented clones. Using the ratiometric GCaMP6f, we determined that the V-ATPase depleted parasites, on average, had a lower change in the ratio of $[Ca^{2+}]_c$ after calcium stimulation than the parental and complemented clones. Parasites that had little to no change in their ratio failed to move at all and these data are in line with previous reports of the importance of Ca^{2+} in the lytic cycle [3, 21].

In addition to storing a variety of ions including Ca^{2+}, the AC is responsible for the synthesis and storage of polyphosphates (polyP). Polyphosphates have been reported to have a wide range of roles from biochemical reactions (from their high energy bond), to signaling and their involvement in regulatory processes, role in virulence, and as a part of the stress response network [57, 58]. The functions of polyP in *Toxoplasma gondii* have not been thoroughly explored. Depletion of TgA1, a Ca^{2+} ATPase that localizes to the AC, had less polyP and showed defects in virulence and attempts to delete components of the VTC complex were unsuccessful suggesting its essentiality [17, 25]. Acidocalcisomes require a proton pump in order to create the acidic environment. We C-terminally Ty1 tagged VTC4, the catalytic subunit responsible for polyphosphate synthesis in the acidocalcisomes [13], and determined that it co-localized with Vha1 in small vesicles. The localization of VTC4-Ty1 was similar to previous reports of other subunits of the VTC complex [17], yet we were able to show that the V-ATPase co-localized with VTC4. We found that V-ATPase depleted parasites had fewer AC organelles and lower amounts of polyPs indicating a link between the V-ATPase and the AC. It was previously shown that

loss of the Vha1 resulted in defects in the formation of the PLV and the AC has been shown to interact with the fully formed PLV [4, 7]. The loss of proper PLV formation in V-ATPase depleted parasites may also result in defects in AC organelle number. This hypothesis is likely true because deletion of VP1, which we demonstrated is also important for polyP synthesis and storage, did not lead to phenotypes associated with defective AC's. Recent reports have shown that polyP are involved in the cell cycle [59, 60]. Although replication was impacted in V-ATPase depleted parasites [7], deletion of VP1 in *T. gondii* resulted in lower levels of polyP but without a replication phenotype [6].

Our work underscores the significance of proton gradients in maintaining a delicate ion equilibrium that when altered will result in detrimental cell functions. In summary, our data demonstrate that the PLV and AC, in conjunction with the ER, play an active role in storing calcium and the proton gradient generated by the activity of the V-ATPase is critically important. We demonstrate that the V-ATPase plays some role in calcium influx, likely through alterations in the membrane potential. Finally, we demonstrate a link between calcium, pH, and polyphosphate that is important for invasion and virulence.

6.6 Acknowledgment

We thank the Georgia Electron microscopy core facilities for the EM images taken during this study. We thank the Biomedical Microscopy Core, Coverdell, for the use of their microscopes.

6.7 Conflict of interest

The authors declare that they have no conflicts of interest with the contents of this article.

6.8 References

1. Black, M.W. and J.C. Boothroyd, *Lytic Cycle of Toxoplasma gondii.* Microbiology and Molecular Biology Reviews, 2000. **64**(3): p. 607.

2. Lourido, S. and S.N.J. Moreno, *The calcium signaling toolkit of the Apicomplexan parasites Toxoplasma gondii and Plasmodium spp.* Cell Calcium, 2015. **57**(3): p. 186-193.

3. Pace, D.A., et al., *Calcium Entry in Toxoplasma gondii and Its Enhancing Effect of Invasion-linked Traits.* Journal of Biological Chemistry, 2014. **289**(28): p. 19637-19647.

4. Miranda, K., et al., *Characterization of a novel organelle in Toxoplasma gondii with similar composition and function to the plant vacuole.* Molecular Microbiology, 2010. **76**(6): p. 1358-1375.

5. Chasen, N.M., et al., *The Vacuolar Zinc Transporter TgZnT Protects Toxoplasma gondii from Zinc Toxicity.* mSphere, 2019.

6. Liu, J., et al., *A vacuolar-H^+-pyrophosphatase (TgVP1) is required for microneme secretion, host cell invasion, and extracellular survival of Toxoplasma gondii.* Molecular Microbiology, 2014. **93**(4): p. 698-712.

7. Stasic, A.J., et al., *The Toxoplasma Vacuolar H^+-ATPase regulates intracellular pH, and impacts the maturation of essential secretory proteins* Cell Reports, 2019.

8. Moreno, N.J.S., et al., *Vacuolar-type H^+-ATPase regulates cytoplasmic pH in Toxoplasma gondii tachyzoites.* Biochemical Journal, 1998. **330**(2): p. 853.

9. Ryan, P.R., I.A. Newmn, and I. Arif, *Rapid calcium exchange for protons and potassium in cell walls of Chara.* Plant, Cell & Environment, 1992. **15**(6): p. 675-683.

10. Schwiening, C.J., H.J. Kennedy, and R.C. Thomas, *Calcium-hydrogen exchange by the plasma membrane Ca-ATPase of voltage-clamped snail neurons.* Proceedings of the Royal Society B, 1993. **253**(1338): p. 285-289.

11. Åkerman, K.E.O., *Changes in membrane potential during calcium ion influx and efflux across the mitochondrial membrane.* Biochimica et Biophysica Acta (BBA) - Bioenergetics, 1978. **502**(2): p. 359-366.

12. Moreno, S.N.J. and L. Zhong, *Acidocalcisomes in Toxoplasma gondii tachyzoites.* Biochemical Journal, 1996. **313**(2): p. 655.

13. Docampo, R. and S.N.J. Moreno, *Acidocalcisomes.* Cell Calcium, 2011. **50**(2): p. 113-119.

14. Docampo, R., et al., *Acidocalcisomes - conserved from bacteria to man.* Nature Reviews Microbiology, 2005. **3**: p. 251.

15. Müller, O., et al., *The Vtc proteins in vacuole fusion: coupling NSF activity to V_0 trans-complex formation.* The EMBO Journal, 2002. **21**(3): p. 259.

16. Bru, S., et al., *Polyphosphate is involved in cell cycle progression and genomic stability in Saccharomyces cerevisiae.* Molecular Microbiology, 2016. **101**(3): p. 367-380.

17. Rooney, P.J., et al., *TgVTC2 is involved in polyphosphate accumulation in Toxoplasma gondii.* Molecular and Biochemical Parasitology, 2011. **176**(2): p. 121-126.

18. Forgac, M., *Vacuolar ATPases: rotary proton pumps in physiology and pathophysiology.* Nat Rev Mol Cell Biol, 2007. **8**(11): p. 917-929.

19. Parussini, F., et al., *Cathepsin L occupies a vacuolar compartment and is a protein maturase within the endo/exocytic system of Toxoplasma gondii.* Molecular Microbiology, 2010. **76**(6): p. 1340-1357.

20. Hortua Triana, M.A., et al., *Calcium signaling and the lytic cycle of the Apicomplexan parasite Toxoplasma gondii.* Biochimica et Biophysica Acta (BBA) - Molecular Cell Research, 2018. **1865**(11, Part B): p. 1846-1856.

21. Borges-Pereira, L., et al., *Calcium Signaling throughout the Toxoplasma gondii Lytic Cycle a study using genetically encoded calcium indicators.* Journal of Biological Chemistry, 2015. **290**(45): p. 26914-26926.

22. Berridge, M.J., M.D. Bootman, and H.L. Roderick, *Calcium signalling: dynamics, homeostasis and remodelling.* Nature Reviews Molecular Cell Biology, 2003. **4**: p. 517.

23. Clapham, D.E., *Calcium signaling.* Cell, 2007. **131**(6): p. 1047-58.

24. Brini, M., et al., *Calcium pumps: why so many?* Compr Physiol, 2012. **2**(2): p. 1045-60.

25. Luo, S., F.A. Ruiz, and S.N.J. Moreno, *The acidocalcisome Ca^{2+}-ATPase (TgA1) of Toxoplasma gondii is required for polyphosphate storage, intracellular calcium homeostasis and virulence.* Molecular Microbiology, 2005. **55**(4): p. 1034-1045.

26. Luo, S., et al., *A plasma membrane-type Ca^{2+}-ATPase co-localizes with a vacuolar H^{+}-pyrophosphatase to acidocalcisomes of Toxoplasma gondii.* The EMBO Journal, 2001. **20**(1-2): p. 55.

27. Rohloff, P., et al., *Calcium Uptake and Proton Transport by Acidocalcisomes of Toxoplasma gondii.* PLOS ONE, 2011. **6**(4): p. e18390.

28. Thastrup, O., et al., *Thapsigargin, a tumor promoter, discharges intracellular Ca^{2+} stores by specific inhibition of the endoplasmic reticulum Ca^{2+}-ATPase.* Proceedings of the National Academy of Sciences, 1990. **87**(7): p. 2466.

29. Haller, T., et al., *The lysosomal compartment as intracellular calcium store in MDCK cells: a possible involvement in InsP3-mediated Ca2+ release.* Cell Calcium, 1996. **19**(2): p. 157-165.

30. Lloyd-Evans, E., et al., *Niemann-Pick disease type C1 is a sphingosine storage disease that causes deregulation of lysosomal calcium.* Nat Med, 2008. **14**(11): p. 1247-1255.

31. Warring, S.D., et al., *Characterization of the Chloroquine Resistance Transporter Homologue in Toxoplasma gondii.* Eukaryotic Cell, 2014. **13**(11): p. 1360-1370.

32. Thornton, L.B., et al., *An ortholog of P. falciparum chloroquine resistance transporter (PfCRT) plays a key role in maintaining the integrity of the endolysosomal system in Toxoplasma gondii to facilitate host invasion.* PLOS Pathogens, 2019.

33. Stasic, A.J., et al., *The Toxoplasma Vacuolar H^{+}-ATPase regulates intracellular pH, and impacts the maturation of essential secretory proteins.* Cell Reports, 2019.

34. Docampo, R., P. Ulrich, and S.N.J. Moreno, *Evolution of acidocalcisomes and their role in polyphosphate storage and osmoregulation in eukaryotic microbes.* Philosophical transactions of the Royal Society of London. Series B, Biological sciences, 2010. **365**(1541): p. 775-784.

35. Lander, N., et al., *Polyphosphate and acidocalcisomes.* Biochemical Society Transactions, 2016. **44**(1): p. 1.

36. Rodrigues, C.O., et al., *Characterization of Isolated Acidocalcisomes from Toxoplasma gondii Tachyzoites Reveals a Novel Pool of Hydrolyzable Polyphosphate.* Journal of Biological Chemistry, 2002. **277**(50): p. 48650-48656.

37. Chen, T.-W., et al., *Ultrasensitive fluorescent proteins for imaging neuronal activity.* Nature, 2013. **499**(7458): p. 295-300.

38. Kim, J.H., et al., *High Cleavage Efficiency of a 2A Peptide Derived from Porcine Teschovirus-1 in Human Cell Lines, Zebrafish and Mice.* PLOS ONE, 2011. **6**(4): p. e18556.

39. Sidik, S.M., et al., *Using a Genetically Encoded Sensor to Identify Inhibitors of Toxoplasma gondii Ca^{2+} Signaling.* Journal of Biological Chemistry, 2016. **291**(18): p. 9566-9580.

40. Carruthers, V.B. and L.D. Sibley, *Mobilization of intracellular calcium stimulates microneme discharge in Toxoplasma gondii.* Molecular Microbiology, 1999. **31**(2): p. 421-428.

41. Fazli, M.S., et al., *Computational motility tracking of calcium dynamics in Toxoplasma gondii.* arXiv preprint arXiv:1708.01871, 2017.

42. Fox, B.A., et al., *Efficient gene replacements in Toxoplasma gondii strains deficient for nonhomologous end joining.* Eukaryot Cell, 2009. **8**(4): p. 520-9.

43. Potapenko, E., et al., *5-Diphosphoinositol pentakisphosphate (5-IP7) regulates phosphate release from acidocalcisomes and yeast vacuoles.* Journal of Biological Chemistry, 2018. **293**(49): p. 19101-19112.

44. Lanzetta, P.A., et al., *An improved assay for nanomole amounts of inorganic phosphate.* Analytical Biochemistry, 1979. **100**(1): p. 95-97.

45. Arrizabalaga, G. and J.C. Boothroyd, *Role of calcium during Toxoplasma gondii invasion and egress.* International Journal for Parasitology, 2004. **34**(3): p. 361-368.

46. Lovett, J.L. and L.D. Sibley, *Intracellular calcium stores in Toxoplasma gondii govern invasion of host cells.* Journal of Cell Science, 2003. **116**(14): p. 3009.

47. R.S. Garcia, C., et al., *InsP3 Signaling in Apicomplexan Parasites.* Current Topics in Medicinal Chemistry, 2017. **17**(19): p. 2158-2165.

48. Parekh, A.B. and J.W. Putney, *Store-Operated Calcium Channels.* Physiological Reviews, 2005. **85**(2): p. 757-810.

49. Kass, G.E. and S. Orrenius, *Calcium signaling and cytotoxicity.* Environmental Health Perspectives, 1999. **107**(suppl 1): p. 25-35.

50. Krebs, J., L.B. Agellon, and M. Michalak, *Ca^{2+} homeostasis and endoplasmic reticulum (ER) stress: An integrated view of calcium signaling.* Biochemical and Biophysical Research Communications, 2015. **460**(1): p. 114-121.

51. Nagamune, K., S.N.J. Moreno, and L.D. Sibley, *Artemisinin-resistant mutants of Toxoplasma gondii have altered calcium homeostasis.* Antimicrobial agents and chemotherapy, 2007. **51**(11): p. 3816-3823.

52. Marshansky, V. and M. Futai, *The V-type H^+-ATPase in vesicular trafficking: targeting, regulation and function.* Current Opinion in Cell Biology, 2008. **20**(4): p. 415-426.

53. Miranda, K., et al., *Acidocalcisomes in Apicomplexan parasites.* Experimental Parasitology, 2008. **118**(1): p. 2-9.

54. Verkhratsky, A. and V. Parpura, *Calcium signalling and calcium channels: evolution and general principles.* Eur J Pharmacol, 2014. **739**: p. 1-3.

55. Arrizabalaga, G., et al., *Ionophore-resistant mutant of Toxoplasma gondii reveals involvement of a sodium/hydrogen exchanger in calcium regulation.* The Journal of Cell Biology, 2004. **165**(5): p. 653.

56. Behringer, E.J. and S.S. Segal, *Membrane potential governs calcium influx into microvascular endothelium: integral role for muscarinic receptor activation.* J Physiol, 2015. **593**(20): p. 4531-48.

57. Jiménez, J., et al., *Polyphosphate: popping up from oblivion.* Current Genetics, 2017. **63**(1): p. 15-18.

58. Albi, T. and A. Serrano, *Inorganic polyphosphate in the microbial world. Emerging roles for a multifaceted biopolymer.* World Journal of Microbiology and Biotechnology, 2016. **32**(2): p. 27.

59. Henry, J.T. and S. Crosson, *Chromosome replication and segregation govern the biogenesis and inheritance of inorganic polyphosphate granules.* Molecular Biology of the Cell, 2013. **24**(20): p. 3177-3186.

60. Boutte, C.C., J.T. Henry, and S. Crosson, *ppGpp and Polyphosphate Modulate Cell Cycle Progression in Caulobacter crescentus.* Journal of Bacteriology, 2012. **194**(1): p. 28.

Figures

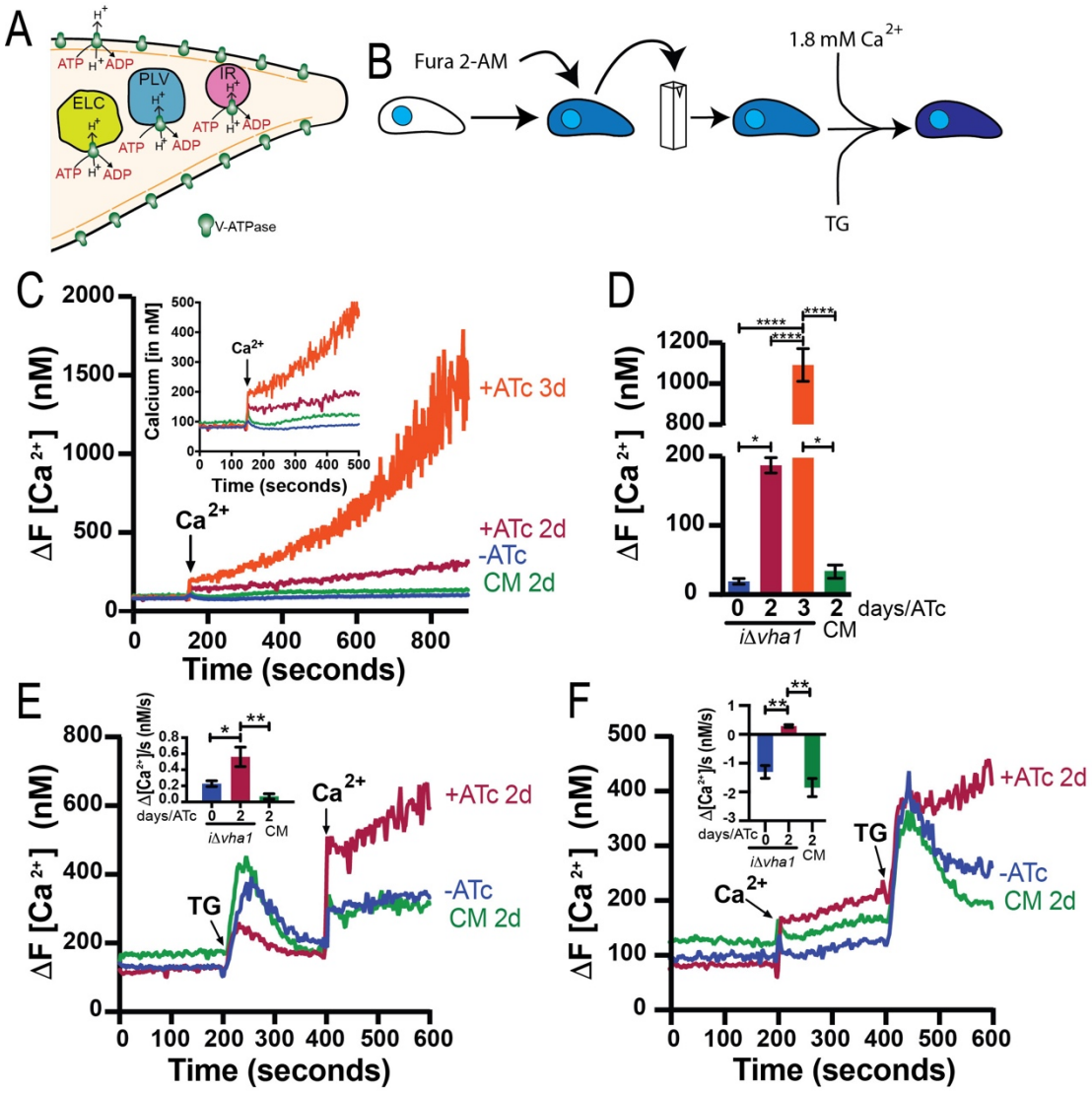

FIGURE 6.1: The PLV acts as a calcium store. A) Localizations of the V-ATPase based on Stasic et al, 2019. B) Schematic of the loading of parasites with Fura2-AM. C) Representative tracing of Fura-2-AM loaded *iΔvha1-HA* and *iΔvha1-HA-CM* parasites previously grown with ATc for the indicated days. 1.8 mM Calcium was added at 150 s (indicated by the arrow). D) Quantification of the change in intracellular calcium levels observed from 200-900s. C-D Data are from 3-5 independent trials. E) Representative

tracings of Fura2-AM loaded *iΔvha1-HA* and *iΔvha1-HA-CM* clones incubated for the indicated days with ATc. Thapsigargin (TG, 2 μM) was added at 200 s and 1.8 mM Ca^{2+} at 400 s. Inset graph shows the quantification of the slope of Ca^{2+} recovery after Ca^{2+} addition (from 450 s to 600 s). F) Representative tracings of Fura2-AM loaded *iΔvha1-HA* and *iΔvha1-HA-CM* clones incubated for the indicated days with ATc. Calcium (1.8 mM) was added at 200 s and 2 μM TG (2 μM) at 400 s. Inset graph shows the quantification of the slope of Ca^{2+} recovery after TG addition (from 475s to 600s). D-F data were compared with one-way ANOVA test from 3 independent trials where $^{**}P < 0.05$; $^{**}P < 0.01$; $^{****}P < 0.0001$.

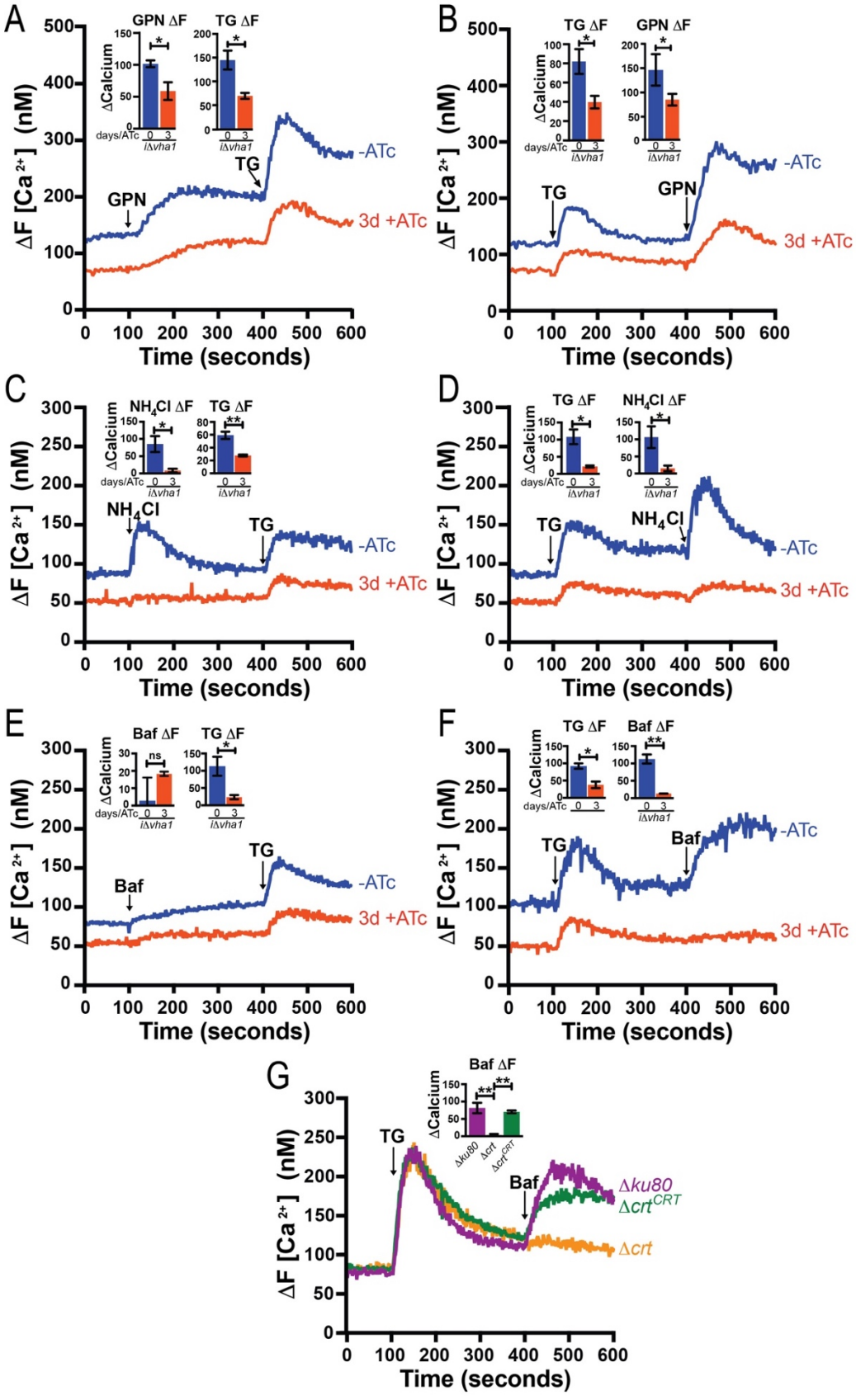
A
GPN ΔF
TG ΔF
ΔCalcium
days/ATc 0 3
iΔvha1
ΔF [Ca 2+] (nM)
GPN
TG
-ATc
3d +ATc
Time (seconds)
B
TG ΔF
GPN ΔF
TG
GPN
C
NH4Cl ΔF
TG ΔF
NH4Cl
D
TG ΔF
NH4Cl ΔF
E
Baf ΔF
TG ΔF
ns
Baf
F
TG ΔF
Baf ΔF
G
Baf ΔF
Δku80
Δcrt
ΔcrtCRT
Δku80
ΔcrtCRT
Δcrt

FIGURE 6.2: Calcium release from acidic stores. Representative tracings of Fura2-AM loaded parasites. A) GPN (30 μM) and TG (1 μM) were added at 100 and 400 seconds, respectively. B) Similar to A with the addition of reagents reversed. C) NH_4Cl (20 mM) and TG (1 μM) were added at 100 and 400 seconds, respectively. D) Similar to C with the addition of reagents reversed. E) Bafilomycin (1 μM) and TG (1 μM) were added at 100 and 400 seconds, respectively. F) Similar to E with the addition of reagents reversed. Panels A-F used *iΔvha1-HA* and *iΔvha1-HA-CM* clones incubated with ATc for 0 or 3 days and G) TG (1 μM) and Bafilomycin (1 μM) were added at 100 and 400 seconds, respectively, to Δku80, Δ*crt*, and Δcrt^{CRT} parasites from [32]. A-G inset graphs show the quantification of the change in calcium levels between the level 10 seconds prior to the addition of the indicated compound and the maximum peak after addition. Panels A-F are from 3-4 independent trials using a student's T-test and panel G was compared with one-way ANOVA test where *$P < 0.05$; **$P < 0.01$; n. s., not significant.

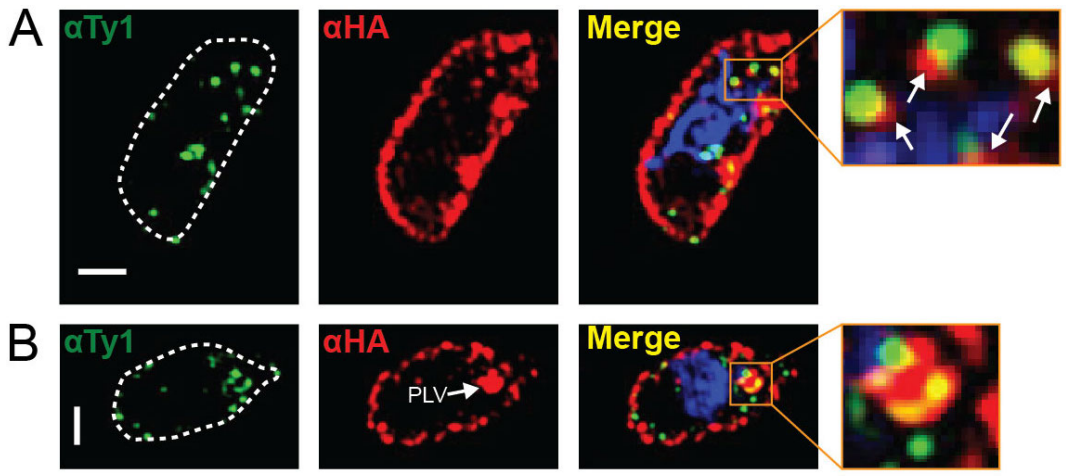
A
αTy1
αHA
Merge
B
αTy1
αHA
PLV
Merge

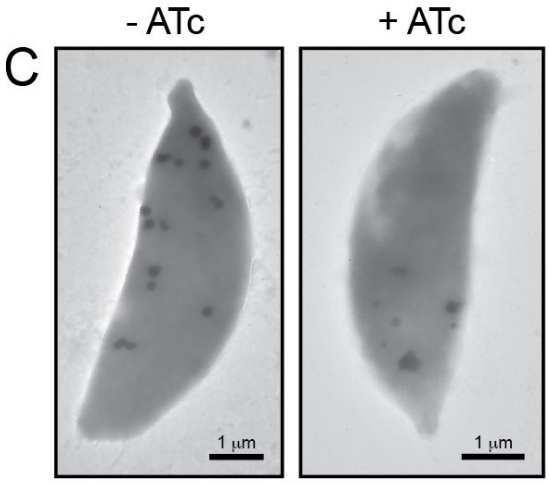
- ATc
+ ATc
C
1 μm
1 μm

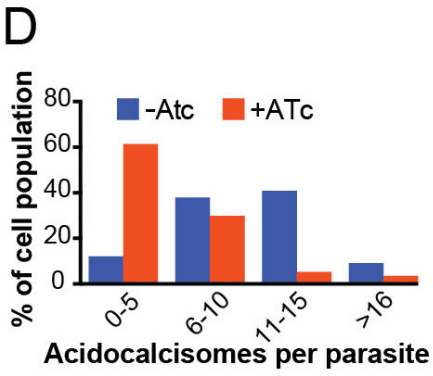
D
% of cell population
80
60
40
20
0
-Atc
+ATc
0-5
6-10
11-15
>16
Acidocalcisomes per parasite

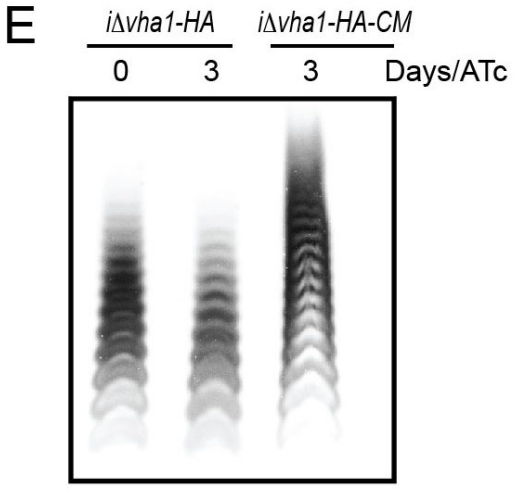
E
iΔvha1-HA
iΔvha1-HA-CM
0
3
3
Days/ATc

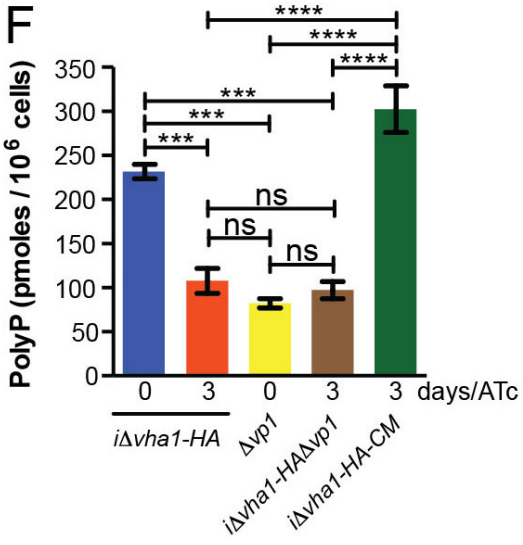
F
PolyP (pmoles / 10^6 cells)
350
300
250
200
150
100
50
0
****
****
****
***
***
***
ns
ns
ns
0
3
0
3
3
days/ATc
iΔvha1-HA
Δvp1
iΔvha1-HAΔvp1
iΔvha1-HA-CM

FIGURE 6.3: Protons are required for polyphosphate storage. A) Super resolution images of *iΔvha1-HA-VTC4-Ty1* parasites showing Vha1 colocalization with VTC4 (arrows in inset). B) Super resolution images of *iΔvha1-HA-VTC4-Ty1* parasites showing Vha1 colocalization with VTC4, highlighting the association with the PLV (inset). Scale bars are 2 μm. Dashed lines are the outline of the parasite. C) Electron microscopy of whole cell *iΔvha1-HA* parasites. D) quantification of acidocalcisome number per parasite. Data are from 2 independent trials where a total of 67 -ATc and 57 +ATc were enumerated. E) Short chain polyphosphate gel from *iΔvha1-HA* and *iΔvha1-HA-CM* parasites incubated with or without ATc on a 30% poly-acrylamide gel. F) Quantification of short chain polyphosphate of *iΔvha1-HA*, *Δvp1*, *iΔvha1-HAΔvp1,* and *iΔvha1-HA-CM.* Panel F was compared with one-way ANOVA test, where ***$P < 0.001$, ****$P < 0.0001$.

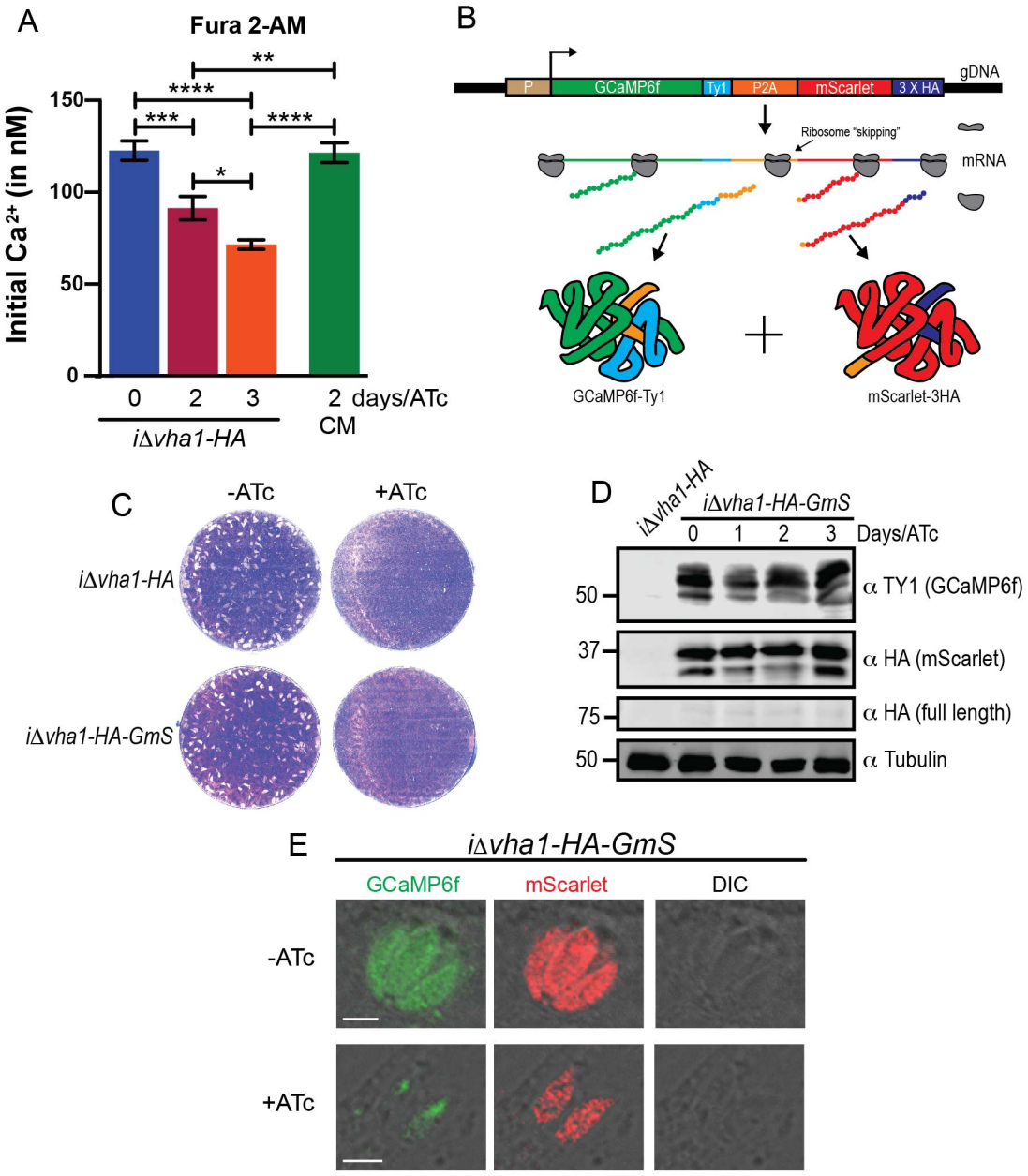

FIGURE 6.4: Vha1 knockdowns contain less intracellular calcium. A) Fura-2-AM loaded *iΔvha1-HA* and *iΔvha1-HA-CM* clones incubated with ATc for the indicated days. Data are reported as the average of the first 60 seconds of basal calcium levels from 6 independent trials. B) Cartoon depicting the ratiometric GCaMP6-mScarlet construct. P, tubulin promoter; GCamp6f, genetically encoded calcium indicator version 6-fast; Ty1,

epitope tag; P2A, porcine teschovirus-1; HA, hemagglutinin. C) Plaque assay comparing the parental strain (*iΔvha1-HA*) and the *iΔvha1-HA-GmS* clone with or without ATc for 8 days. D) Western blots comparing parental strain (*iΔvha1-HA*) with the *iΔvha1-HA-GmS* clone with the addition of ATc for the indicated time. Anti Ty1 1:1,000; Anti-HA 1:200; Anti-Tubulin 1:30,000. E) Live cell microscopy of *iΔvha1-HA-GmS* incubated with or without ATc for 2 days. Scale bars are 2 μm. Panel A was compared with one-way ANOVA test, where $^{**}P < 0.01$ and $^{****}P < 0.0001$.

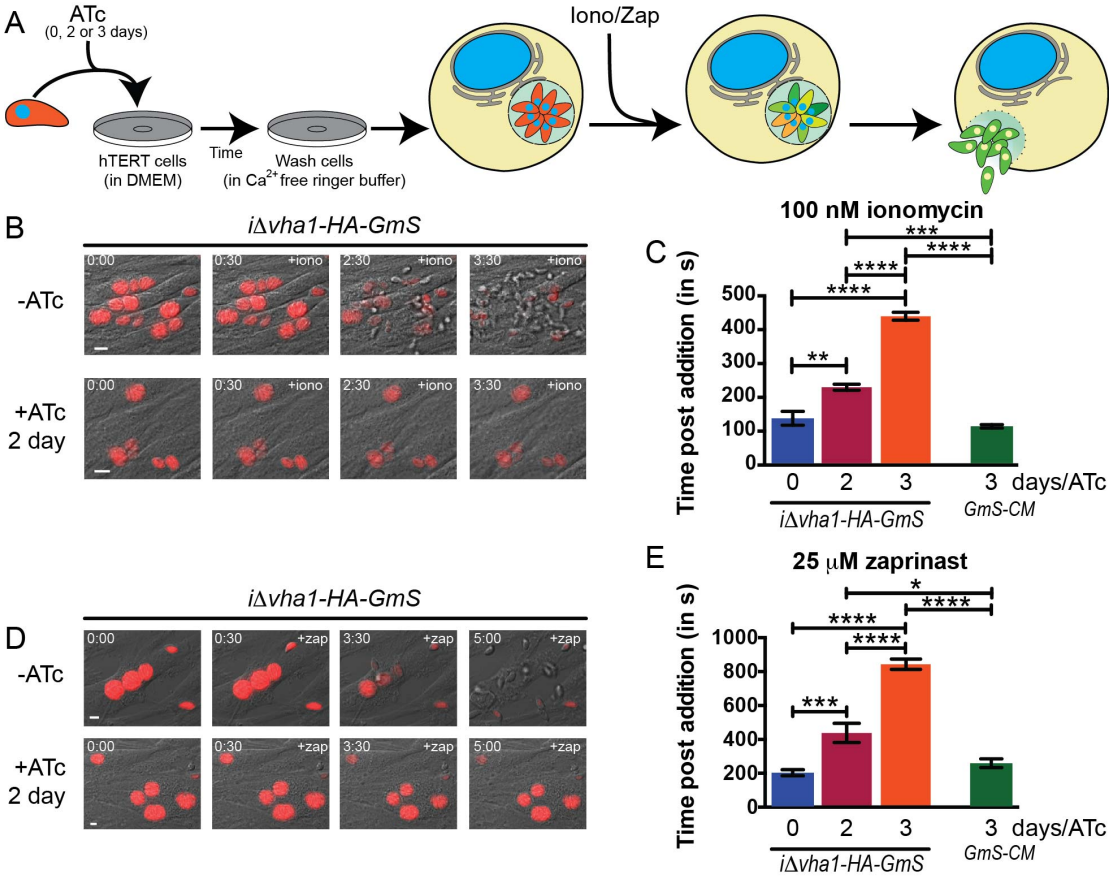

FIGURE 6.5: Vha1 knockdowns have a delayed egress. A) Cartoon depicting the measurement of parasite egress. B) *iΔvha1-HA-GmS* clones were incubated with ATc for 0, 2 or 3 days (day 3 video not shown). After 30 seconds of the time lapse, 100 nM ionomycin was added. C) Quantification of the time to egress. Data are reported as the average time of the first parasite to egress from the first 5 parasitophorous vacuoles. D) *iΔvha1-HA-GC6-mS* clones were incubated with ATc for 0, 2 or 3 days (day 3 video not shown). After 30 seconds of the time lapse, 25 μM zaprinast was added. E) Quantification of egress time. Data are reported as the average time of the parasite to egress from the first 5 parasitophorous vacuoles. For the purpose of clarity only the red channel is shown in

panels B and D. Panels C and D were compared with one-way ANOVA test, *$P < 0.05$; **$P < 0.01$; ***$P < 0.001$, ****$P < 0.0001$.

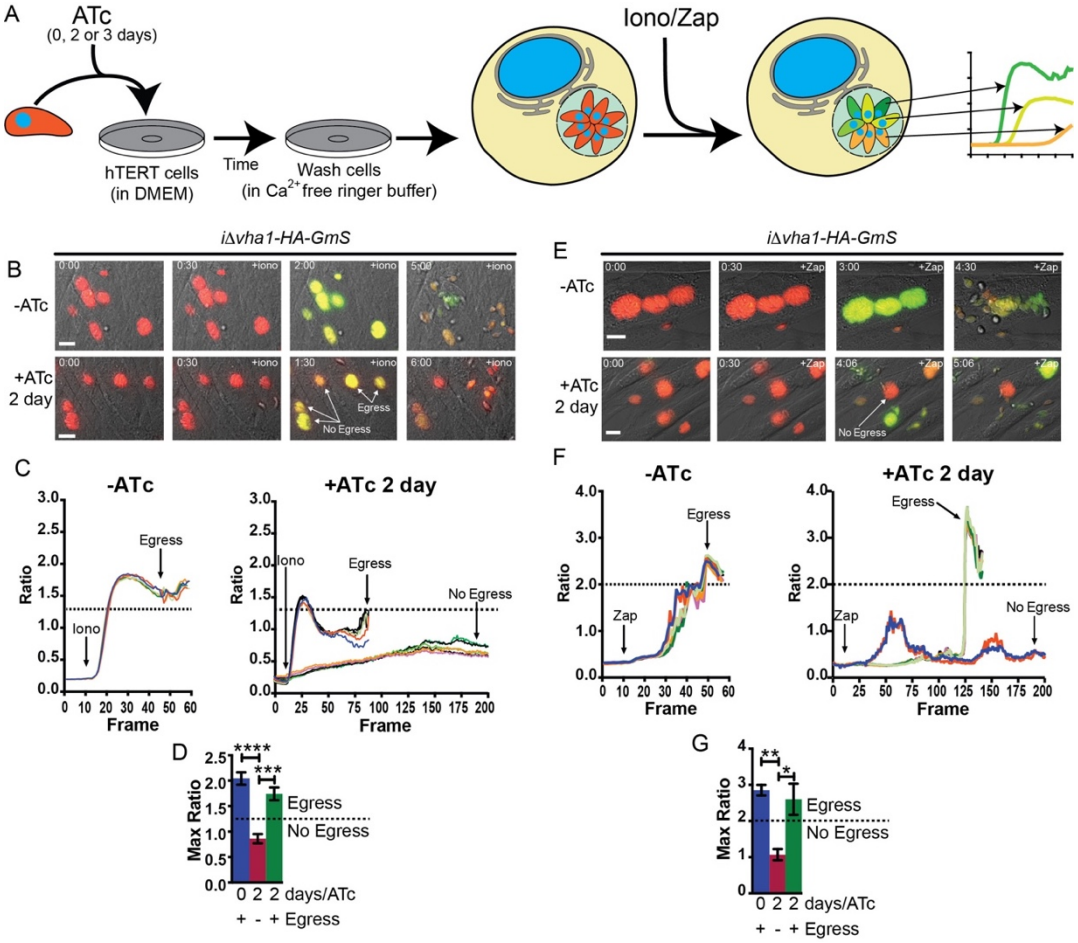

FIGURE 6.6: A threshold for calcium is required for egress. A) Cartoon showing the protocol for measurements of egress of individual parasites from a single parasitophorous vacuole in response to calcium agonists. B) *iΔvha1-HA-GmS* clones were incubated with ATc for 0, 2 or 3 days (day 3 video not shown). After 30 seconds of the time lapse, 100 nM ionomycin was added. Arrows indicated the addition of 100 nM ionomycin and the time of the egress of the first parasite. C) Representative tracings of the ratio of red to green fluorescence of all the parasites in a single parasitophorous vacuole. For clones incubated with ATc, some parasites failed to egress from the parasitophorous vacuole and a representative tracing is overlaid. D) The peak ratio observed before egress of all

members of the parasitophorous vacuole were averaged into a single value of 6 independent trials. E) *i⊿vha1-HA-GmS* clones were incubated with ATc for 0, 2 or 3 days (day 3 video not shown). After 30 seconds of time lapse, 25 μM zaprinast was added. Arrows indicated the addition of 25 μM zaprinast and the time of egress of the first parasite. G) The peak ratio, prior to egress, of all members in the parasitophorous vacuole were averaged into a single value of 6 independent trials. One-way ANOVA was performed where $*P < 0.05$; $**P < 0.01$; $**P < 0.001$; $****P < 0.0001$.

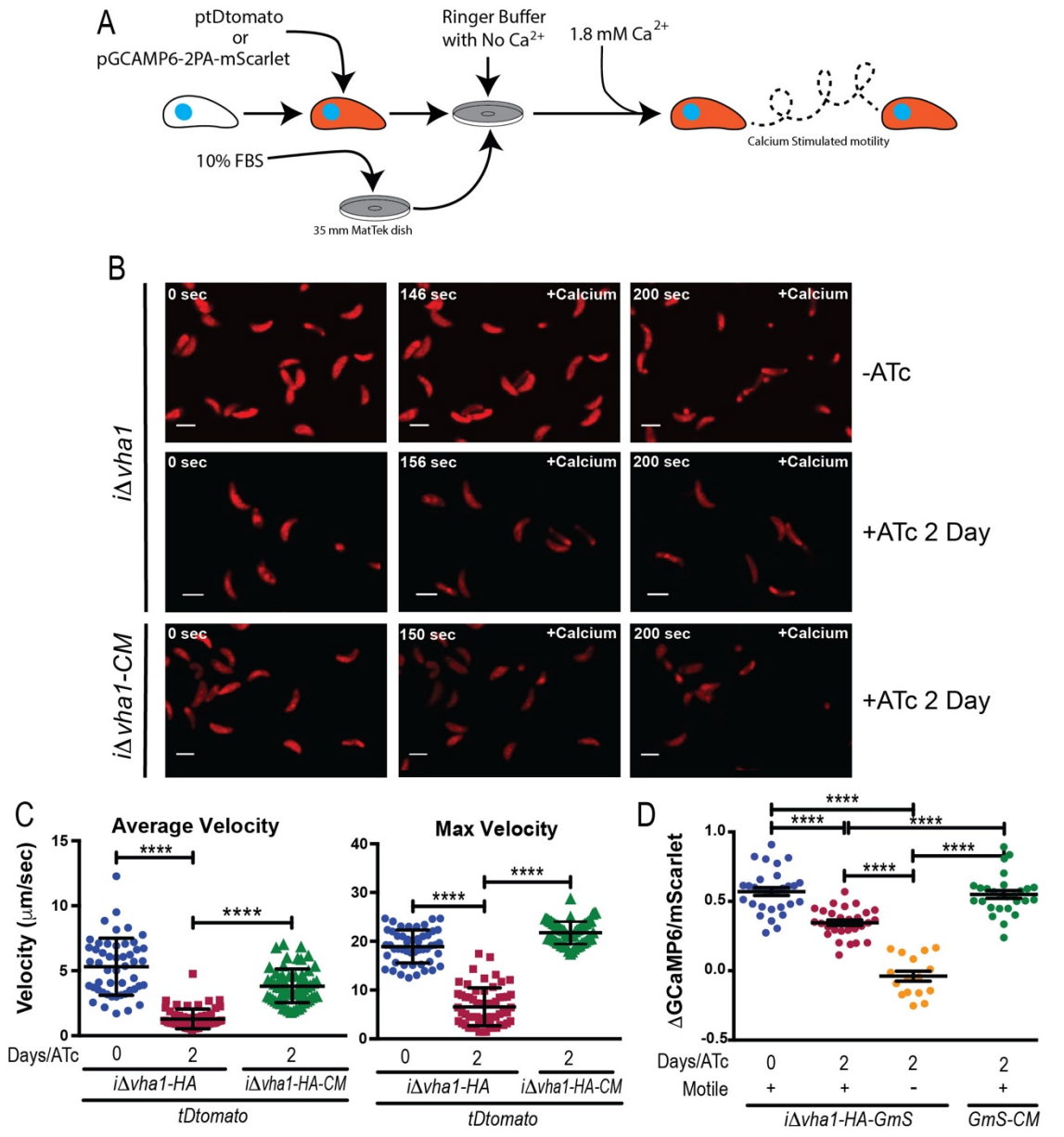

FIGURE 6.7: Vha1 knockdowns have a reduction in velocity due to reduced intracellular calcium levels. A) Cartoon showing the protocol to measure calcium-stimulated motility. B) Time lapse microscopy where tdTomato expressing *iΔvha1-HA* and *iΔvha1-HA-CM* were incubated with or without ATc for 0 or 2 days. At the indicated time, 1.8 mM calcium was added. C) Motility assaying average velocity or maximum (top

speed) velocity of tdTomato expressing *iΔvha1-HA* and *iΔvha1-HA-CM* with or without ATc. The motility of 40-80 individual parasites from 3 independent trials per clone were tracked and then sorted as fastest to slowest where the top 20 per independent trial were used for quantification. Displayed are the top 20 velocities (60 data points in total from 3 independent trials) per trial and clone. Error bars are SEM and data were analyzed by GraphPad Prism 6. D) Quantification of the change in ratio at the start of the time lapse to one frame before movement of *iΔvha1-HA-GmS* and *iΔvha1-HA-GmS-CM* clones incubated with ATc for 0 or 2 days. One-way ANOVA was performed where ****$P <$ 0.0001.

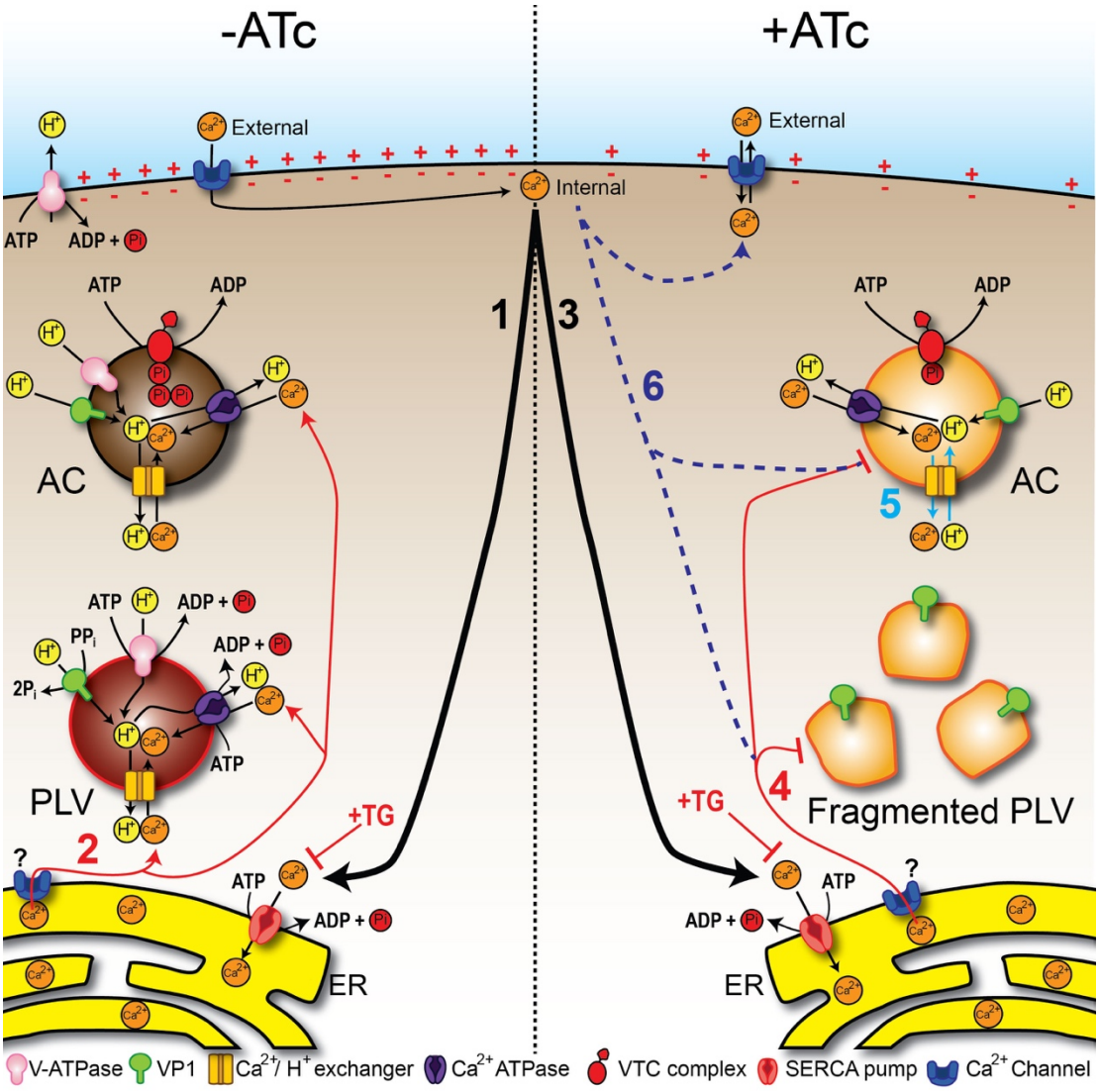

FIGURE 6.8: Model of crosstalk between calcium, pH, and polyphosphate. Model showing the relationship of calcium, pH, and their interaction with the stores, the endoplasmic reticulum (ER), plant-like vacuole (PLV), and acidocalcisome (AC). ***Step 1***: In wild type parasites, extracellular calcium enters the cytoplasm resulting in a cytoplasmic increase. Excess calcium is taken up largely by the ER pumped by the SERCA-Ca^{2+}-ATPase. ***Step 2***: When the SERCA pump is inhibited by thapsigargin (TG), calcium leaks

out of the ER by an unknown mechanism. The increase in cytosolic calcium activated the uptake by the PLV and acidocalcisomes. ***Step 3***: In *i*Δ*vha1-HA* parasites incubated with ATc, extracellular calcium enters the cytoplasm and results in increased cytoplasmic calcium. Excess calcium is taken up largely by the ER with the SERCA-Ca^{2+}-ATPase pump. ***Step 4***: When TG is added to *i*Δ*vha1-HA*+ATc parasites, Ca^{2+} leaked by the ER is unable to enter the PLV due to its fragmentation or the AC due to its decreased acidification. ***Step 5***: The reduced acidity of the AC results in the Ca^{2+}/H^{+} exchanger to change direction and allow calcium out of the organelle, thus leading to a decrease calcium in the AC. Due to the reduced acidity and calcium concentration, the VTC complex is unable to maintain the polyP concentration into the AC. ***Step 6***: The altered membrane potential causes *i*Δ*vha1-HA*+ATc parasites to equilibrate their calcium levels with their surrounding environment and lose the ability to regulate calcium homeostasis. This leads to severe defects in egress and motility.

CHAPTER 7

CONCLUSIONS AND FUTURE WORK

7.1 Introduction

In this dissertation, I aimed to characterize the function and the importance of the *Toxoplasma gondii* V-ATPase. Prior to this investigation, very little was known about this pump in *T. gondii* and investigations were largely limited to biochemical observations driven by chemical inactivation. In this dissertation, I C-terminally HA tagged Vha1 and then created a conditional knockout to study the function of this pump at the molecular level. Upon characterization of this complex through its absence in the parasite, I demonstrated that the V-ATPase plays numerous roles in the propagation of the parasite as well as performing some housekeeping functions. I demonstrate that the major steps of the lytic cycle were impacted by depletion of the V-ATPase. The evidence I present suggests that the defects in the lytic cycle are due to a combination of losses in the endolysosomal system, loss of vesicular trafficking, disruption of key proteases, disruption in key secretory proteins, and the loss of ionic homeostasis. Collectively, these functions demonstrate the importance of the pump for the parasite.

7.2 Future work

7.2.1 Vha1 translocation to the PLV

While this dissertation makes great strides identifying the roles of the V-ATPase, there are unanswered questions or other observations the require further characterization. Routine IFA's showed the V-ATPase formed a large punctum that appeared to detach from

the plasma membrane and transit to the PLV. The ingestion pathway (host proteins making their way to the PLV) in *T. gondii* remains a mystery [1] and these translocation observations are a curious observation. Another observation is that the localization of the large punctum is often in the area where the micropore typically resides. Due to the trafficking properties of the V-ATPase and its translocation to the PLV after egress, further investigations should determine if the translocation event is involved in bringing host material to the PLV or at the micropore. Data presented in this dissertation demonstrates that the translocation to the PLV is not a result of membrane recycling, consequently the parasites are actively translocating this pump to the PLV to perform specific functions, some of them I characterized in this work.

7.2.2 Only select subunits of the V-ATPase were investigated

In this study, I tagged three subunits of the V-ATPase (Vha1, VhG, and VhE). I extensively investigated Vha1 and only tagged VhG and VhE. The effect of loss of either of these subunits remains unknown but presumably the phenotypes would be similar to the loss of Vha1. Curiously, of all the V-ATPase subunits, VhG has the third highest essentiality score and VhE is the most dispensable (see **Table 5.1**).

There are several other subunits which BLAST with yeast subunits that were not tagged nor investigated (see **Table 5.1**). For example, *T. gondii* possess two *a* subunit isomers, Vha1 and Vha2. Both of the *a* isomers were able to complement in *Δvph1Δstv1* yeast (see **Fig. S5.3**), but Vha2 was difficult to tag and visualize once tagged. This was largely due to its decreased expression. Attempts to tag with stronger and more fluorescent tag were unsuccessful. Thus, the function of Vha2 remains unknown in *T. gondii*. Because loss of Vha1 resulted in severe phenotypes, it is likely that Vha2 is unable to compensate

for loss of Vha1 even though it can function similarly to Vha1 in yeast. Many of the other subunits have not been tagged nor investigated to confirm their association with the V-ATPase. With the exception of Vha1, the specific function of each subunit has not been identified. Because the complex itself is essential, the fact that the essentiality scores for all subunits are not similar could indicate that some subunits perform additional important, yet unidentified roles. In yeast, many of the V-ATPase subunits have additional functions or binding partners that interact with the V-ATPase. Aside from all other subunits of the V-ATPase, none of the interacting partners nor the specific function of the other subunits in *T. gondii* are known. All assumptions of their presumed function are solely based on other organisms such as yeast.

7.2.3 Importance of separating proton translocation versus targeting functions of the V-ATPase

Separating the pumping function from any trafficking function has proven extremely difficult to dissect in *T. gondii*. Mutation of arginine 735 in yeast results in defective pumping of protons [2]. Similar mutations were made in cDNA of *vha1,* but stable clones were not possible after numerous attempts. It is possible that over expression of the mutant cDNA could be creating a dominant negative effect and killing the parasites due to faulty proton translocation; or it is also possible that the proton translocating activity is absolutely essential. Unfortunately, negative data cannot determine if the latter is true. The *vha1* gene also encodes a signal peptide that likely ensures proper localization. Interestingly, *vha2* does not contain any predicted signal peptide. A construct that consisted of an ablation of the signal peptide in *vha1* cDNA was made but never successfully transfected. Thus, the importance of the localization of Vha1 to *T. gondii*

remains unknown. However, there was evidence of palmitoylation present in Vha1. I observed that mutation of cystine[26] to alanine (this strain was termed *Δku80vha*^{C26A}) did seem to impact localization whereas complementation back of the WT gene (this strain was termed *Δku80vha*^{WT}) restored Vha1 and VP1 colocalization. These observations were curious but proper follow up experiments need to be performed to fully understand the role of palmitoylation and its translocation back to the PLV. Curiously, the palmitoylation mutant seemed to have a more fragmented PLV than the WT. In general, future studies should be directed at separating the proton translocating activity from its trafficking functions.

7.2.4 Rhoptry biogenesis and the role of the V-ATPase

I report that the V-ATPase encircles the forming rhoptries and postulate that the complex could play a role in their maturation. While I demonstrate that the V-ATPase plays a role in the maturation of their contents, not much is known about the biogenesis of this important secretory organelle and how it becomes acidic and neutral after maturation. Thus, the role of the V-ATPase in the conversion of immature to mature rhoptries is not known. While IFA's failed to show co-localization of the V-ATPase in mature rhoptry membrane, recent immunoelectron microscopy suggests that the V-ATPase may be present in the mature rhoptry membrane. Further studies should be directed to confirming the localization of the V-ATPase in mature rhoptries and its function (if present).

7.2.5 The V-ATPase and calcium

Calcium entry across the *T. gondii* plasma membrane is poorly understood. Data presented in this dissertation demonstrate that the V-ATPase is important in part to calcium entry. However, a full characterization of the contribution of the V-ATPase in calcium

entry at the plasma needs further study. I postulate that the differences in membrane potential in Vha1 depleted parasites is responsible for our observations on calcium movement in the parasites. A further characterization of how the membrane potential, the V-ATPase, and calcium entry are related should be performed to understand this link.

7.3 Conclusion

The research presented in this dissertation provides significant insights of the *T. gondii* V-ATPase into the molecular function, importance to the parasite, and importance to the physiology of the parasite. However, there remain numerous avenues for further exploration. New insights to the role of the V-ATPase could be valuable in understanding the endolysosomal system, new functions of the plant-like vacuole, vesicular trafficking, the maturation of key proteases and secretory proteins, calcium entry, polyphosphate synthesis and storage, and how the parasite copes with changing ionic concentrations.

7.4 References

1. Dou, Z., et al., *Toxoplasma gondii Ingests and Digests Host Cytosolic Proteins.* mBio, 2014. **5**(4).
2. Kawasaki-Nishi, S., T. Nishi, and M. Forgac, *Arg-735 of the 100-kDa subunit a of the yeast V-ATPase is essential for proton translocation.* Proceedings of the National Academy of Sciences, 2001. **98**(22): p. 12397.